Danish Windatlas

A Rational Method of Wind Energy Siting

Lundtang Petersen, Erik; Troen, Ib; Frandsen, Sten Tronæs; Hedegaard, K.

Publication date:
1981

Document Version
Publisher's PDF, also known as Version of record

WINDATLAS FOR DENMARK

Erik Lundtang Petersen
Ib Troen
Sten Frandsen
Klaus Hedegaard

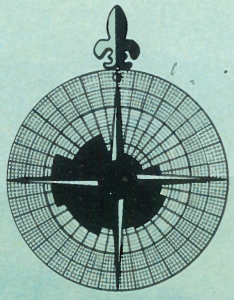

RISØ
JANUARY 1981

RISØ-R-428

DANISH WINDATLAS
A RATIONAL METHOD OF WIND ENERGY SITING

Erik Lundtang Petersen
Ib Troen
Sten Frandsen
Meteorology Section
Physics Department
Risø National Laboratory

and

Klaus Hedegaard
Weather Service
Danish Meteorological Institute
Lyngbyvej 100, DK-2100 Copenhagen Ø

January 1981
Risø National Laboratory, DK-4000 Roskilde, Denmark

Sales distributors:
Jul. Gjellerup, Sølvgade 87,
DK-1307 Copenhagen K, Denmark

Available on exchange from:
Risø Library, Risø National Laboratory,
P.O. Box 49, DK-4000 Roskilde, Denmark

Abstract. A method is presented which makes it possible to obtain an accurate estimate of the probability distribution of the wind velocity of a given height above a specified terrain. The physical base for the method is the similarity theory for the planetary boundary layer. The method requires a long series of surface pressure observations from a reasonably dense network. The method is applied to Denmark using 13 years of data from 55 synoptic stations. The Weibull distribution is found to give excellent fit to the calculated wind speed distributions and the results are presented as charts giving the Weibull parameters for Denmark as function of type of terrain, direction sector and height up to 200 meters. Simple computational procedures are described which make it possible to estimate the wind distribution over inhomogeneous terrain, and in the presence of topographical and shelter effects. The method is found to accurately reproduce observed wind distributions over a wide range of conditions. The Atlas is especially well-suited for wind power assesment. The problems of the persistance of power production and the effect of the geographical distribution of wind turbines on the mean power are also discussed.

UDC 551.55 (489)

ISBN 87-550-0738-4
ISSN 0106-2840

Cover by Eva Floryan
Cover printing Elsgaard Press, Roskilde

Risø repro 1981

CONTENTS

page

FOREWORD

"Danish Windatlas" is an investigation of the Danish climatic wind conditions. Its objective is the evaluation of wind resources for the purpose of locating large wind power stations in Denmark. The investigations have been carried out jointly by the Risø National Laboratory and the Danish Meteorological Institute under the sponsorship of the Wind Power Program of the Danish Energy Ministry and the Danish Utilities. Risø National Laboratory has had the overall responsibility for project coordination while the Meteorological Institute has been mainly responsible for the collection of pressure data and pressure analysis (Chapter 4), along with the collection of other meteorological data from synoptic stations.

A number of people at the two institutions have taken an active role in the analysis. In the Meteorological Section of Risø, Ole Christensen has had an appreciable influence on the choice of the method upon which the investigation is based; Niels Otto Jensen and Søren Larsen have helped with the solutions of a number of problems.

Personnel of the Meteorological Institute who have contributed to this program include: Mogens Rønnebæk who organized the pressure, temperature and wind data, Jørgen Heesche who deciphered the data tapes that were received from foreign countries, and Peter Aakjær who organized and processed the radiosonde data.

The preparation of the Windatlas has been dependent upon the meteorological data contributed by several foreign countries. The cooperation which has been received from the meteorological services in the neighbouring countries is gratefully acknowledged; in particular, the Norwegian Meteorological Institute, Oslo, the Swedish Meteorological and Hydrological Institute, Norrköping, Deutsches Wetterdienst, Offenbach, Meteorological Dienst der DDR, Potsdam, and the Instytut Meteorologii in Gospodarki Wodnej Warsaw.

We direct special thanks to I.K. Ebbesen, Weather Service Inspector of the Defence Command, and to the associated weather services of the airports at Aalborg, Karup, Tirstrup, Skrydstrup, Avnø, and Værløse for the willingness with which they have delivered information to the project. We also thank the weather services at the airports at Beldringe and Rønne together with the observers at Skagen, Hanstholm, Thyborøn, Lyngvig and Keldsnor and the Weather Observatory Department of the Meteorological Institute for their help in determining the anemometer conditions at the various observation sites.

The English edition of this report is largely a translation of "Vindatlas for Danmark" which is in Danish. The authors are grateful to William K. George, Professor of Mechanical and Aerospace Engineering at the State University of New York at Buffalo and Visiting Scientist at Risø 1980-81, for assisting with the translation and editing of this version.

1. INTRODUCTION

1.1. The meteorological basis of the Windatlas

The meteorological criteria which are the basis for the Windatlas are built especially on the fact that the wind speed at a given location and height within the lowest few hundred meters of the atmosphere is strongly dependent upon the nature of the surroundings. This dependence arises from the frictional retardation of the wind by the earth's surface. In many circumstances, a surface can be characterised by determining its roughness since the greater the roughness of the surface, the greater will be the retardation.

For the purpose of the Windatlas, the Danish landscape has been classified into four roughness classes as shown in Table 1.1. Also shown in Table 1.1 is the roughness length, a concept which will be explained in Appendix C. The importance of roughness for the wind energy potential of a terrain is illustrated in the table by the calculated wind energy at a height of 50 m above the surface. The numbers are relative and the energy for water areas is arbitrarily chosen as 10.

At a height of approximately 1000 m the wind is not affected by the character of the earth's surface. In Chapter 4 it is shown that the statistics of this so-called "free wind" can be considered to be the same over the whole analysed region. In other words, even though at a given moment the speed and direction of the wind can vary from one place to another in the region, the "free wind's" statistical characteristics (such as its probability density function) will not show a geographic variation over Denmark.

The free wind can be calculated from a set of surface pressure measurements by means of the geostrophic approximation, and the wind at a given height over the surface can then be calculated using the geostrophic resistance law as shown in Chapter 2.

Table 1.1. Types of terrain, roughness classes, and roughness lengths.

Roughness class	Terrain	Roughness length	Relative energy
0	- water areas	0-1 mm	10
1	- open country areas with very few bushes, trees, and buildings	1 cm	7
2	- farmland with scattered buildings and hedges with separation in excess of 1000 m	5 cm	5
3	- built-up areas, forests, and farmland with many hedges	30 cm	3

1.2. Use of the Windatlas

A given wind turbine's average energy production at a given place can be calculated if the wind turbine's power curve and the probability density for the wind speed at hub height are known. Typical examples of these are illustrated below.

Wind turbine's power curve (power vs. wind speed)

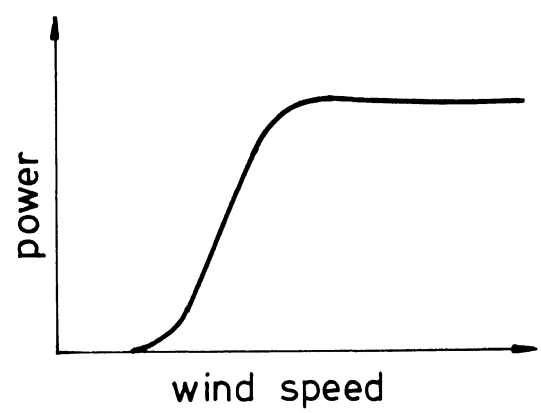

Probability density function for the wind speed at hub height (probability vs. wind speed)

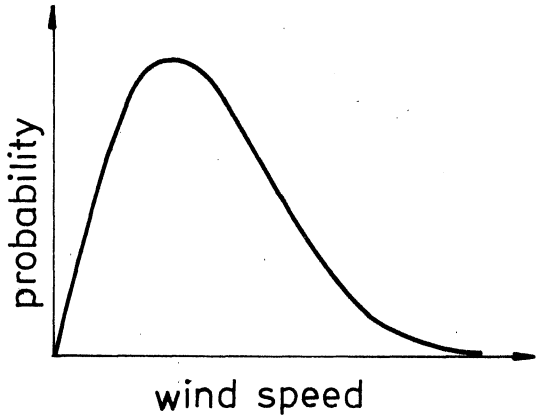

Multiplication of the ordinates of these two functions yields the wind turbine's

energy production curve (production vs. wind speed),

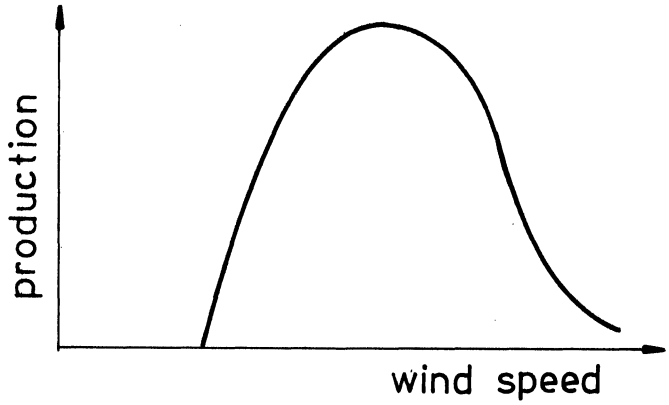

and the area under this curve is equal to the average energy production of the turbine.

The probability density function is described in Chapter 3 and the power curve in Chapter 5. The power curve of the turbine is usually supplied by the manufacturer; the purpose of the Windatlas is to be a tool for the determination of the probability density function of the wind speed at hub height.

It is well-known that the wind speed probability density function is given by the Weibull distribution to an acceptable approximation. This has been demonstrated in a number of articles, e.g. Justus and Mikhail (1976), Hennessey (1977), and Stewart and Essenwanger (1978). The Weibull distribution is described by two parameters, a scale parameter A, and a shape parameter C.

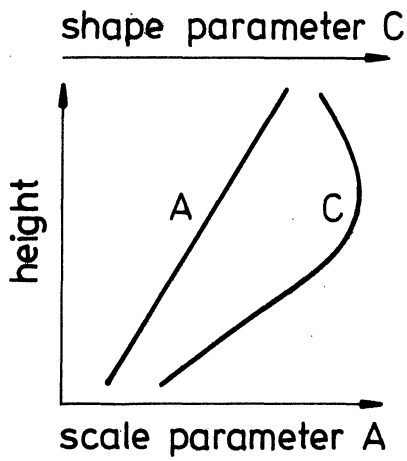

Weibull parameter variation with height

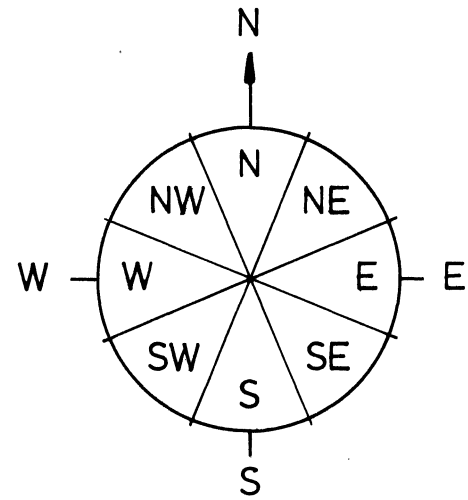

Division by sectors

The Windatlas provides a method for the calculation of these scale and shape parameters at a given height over the surface of the earth at a specified place in Denmark. Such a calculation is carried out using the tables and graphs in Appendix A. These show how A and C vary with height for a given wind direction sector and a given roughness class.

The Windatlas charts are based on wind direction sectors of 45° and on four surface roughness classes. In addition to the 32 charts generated by this division, an additional chart has been prepared for each roughness class under the assumption that the roughness is the same in all sectors. Thus, there are in all 36 charts in Appendix A.

The wind speed probability density function (and thereby a given wind turbine's average energy production) is determined by the following method:

1) The roughness class for each of eight direction sectors is determined.

2) From the 36 charts, those curves specifically corresponding to the appropriate roughness classes are chosen. If the roughness of the terrain changes with the sector direction, eight charts are chosen. If the terrain is of uniform roughness, one chart is sufficient.
3) The shape and scale parameters for the Weibull distribution at the hub height of the wind turbine are read from each of the selected charts.
4) Calculations corresponding to those in Example 5.5 of Chapter 5 are carried out, and the wind speed's probability density function is obtained.

The wind turbine's average energy production can now be determined if the power curve of the turbine is known. If the power curve is of a form where the portions are approximately piecewise linear the tables in Chapter 5 can be used directly.

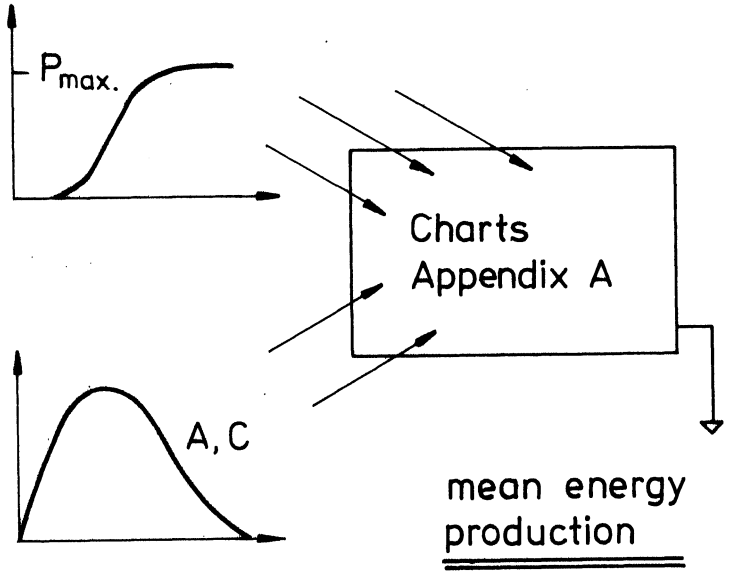

Sketch of the mean energy production determination

The error of the calculated mean energy production is estimated to be less than 5% if the calculations are made for a terrain which is not too complicated.

This 5%-error estimate is not based on theoretical considerations but is obtained by comparisons between measured energy outputs of wind turbines and those calculated by means of the Windatlas. The wind turbines used for this validation were the Gedser wind turbine, the small wind turbine analyzed in Chapter 5, and two identical small wind turbines whose outputs were measured over a period of one year. The two identical wind turbines showed a difference in production over the year of 25% which was attributable to the terrain surrounding the turbines. The Windatlas reproduced the output of each of these wind turbines to within 5% and also reproduced the difference in the output caused by the dissimilar terrain surrounding the two wind turbines.

In addition the verifications in Chapter 6 support the 5%-error estimate.

1.3. Previous climatic wind energy investigations

The Windatlas can be regarded as an extension of the work done by Martin Jensen for the Danish Wind Power Program in the period 1957-1961 (Wind Power Committee's Report, 1962). At the Danish locations Gedser, Tune, and Torsminde, the maximum wind speeds and the wind energy probability density distribution functions were measured. The sites were chosen such that the coastal sites Torsminde and Gedser were representative of optimal Danish wind turbine sites, while Tune was a typical Danish inland site. These measurements are compared with the Windatlas in Chapter 6. The measurements of the extreme winds made during these investigations have formed the basis for the Danish Wind Code (Actions on Building Structures 2. Wind Load, 1977).

Martin Jensen's measurements were performed in order to determine the wind power potential for typical wind turbine sites in the Danish countryside. Comparable investigations have been made at other places in the world; for example, the Dutch investigations of 1952-57 (Dutch Windmills 1960). One of the purposes of that report was to determine the suitability of wind turbine sitings along the Dutch North Sea coast. Unfortunately the re-

sults of that investigation, like many other similar older investigations, are presented in such a way that it is difficult to compare them to the results of the Windatlas.

It would lead too far astray to examine more closely all of the wind energy studies that have been made. A great many of them are concerned with the special conditions that prevail in mountainous regions, a subject that will not be addressed in the Windatlas. Other investigations make an attempt to estimate the geographical distribution of wind power potential over large areas taken as a whole; for example, the eastern and midwestern U.S.A. (Justus, 1978), the Pacific northwest states (Baker, et al., 1979), the entire U.S.A. considered as a whole (Justus, 1976), and Sweden (Smedman-Högström and Högström, 1978 and Kvick and Karlström, 1977). The investigations mentioned generally follow a procedure where a number of suitably scattered synoptic measurement stations are chosen for the area under consideration. The wind measured at 10-meter height is extrapolated to the desired height, and statistical calculations on the extrapolated wind speeds are performed.

The simplest extrapolation method is based on the "1/7 power law", $u_1/u_2 = (z_1/z_2)^{1/7}$, where u_1 and u_2 are the wind speeds at the heights z_1 and z_2. This method is often preferable to more complicated empirical methods (Peterson and Hennessey, 1978; Justus and Mikhail, 1976).

Smedman-Högström and Högström (1978) have presented a method which includes the dependence of the wind on the roughness of the terrain, the stability of the atmosphere, and the height above the terrain. Determination of the average power production of a wind turbine at a given place by this method requires that meteorological measurements be taken several times a day over a period of years at the location in question. Moreover, a detailed mapping of the roughness of the surrounding terrain is needed. These calculations can only be carried out by computer. Kvick and Karlström (1977) have applied this method to 45 Swedish stations in order to obtain a statistical view of the

geographical variation of the wind speed. A discussion of this method along with the Windatlas's method is given in Chapter 2, section 2.5.

1.4. Contents of the Windatlas

In the following chapter the physical model that forms the basis for the Windatlas is described. Concepts such as geostrophic wind, boundary layer stability, and similarity theories are introduced and defined. In Chapter 3 the basic statistical principles are examined, first with a discussion of the proper choice of averaging for measuring wind speeds, and then with a description of the Weibull distribution and the methods for estimating its parameters. Chapter 4 deals with the pressure analysis and the calculation of the geostrophic wind. The geographical variation of the geostrophic wind, the effects of the gradient wind, and baroclinicity, and the percentage of error in the calculations are also discussed.

Chapter 5 together with Appendix A constitutes the practical part of the Windatlas. Procedures for determining the terrain's roughness as well as the effects of various forms of shelter and topographical features are outlined in Chapter 5; a number of examples are presented to illustrate the application of the method proposed. In Chapter 6, a comparison is made between the distributions of wind speeds predicted by the Windatlas and the speeds actually measured at a series of stations evenly distributed over Denmark. These comparisons are the conclusive proof for applicability of the Windatlas.

Chapter 7 provides an overall assessment of the Windatlas.
In Appendix B, an analysis of the time variation and geographic variation of production from specific wind turbines is made, and finally, in Appendix C the concept of roughness length is discussed.

2. THE PHYSICAL MODEL

2.1. The equations of motion

Meteorology is the science which deals with the dynamical processes which take place in the earth's atmosphere. As such it employs many physical disciplines, the most important being geophysical fluid dynamics which includes the study of flow systems in rotating stratified fluids.

All types of flow that are dealt with in meteorology are governed by the same set of physical equations; namely equations for mass and momentum conservation, together with the first law of thermodynamics and the equation of state. This set of governing equations has no general solution. Moreover, as they are coupled nonlinear partial differential equations, they present in their most general form an extremely complicated mathematical problem. Nonetheless they appear in a simple and elegant form, and describe the motion of extremely complicated flow systems with only very few symbols.

2.2. The geostrophic wind

A flow system that is often seen on weather maps is one where the wind at a height of approximately 1000 meters over the earth's surface blows parallel to the isobars (lines of constant pressure) with the low pressure to the left* and with a velocity that is proportional to the pressure gradient (i.e. inversely proportional to the spacing of the isobars).

If an air parcel starts to move toward the low pressure, the Coriolis force (a force arising from the earth's rotation) will influence the parcel and turn it towards the right*. The result will be that the parcel circles around the low pressure and

*In the northern hemisphere

never reaches it. When the isobars are close to being straight lines, the wind velocity calculated from the assumption of equilibrium between the Coriolis and the pressure gradient forces is often a very good approximation to the velocity observed at a height of one kilometer above the terrain. This wind velocity is called the geostrophic wind, and it is illustrated on Fig. 2.1.

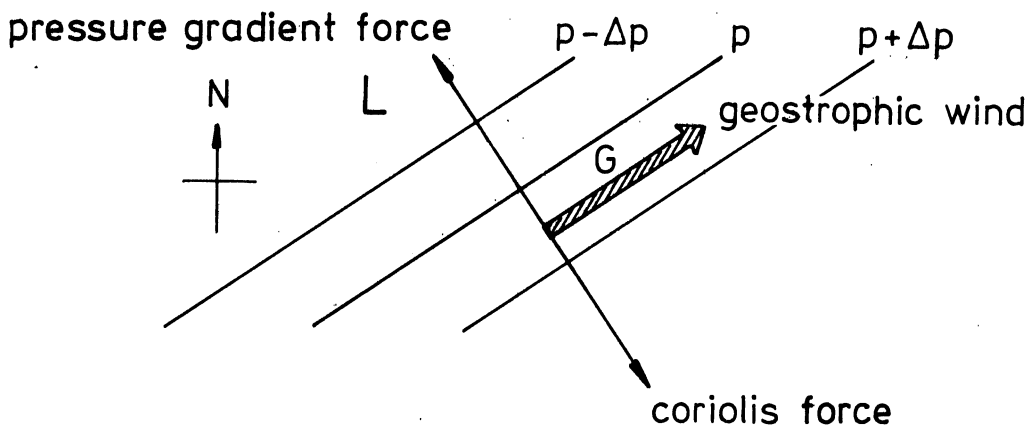

Fig. 2.1. The geostrophic wind

The geostrophic wind is a good approximation as long as the acceleration of the air and the frictional forces acting upon it are negligible. These conditions are further discussed in Chapter 4.

The geostrophic wind is an important concept in meteorology because it gives a direct relation between the mass distribution over a certain area in the atmosphere and the wind field in the same area.

2.3. The planetary boundary layer

The geostrophic approximation cannot be used where frictional forces are comparable to the pressure and Coriolis forces. Such is the case with the layer next to the earth's surface where the wind is influenced by frictional forces acting on the surface. This layer is called the planetary boundary layer. On a cloudy day with a strong wind, this layer is of the order of one kilometer in thickness. On a cloudless night with light wind the thickness of the layer can be less than one hundred meters.

Under a number of simplifying conditions* which will be discussed below, the following simple picture of the boundary layer is valid. In the lowest small fraction of the boundary layer, denoted the surface layer, the vertical fluxes of momentum and heat are essentially constant, the wind speed changes with height, but the mean direction of the wind is constant. In this layer energy is extracted from the mean wind to produce turbulent eddy energy (ultimately converted into heat). The turbulent eddies cause a momentum drain on the mean wind, the momentum is carried downward to the surface where it replenishes the momentum loss to the ground caused by the aerodynamic drag forces acting on the surface roughness elements. The momentum lost to the surface is replenished by turbulent transport of momentum from the boundary layer above the surface layer.

In the boundary layer the wind vector is turned a small angle anticlockwise (on the northern hemisphere) compared with the direction of the geostrophic wind. The wind vector thus has a component down the pressure gradient resulting in net generation of kinetic energy to make up for the loss to turbulence.

---

*The boundary layer is horizontally homogeneous, the geostrophic wind is constant with height (barotropy) and time (stationarity) and the boundary layer is unstratified (neutral conditions, see below).

2.4. The stability of the boundary layer

A concept which is of major importance in describing the dynamical behaviour of the planetary boundary layer is the static stability.

Stability can be illustrated by the following example:

If a small parcel of air is moved upward (or downward), it will expand (or be compressed) because the pressure in the atmosphere decreases with height. As the parcel's volume changes, so does its temperature, a decrease in temperature corresponding to expansion and vice versa. This type of thermodynamic process where no heat is transfered is called an adiabatic expansion (or compression) and the change in temperature which occurs can be computed if the variation of pressure with height is specified. In the lower atmosphere the temperature change with height for an adiabatic expansion is $-1^{o}C$ per 100 m. altitude increase.

If the surrounding atmosphere has a temperature distribution that decreases with height at the same rate, the air parcels will be in equilibrium with each other. The atmosphere's condition in this case is said to be neutral. Under situations of neutral stability, atmospheric turbulence appears only as a result of friction with the earth's surface.

If the temperature in the atmosphere falls more than $1^{o}C$ for a height increase of 100 m, a parcel which is moved upward will arrive at surroundings that are relatively colder. As a result, the lighter parcel will have a positive buoyancy and the upward movement will continue. If on the other hand the parcel is moved downwards it will arrive at surroundings that are relatively warmer, and the movement will therefore continue downward. In such unstable conditions where each movement in the vertical direction is increased, a stronger turbulence results than in a neutral situation. If a condition like this prevails, the atmosphere is said to be unstable.

If the temperature in the atmosphere falls less than $1^{o}C$ for a height increase of 100 m or if the temperature rises with increasing height, it can be seen by arguments analogous to those above that turbulent motions will be suppressed. In such situations where buoyancy forces act to oppose vertical motions the condition of the atmosphere is said to be stable. In a stable atmosphere, the turbulence level is less than in the neutral atmosphere, and in case of strong stability the turbulent motions can be nearly eliminated.

Measurements from Risø's meteorological mast taken continuously over a period of 10 years show that unstable, neutral, and stable atmospheric conditions occur approximately, 6%, 60%, and 34% of the time respectively (Jensen, 1973).

Stability conditions in the portion of the atmosphere closest to the earth have a strong influence on wind conditions. For a given geostrophic wind, unstable conditions will cause increased wind speeds relative to those expected in neutral conditions, while stable conditions normally give rise to relatively smaller wind speeds.

2.5. Choice of method

The basis of the method which is used in the Windatlas is the geostrophic resistance law. This law expresses the frictional force at the earth's surface as a function of the geostrophic wind, which is treated as external driving force. The theoretical foundations of this law are based on similarity considerations; therefore, it can be used only under quite simplified conditions. The most important of these is that the turbulent boundary layer be in equilibrium with a geostrophic wind which is constant with height, and that the static stability in the boundary layer be constant with height. In practice, these two conditions are not often fulfilled in the atmosphere and a more complete theory would be desirable. In principle, the dynamic equations can be solved for boundary layers by the use of the analysed pressure fields and a simple boundary layer

model. However, the computer time required by even the simplest models makes such an approach impossible. In the preparation of the Windatlas the choice has, therefore, been between a statistical analysis of existing wind measurements and an application of a similarity theory in conjunction with the analysed pressure field.

Use of the first method requires that one be in possession of measurements of wind speeds from meteorological masts placed in reasonably homogeneous areas. Furthermore, high quality measurements at a number of heights are required. As will be shown later, wind measurements, especially at relatively low heights, can be strongly influenced by the immediate surroundings; it is therefore difficult to systemize wind measurements from different locations without using a theoretical method that makes it possible to distinquish between important and unimportant influences. Because of the small number of measurement series that can be used in practice, such an analysis will employ similarity theory to a high degree in order to make possible generalizations beyond a reproduction of the measured statistics.

In the Windatlas, a similarity theory was used directly to calculate the probability density function of the wind speed at a given height over a specified terrain. There are two important advantages of such a procedure: First, the measurements required are the surface pressure observations which are much less influenced by the local conditions than are the wind measurements; moreover, they are available from a large number of stations in the synoptic network. Second, wind observations are not used for the determination of the wind distributions. Therefore, the existing measurements of the wind can be used for validation of the procedure.

2.6. Similarity theory

The arguments leading to the establishment of the similarity relationships used in this study are treated in, for example, Tennekes & Lumley (1972), Eskinazi (1975), and will not be set forth here. With the assumption of barotropic conditions and equilibrium, the following expressions can be obtained for the geostrophic drag law, which gives a relation between the surface stress and the geostrophic wind:

$$\ln\left(Ro \cdot \frac{u_*}{G}\right) = B(\mu_o) + \left[-\frac{k^2}{(u_*/G)^2} - A^2(\mu_o)\right]^{\frac{1}{2}} \qquad (2.1)$$

$$\sin\alpha = - A(\mu_o) \cdot \frac{u_*}{kG} \qquad (2.2)$$

where

u_* = friction velocity ($u_*^2 \cdot \rho \equiv$ surface stress)
p = air density
Ro = surface Rossby number (G/fz_o)
f = Coriolis parameter ($1.21 \cdot 10^{-4} s^{-1}$ at 56^oN)
μ_o = stability parameter (see below)
k = von Karmans constant (0.4)
α = angle between the geostrophic wind and the wind near the surface
$A(\mu_o)$, $B(\mu_o)$ = empirical functions

If one assumes the A and B functions to be known, these relationships make it possible to determine u_* and α for a given value of the geostrophic wind G. Knowing u_*, the wind speed near the surface can be calculated from the following expressions:

$$\frac{V(z)}{u_*} = \frac{1}{k}\left(\ln\frac{z}{z_o} - \psi_1\left(\frac{z}{L}\right)\right) \qquad (2.3)$$

where

$\psi_1(\frac{z}{L})$ is an empirical function, and L is the Monin-Obukhov length which is a stability measure.

The two measures of stability μ_o and L are related by:

$$\mu_o = \frac{ku_*}{fL} \tag{2.4}$$

In addition to the geostrophic wind speed, it is also necessary to know L in order to be able to use the similarity expressions above. L can be determined from profile measurements of wind speed and temperature with the aid of Eq. (2.3) and the corresponding relation for the temperature profile given by:

$$\frac{\Delta\theta}{\theta_*} = .74\left(\ln \frac{z}{z_o} - \psi_2\left(\frac{z}{L}\right)\right) \tag{2.5}$$

where

$\Delta\theta = \Delta T + 0.01 \cdot \Delta z$ is the change in the potential temperature θ over the height Δz

$\psi_2(\frac{z}{L})$ is an empirical function

$L = -\frac{T_o u_*^2}{g\, k\theta_*}$ is the Monin-Obukhov length

T_o is the absolute temperature near the surface

$\theta_* u_*$ is a measure of the heat flux at the surface

The determination of L from the profile measurements of T(z) and V(z) and Eqs. (2.3), (2.5), and (2.6), requires an iterative process.

2.7. Determination of stability

There exist different possibilities for the determination of stability:

1) L can be calculated from profile measurements.
2) ΔT can be calculated from profile measurements, and the relations above can then be used iteratively together with the geostrophic wind G for the determination of u_* and L.
3) The wind speed measured at a particular height together with the temperature difference between two heights can be used for the calculation of a "bulk"-Richardson number defined as

$$Ri_B = \frac{g}{T} \frac{\Delta\theta \cdot z}{V^2} \qquad (2.7)$$

Equations (2.3), (2.5) and (2.6) can thereafter be used for the calculation of L.

4) μ_o can be determined with the help of profile measurements.

In the Windatlas it is assumed that a stability measure can be chosen which with sufficient accuracy in a statistical sense, can be regarded as being constant over Denmark. This assumption is necessary because the determination of stability requires long measurement series of wind and temperature from high meteorological masts, and the only such measurements available were those from the Risø mast. Because of this assumption, an important aspect of this investigation has been to evaluate the extent to which these measurements taken at a single location describe the conditions in the rest of the country. As mentioned above the wind speed is strongly influenced by the surrounding terrain's roughness; therefore, the different stability measures will to a varying extent be influenced by the local conditions. A thorough analysis of these conditions is quite complicated and lies outside the framework of the present investigation. Two important conditions make such an analysis less critical with regard to the Windatlas. In the first place, the primary interest is in moderate and high wind speeds for which near-

neutral conditions can be expected and the geostrophic wind is well-defined in both strength and direction. In the second place, the cause of the largest portion of the variation of stability at a given location is the daily and yearly variations which are essentially the same over the entire country.

Comparisons between the stability measured at the same time at meteorological masts placed in different parts of Denmark show that if the stability defined from $\Delta T/\Delta z$ is divided into three categories: unstable ($\Delta T/\Delta z < -1.5K/100$ m), neutral ($-1.5K/100$ m $< \Delta T/\Delta z < 1.5K/100$ m), and stable ($\Delta T/\Delta z > 1.5K/100$ m), situations where the stability is the same account for more than 70% of all observations when the wind speed at 40 m exceeded 4 ms^{-1}. Measurements made in the year 1976 from Margretheholm, Fredericia and Risø were used in this analysis. Margretheholm is situated at the coast of Øresund, and Fredericia in the eastern part of Jutland. The separation between the two sites is about 300 km. The stabilities for these sites calculated from a bulk-Richardson number also showed close agreement, although they were a few per cent smaller.

In the Windatlas the stability measurement has been chosen as the bulk-Richardson number measured at the Risø mast and defined as

$$Ri_B = \frac{g}{T_2} \frac{\Delta\theta \cdot (11\ m)}{V_{11}^2} , \qquad (2.8)$$

where T_2 is the absolute temperature measured at 2 meters height and $\Delta\theta$ is the difference in the potential temperature between 2 and 117 meters:

$$\Delta\theta = (T_{117} - T_2 + 1.15) \cdot \frac{11}{115} \qquad (2.9)$$

This definition of $\Delta\theta$ implies an artificial increase in the numerical value of the Monin-Obukhov length L in the calculations. This means that very stable and very unstable conditions are treated as being closer to neutral, while conditions close to neutral are unchanged. If instead a bulk-Richardson number

calculated over a larger height difference is used, unrealistic wind speeds result at heights over 50 m, especially under very stable conditions. This is because the validity of Eq. (2.3) in such situations does not extend to heights of more than 50 m at most. As an alternative to this method the profile expressions Eqs. (2.3) and (2.5) could be used for only low heights (for example 10 m) and the analysis completed as described below for that height alone. Empirical expressions would then be needed for the extrapolation of the statistical wind distribution to a suitable height.

2.8. Similarity functions

In order to use the relationships that are cited in the previous sections, it is necessary to have the empirical similarity functions established. The two functions ψ_1 and ψ_2 which occur in the profile relationships of Eqs. (2.3) and (2.5) are obtained by the integration of the flux-profile relations obtained from the 1968 Kansas experiment (Businger 1973, Paulson, 1970). The results are:

$$\psi_1\left(\frac{z}{L}\right) = \begin{cases} 2\ln[(1+x)/2] + \ln[(1+x^2)/2] - 2\tan^{-1}x + \frac{\pi}{2}; & L < 0 \\ -4.7\,\frac{z}{L} & L > 0 \end{cases}$$

$$\text{where } x = \left(1 - 15\,\frac{z}{L}\right)^{1/4} \qquad (2.10)$$

$$\psi_2\left(\frac{z}{L}\right) = \begin{cases} \ln[(1+y)/2] \quad \text{where } y = \left(1 - 9\,\frac{z}{L}\right)^{\frac{1}{2}}; & L < 0 \\ -6.4\,\frac{z}{L} & L > 0 \end{cases} \qquad (2.11)$$

Equations (2.3), (2.10) and (2.11) are used directly with u_* and L to derive V(z) at the five heights 10, 25, 50, 100, and 200 m. As mentioned above the Monin-Obukhov length is derived from the measured Richardson number. Formally this can be done by combining Eqs. (2.3) and (2.5) and solving the resulting

equation in L by an iterative process. The Windatlas uses instead a direct method based on series expansions in Ri_B (Louis, 1977).

The two similarity functions $A(\mu_o)$ and $B(\mu_o)$ which occur in the similarity relations, Eqs. (2.1) and (2.2), have been estimated by the use of a series of experiments. In the Windatlas the expressions used have been determined by a fitting of theoretically based asymptotic expressions to data taken in unstable and stable situations (Konstantinov and Dzkolov, 1977). When conditions are near neutral, these expressions cannot be used; therefore, in the Windatlas the functions have been combined with linear functions near the neutral state to get continuous functions of μ_o which are correct in the limit as $\mu_o \to 0$, i.e. the neutral state.

A number of values can be found in the literature for the function values at neutral; in the Windatlas the values $A(0) = 6$ and $B(0) = 2$ have been selected. The resulting expressions can be summarized as:

$$A(\mu_o) = \begin{cases} 28|\mu_o|^{-\frac{1}{2}} ; & \mu_o < -49 \\ 6 + 0.04\ \mu_o ; & -49 < \mu_o < 8.3 \\ 2.2\ \mu_o^{\frac{1}{2}} ; & 8.3 < \mu_o \end{cases} \qquad (2.12)$$

$$B(\mu_o) = \begin{cases} \ln(|\mu_o|) + 6\ |\mu_o|^{-\frac{1}{2}} ; & \mu_o < -10 \\ 4.2 - 0.22(10 + \mu_o) ; & -10 < \mu_o < 0 \\ 2 - 0.86 \cdot \mu_o ; & 0 < \mu_o < 10 \\ \ln(\mu_o) - 2.8 \cdot \mu_o^{\frac{1}{2}} ; & 10 < \mu_o \end{cases} \qquad (2.13)$$

In the literature a number of other expressions for the two functions appear. Unfortunately, none of them can be claimed to

have been sufficiently verified by experiments or supported sufficiently by an acceptable theory. In the experimental determinations of the two functions, simultaneous measurements of u_*, L and the geostrophic wind G have been used. The accuracy with which the functions can be determined is dependent on how precisely the measurements of these parameters can be estimated. A rough estimate of how the uncertainties in the parameters influence the determination of the two functions can be obtained by calculating the total differential from Eq. (2.1). Defining $x = \frac{u_*}{G}$, $B = B(\mu_o)$, $A = A(\mu_o)$, Eq. (2.1) can be written as

$$\ln(Ro \cdot x) - B - \sqrt{k^2 x^{-2} - A^2} = 0 \qquad (2.14)$$

from which it follows that

$$\frac{dx}{x} - dB + (k^2 x^{-2} - A^2)^{-\frac{1}{2}} \cdot (k^2 x^{-2} \frac{dx}{x} + AdA) = 0 \qquad (2.15)$$

For conditions near neutral, substitution of the appropriate function values yields:

$$15 \frac{dx}{x} - 2 \frac{dB}{B} + 3 \frac{dA}{A} = 0 \qquad (2.16)$$

Thus the error in the determination of A and B is at least five times larger than the error in the determination of x. On the other hand, if Eq. (2.1) can be taken as correct, the accuracy with which the shape of $A(\mu_o)$ and $B(\mu_o)$ are determined has a correspondingly smaller influence on the determination of u_*.

As mentioned earlier, the similarity theories build on the assumptions of equilibrium and a geostrophic wind which is constant with height. These conditions are not often found in the atmosphere. The assumption of equilibrium is especially problematic because the time needed for the boundary layer to reach equilibrium with the geostrophic wind is of the same order of magnitude as the time for changes caused by the daily variation in stability. This is especially true in situations with strong radiation cooling at night where the boundary layer scarcely

reaches equilibrium until the following day. Similarly, changes in the pressure field and thereby the geostrophic wind will often occur so quickly that a balance cannot be reached. Included here are nonstationarity, advective and isallobaric effects. It is possible to a certain extent to include these effects in the framework of similarity theory (Hasse, 1976), but this has not been attempted in the Windatlas.

The condition that the geostrophic wind is constant with height is called barotropy, and in situations where this is not true, baroclinic conditions prevail. Strong baroclinicity is attached to frontal zones and is most often transient. The baroclinic boundary layer has been treated in the framework of similarity theory in several papers (Hess, 1973, Romanov, 1977), but theory for such extensions is still incomplete. Simple physical arguments show that it is reasonable to assume that the geostrophic shear can be included by substituting for the geostrophic wind an appropriately chosen mean geostrophic wind in the boundary layer. The depth over which the mean value is averaged for the convective boundary layer must be the whole layer's depth (Arya and Wyngaard, 1975), while the depth in the neutral and stable boundary layer is dependent upon u_*.

As described in Chapter 4, a series of wind velocities at 1500 m height (determined from the radiosonde data from Copenhagen) was used together with the surface geostrophic wind to calculate the average geostrophic windshear (thermal wind) for a two year period. The purpose of this analysis was to investigate whether the physical model could be improved by a simple model for including the effect of the baroclinicity. For this period the model was used with an effective geostrophic wind G' defined as

$$G' = G + \frac{\partial G}{\partial z} \cdot \Delta \qquad (2.17)$$

where G is the geostrophic wind at Risø's location derived from the pressure analysis (Chapter 4), $\frac{\partial G}{\partial z}$ is the thermal wind and Δ may depend on u_*. For moderate and large values of u_* it was expected that a value of Δ could be determined which gave better correlation between calculated and observed wind speed than

that obtained by neglecting the influence of baroclinicity (i.e. $\Delta = 0$). Contrary to expectations, a comparison between observed and calculated wind speeds for Risø showed no significant improvement in the correlation. Therefore, the effect of baroclinicity is neglected in the analysis that forms the basis for the Windatlas. A reason for the lack of influence of baroclinicity in a statistical sense is that strong baroclinic situations are relatively rare and transient. There is no doubt, however, that if one wishes to use the similarity model for a prediction of the wind speed in isolated situations, baroclinicity must be taken into account. In such circumstances, it seems to be necessary to also include the effects that are mentioned above, since generally the effects of baroclinicity, advection, and non-stationarity cannot be seperated in the real atmosphere.

In the Windatlas the effect caused by the fact that the isobars are curved instead of straight has also been neglected. Taking the curvature into account would require the wind speed in the free atmosphere to be calculated by means of the so-called gradient wind, rather than the geostrophic wind. The effect of the curvature is discussed in Chapter 4, where it is seen to be proportional to the wind speed squared. Since the wind speed in the bottom half of the layer is considerably smaller than the geostrophic wind, the effect on the wind near the surface is substantially less than on the free wind.

2.9. Application of the physical model

The physical expressions which are the basis for the Windatlas have been described in the previous sections. How these expressions are to be used in the practical calculations is summarized below:

1) The magnitude G and the direction α_o of the geostrophic wind are determined from the pressure analysis (Chapter 4) for Risø's geographical position. In order to avoid analyses with large deviations between observed and analysed pressure fields, which apparently arise from erroneous obser-

vations, only those analyses are included where data from more than 25 stations are available and the standard deviation is less than 1 mb (see Chapter 4).

2) For each pressure analysis the Richardson number (at the corresponding time) is determined from the Risø mast data (section 2.8).
3) The stability parameter L is calculated for roughness z_o by using a direct calculation process based on the similarity expressions Eqs. (2.3) and (2.5).
4) The corresponding values of u_* and α are determined with an iterative process by using the similarity expressions Eqs. (2.1) and (2.2) along with the definition of μ_o, Eq. (2.4), and the similarity functions $A(\mu_o)$ and $B(\mu_o)$ specified by Eqs. (2.12) and (2.13).
5) The wind speed is determined at the desired height z by using the profile expression Eq. (2.3), the specified roughness z_o, and the calculated value of the friction velocity u_*. The direction of the wind is given by $D = \alpha_o - \alpha$.

The calculations described above are carried out consecutively for each observation period, eg. every third hour. From the results, the frequency distribution of the wind is constructed for the eight 45^o-direction sectors, centered around North, Northeast, East, etc. In these frequency distributions the wind speed is discretized in intervals of 1 m/s.

For each of the four roughness lengths chosen to characterize the four terrain types the calculations are performed for the five heights 10, 25, 50, 100, and 200 m. The Weibull distribution parameters (which is the desired result) are obtained from the frequency distributions by first estimating the parameters by the method of moments and then by using these estimates as starting values in an iterative process which determines the final parameters from a maximum - likeness criterion (Chapter 3).

The results of the calculations are shown in appendix A as curves giving the vertical variation of the Weibull parameters for every roughness class and direction sector.

3. THE STATISTICAL BASIS

3.1. Power density

The energy flux (power density) in a flow of air through an area at right angles to the earth's surface is given by

$$E(V) = \frac{1}{2} \text{ (mass per second per } m^2) (\text{speed})^2$$

$$= \frac{1}{2} \rho V^3 \ (kgs^{-3}) = \frac{1}{2} \rho V^3 \ (Wm^{-2}) \qquad (3.1)$$

where

$E(V)$ = power density at wind speed V (Wm^{-2})

ρ = density of air ($\cong$ 1.23 kgm^{-3})

V = horizontal wind speed (ms^{-1})

3.2. Averaging time

In Eq. (3.1) V is the instantaneous horizontal wind speed at a given point. In practical applications the wind speed will always be a measured quantity V_T which is created from V by averaging over the time interval T.

In choosing the correct averaging time for wind energy evaluations there are two important constraints that must be considered. Firstly, the averaging time must not be chosen too long because then the potential for wind power production will be underestimated. Secondly, the averaging time should not be chosen shorter than the averaging time applicable for experimental determination of the power curves of wind turbines.

With regard to the second constraint, a series of experiments that were carried out at the Gedser wind turbine in 1977-79 (Lundsager, Christensen, and Frandsen, 1979) showed that the

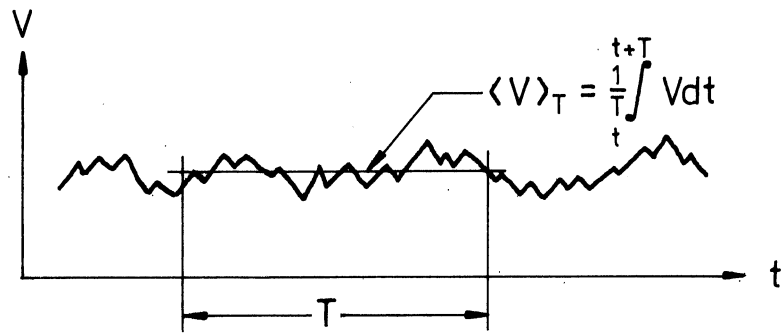

Fig. 3.1. Averaging V over the time interval T

turbine's power curve P(V) could not be unequivocally determined when the wind speed was averaged for less than one minute.

As mentioned in Chapter 1,the power curve of the wind turbine gives the energy it can produce at a given wind speed. If the turbine could make use of all the energy in the wind, the turbine's power curve would be identical to Eq. (3.1). In practice a wind turbine will, typically, only be able to use 20-30% of the available energy.

Figure (3.2) summarizes the results of the experiments on the Gedser wind turbine. While the results for an averaging time of two seconds show considerable scatter,those with an averaging time of ten minutes are well defined. It is also seen that the power curve is close to a straight line in contrast to the cubic variation of E(V), which is shown for comparison.

The results from the Gedser wind turbine demonstrate that the averaging time apparently should not be chosen shorter than of the order one minute.

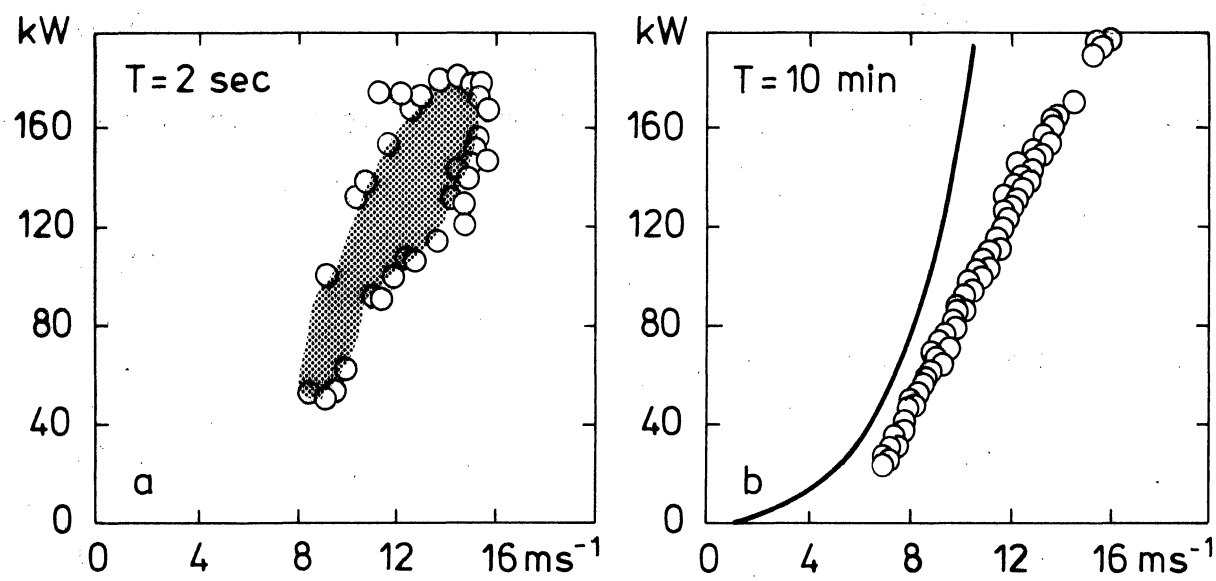

Fig. 3.2. Power curve of the Gedser wind turbine obtained with different averaging times (Lundsager, Christensen and Frandsen, 1979).

The implications of first constraint, i.e. the upper limit for the averaging time, can be illustrated by an analysis of Eq. (3.1).

From Eq. (3.1), the mean value of the power density of the wind can be represented as

$$\langle E \rangle_T = \langle \tfrac{1}{2} \rho V^3 \rangle_T \qquad (3.2)$$

where a parentheses $\langle \ \rangle_T$ around a quantity indicates a mean value obtained by averaging over time T

$$\langle V \rangle_T \equiv \frac{1}{T} \int_0^T V dt$$

In Eq. (3.2) the density of the air can be taken as constant over the range of conditions of interest here with an error of less than 5%. Hence Eq. (3.2) becomes

$$\langle E \rangle_T = \tfrac{1}{2}\rho \langle V^3 \rangle_T \tag{3.3}$$

The instantaneous wind speed can be written as a mean value plus a deviation

$$V = \langle V \rangle_T + V' \tag{3.4}$$

Straightforward operations give

$$\langle V' \rangle_T = 0 \tag{3.5}$$

$$\langle V'^2 \rangle_T = \langle V^2 \rangle_T - \langle V \rangle_T^2 \tag{3.6}$$

$$\langle V^3 \rangle_T = \langle V^3 \rangle_T + \langle V'^3 \rangle_T + 3\langle V'^2 \rangle_T \langle V \rangle_T \tag{3.7}$$

For the sake of clarity the following commonly used symbols are introduced:

$$\begin{aligned} M &= \langle V \rangle_T && \text{mean value} \\ S^2 &= \langle V'^2 \rangle_T && \text{variance} \\ \sqrt{\beta_1} &= \frac{\langle V'^3 \rangle_T}{S^3} && \text{skewness} \end{aligned} \tag{3.8}$$

Combining Eqs. (3.3), (3.7), and (3.8) yields

$$\langle E \rangle_T = \tfrac{1}{2}\rho M^3 \left(1 + 3\left(\frac{S}{M}\right)^2 + \sqrt{\beta_1}\left(\frac{S}{M}\right)^3\right) \tag{3.9}$$

The last two terms in the parenthesis in Eq. (3.9) represent the contribution to the average power density from the variance and skewness of the wind speed in the time interval considered. In the Table (3.1) the values for the right hand side of Eq. (3.9) are given for averaging times of 10 minutes and 10 years.

T	M ms^{-1}	$\sqrt{S^2}$ ms^{-1}	$\frac{\sqrt{S^2}}{M}$	$\sqrt{\beta}_1$
10 min*	5	0.5	0.1	0
10 år**	5	3	0.6	0.7

Table 3.1. Dependence of the mean value, variance, and skewness on averaging time.
* data: turbulence experiments
**data: Risø mast 1958-67

Substitution of the values given in Table (3.1) into Eq. (3.9) yields the following estimates for the average power density:

$$\begin{aligned} \langle E \rangle_{T=10\ \text{min}} &= (\tfrac{1}{2}\rho) \cdot 125 \cdot (1 + 3 \cdot 0.01 + 0) \\ \langle E \rangle_{T=10\ \text{years}} &= (\tfrac{1}{2}\rho) \cdot 125 \cdot (1 + 3 \cdot 0.36 + 0.7 \cdot 0.216) \end{aligned} \qquad (3.10)$$

Eq. (3.10) illustrates that the calculation of the mean power over a 10 minute interval only requires a knowledge of the corresponding 10 minute mean value of the wind because neglect of the higher terms only introduces an error of about 3 per cent. On the other hand, if the same procedure is followed for calculating the mean power over a 10 year period the error will be more than 100%. Thus for a reasonable estimate of the mean power density over a period typical of the lifetime of a wind turbine, it is crucial that the variance and the skewness be included in the calculations, and this can be achieved by using a long record of 10 minute averages of the horizontal wind speed.

To facilitate the understanding of the connection between averaging time and a reasonable estimate of the mean power, a typical form of the variance spectrum of the horizontal wind

speed is presented in fig. (3.3). The variance spectrum has the property that the area under it is proportional to the variance; moreover it shows how geophysical phenomena of differing time-scales contribute to the variance in the wind. The spectrum's horizontal axis is given in Hz (cycles per second) and the corresponding periods. The various contributing influences to the spectrum can be loosely grouped according to their periods and the geophysical phenomena responsible for them. For example, turbulence covers periods from a fraction of a second to hours, weather covers periods from hours to weeks, climate weeks to a half century, and climate fluctuations anything longer.

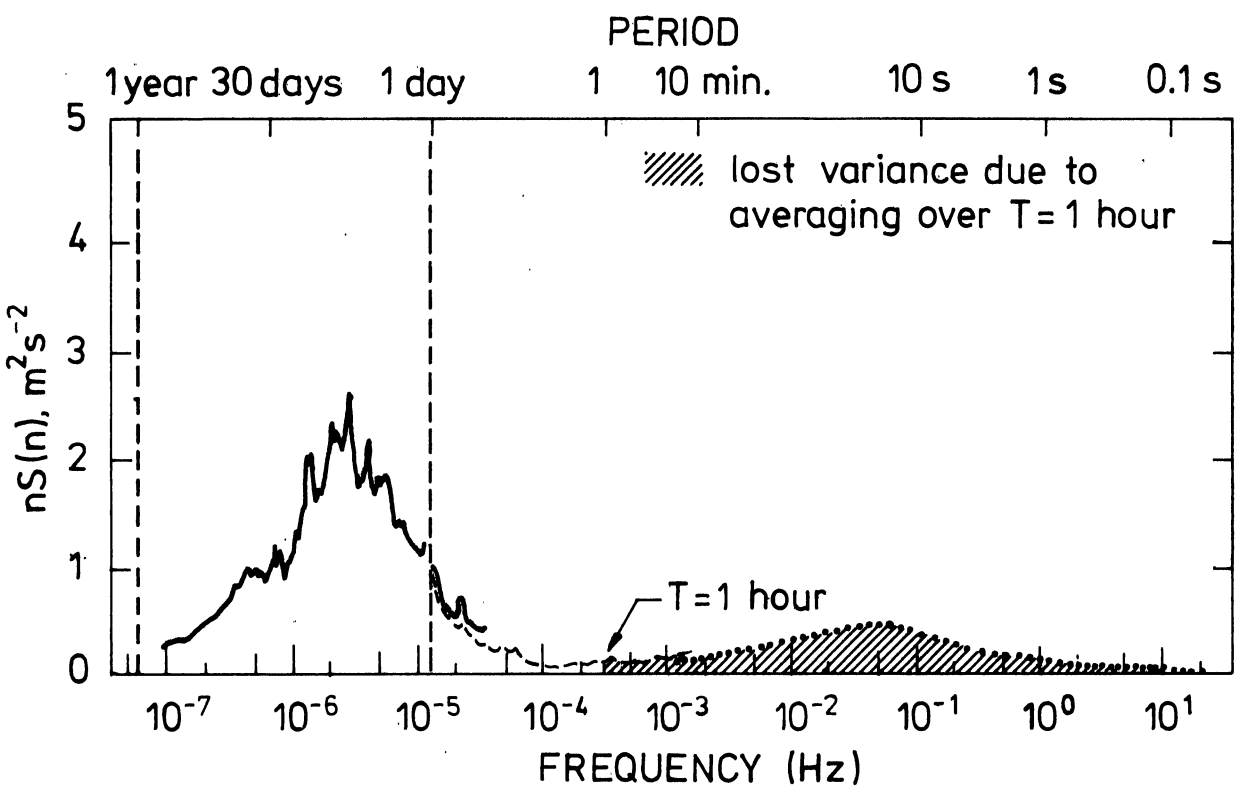

Fig. 3.3. Variance spectrum of the horizontal wind speed 6 meters over the terrain. The figure contains the results of many measurement series (Petersen, 1975).

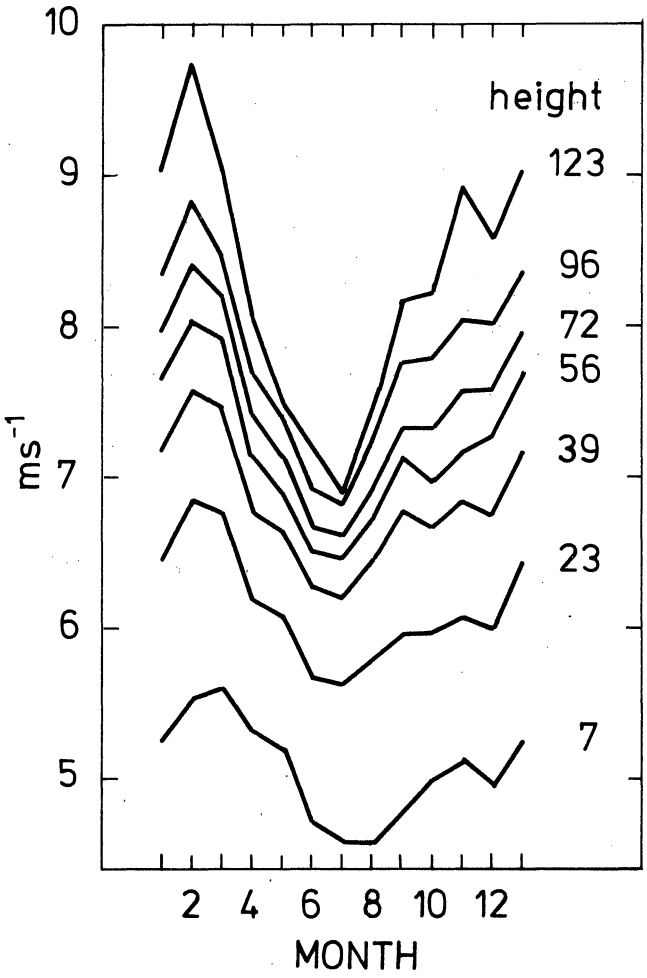

Fig. 3.4. The variation over the year of the monthly mean wind speeds as measured at Risø at seven heights in the period 1958-67 (Petersen, 1975).

The consequences of averaging the wind fluctuations over time T is that the portion of the variance for periods less than T is lost (i.e. the fluctuations of frequency higher than T^{-1} are averaged out). This is illustrated in fig. (3.3) for T=1 hour where the shaded area represents that portion of the variance which is lost. From the figure, it is clear that when the averaging time becomes more than a few hours, the variance loss begins to be of importance.

On fig. (3.3) are shown two dashed lines, which mark contributions to the spectrum from the daily and yearly variation of

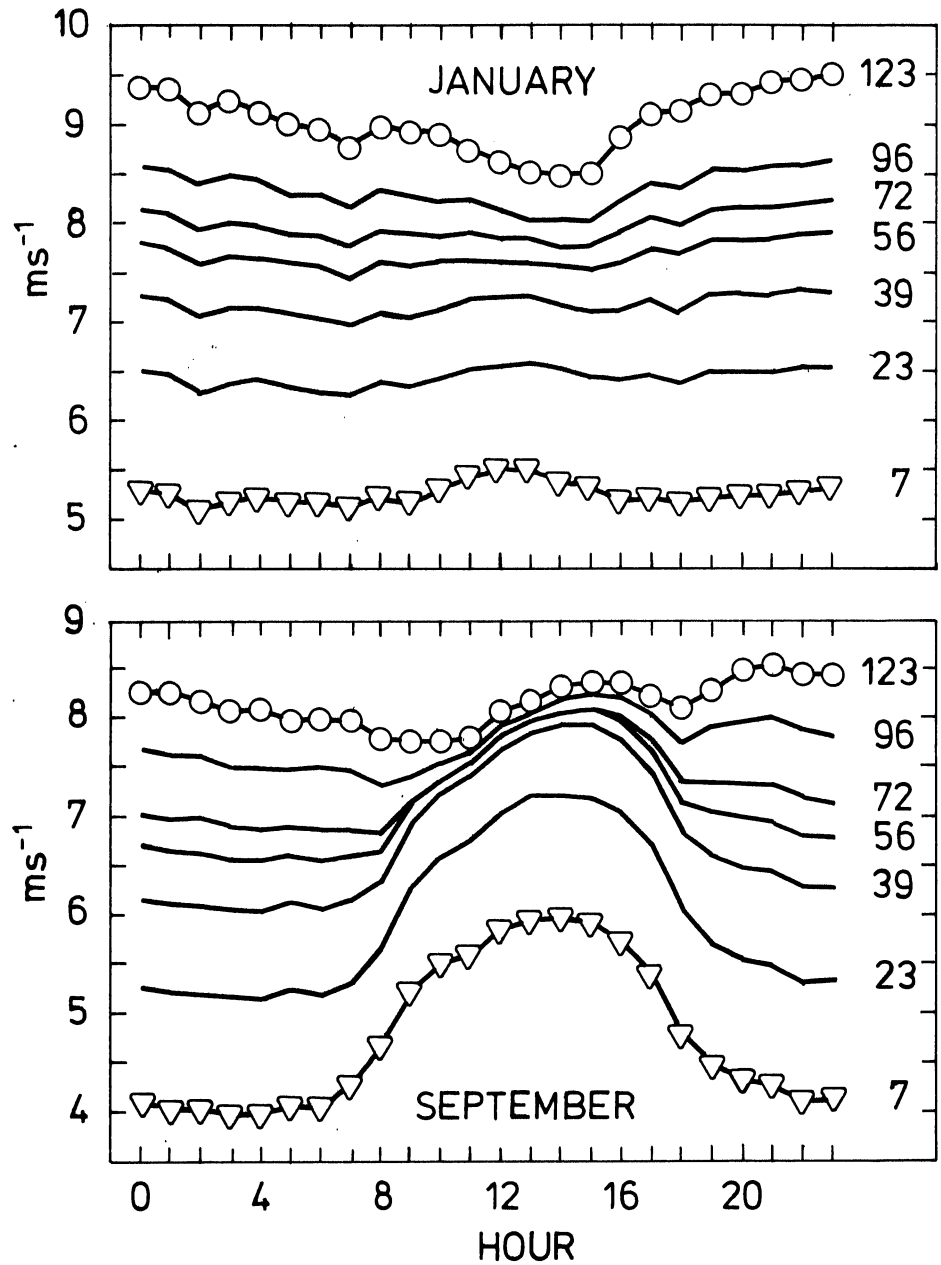

Fig. 3.5. The daily variation of the wind speed in the months January and September. On the individual curves are given the measurement heights. The measurement were made at Risø 1958-67 (Petersen, 1975).

the wind. These variations are described in Petersen (1975) and are illustrated by figs. (3.4) and (3.5). Note that the variations change with height over the terrain.

Finally it should be noted that wind speed statistics calculated by means of the Windatlas can be considered to pertain to averages over 10 minutes to one hour. This is fully satisfactory for wind energy purposes, because as was shown above fluctuations with periods less than 10 minutes to one hour only contribute approximately three percent of the total energy.

3.3. The probability density function

The mean energy production, <P>, for a wind turbine with power characteristic P(V) can be determined by

$$<P> = Pr_1 P(V_1) + Pr_2 P(V_2) + \cdots \qquad (3.11)$$

where the Pr's are weights that reflect the frequency of occurence of the wind speed in a given interval. Pr_1, for example, could be the fraction of time the wind speed is in the interval from 0 to 1 ms^{-1}, and $P(V_1)$ would be taken as the value of the power characteristic at the mid-point of this interval. Figure (3.6) illustrates the weighting function Pr; this function is usually called the histogram. The sum of Pr's is exactly 1 (or 100%).

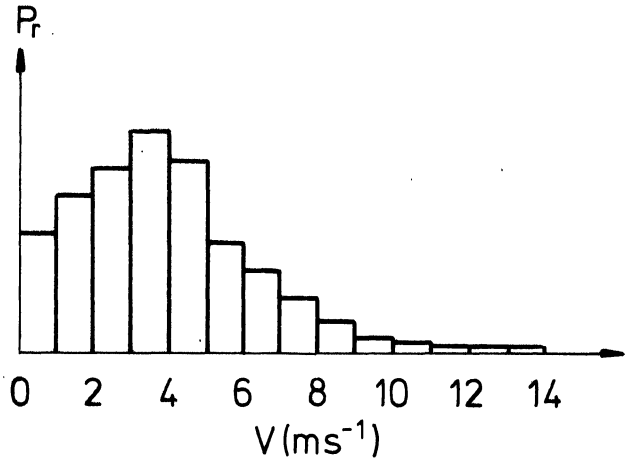

Fig. 3.6. Weighting function Pr. Histogram of wind speeds.

If the wind speed intervals are made smaller and smaller, then (under certain conditions) the histogram becomes a continuous function, the so-called probability density function. This function is sketched in fig. (3.7). The shaded area gives the probability that the wind speed lies in the interval of V to

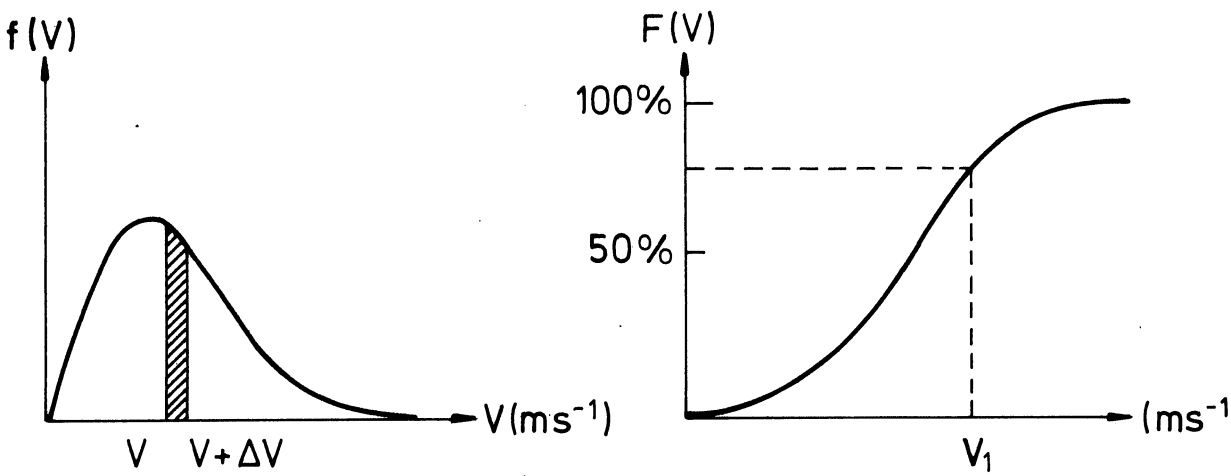

Fig. 3.7. Probability density function f(V) and accumulated probability density function F(V).

V + ΔV. Figure (3.6) also shows the accumulated probability density function F(V) which gives the probability of wind speeds less than V. The probability that the wind speed is larger than V is given by 1-F(V).

The relationship between f(V) and F(V) is

$$F(V) = \int_{o}^{V} f(V)\ dV \qquad (3.12)$$

The probability density function can be used to rewrite Eq. (3.11) as

$$\langle P \rangle = \int_0^\infty f(V)\,P(V)\,dV \qquad (3.13)$$

Equation (3.13) shows clearly why it is so essential for wind energy purposes to determine the probability density function of the wind speed. Not only can the mean energy production $\langle P \rangle$ be obtained, but also the form of the power curve $P(V)$ can be adapted to the form of $f(V)$, so that $\langle P \rangle$ becomes as large as possible, thus maximizing the wind turbine's output.

The first, second, and third moment of the wind speed can be directly calculated from the wind speed probability density function by the following:

$$\langle V^n \rangle = \int V^n f(V)\,dV \;,\; n = 1,2,3,... \qquad (3.14)$$

It follows that the mean energy density is given by

$$\langle E \rangle = \tfrac{1}{2}\rho \int_0^\infty V^3 f(V)\,dV \qquad (3.15)$$

The probability density function $f(V)$ can be obtained from measurements of the wind speed over an appropriate time span and with an suitable averaging time. As previously discussed the averaging time should be of the order of 10 minutes. The length of the measurement series depends upon the form of the power curve since this curve typically eliminates the influence of small wind speeds and damps the importance of the large wind speeds. This means that for wind energy purposes, shorter measurement series can be used than are normally required for general wind climatological investigations.

Usually there will not exist a measurement series of wind speeds at the location where one wishes to place a wind turbine, and most certainly not at the relevant height over the terrain - the hub height. As already mentioned in Chapter 2, the method that is used in the Windatlas for the determination of the probability density function $f(V)$ at a given location and height builds on the fact that the measured wind speeds almost always

follow a Weibull-distribution. This special distribution is described in detail in the following section.

3.4. The Weibull distribution

The Weibull distribution is expressed mathematically as

$$f(V) = aCV^{C-1} \exp(-aV^{C}) \qquad (3.16)$$

where

$$V \geq 0, \quad a > 0, \quad C > 0,$$

and where C is called the shape parameter and $a^{-1/C}$ is a scaling parameter that is represented in the Windatlas by the letter A. The influence of the shape parameter on the shape of f(V) is illustrated in fig. 3.8. For $C > 1$ the function has a maximum away from the origin, while for $C \leq 1$ it is monotonically decreasing. For $C = 1$ the distribution is exponential, $C = 2$ gives the Rayleigh distribution and $C = 3.5$ gives an approximation to the normal distribution (Gaussian distribution). The distributions found in the Windatlas have a C value between 1.5 and 2.6 and the value is often close to 2.0.

The accumulated Weibull distribution F(V) which gives the probability of having a wind speed equal to or less than V is obtained by integrating Eq. (3.16) with the result:

$$F(V) = 1 - \exp(-aV^{C}) \qquad (3.17)$$

A special consequence of the Weibull distribution is that if V is Weibull-distributed, so is V^{m}. This can be seen as follows:

Let V be Weibull-distributed with parameters a and C, and let g(Y) represent the distribution function of $Y = V^{m}$. Since the probability that Y is in the interval Y + dY is g(Y)dY and since this must be the same as f(V)dV, it follows that

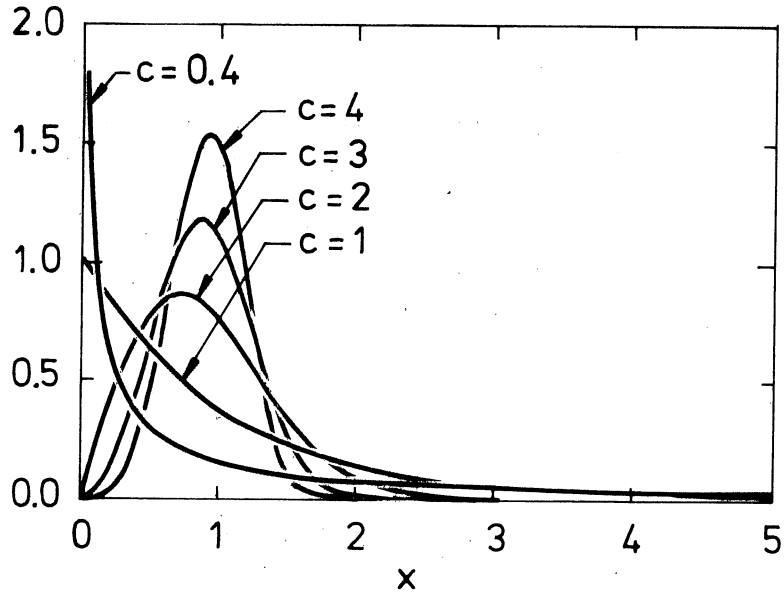

Fig. 3.8. The importance of the shape parameter C for the shape of the Weibull distribution.

$$g(Y) = f(V)\frac{dV}{dY} = f(Y^{\frac{1}{m}})\frac{d}{dY}(Y^{\frac{1}{m}})$$

$$= f(Y^{\frac{1}{m}})\frac{1}{m}Y^{\frac{1}{m}-1} \qquad (3.18)$$

$$= aC(Y^{\frac{1}{m}})^{C-1}\exp(-a(Y^{\frac{1}{m}})^{C})\frac{1}{m}Y^{\frac{1}{m}-1}$$

$$= a\frac{C}{m}Y^{\frac{C}{m}-1}\exp(-aY^{\frac{C}{m}}) .$$

A comparison with Eq. (3.16) shows that $Y = V^m$ is Weibull-distributed with parameters:

$$a_m = a$$

$$C_m = \frac{C}{m} \qquad (3.19)$$

and has the following accumulated distribution function

$$F_m(Y) = 1 - \exp(-aY^{\frac{C}{m}}) \quad . \tag{3.20}$$

It follows from the definition of the mean value that

$$\langle V^m \rangle = \int g(Y)\, Y dY$$

which can be calculated to be

$$\langle V^m \rangle = (\frac{1}{a})^{\frac{m}{C}} \Gamma(1 + \frac{m}{C}) \tag{3.21}$$

where $\Gamma(x)$ is the gamma function defined by

$$\Gamma(x) = \int_0^\infty \xi^{x-1} \exp(-\xi) d\xi \tag{3.22}$$

and where $\Gamma(x+1) = x\Gamma(x)$ and $\Gamma(n) = (n-1)!$ where x is real and n is a positive integer.

The variance of V^m is given by

$$\langle (V^m - \langle V^m \rangle)^2 \rangle = (\frac{1}{a})^{\frac{2m}{C}} (\Gamma(1 + \frac{2m}{C}) - \Gamma^2(1 + \frac{m}{C})) \tag{3.23}$$

The mean value and variance of V are obtained from Eqs. (3.21) and (3.23) by setting m = 1:

$$\langle V \rangle = (\frac{1}{a})^{\frac{1}{C}} \Gamma(1 + \frac{1}{C})$$

$$\langle (V - \langle V \rangle)^2 \rangle = (\frac{1}{a})^{\frac{2}{C}} (\Gamma(1 + \frac{2}{C}) - \Gamma^2(1 + \frac{1}{C})) \tag{3.24}$$

Similarly $\langle V^2 \rangle$ can be obtained by setting m = 2 in Eq. (3.21) with the result

$$\langle V^2 \rangle = (\frac{1}{a})^{\frac{2}{C}} \Gamma(1 + \frac{2}{C}) \tag{3.25}$$

The mean energy density, given by Eq. (3.2) as

$$\langle E \rangle = \tfrac{1}{2}\rho \langle V^3 \rangle$$

can be readily obtained from Eq. (3.21) with m = 3 as

$$\langle E \rangle = \tfrac{1}{2}\rho \left(\frac{1}{a}\right)^{\frac{3}{C}} \Gamma\left(1 + \frac{3}{C}\right) \qquad (3.26)$$

Similarly, the variance of E can be obtained from Eq. (3.23) by setting m = 3.

Another example is the distribution of $Y = V^{-1}$ where Eqs. (3.18) and (3.19) with m = -1 give:

$$f(Y) = aC(Y)^{-C-1} \exp(-aY^{-C}) \ .$$

This distribution has some applications for air pollution studies.

For the use in Chapter 6 some of the most important statistical quantities of the Weibull-distributed variable V are listed below with the scale parameter inserted.

Accumulated distribution	$1 - \exp\left(-\left(\frac{V}{A}\right)^C\right)$
Mean value	$A\Gamma\left(1 + \frac{1}{C}\right)$
Variance	$A^2\left(\Gamma\left(1 + \frac{2}{C}\right) - \Gamma^2\left(1 + \frac{1}{C}\right)\right)$
Mean square	$A^2\Gamma\left(1 + \frac{2}{C}\right)$ (3.27)
Modal value	$A\left(\frac{C-1}{C}\right)^{\frac{1}{C}}$
Median value	$A(\ln 2)^{\frac{1}{C}}$

$V^m \cdot f(V)$ has its maximum for V equal to $A\left(\frac{C-1+m}{C}\right)^{\frac{1}{C}}$

3.5. Determination of the Weibull parameters

The determination of those values of the shape and scale parameters which give the best fit to a given set of observations (V_1, V_2, ... , V_n) has in this investigation been performed by means of moment estimates and the use of maximum likelihood and maximum likeness criteria. These concepts are briefly described in this section.

3.5.1. Maximum likelihood

If the V's are assumed to be independent and Weibull-distributed, the probability density function for the observation set is given by the product

$$\prod_{i=1}^{n} aCV_i^{C-1} \exp(-aV_i^C) \qquad (3.28)$$

If the individual observations V_1, ..., V_n are substituted into Eq. (3.28), a quantity L(a,C) is obtained which is a function of a and C. It is intuitively clear that a and C should be choosen so that L(a,C) becomes as large as possible. Maximizing L in this manner achieves "the maximum likelihood" that the observations are Weibull-distributed with parameters a and C.

To avoid the complexities arising in directly maximizing L(a,C), it is more convenient to maximize ln(L(a,C)); that is

$$L(a,C) = a^n C^n \prod V_i^{C-1} e^{-a\Sigma V_i^C}$$

$$\ln L(a,C) = n\ln a + n\ln C + (C-1)\Sigma \ln V_i - a\Sigma V_i^C$$

The maximum of ln(L(a,C)) is unambiguously determined when a and C are choosen to satisfy the equations

$$\frac{d\ln(L(a,C))}{da} = \frac{d\ln(L(a,C))}{dc} = 0$$

Carrying out the differentation yields

$$\frac{n}{a} - a\Sigma V_i^C = 0$$

$$\frac{n}{C} + \Sigma \ln V_i - a\Sigma(\ln V_i)V_i^C = 0 \qquad (3.29)$$

3.5.2. Maximum likeness

The maximum likelihood method described above uses the individual observations in a measurement series for the determination of a and C (cf. Eq. (3.29)). Another method is to group the data first in order to obtain a histogram and thereafter choose a and C so that the corresponding Weibull distribution has the best possible agreement with the histogram. For this a "maximum likeness" criterion (Barndorff-Nielsen, 1977) can be applied. This criterion requires choosing the values of a and C to maximize the expression

$$\sum \hat{Pr}_i \ln Pr_i(a,C) \qquad (3.30)$$

where $Pr_i(a,C)$ is the theoretical probability density in the i'th interval, and $\hat{Pr}_i$ is the corresponding probability density derived from the observations. Unlike the maximum likelihood method, the maximum likeness method does not assume that the observations are independent. If the observations are independent the two criteria yield the same result.

It can be shown that maximizing Eq. (3.30) corresponds to minimizing

$$\sum Pr_i \ln \frac{\hat{Pr}_i}{Pr_i(a,C)} \qquad (3.31)$$

The determination of maximum likelihood and likeness estimates for a and C are carried out numerically on a computer using an iterative algorithm. The calculations are initiated by making a guess for a and C. This guess is often based on estimates of the moments.

3.5.3. Estimates of the moments

The mean and mean square values in the Weibull distribution are given by Eqs. (3.24) and (3.25) as:

$$\langle V \rangle = \left(\frac{1}{a}\right)^{\frac{1}{C}} \Gamma\left(1 + \frac{1}{C}\right)$$

$$\langle V^2 \rangle = \left(\frac{1}{a}\right)^{\frac{2}{C}} \Gamma\left(1 + \frac{2}{C}\right)$$

Defining

$$x_1(C) = \Gamma\left(1 + \frac{2}{C}\right)\Gamma^{-2}\left(1 + \frac{1}{C}\right)$$

$$x_2(C) = \Gamma\left(1 + \frac{1}{C}\right)\Gamma^{-1}\left(1 + \frac{2}{C}\right) \qquad (3.32)$$

leads immediately to the following equations for a and C:

$$x_1(C) = \frac{\langle V^2 \rangle}{\langle V \rangle^2}$$

$$\left(\frac{1}{a}\right)^{\frac{1}{C}} = \frac{\langle V^2 \rangle}{\langle V \rangle} x_2(C) \qquad (3.33)$$

The moment estimates for $\langle V \rangle$ and $\langle V^2 \rangle$ are calculated from the set of observations by

$$\langle V \rangle = \frac{1}{N} \sum V_i$$

$$\langle V^2 \rangle = \frac{1}{N} \sum V_i^2$$

Use of these estimates in Eq. (3.33) yields a set of equations which can easily be solved iteratively to obtain "moment estimates" for a and C.

3.5.4. Calculation procedure in the Windatlas

In the practical calculations the moment estimates were calculated first. From these the starting values for maximum likeness parameters were chosen and an iterative solution was

initiated. The iterative procedure was stopped when the relative change of the parameters became less than 1%.

In the construction of the Windatlas, visual comparison of the observed and calculated distributions has been important. A physical explanation for the difference between them has been sought, both by a closer study of the observation material and by varying the parameters in the physical model. There has, therefore, not been any significant need for using statistical criteria for the agreement between the observed and calculated distributions.

3.6. Extreme values

For the purpose of wind energy production the probability of extreme high winds is only of secondary concern. Therefore, whether the calculated distributions are reliable for very high wind speeds has not been investigated in the Windatlas; however, the comparisons between calculated and measured distributions given in Chapter 6 show very good agreement for all wind speeds. Nonetheless, the extreme wind speed probabilities calculated by means of the Windatlas should be used only with great caution for two reasons: Firstly, the physical model which forms the basis for the Windatlas can only be expected to produce reliable wind speeds outside the extreme range; secondly, from a statistical point of view, the variance of the extreme values will be so large that it itself strongly limits their applications.

For the sake of completeness it should be noted that the Weibull distribution belongs to the class of "the asymptotic extreme-value distributions" (Gumbel, 1958).

4. THE PRESSURE ANALYSIS AND THE DETERMINATION OF THE GEOSTROPHIC WIND

4.1. The pressure analysis

The geostrophic wind can be calculated directly from a set of pressure measurements. This procedure is, however, not without complications. This is because the pressure measurements are encumbered with errors which impair the determination of the pressure gradients. Furthermore, this procedure can only give point values of the geostrophic wind.

In order to partially eliminate errors in the pressure measurements and to make possible the determination of the geostrophic wind at an arbitrary point, a third order polynomial surface has been fitted to the pressure values. The geostrophic wind is then readily determined from the surface gradient. The fitting of the third order surface was accomplished by using the method of least squares.

4.1.1. The synoptic stations used

The pressure analysis was performed for the years 1965-77 and was based on the pressure measurements taken every third hour in Denmark and the neighbouring countries. The stations used are shown in fig. 4.1. Since some of the stations either did not exist or did not measure for the whole period, the same stations do not always appear in the analyses for the various years. A list of those stations which do not appear in all the analyses is provided in Table 4.1.

4.1.2. The coordinate system

Since the analysed area is only of limited extent, it can be regarded as a plane, thereby simplifying the calculations. The area has been mapped using a polar sterographic projection at 56^{o}N. Coordinates are located within a Cartesian system whose

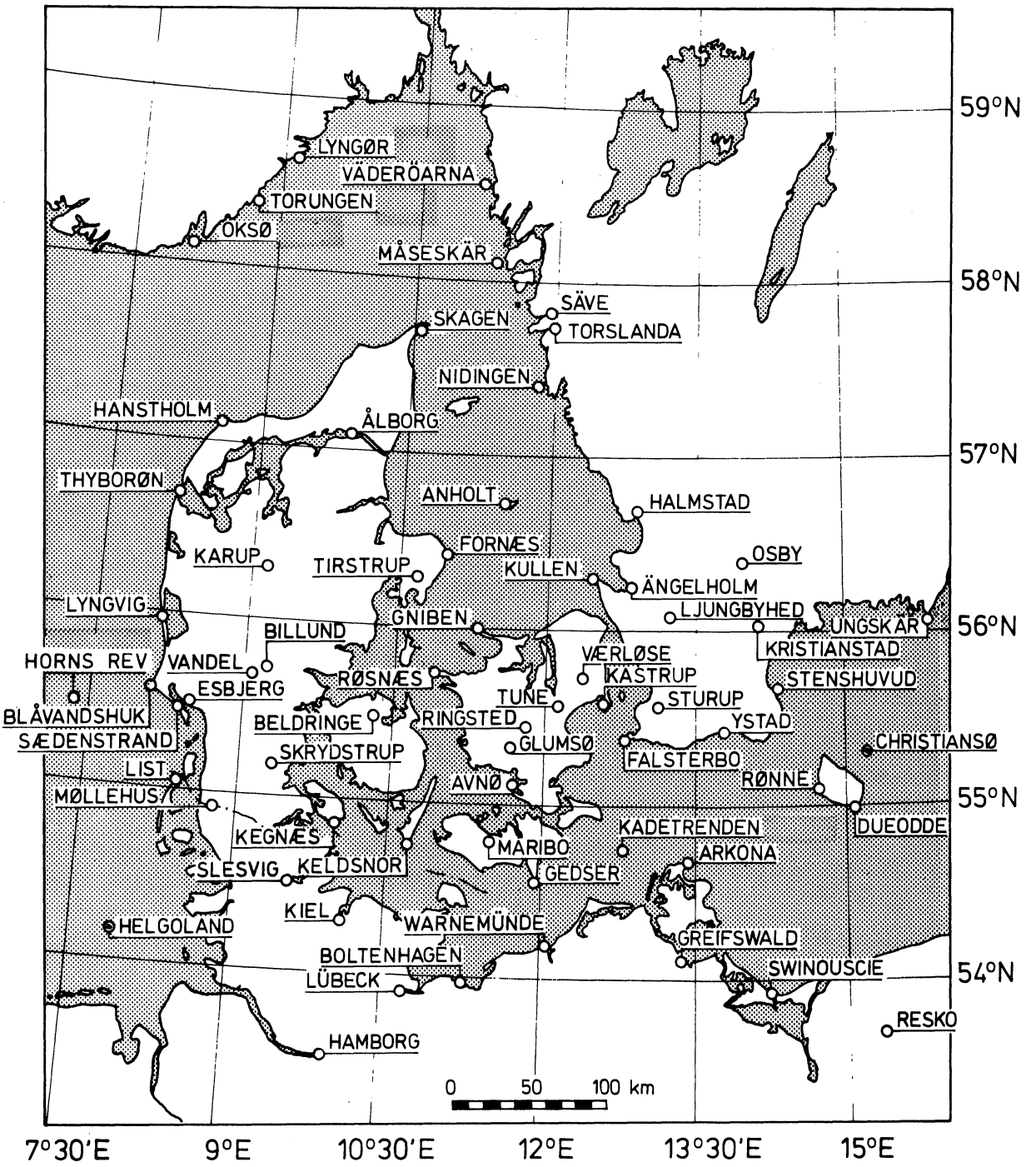

Fig. 4.1. Location of the synoptic stations used.

Anholt	1965, 1967-77
Blåvandshuk	1965-68
Sædenstrand	1968-77
Billund	1971-77
Horns Rev fyrskib	1969-77
Møllehus	1969-74
Maribo	1973-77
Kadetrenden fyrskib	1968-77
Gedser	1965-68
Glumsø	1972-77
Ringsted	1965-71
Tune	1973-77
Väderöarna	1966-77
Nidingen	1969-77
Ängelholm	1970-77
Sturup	1965-66, 1973-77
Stenshuvud	1972-77
Helgoland	1965-72
List	1965-72
Slesvig	1965-72
Kiel	1965-72
Hamborg	1965-72
Lübeck	1965-72
Arkona	1967-77
Boltenhagen	1967-77
Warnemünde	1967-77
Greifswald	1967-77
Swinoujscie	1966-77
Resko	1966-77

Table 4.1. List of the stations where the pressure data has only been used for a portion of the analysed period, along with information about the time periods they were used. All other stations were used for the entire period 1965-77.

origin is at (56^{o}N, 10^{o}E), the z-axis is normal to the surface and the y-axis is directed to the North.

If $\begin{pmatrix} dsx \\ dsy \end{pmatrix}$ is a line element on a sphere it will be mapped by a polar stereographic projection onto a line element in the plane $\begin{pmatrix} dx \\ dy \end{pmatrix}$ given by

$$\begin{Bmatrix} dx \\ dy \end{Bmatrix} = \frac{1+\sin\phi_o}{1+\sin\phi} \begin{Bmatrix} \cos(\lambda-\lambda_o) & -\sin(\lambda-\lambda_o) \\ \sin(\lambda-\lambda_o) & \cos(\lambda-\lambda_o) \end{Bmatrix} \begin{Bmatrix} dsx \\ dsu \end{Bmatrix} \qquad (4.1)$$

The mapping is therefore not isometric; the degree of stretching is given by

$$A(\phi) \equiv \frac{1+\sin\phi_o}{1+\sin\phi}$$

In the observed area ϕ varies approximately between 54^{o}N and 58^{o}N from which it follows that $A(\phi)$ varies between 0.99 and 1.01. The error which arises in the gradient calculation on the projected plane is thus about 1%, and is therefore negligible.

4.1.3. The objective analysis

In order to objectively analyze the pressure measured at different points, it is desirable to fit the observations with an empirical expression which describes the variation of the pressure field in space. The method which will be employed here treats the pressure field as a surface which is given by an n^{th} order polynomial; in particular,

$$p_a(x,y) = \sum_{j=0}^{n} \sum_{k=0}^{(n-j)} \beta_{jk} x^j y^k \ , \qquad (4.2)$$

In the analysis which follows, the coefficients β_{jk} will be determined by fitting Eq. (4.2) to the measured pressures at their appropriate locations as described above.

In general, the number of coefficients which must be determined is given by:

$$\sum_{\ell=0}^{n} (1+(n-\ell)) = \frac{(n+1)(n+2)}{2}$$

In the Windatlas a third order surface is employed; therefore ten coefficients must be determined. Hence at least ten measurement points are necessary. If there are exactly ten, the surface determined by Eq. (4.2) will be in perfect agreement with the measurements at the measuring sites. Because of measurement errors, however, it is necessary to provide some smoothing. If the system is overdetermined (that is to say there are more then ten measuring points), a smoothing can be obtained by determining the coefficients $\beta_{j_o k_o}$ so that the square of the deviation between the empirical surface and the measured values is minimized. If $p(x_i,y_i)$ is the measured pressure at station i which has coordinates (x_i,y_i), the mean square deviation S^2 is given by

$$NS^2 = \sum_{i=1}^{N} (p_a(x_i,y_i) - p(x_i,y_i))^2 , \qquad (4.3)$$

where N is the number of stations. The coefficients $\beta_{j_o k_o}$ are obtained by the conditions

$$\frac{\partial S^2}{\partial \beta_{j_o k_o}} = 0 \qquad (4.4)$$

Equations (4.3) and (4.4) can be combined to yield

$$\sum_{i=1}^{N} \frac{\partial p_a(x_i,y_i)}{\partial \beta_{j_o k_o}} (p_a(x_i,y_i) - p(x_i,y_i)) = 0 .$$

This can be applied to Eq. (4.2); for n=3 the result is

$$\sum_{i=1}^{N} x_i^{j_o} y_i^{k_o} \cdot p_a(x_i,y_i) = \sum_{i=1}^{N} p(x_i,y_i) x_i^{j_o} y_i^{k_o} \qquad (4.5)$$

Again using Eq. (4.2) for p_a, and changing the order of summation in Eq. (4.5) yields the following equation for the determination of the coefficients

$$\sum_{j=o}^{3}\sum_{k=0}^{(3-j)}\left(\sum_{i=1}^{N} x_i^{(j_o+j)}\cdot y_i^{(k_o+k)}\right)\cdot\beta_{jk} = \sum_{i=1}^{N} x_i^{j_o}\, y_i^{k_o}\, p(x_i,y_i) \tag{4.6}$$

Since both j_o and k_o can vary in Eq. (4.6) a system of equations appears which is most efficiently expressed in matrix notation:

$$A_{rs}\cdot X_s = P_s \tag{4.7}$$

where r and s are defined as

$$r = j_o + j_o\cdot k_o \;;\quad s = j + j\cdot k.$$

$\underline{\underline{A}}$ is a 10 x 10 matrix with elements of the form $\Sigma\, x_i^{(j_o+j)}\cdot y_i^{(k_o+k)}$, and it depends only on the number and the position of the stations. In the following this matrix will be called the station matrix. The unknown coefficients $\beta_{j_ok_o}$ are contained in the vector X_s; the vector P_s contains the input data from the measured pressures in the following form

$$\sum_{i=1}^{N} x_i^{j_o}\, y_i^{k_o}\, p(x_i,y_i)\ .$$

The system of equations given by Eq. (4.7) can be solved by standard methods to yield the expansion coefficients $\beta_{j_ok_o}$ directly.

4.2. The calculation procedure for the pressure analysis

Because of missing observations the pressure measurements from the individual stations do not always constitute an unbroken data series. Since a large number of stations were used (on the average 55), the probability for exactly same set of stations appearing in two consecutive calculations was rather small. This means that a new calculation of the station matrix would be required for each observation period. If such a procedure had been followed the calculation of the coefficients in the station matrix would have been quite time consuming.

To avoid the necessity for recalculating the station matrix for each observation period a fixed station matrix was chosen for each year, and the missing data were reconstructed by interpolation in time or space. This method has the additional advantage that at any particular time there will not be any large areas which are not covered by stations. Had such been the case the polynomial would be unconstrained in these regions and the approximated pressure could differ greatly from the true pressure.

4.2.1. Reconstruction of data

In order to reconstruct missing data, it was necessary to constantly operate with three time levels, $t-\Delta t$, t and $t+\Delta t$, where Δt = 3 hours. The synoptic observations also include the pressure tendency $\Delta p(t)$ defined as the pressure change in the last three hours, i.e. $\Delta p(t) = p(t) - p(t-\Delta t)$. If it is assumed that the pressure $p_i(t)$ at station i is missing at time t, this value can then be reconstructed or approximated through any of the following procedures:

1. If $p_i(t+\Delta t)$ and $\Delta p_i(t+\Delta t)$ exist then

$$p_i(t) = p_i(t+\Delta t) - \Delta p_i(t+\Delta t) \ ,$$

2. If $p_i(t-\Delta t)$ and $\Delta p_i(t)$ exist then

$$p_i(t) = p_i(t-\Delta t) + \Delta p_i(t) \ ,$$

3. If $p_i(t-\Delta t)$ and $p_i(t+\Delta t)$ exist then

$$p_i(t) = 0.5 \cdot (p_i(t-\Delta t) + p_i(t+\Delta t)) \ ,$$

4. $$p_i(t) = p_{a,i}(t-\Delta t) \ ,$$

where $p_{a,i}$ is the pressure at station i determined from the 3rd order polynomial surface.

In a situation with large pressure changes the last approximation can be quite rough. However, because of the large number of stations, the error will not affect the determination of the approximating polynomial to an appreciable degree; moreover, the error will be eliminated by subsequent error filtering.

4.2.2. Elimination of errors

In order to remove the influence of errors in the input data (i.e. both measured and reconstructed pressure values), it is required that the condition $|p_i(t) - p_{a,i}(t)| \leq 2$ mb be satisfied. The value 2 mb was a compromise between measurement errors of the order of 1 mb on the one hand, and sporadic reporting errors, characteristically 5 or 10 mb. If this condition is not satisfied, the value is replaced by the value of the approximating polynomial, and the approximating 3rd order polynomial is thereafter re-calculated.

4.3. Evaluation of the analysis method

For each approximation, the mean square deviation between the approximated and the measured values was determined. This is expressed by

$$S^2 = \frac{1}{N} \sum_{i=1}^{N} (p_i - p_{a,i})^2 \qquad (4.9)$$

Using $\Delta p_i \equiv p_i - p_{a,i}$ and the fact that the average value of Δp_i is zero, S^2 is seen to be the variance of Δp_i.

If it is assumed that the Δp_i are mutually independent, and that Δp_i has a normal distribution with variance σ^2, then $NS^2\sigma^{-2}$ is χ^2-distributed with N-1 degrees of freedom. The mean value of $NS^2\sigma^{-2}$ is therefore (N-1), from which follows that $\sigma^2 = \frac{N}{N-1} \langle S^2 \rangle$. The value of $\langle S^2 \rangle$ has been determined as 0.29 from the data; therefore the standard deviation σ for the distribution of Δp_i is 0.5 mb since N was approximately 50.

In order to investigate whether the Δp_i are in fact normally distributed, the χ^2-distribution for $NS^2\sigma^{-2}$ with N = 48 (the smallest number of stations used) has been compared with the actual distribution for S^2. These are plotted together in fig. 4.2. It is clear that the distribution of S^2 does not correspond closely to a χ^2-distribution. This is a consequence of the fact that that the Δp_i cannot be attributed entirely to measurement errors. Contributions to Δp_i can also be attributed to the inability of a 3rd order surface to adequately describe the true pressure field in certain circumstances.

Since the χ^2-distribution is practically symmetric because of the large number of degrees of freedom, the frequency of the situations where the 3rd order polynomial cannot approximate the pressure field sufficiently accurately, can be estimated from fig. 4.2. This is found to represent 10% of all the situations.

These situations appear in connection with the passage of fronts where a first order discontinuity exists in the pressure distribution because of air mass differences. This can only be approximately described by a third order surface, and therefore gives rise to larger standard deviations than those which arise from measurement errors.

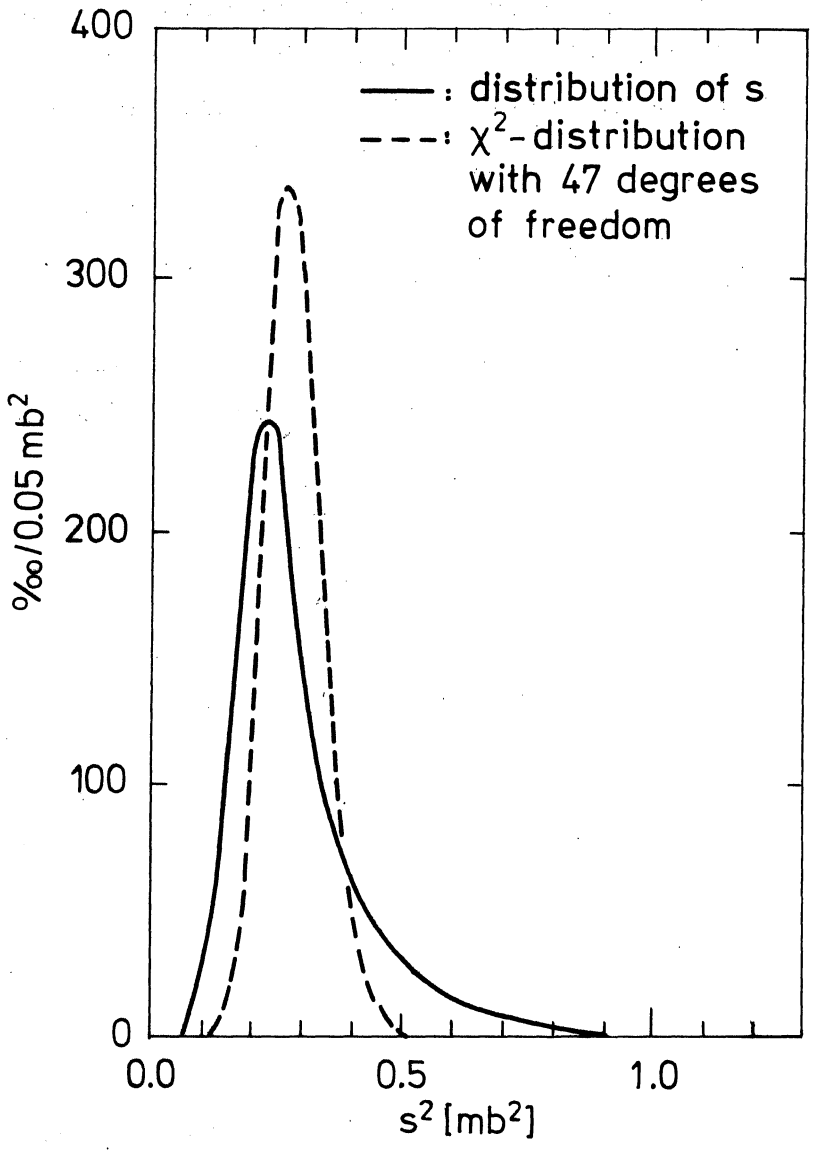

Fig. 4.2. The distribution of S^2 and a χ^2-distribution with 47 degrees of freedom.

For the majority of situations, the standard deviation in the analysis is in agreement with that which might be expected from measurement errors. The inaccuracy which arises in the determination of the geostrophic wind as a result of both types of errors will be more closely considered in the next section.

4.4. The geostrophic wind

Horizontal motions influenced only by the Coriolis force and the pressure gradient are governed by the following equations for the horizontal acceleration (see for example Haltiner and Martin, 1957),

$$\frac{d\vec{V}}{dt}\Big|_H = -\frac{1}{\rho}\vec{\nabla}_H p - f\vec{k}\times\vec{V}, \tag{4.10}$$

where $\vec{V}$ is the horizontal wind vector, ρ is the air density, $\vec{k}$ is a unit vector in the z direction, and f is the Coriolis parameter defined by

$$f = 2\Omega\sin\phi,$$

where Ω is the earth's angular speed of rotation, and ϕ is the latitude. The friction terms have been neglected in Eq. (4.10); therefore, the solutions are only valid in the friction-free zone away from the planetary boundary layer. The geostrophic wind $\vec{G}$ is defined to be the solution to Eq. (4.10) with $\frac{d\vec{V}}{dt}\Big|_H = 0$, and is given by

$$\vec{G} = \frac{1}{\rho f}\vec{k}\times\vec{\nabla}_H p \tag{4.11}$$

$\vec{G}$ can be a solution to Eq. (4.10) only if the isobars are straight, since a curved motion implies a centripetal acceleration.

There is a solution to Eq. (4.10) where the centripetal acceleration is taken into account but where the tangential acceleration is still assumed zero. This solution is called the gradient wind $\vec{V}_{gr}$, and is given by the following equation

$$\vec{V}_{gr}\cdot\left(1+\sigma\frac{|\vec{V}_{gr}|}{Rf}\right) = \vec{G}\ , \tag{4.12}$$

where R is the radius of curvature (always positive) and $\sigma = -1$

for anticyclones (high pressure regions) and $\sigma = +1$ for cyclones (low pressure regions). In the case of anticyclonal motion the gradient wind is larger than the geostrophic wind; the reverse is true for cyclonal motion.

4.4.1. The effect of the radius of curvature

For stationary conditions with circular isobars, the gradient wind is the real wind above the boundary layer. In boundary layer calculations, however, one cannot directly substitute for the geostrophic wind with the gradient wind since Eq. (4.10) is not valid there. Here the centripetal acceleration must be based on the real wind which, even in cases where stationarity can be assumed, is a complicated function of the geostrophic wind, roughness and stability (cfr. Chapter 2). Consideration of the effects of isobar curvature will complicate the calculations even further.

Because only stationary solutions will be considered (and in fact, only the wind's statistical characteristics), the effects of curvature and centripetal accelerations have been neglected. Whether this increases or decreases the wind depends on location relative to the curve. Therefore, this curvature effect will not influence the average value to a significant degree; it will, however, weaken the correlation between the surface wind and the geostrophic wind.

In order to get an approximate measure of the influence of the centripetal acceleration, a statistical investigation of the relationship between $\vec{G}$ and $\vec{V}_{gr}$ was carried out for the point (0,0), identical to (56^{o}N, 10^{o}E). The results are shown in Table 4.1.

The missing 4% are those cases where a solution to the gradient wind equation does not exist. The average deviation between the gradient wind and the geostrophic wind is small, as expected. The standard deviation of $\vec{V}_{gr} - \vec{G}$ is 2.4 ms^{-1} while that of V_{gr}/G is only 0.18. These values can be taken as conservative estimates of the uncertainty in the determination of the free

Table 4.1. Investigation of the relationship between the gradient wind $\vec{V}_{gr}$ and the geostrophic wind $\vec{G}$ for the position (56°N, 10°E) in the period 1965-77. The deviation from the mean value is indicated by an apostroph and the mean value by < >.

	Number of cases %	$\langle V_{gr}-G \rangle$ m/s	$\langle (V_{gr}-G)'^2 \rangle^{\frac{1}{2}}$ m/s	$\langle V_{gr}/G \rangle$	$\langle (V_{gr}/G)'^2 \rangle^{\frac{1}{2}}$
Anticyclonic curvature	33	1.4	1.9	1.15	0.15
Cyclonic curvature	63	-1.7	1.9	0.86	0.09
Total	96	-0.6	2.4	0.96	0.18

wind when the centripetal acceleration is neglected. The effect will not have a significant influence on the statistical distribution of the wind, but it does contribute to a weakening of the correlation between the geostrophic wind and the calculated surface wind.

4.4.2. Calculation of the geostrophic wind

The geostrophic wind is given by Eq. (4.11) and can be expressed as

$$\vec{G} = (u_g, v_g) = \frac{1}{\rho f}\left(-\frac{\partial p}{\partial y}, \frac{\partial p}{\partial x}\right) \qquad (4.13)$$

For f the value $1.21 \times 10^{-4} s^{-1}$ is valid for 56°N, ρ is determined from $\rho = \bar{p}/R\bar{T}$, where R is the gas constant for dry air, and $\bar{p}$ and $\bar{T}$ are the mean values of pressure and temperature over the area at a given time. By using a third order expansion of $\bar{p}$, Eq. (4.2) gives with n=3:

$$\vec{G}(x,y) = \frac{R\bar{T}}{\bar{p}f}\left(-\sum_{j=0}^{3}\sum_{k=0}^{(3-j)} \beta_{jk}\cdot k\cdot x^{j}y^{(k-1)}\right.,$$

$$\left.\sum_{j=1}^{3}\sum_{k=0}^{(3-j)} \beta_{jk}\cdot j\cdot x^{(j-1)}y^{k}\right) \qquad (4.14)$$

By introducing the values of β_{jk} determined by the least squares method, Eq. (4.14) becomes an expression for the geostrophic wind at an arbitrary point inside the analysed area.

4.5. The uncertainty in the determination of the geostrophic wind

The geostrophic wind is determined with an uncertainty which is directly related to the uncertainty in the determination of the polynomial which approximates the pressure field. This uncertainty is, as already mentioned, due partially to the measurement error and partially to the inaccuracy of the third order approximation.

4.5.1. The uncertainty due to measurement errors

In section 4.3 it was stated that the error in the pressure measurements was approximately 0.5 mb. Even though the fitting of the polynomial is made by minimizing the mean square deviation, the error in the pressure measurements can generate errors in the geostrophic wind. The magnitude of these errors can be found as follows:

The coefficients β_{jk} in the polynomial are the solution to the matrix equation

$$\underline{\underline{A}} \cdot \underline{x} = \underline{p}$$

The introduction of $\Delta p(x_i,y_i)$ as an expression for the error in the pressure measurements so that

$$p(x_i,y_i) = p_t(x_i,y_i) + \Delta p(x_i,y_i) \ .$$

leads to an input matrix of the form

$$\underset{=}{p} = \underset{=}{p}_t + \underset{=}{p}_e$$

where $\underset{=}{x}_e$ can be defined as the solution to

$$\underset{=}{A} \cdot \underset{=}{x} = \underset{=}{p}_e$$

from which it follows that

$$\underset{=}{x}_t = \underset{=}{x} - \underset{=}{x}_e$$

where $\underset{=}{x}_t$ is the solution to

$$\underset{=}{A} \cdot \underset{=}{x} = \underset{=}{p}_t \ .$$

By assuming the errors in the pressure measurements to be random noise in time and space with an amplitude of 0.5 mb, $\underset{=}{x}_e$ can be determined and the influence of the measurement errors on the geostrophic wind can be assessed.

The uncertainty in the geostrophic wind will be defined as the standard deviation in the distribution of "the wind" calculated from this noise model. The standard deviation within Denmark was found to be 0.9 ms^{-1}. As expected, the deviation is small and will only have practical meaning for relatively weak geostrophic winds.

4.5.2. The uncertainty due to the pressure surface approximation

It was concluded earlier that in about ten per cent of all cases the standard deviation is larger than would have been expected from measurement errors alone. It was also concluded that these cases were associated with the passage of fronts. It is very difficult to estimate the error in the geostrophic wind in these situations.

The pressure surface approximation is, in effect, a spatial smoothing of the true pressure field. This smoothing means that the geostrophic wind which is calculated at a given point will represent the average value over a time period which is estimated to be about one hour. As described in Chapter 3, this means that the calculated surface wind distribution will have less variance than one which was determined by ten minute averages. Although this variance deficit increases with height over the surface, it is estimated not to be of significance for heights up to 200 m.

The smoothing does contribute to a weakening of the correlation between the surface wind and the geostrophic wind. However, since the statistical distribution is not expected to be influenced to a significant degree, the pressure surface approximation will be accepted as being sufficiently accurate for the determination of the geostrophic wind. To what extent this assumption is correct or sufficiently good for the purpose of the Windatlas will in the final analysis be determined by the succes of the entire physical model.

4.6. The geographic variation of the geostrophic wind

When the limited geographical extent of Denmark is considered, one does not expect to find any statistical variation of the geostrophic wind over Denmark. The reason for this is that the horizontal extent of a typical atmospheric pressure system is usually many times larger than Denmark.

For a number of selected points the mean values and standard deviations for the geostrophic wind for the period 1965-77 were calculated. These points and the calculated values are shown on the map in fig. 4.3. As can be seen from the figure, the mean value and the standard deviation can be taken as the same over the entire country. The somewhat higher values for points B and C can be ascribed to boundary effects introduced by the method of analysis. This can be most clearly seen for point C where the dropping of the West German stations after 1972 caused

an increase in both the mean value and the standard deviation compared to the other points. As for point B, it lies close to the boundary for the whole of the calculation period (cfr. fig. 4.1). The somewhat higher values for this point can therefore be ascribed to a boundary effect.

The existence of the boundary effects is due to the analysis method (cfr. section 4.1.3). Since all the stations are used in the calculation with the same weight, the restrictions on the approximating polynomial are smallest in the outer areas. This introduces relatively larger pressure gradients at the boundary; as a consequence, both the mean value and the standard deviation of the geostrophic wind are increased.

There is therefore no reason to expect that there are any appreciable differences in the statistical characteristics of the geostrophic wind over the country. As a consequence it is fully reasonable to use the geostrophic wind calculated at an interior point in Denmark, namely Risø. This hypothesis is then the basis for all further analysis.

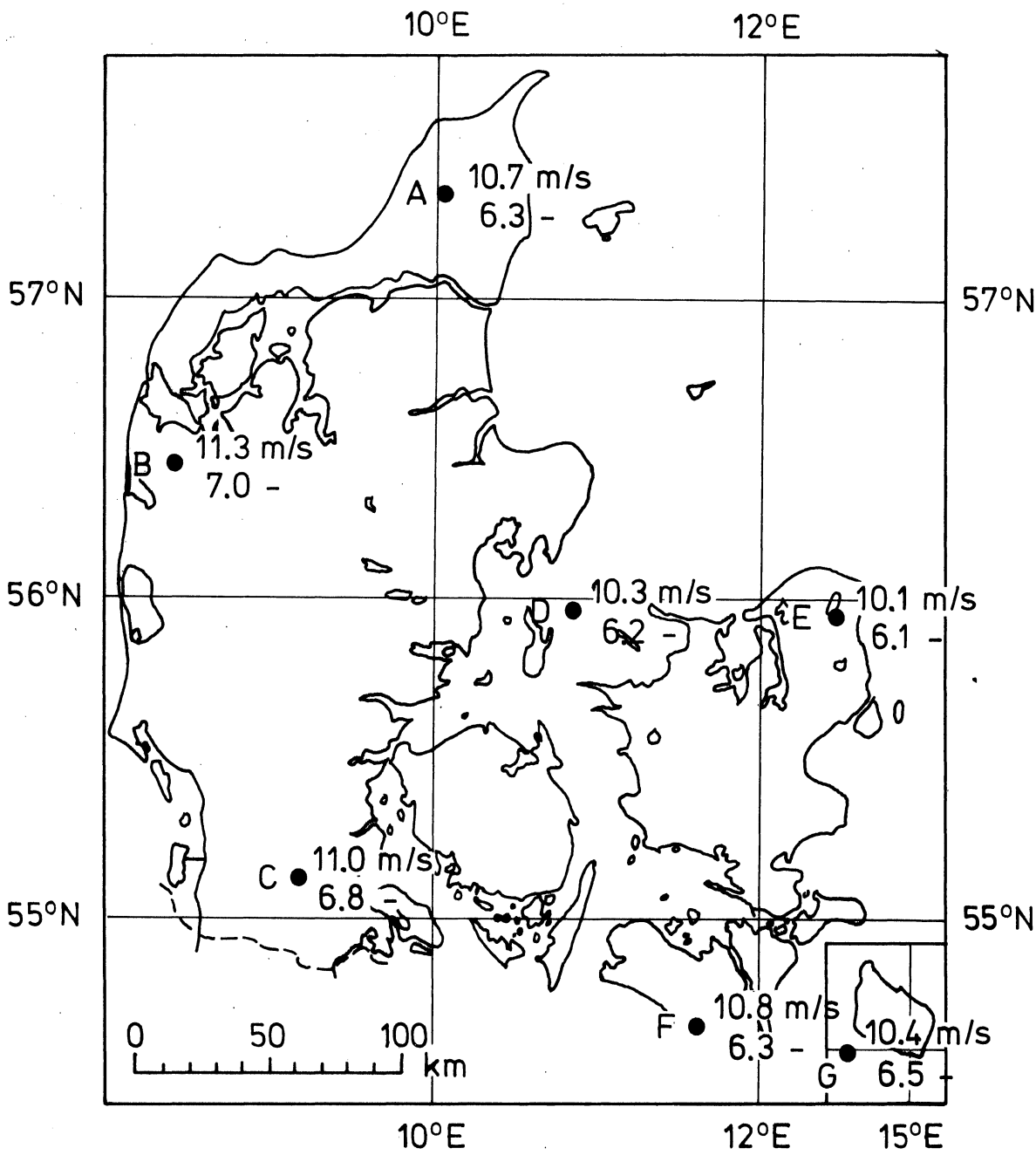

Fig. 4.3. Calculated mean values and standard deviations of the geostrophic wind for selected points for the period 1965-77. The upper value is the mean and the lower value is the standard deviation.

4.7. The baroclinity

It is customary to distinguish between whether the atmosphere is in a barotropic or a baroclinic state. By a barotropic state it is understood that the surfaces of constant pressure and temperature coincide. In this situation the magnitude and direction of the geostrophic wind do not change with height. In the baroclinic state the surfaces of constant pressure and temperature intersect each other at an angle. In this situation the geostrophic wind is not constant in the planetary boundary layer. Since the free wind to a good approximation can be regarded as geostrophic, it is clear that baroclinity is most often related to advection of either cold or warm air.

If cold air advection occurs, then the geostrophic wind turns to the left with height, and the geostrophic wind at the top of the boundary layer is therefore close to the direction of the surface wind. With warm air advection, the geostrophic wind turns to the right with height, and the difference in direction between the surface wind and the geostrophic wind near the top of the boundary layer is considerably larger than between the geostrophic wind at the surface and the real surface wind.

A measure of baroclinity in the planetary boundary layer is the difference between the geostrophic wind at the surface and the corresponding wind at the top of the boundary layer, $\vec{V}_T = \vec{G}(h) - G(0)$, where h is the height of the boundary layer, and $\vec{V}_T$ is usually referred to as the thermal wind.

The thermal wind in the planetary boundary layer can be obtained either through a detailed knowledge of the tilting of the pressure- and temperature surfaces, or from wind measurements near the top of the boundary layer.

The net of radiosonde stations in and around Denmark is relatively dense; however, the distances are too large for the use of the first method for the planetary boundary layer. On the other hand one can determine the thermal wind from a single radiosonde station with very good accuracy, if the geostrophic wind at the surface has already been determined.

The last method was applied to data from the radiosonde station in Jægersborg based on the original measurements of the wind speed at 300 m height intervals.

The thermal wind was determined as the difference between the wind at a height of 1500 m and the geostrophic wind at the surface. The former was determined by fitting a sixth or seventh order polynomial to the measured wind speeds. Various tests showed that such a fitting produces the most realistic profiles. The thermal wind was so determined twice daily for the period from May 1974 to November 1976.

As described in section 2.8, the thermal wind was incorporated into the physical model in a preliminary investigation to decide whether such an extension of the model would lead to improved accuracy in the calculation of the surface wind. No significant improvement was found, and the thermal wind data consequently have not been employed in the final analysis described in section 2.9.

4.8. Meteorological data

The network of meteorological stations that are used in the weather observation and warning services is normally called the synoptic network.

The observation posts must of necessity be placed in areas where personnel are present the whole day for reasons other than weather monitoring; for example, at lighthouses. At the airports it is necessary on purely aeronautical grounds to take meteorological measurements, and these measurements are naturally included in the synoptic network.

The meteorological parameters from the synoptic stations which are used in the Windatlas are the atmospheric pressure, the wind speed, and wind direction. For the measurement of pressure, the placement of the station is not especially critical. On the other hand, the measurement of the wind parameters (especially

the wind speed) can be very dependent on the local conditions. Since the placement of the stations is partially chosen for the convenience of the personnel, the measurement site is not always appropriate for detailed wind measurements. For normal synoptic use these measurements are usually satisfactory because the uncertainty in the measurements is smaller than the uncertainty with which the winds can be forecast. This is not the case, however, at the airports where it is very important to measure the wind with good accuracy. Furthermore, airports are for obvious reasons placed in large flat and horizontally homogeneous areas. Measurements from airports are therefore usually of high quality; since they are, in addition, also evenly distributed over the country, these data have been vital for the validation of the Windatlas.

4.9. The frequency distribution of the surface geostrophic wind

The frequency distributions of the surface geostrophic wind calculated as described in the preceeding sections are shown in the following nine figures. On each figure a histogram calculated from the observed pressure fields is plotted together with a continuous curve which represents the fitted Weibull-distribution. The mean value (G), the standard deviation (S), the Weibull parameters (A and C), and the frequency of occurrence in the various sectors (f) are listed on the figures.

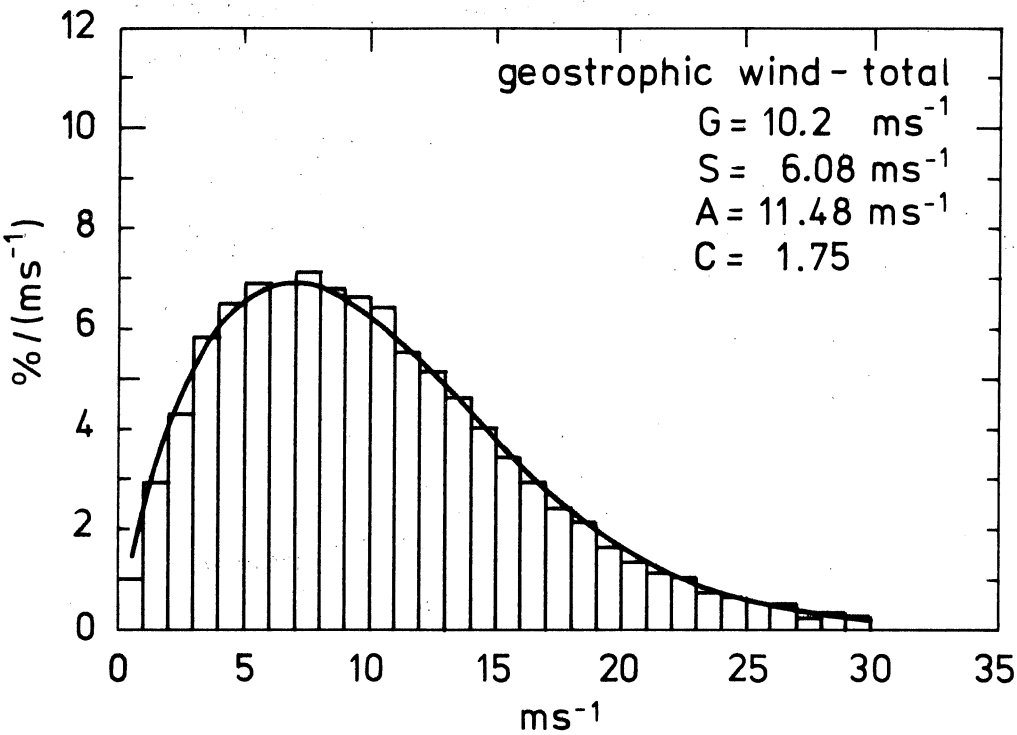

Fig. 4.4. The distribution of the geostrophic wind. The first figure shows the total distribution, and on the following eight figures, the sectorwise distributions are shown.

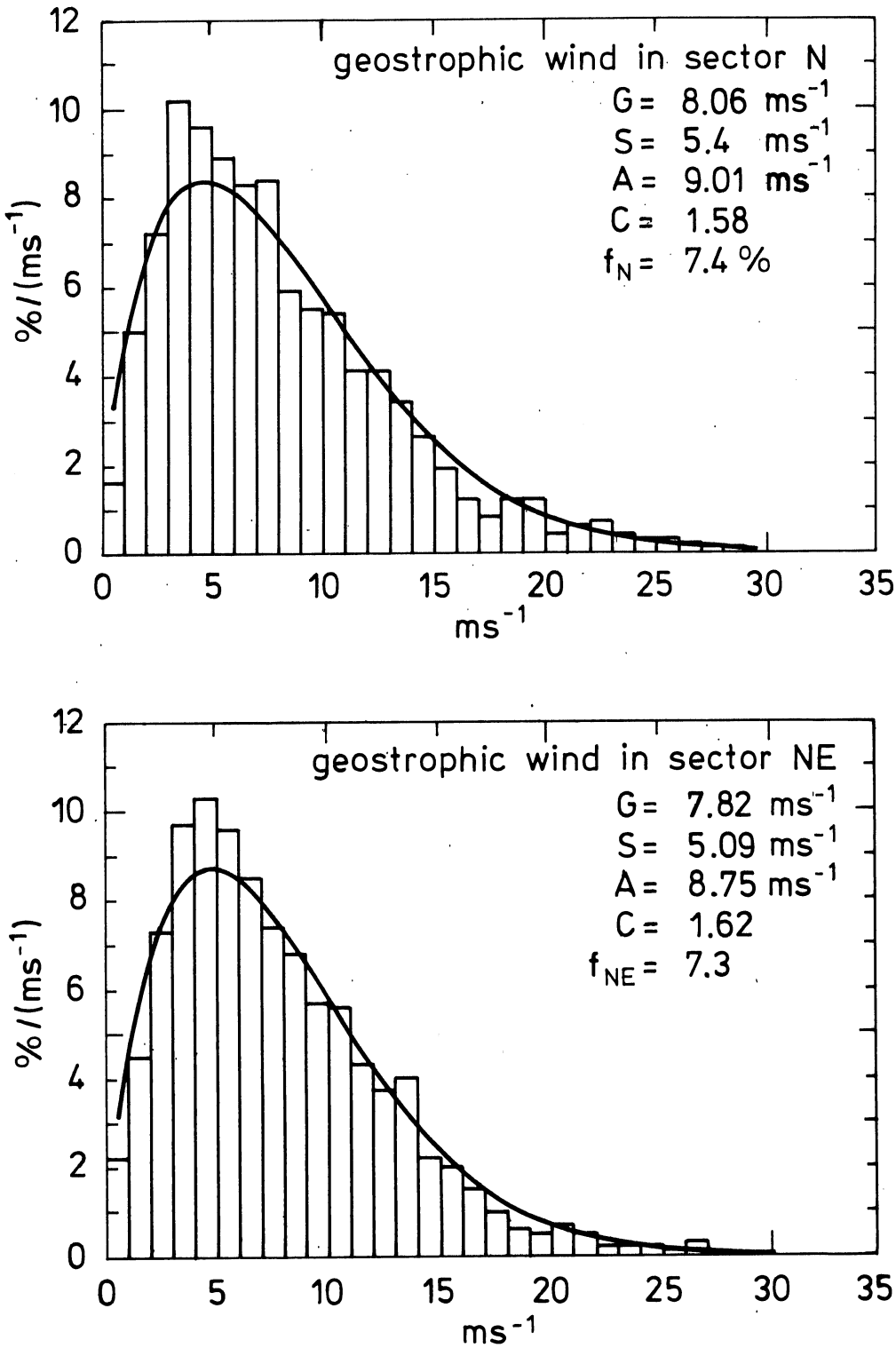

Fig. 4.4. Continued.

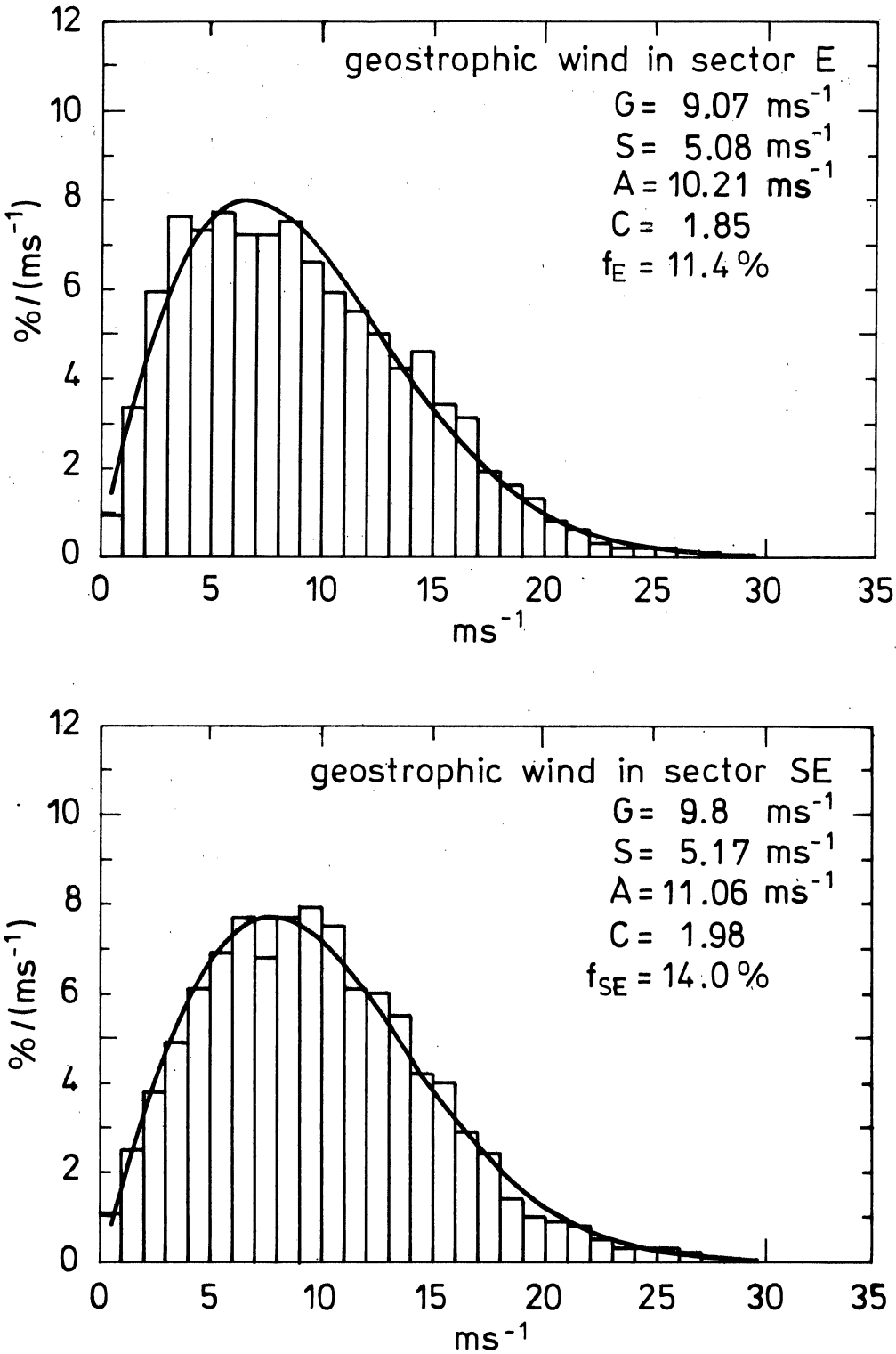

Fig. 4.4. Continued.

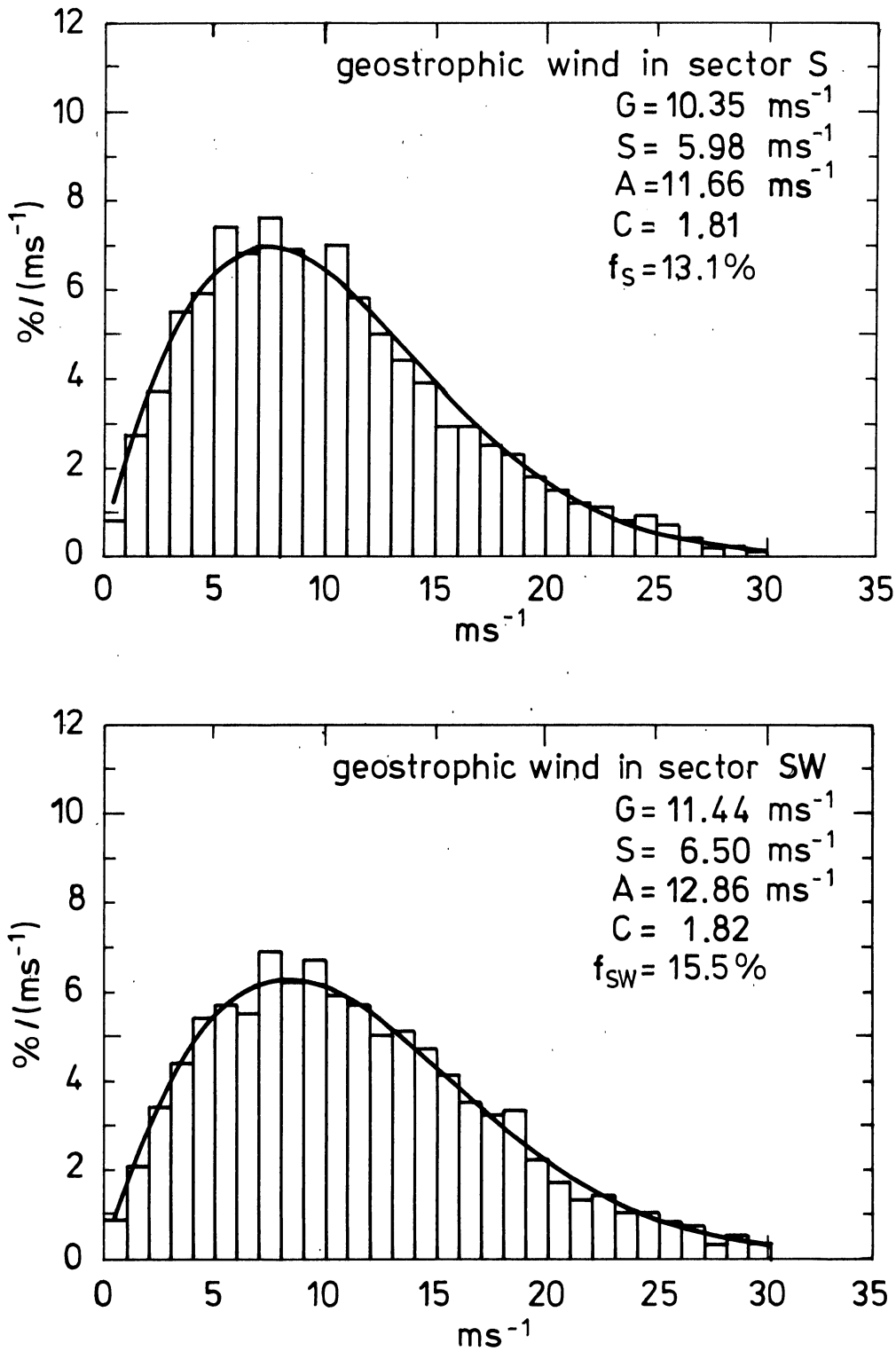

Fig. 4.4. Continued.

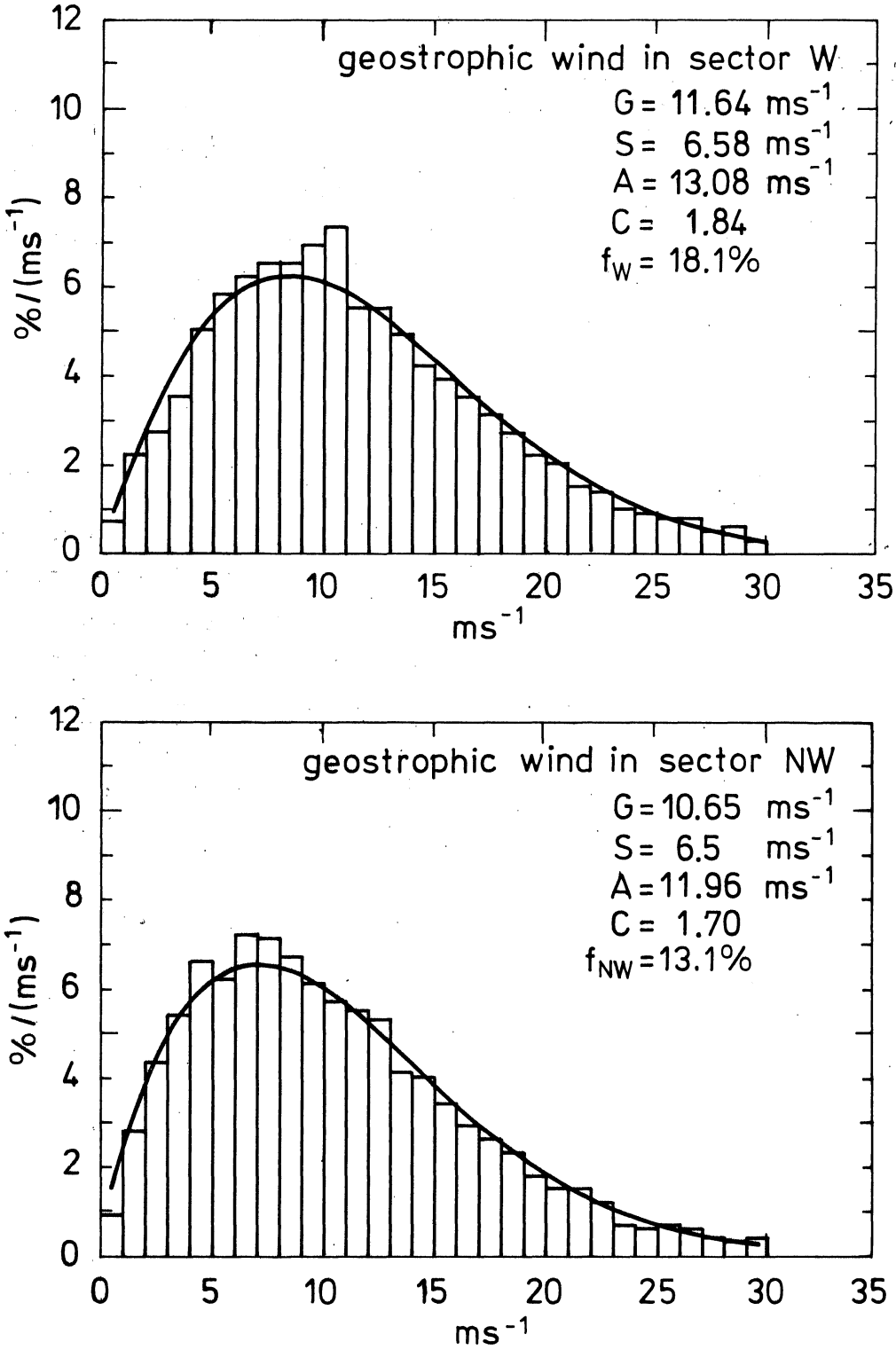

Fig. 4.4. Continued.

5. APPLICATION OF THE WINDATLAS

This chapter describes how the Windatlas can be used for practical calculations. Each section includes examples, which can serve as a guide when applying the Windatlas. The chapter is self-contained and can be used independent of the preceding theoretical analyses.

5.1. Roughness classification

The collective action on the wind of the surface of the terrain and the obstacles in the terrain is called the roughness of the terrain. The effect is parameterized through the roughness length, a quantity which is discussed in Appendix C. In the Windatlas the Danish landscape has been divided into four roughness classes. These are shown in Table 1.1 together with the corresponding type of terrain and roughness length. A short description of each roughness class is given below; examples of classifications are found in Chapter 6.

Roughness class 0. Waterareas: The sea, fjords and lakes.

Roughness class 1. Open areas without significant windbreaks: The terrain appears to be very open because there are only very few windbreaks, if any. The terrain is flat or very gently rolling. Single farms and stands of low bushes can be found. Fig. 5.1 shows an example of this roughness class.

Roughness class 2. Farmland with windbreaks having a mean separation in excess of 1000 m, and some scattered built-up areas: The terrain is characterized by large open areas between the many windbreaks, giving the landscape an open apperance. The terrain can be flat or strongly undulating. Trees and buildings are common. Fig. 5.2 shows an example of this roughness class.

The figures 5.1, 5.2, and 5.3 are by Søren Rasmussen

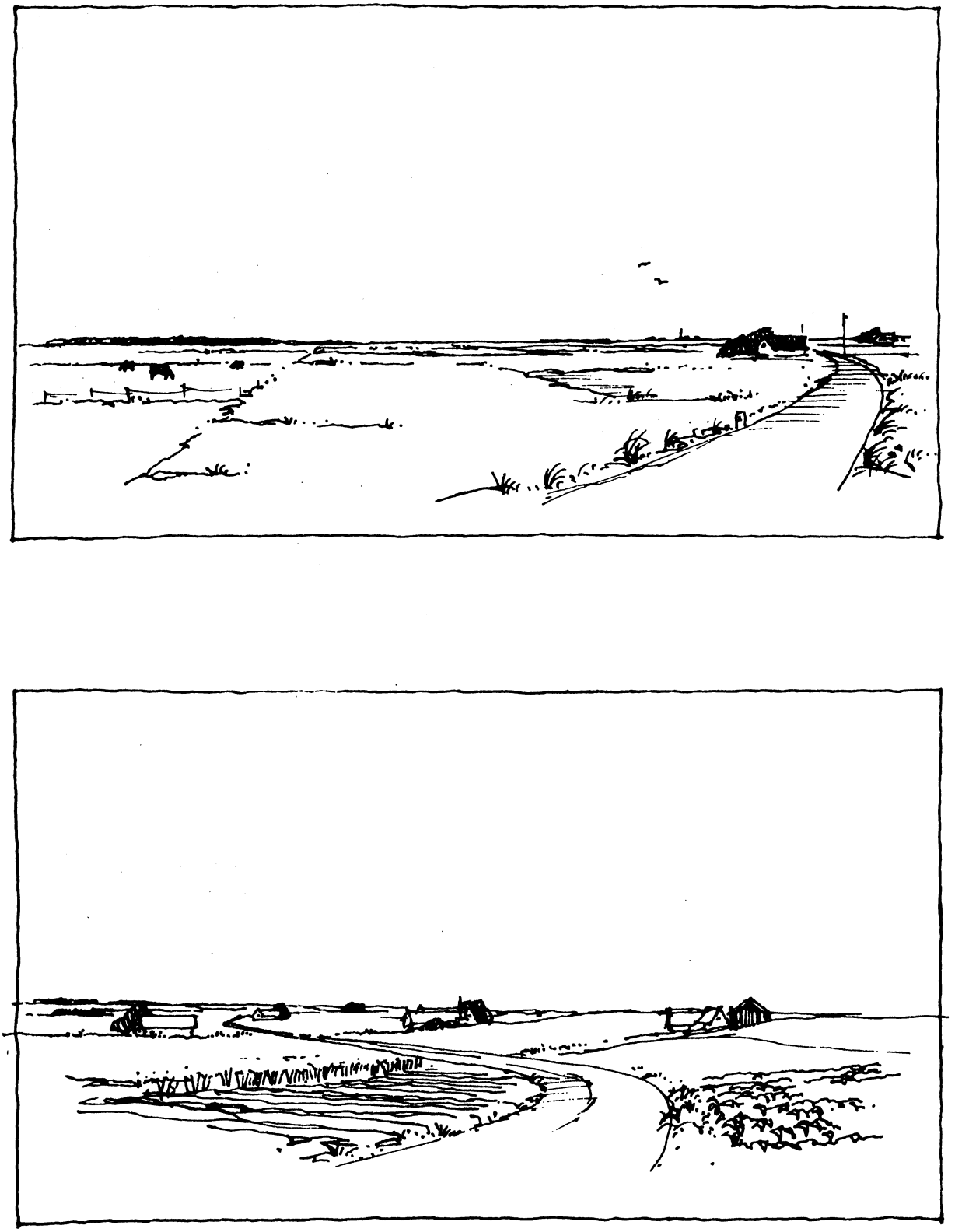

Fig. 5.1. Examples of terrains corresponding to roughness class 1.

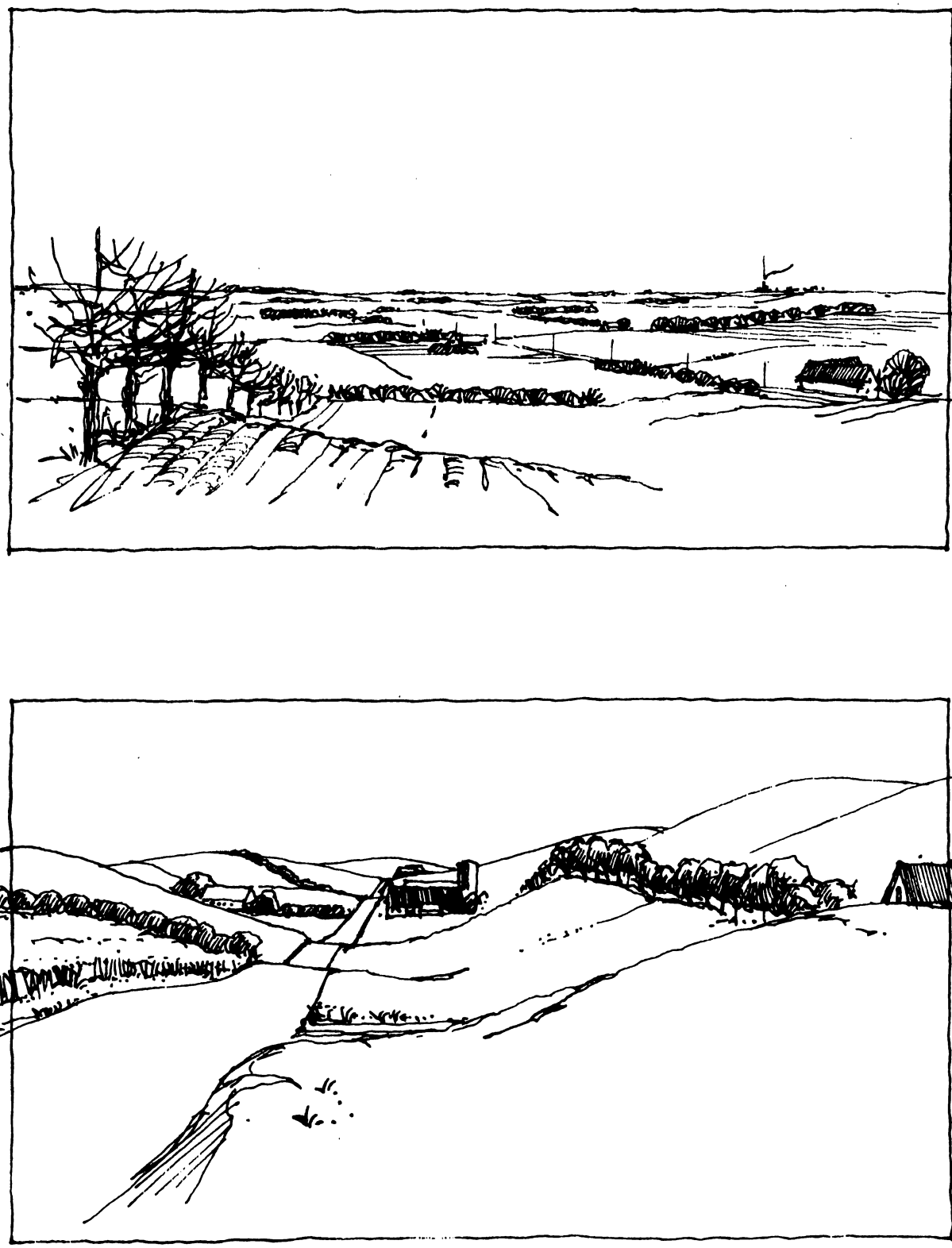

Fig. 5.2. Examples of terrains corresponding to roughness class 2.

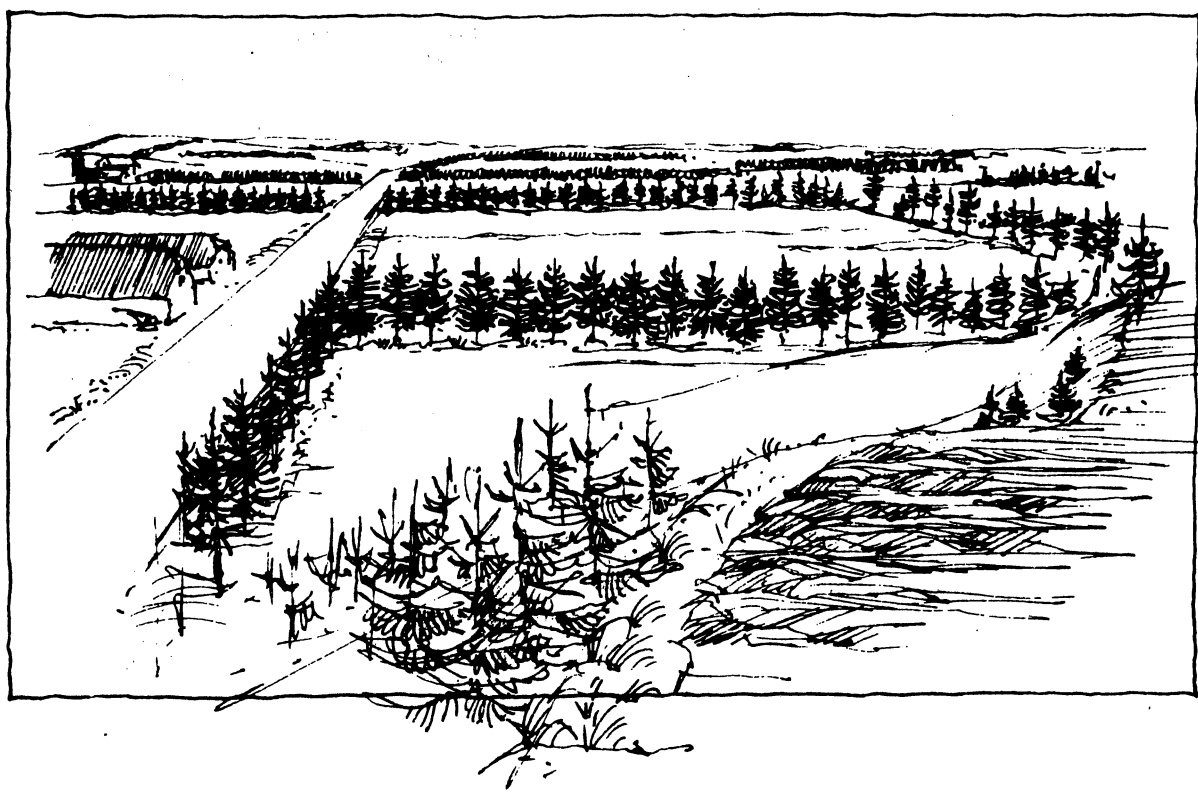

Fig. 5.3. Example of a terrain corresponding to roughness class 3.

Roughness class 3. Urban districts, forests, and farmland with many windbreaks: The farmland is characterized by the many closely spaced windbreaks, the average seperation being a few hundred meters. Forest and urban areas belongs to the class. Fig. 5.3 shows an example of this roughness class.

The roughness classification of a terrain is in its most simple form a matter of determining to which of the four roughness classes the various areas of the terrain belong. When this has been done and marked on a map together with significant obstacles and other complications, the possible sites for one or more turbines can be selected.

For each site the roughness of the terrain must be determined for the eight 45-degree direction sectors centered on the directions N, NE, E, SE, S, SW, W, NW, and each sector must be assigned a roughness class. Next, the Weibull parameters corresponding to the chosen roughness classes are found for each sector from the charts in appendix A. The heading on each chart tells which sector is referred to, the frequency with which the wind direction occurs in this sector, and the roughness class. The graphs on the chart show how the Weibull parameters corresponding to this set of parameters vary as a function of the height over terrain. For each roughness class graphs are included which give the Weibull parameters for the special case of homogeneous terrain, i.e. the roughness class is the same for all sectors.

5.2. Determination of the probability of a given wind speed

As described in Chapter 3 the Weibull distribution gives a measure of the probability of a given wind speed. The simplest application is the estimation of the probability of the wind speed V at a given height z over a homogeneous terrain of a given roughness class. The Weibull parameters corresponding to this situation can be found directly from the charts for homogeneous conditions. Once the parameters A and C are determined, the probability for a wind speed between V_1 and V_2 is given by

$$\Pr(V_1 < V < V_2) = \exp\left(-\left(\frac{V_1}{A}\right)^C\right) - \exp\left(-\left(\frac{V_2}{A}\right)^C\right) \qquad (5.1)$$

Example 5.1

The frequency with which the wind speed can be expected between 15 and 20 ms^{-1} is desired for a homogeneous area of roughness class 2 (roughness length 5 cm). The estimate should correspond to a height of 40 meters over the terrain.

From the chart corresponding to roughness class 2 and sector "total", the Weibull parameters corresponding to the height 40 meters on the vertical axis are A = 7 ms^{-1} and C = 1.93. Using these in the expression above yields

$$\Pr(15 < V < 20) = 0.012$$

Thus, for 1.2% of the time, the wind speed can be expected to be in this interval.

——— • ———

If it is desired to know the frequency of occurence of the wind in a given speed interval and in a given direction sector, the curves corresponding to the sector concerned must be used. The frequency is obtained by multiplying the frequency calculated above by the sector frequency given in the heading of the appropriate chart.

Example 5.2

As in the example above, it is required to have an evaluation of the frequency with which the wind speed is between 15 and 20 ms^{-1} at a height of 40 meters over a terrain of roughness class 2, but now with the additional constraint that the wind direction is in the East-sector.

From the appropriate chart, the Weibull parameters and frequency of occurrence in this sector are given by:

$$A = 6.6 \text{ ms}^{-1} \; ; \quad C = 2.29 \quad \text{and} \quad f_E = 12.7\%$$

Substituting these into Eq. (5.1) yields:

$$\Pr(15<V<20, \text{ East}) = 0.127 \cdot \left(\exp\left(-\left(\frac{15}{6.6} \right)^{2.29} \right) - \exp\left(-\left(\frac{20}{6.6} \right)^{2.29} \right) \right)$$

$$= 1.8 \cdot 10^{-4}$$

This result can be multiplied by the number of hours in 10 years (87660) to obtain

$$1.8 \cdot 10^{-4} \cdot 87660 \text{ hours} = 16 \text{ hours}$$

Thus, the wind (at 40 meters height over a homogeneous terrain of roughness class 2) can be expected to come from the East within the specified speed interval for an average of 16 hours over a 10 years period.

——— • ———

Normally, the frequency of occurrence of a given wind speed in a given direction sector is not of interest; rather, it is the frequency of occurrence independent of direction which is most interesting. This is especially true for estimation of wind power production. As mentioned above, the Weibull parameters corresponding to the total wind distribution over homogeneous terrain can be directly read from the charts in appendix A. In general, however, the fact that the terrain roughness is not the same in all directions must be taken into account. To illustrate this, consider a coastal site, where the sea sectors will be of roughness class zero while the land sectors will be characterized by roughness classes 1-3 depending on the nature of the terrain. In such situations the frequency is first calculated for each individual sector; then the total frequency is obtained as the sum of these frequencies.

Example 5.3

Suppose, as in the examples above, that the frequency of occurrence of the wind between 15 and 20 ms^{-1} at a height of 40 meters is desired. This time, however, the roughness class in the sectors N, NE, E, SE and S is 2 while the remaining sectors are described by the roughness class 0.

From Eq. (5.1) and the appropriate charts in appendix A the following information can be obtained:

Sector/ class	Weibull param. A	C	Freq. f	f·Pr
N 2	5.5	1.86	0.066	0.00010
NE 2	5.9	1.95	0.092	0.00019
E 2	6.6	2.29	0.127	0.00018
SE 2	6.8	2.07	0.122	0.00070
S 2	7.6	2.00	0.157	0.00304
SW 0	10.2	2.08	0.172	0.01551
W 0	10.4	2.03	0.198	0.01961
NW 0	7.7	1.72	0.089	0.00331
			1.023	0.0426

from which

$$Pr(15 < V < 20) = \frac{0.0426}{1.02} = 4.2\%$$

Note the large difference between this result and the result obtained in example 5.1.

——— • ———

It should be noted that in a situation with an inhomogeneous terrain, such as the example above, the sum of the frequencies

of the wind from the individual direction sectors is not exactly 100%. This is because the angle between the geostrophic wind and the surface wind depends upon the surface roughness as described in Chapter 2. This deviation is quite small and can be neglected, even though it in principle can be taken into account as shown in the example.

5.3. Determination of the total mean power

For purposes of wind power applications the primary interest is: What power production can be expected from a wind turbine placed at a given site? For such a calculation, it is necessary to know the production characteristics of the wind turbine in addition to the wind statistics. More specifically, one must know how the turbine's power output depends on the wind speed. This will be considered in detail below.

For a first comparison between different possible sites for a turbine, it can be helpful to evaluate the total power that is available in the wind as a function of hub height and terrain roughness. This maximum available power is (as stated earlier) given by

$$\langle E \rangle = \tfrac{1}{2}\rho\langle V^3 \rangle \qquad (5.2)$$

where $\langle E \rangle$ is the average kinetic energy flux per unit area, ρ is the density of air, and $\langle V^3 \rangle$ is the mean value of the third power of the wind speed. With the help of the Weibull parameters this quantity can be calculated as

$$\langle E \rangle = A^3 \cdot F_E(C) \qquad (kWh/m^2/year) \qquad (5.3)$$

The brackets < > will be omitted in the rest of this chapter.

The function $F_E(C)$ has been tabulated in table A1. Thus E can be calculated for each direction sector. The total available power density is then given by the weighted sum:

$$E = f_N \cdot E_N + f_{NE} \cdot E_{NE} + \cdots + f_{NW} \cdot E_{NW} \qquad (5.4)$$

where f_N, f_{NE} ... are the occurrence frequencies for the individual sectors (obtained from the charts), and E_N, E_{NE}, etc. are the power densities calculated by using Eq. (5.3) for each sector.

Example 5.4

In the situation described in the previous example, an estimate of the power contained in the wind at a height of 40 meters is desired.

The required information from the charts is summarized below:

Sector/ class	Weibull param. A	C	Freq. f	E	f·E
N 2	5.5	1.86	0.066	1295	85
NE 2	5.9	1.95	0.092	1513	139
E 2	6.6	2.29	0.127	1819	231
SE 2	6.8	2.07	0.122	2176	265
S 2	7.6	2.00	0.157	3146	494
SW 0	10.2	2.08	0.172	7309	1257
W 0	10.4	2.03	0.198	7938	1572
NW 0	7.7	1.72	0.089	3940	351
			1.023		4394

then

$$E = \frac{4394}{1.02} = 4295 \text{ kWh/m}^2\text{/year}$$

It should be noted that no wind turbine can produce this power; in practice only about 25-40% of the available power can be

utilized. (Simple aerodynamical considerations give a theoretical maximum efficiency of 59%).

5.4. Determination of the Weibull distribution in cases of changing roughness

As mentioned above the Weibull parameters corresponding to the case of a homogeneous terrain can be directly read from the charts. In the more general case where the roughness is not the same in all the sectors, the Weibull parameters can be calculated to a good approximation by use of the mean and mean square values (Chapter 3).

$$\begin{aligned} M &= A \cdot \Gamma(1 + \tfrac{1}{C}) \\ V^2 &= A^2 \cdot \Gamma(1 + \tfrac{2}{C}) \ , \end{aligned} \tag{5.5}$$

where M is the mean value, V^2 is the mean square value in a Weibull distribution with parameters A and C, and Γ is the gamma-function. For each direction sector M and V^2 can be determined using these equations. The corresponding values for the total distribution are then given by the weighted sums

$$\begin{aligned} M &= f_N \cdot M_N + f_{NE} \cdot M_{NE} + \cdots + f_{NW} \cdot M_{NW} \\ V^2 &= f_N \cdot V_N^2 + f_{NE} \cdot V_{NE}^2 + \cdots + f_{NW} \cdot V_{NW}^2 \end{aligned} \tag{5.6}$$

The Weibull parameters corresponding to the total distribution can now be estimated by the use of the expressions:

$$\frac{M^2}{V^2} = \frac{\Gamma^2(1 + \frac{1}{C})}{\Gamma(1 + \frac{2}{C})} \quad \text{and} \quad M = A \cdot \Gamma(1 + \tfrac{1}{C}) \tag{5.7}$$

where A and C now represent the parameters in the total distribution.

These equations are transcendental equations and can only be solved by the use of numerical methods. To assist in practical applications, the solutions have been tabulated in tables A4 and A5. Likewise the gammafunction has been tabulated in tables A2 and A3 for the range of values which occur in the above expressions.

The procedure for the determination of the Weibull parameters for the total distribution can be summarized by the following steps:

1) Determine A and C together with f for each sector.
2) Determine $F_M(C)$ by using table A2 for each sector; then multiply by A for the sector to obtain $M_N, M_{NE}, \cdots, M_{NW}$.
3) Determine V^2 for each sector (i.e. $V_N^2, V_{NE}^2, \cdots, V_{NW}^2$) with the help of $F_V(C)$ from table A3 and $V^2 = A^2 \cdot F_V(C)$.
4) Compute the weighted sum of the mean values and the mean squares to obtain the mean value M and mean square value V^2 for the total distribution.
5) Calculate M^2/V^2 and use this value in table A4 to obtain C for the total distribution.
6) Use the C from step 5 in table A5 to obtain $F_A(C)$ and use $A = M \cdot F_A(C)$ with M obtained in step 4 to find A for the total distribution.

These calculations are easily carried out as illustrated in the following examples.

Example 5.5

Consider the situation in the previous example and assume that it is desired to know the Weibull parameters for the wind speed distribution.

The information obtained from the charts and the procedure outlined above is summarized in the following table:

Sector/ class	A	C	f	M	V^2	fM	fV^2
N 2	5.5	1.86	0.066	4.88	31.3	0.322	2.07
NE 2	5.9	1.95	0.092	5.23	35.2	0.481	3.24
E 2	6.6	2.29	0.127	5.85	41.5	0.743	5.27
SW 2	6.8	2.07	0.122	6.02	45.6	0.734	5.56
S 2	7.6	2.00	0.157	6.73	57.8	1.057	9.07
SW 0	10.2	2.08	0.172	9.04	102.4	1.555	17.61
W 0	10.4	2.03	0.198	9.21	107.5	1.824	21.29
NW 0	7.7	1.72	0.089	6.87	64.0	0.611	5.70
			1.02			7.327	69.81
				Division		7.18	68.4
					$\frac{M^2}{V^2}$ =	0.754	

$$M = \frac{7.33}{1.02} = 7.18$$

$$\frac{M^2}{V^2} = 0.754 \Rightarrow$$

$$V^2 = \frac{69.8}{1.02} = 68.4$$

$$C = F_C(0.754) = 1.81 \qquad \text{(table A4)}$$

$$A = F_A \cdot (1.81) \cdot 7.18 = 8.1 \text{ ms}^{-1} \qquad \text{(table A5)}$$

Table A1 can now be used to estimate the total available power density as

$$E = (8.1)^3 \cdot F_E(1.81) = 4280 \text{ kWh/m}^2\text{/year}$$

This number can be compared with the result obtained in the previous example (4295 kWh/m^2/year). The relative difference is less than 1% and can be attributed to roundoff errors.

——— • ———

It must be noted that the procedure used here assumes that the total distribution is very nearly a Weibull distribution; therefore, it can only be used in such situations. As shown earlier in the Windatlas the wind speeds may be assumed Weibull-distributed with a very good accuracy. Moreover, investigations described later have shown that the method is more than acceptably accurate for purposes of the Windatlas.

5.5. Change of roughness within one or more sectors

In the preceding sections it has been described how the Weibull parameters can be estimated in the case when the roughness class is not the same for all direction sectors. It is not uncommon, however, to encounter situations where the terrain in one or more sectors cannot be thought of as homogeneous because of marked roughness changes which occur at some distance from the point of interest. In order to be able to estimate the Weibull parameters in such cases, a method must be devised which makes it possible to calculate how the parameters change from one type of terrain to another. With such a method, the Weibull parameters in each sector can be calculated and the method described in section 5.4 can be employed to calculate the parameters corresponding to the total distribution. The method used here builds on the experimental evidence that an internal boundary layer develops downstream from a change in the terrain roughness. The height of this boundary layer increases with downstream distance. Outside this layer the roughness change is not felt and the wind speed is determined by the upstream terrain roughness. Within the boundary layer is a transition zone in which the wind speed depends on both the upstream and downstream roughnesses. At a certain distance from the roughness change and under a certain height the wind speed inside the

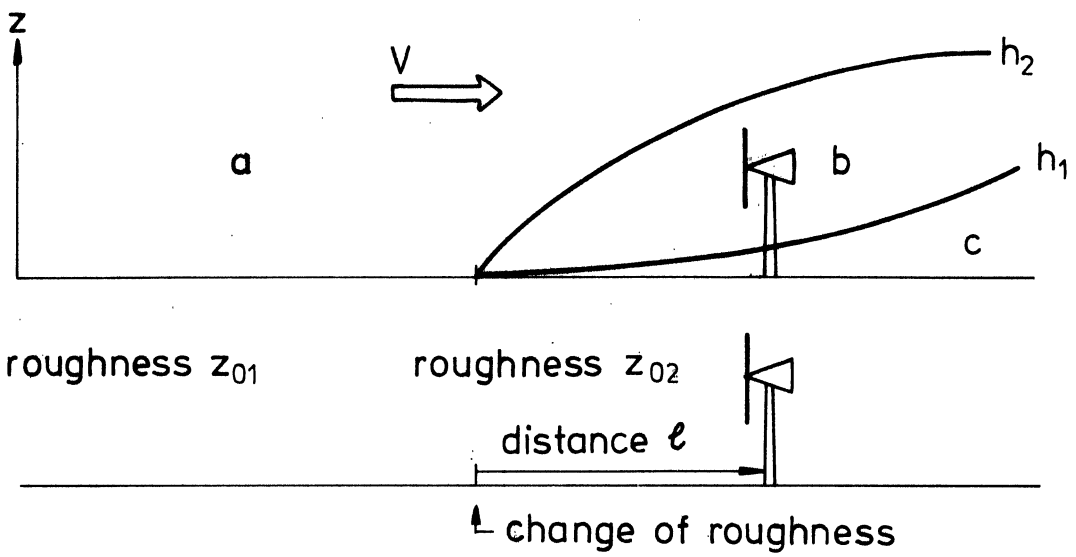

Fig. 5.4. Change of roughness class

boundary layer will be determined by the downstream roughness only. It is well-documented experimentally that the height of the boundary layer grows as shown for the height h_2 in fig. 5.4. It is not finally settled how the wind speed depends on both roughnesses in the transition zone. For purposes of the Wind-atlas a "computational" layer is introduced, the height of which is indicated by h_1 on fig. 5.4. This choice is based on physical considerations and on the desire to obtain a reasonably simple computational procedure.

The situation with a roughness change, depicted in fig. 5.4, is then as follows: The air passes over an area with surface roughness z_{01} onto an area with surface roughness z_{02}. Upstream from the roughness change and above the developing internal boundary layer (the area denoted by "a" on fig. 5.4), the wind speed is determined by the upstream roughness z_{01}. Below the height h_1 downstream from the roughness change, a new equilibrium has been reached where the wind speed depends only on the

roughness z_{02} (the area "c" in the figure). In the intermediate zone between h_1 and h_2 a gradual transition between the two wind speeds takes place. The heights h_1 and h_2 can be read from fig. 5.5; h_1 should be taken from the curve corresponding to the roughness class downstream from the roughness change, while the largest of the two roughness classes must be used for h_2.

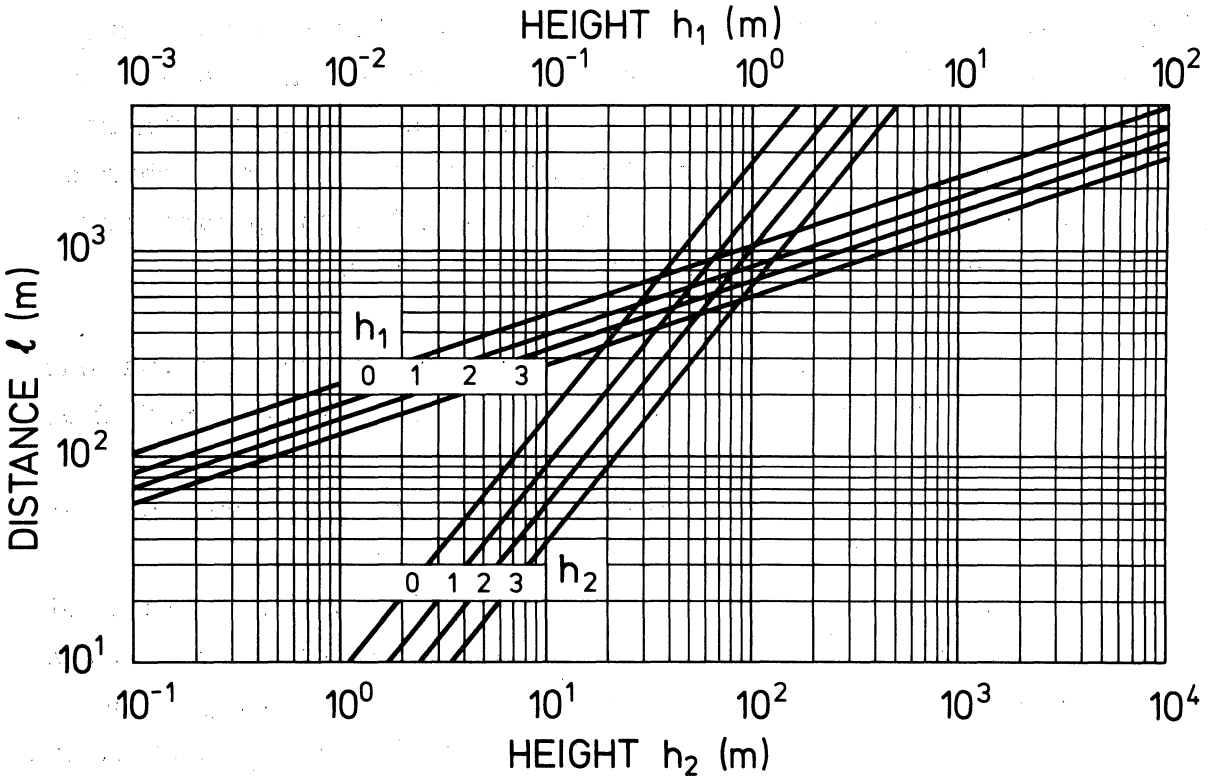

Fig. 5.5. Height of the internal boundary layer h_2 and of computational layer h_1 as function of distance ℓ downstream from a roughness change.

The mathemathical expressions for h_1 and h_2 are:

$$h_1 = 0.7 \cdot 10^{-8} \; z_o^{0.3} \; \ell^3$$

$$h_2 = 0.7 \; z_o \left(\frac{\ell}{z_o}\right)^{0.8} \quad .$$

(h_1, h_2, z_o, and ℓ in meters)

The graph of h_1 versus distance also gives the smallest distance L for which the terrain can be considered homogeneous. L is the value of ℓ corresponding to $h = h_1$. Thus, if the terrain is homogeneous out to a distance L it is not necessary to take into consideration inhomogeneities at greater distances. On the other hand, if a roughness change is encountered within the distance L from the point of interest, the Weibull parameters must be modified to account for the effect of the roughness change on the wind speed distribution and a roughness change procedure should be employed. The recommended procedure for correcting the Weibull parameter is as follows:

1) The Weibull parameters A_1 and C_1 corresponding to the hub height h and the upwind roughness class are obtained from the appropriate chart.
2) Similarly, the Weibull parameters A_2 and C_2 corresponding to the downwind roughness class are determined.
3) The distance to the roughness change ℓ and the greater of the two roughness classes in question determine the height h_2 which is read from fig. 5.5. The downwind roughness class and ℓ determine the height h_1 which is read from the same figure.
4) The corrected Weibull parameters are obtained by using the following expressions:

$$\left.\begin{aligned} A &= A_1 \\ C &= C_1 \end{aligned}\right\} \qquad \text{for} \qquad h \geq h_2$$

$$\left.\begin{aligned} A &= A_2 \\ C &= C_2 \end{aligned}\right\} \qquad \text{for} \qquad h \leq h_1 \qquad (5.8)$$

$$\left.\begin{aligned} A &= w_1 A_1 + w_2 A_2 \\ C &= w_1 C_1 + w_2 C_2 \end{aligned}\right\} \qquad \text{for} \qquad h_1 < h < h_2$$

with

$$w_1 = \frac{\ln\left(\frac{h}{h_1}\right)}{\ln\left(\frac{h_2}{h_1}\right)} \qquad \text{and} \qquad w_2 = 1 - w_1 \qquad (5.9)$$

5) The Weibull parameters corresponding to the total distribution are calculated as described in section 5.4 using the corrected parameters obtained above.

Example 5.6

Consider the situation illustrated in fig. 5.6 where a wind turbine with hub height 25 metres is located 500 meters from a straight coastline.

The distance to the coastline is determined for each sector as the distance from the turbine to the coastline at the middle of the sector:

$$\ell = 500 \text{ m} \cdot \frac{1}{\cos\phi}$$

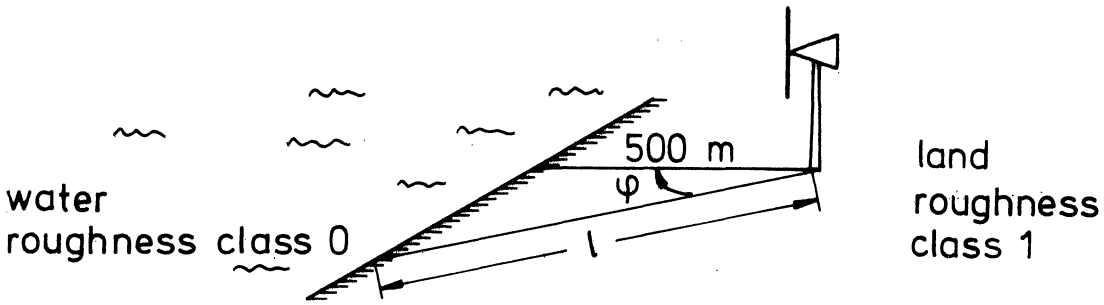

Fig. 5.6. Roughness change at a coastline.

this gives

sector	N	NE	E	SE	S	SW	W	NW
ℓ (m)	-	-	-	-	-	708	500	708

For the five sectors N-S the Weibull parameters corresponding to the appropriate roughness can be used directly. For the three westward sectors, however, the correction procedure outlined above must be employed. The procedure and the corrected Weibull parameters are summarized in the following tables:

Sector	Class 0		Class 2		(m)		W_1	W_2	A	C
	A_1	C_1	A_2	C_2	h_1	h_2				
SW	9.0	2.06	7.2	2.02	1.0	76	0.74	0.26	9.1	2.05
W	10.0	2.02	7.3	1.94	0.35	56	0.84	0.16	9.6	2.01
NW	7.4	1.72	5.1	1.66	1.0	76	0.74	0.26	6.8	1.70

Sector/ class	A	C	f	M	V^2	fM	fV^2
N 2	5.1	1.84	0.066	4.53	27.1	0.299	1.79
NE 2	5.3	1.92	0.092	4.69	28.6	0.431	2.63
E 2	6.0	2.23	0.127	5.32	34.6	0.676	4.39
SE 2	6.2	2.02	0.122	5.49	38.3	0.670	4.67
S 2	7.0	1.95	0.157	6.20	49.5	0.973	7.77
SW 0-2	9.1	2.05	0.174	8.06	82.0	1.402	14.27
W 0-2	9.6	2.01	0.195	8.51	92.0	1.659	17.94
NW 0-2	6.8	1.70	0.086	6.07	50.3	0.522	4.33
			1.02			6.63	57.8
						6.50	56.7
					$\frac{M^2}{V^2}$ =	0.745	

The parameters for the total distribution are then computed, following the procedure described in section 5.4:

A = 7.3
C = 1.77

This result can be compared with that obtained below in example 5.8 where the situation is the same as in this example with the single exception that the turbine is located at the coastline instead of 500 meters behind it. The Weibull parameters are seen to have been affected only slightly by the roughness change. A comparison of the total energy densities shows that it is 12% less for the inland site than for the coastal site.

—— • ——

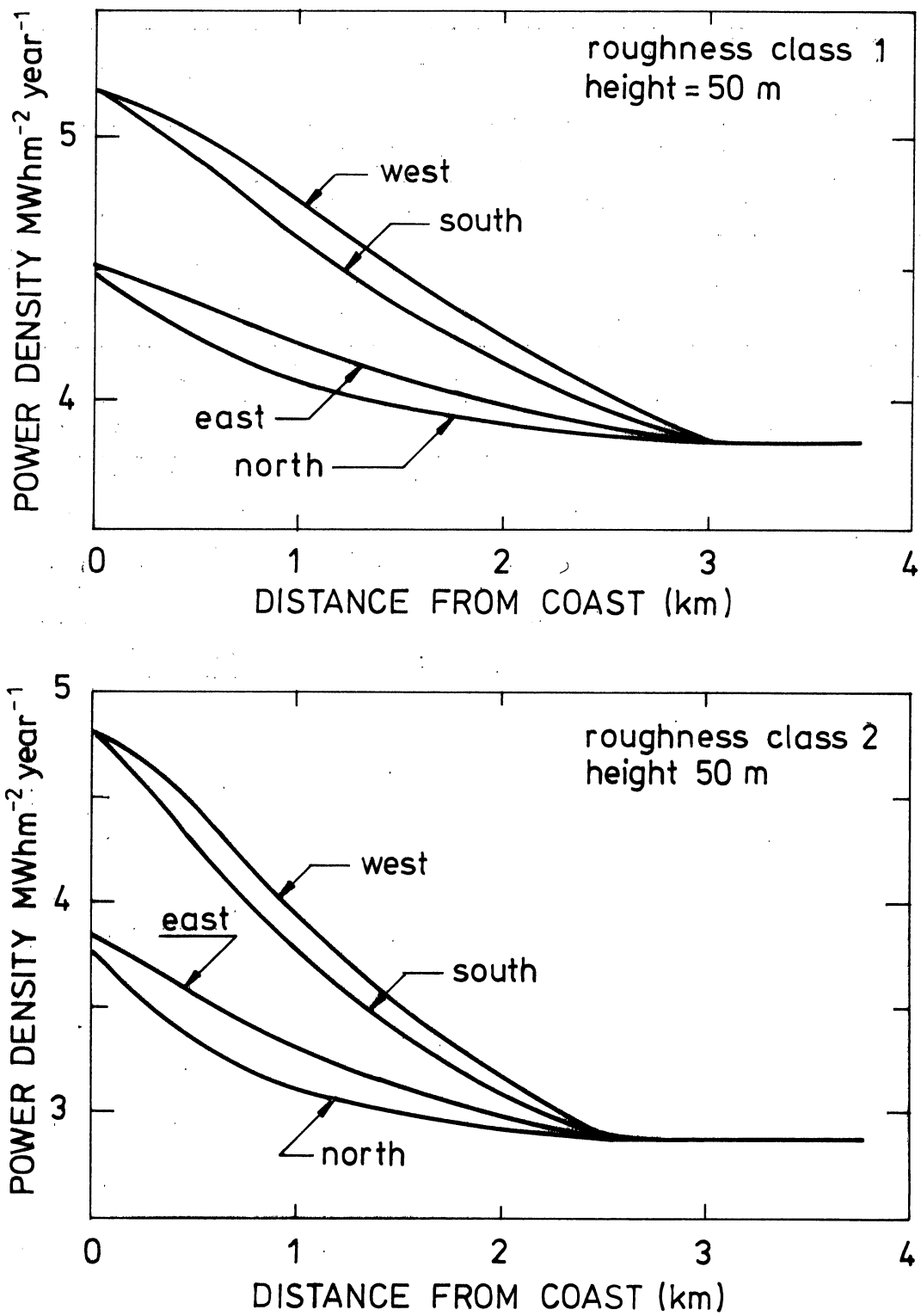

Fig. 5.7. The power density in the wind at 50 meters height as function of the distance to a coastline. The upper graph is for the case that the land roughness is class 1 and the lower one for the case of roughness class 2. In both cases the power density is shown for four orientations of the coastline as indicated.

Because of the importance attached to the coastal siting of large wind turbines, it is of interest to estimate the reduction in the power density as the distance from the coastline is increased. Such calculations have been carried out for various orientations of the coastline. The results are summarized in figure 5.7 which shows the power density at a height of 50 meters as function of the distance from the coast. The upper graph shows the result when the land is assumed to be of roughness class 1, and the lower graph the result when the land roughness class is 2.

5.6. Correction of the Weibull parameters due to shelter effects

Shelter is defined as the relative decrease in the wind speed caused by an obstacle in the terrain. The shelter at a given point is then given by

$$R = \frac{V-V_1}{V} \qquad (5.10)$$

where V is the unobstructed wind speed at the point, and V_1 is the wind speed at the point when the sheltering obstacle is present.

The necessary distance from a sheltering obstacle to a wind turbine depends on the hub height of the turbine and the dimensions of the obstacle. The wind speed, for example, is strongly influenced by the presence of a building; the effect extends up to approximately two times the height of the building and far downstream of the building. Behind the building large eddies can cause wind speeds as large as the wind speed in front of the building, but with the direction reversed.

If a wind turbine has to be placed closer to a building than approximately four times the height of the building, then the area swept by the rotor should not be allowed to reach below two times the height of the building, i.e. the hub height should be at least three times the height of the building. If this

rule is followed, the Weibull A and C parameters can be determined as if the building were not present. For larger distances from the building than four times the height of the building and for other choices of the hub height, fig. 5.8 can be used for approximate calculations of the reduction of the A parameter. The upper figure has two sets of graphs: The full lines give the reduction of the A parameter behind an infinitely long building, and the broken lines give the reduction behind a building where the length is five times the height of the building. The reason why the shelter effect disappears more quickly behind a building of limited length than behind a building of infinite length is that the wind speed not only rebuilds its strength from momentum brought down from above, but also from momentum carried in from the sides; furthermore, the limited building obstructs less of a sector as the distance between the turbine and building becomes larger.

For other lengths of the building than five times the height, the lower figure can be used. The graphs give the reduction factor which must be used together with the full graph from the upper figure. For a building of limited length the reduction factor R_2 corresponding to the actual length L is read from the lower figure and R_2 is thereafter multiplied by the reduction R_1 read from the upper figure. It is only the A parameter that is reduced:

$$R = R_1 \times R_2$$

$$A_{reduced} = A(100-R)/100 \qquad (5.11)$$

The data of Martin Jensen (1959) has been used in the construction of the full graphs in the upper figure of fig. 5.8.

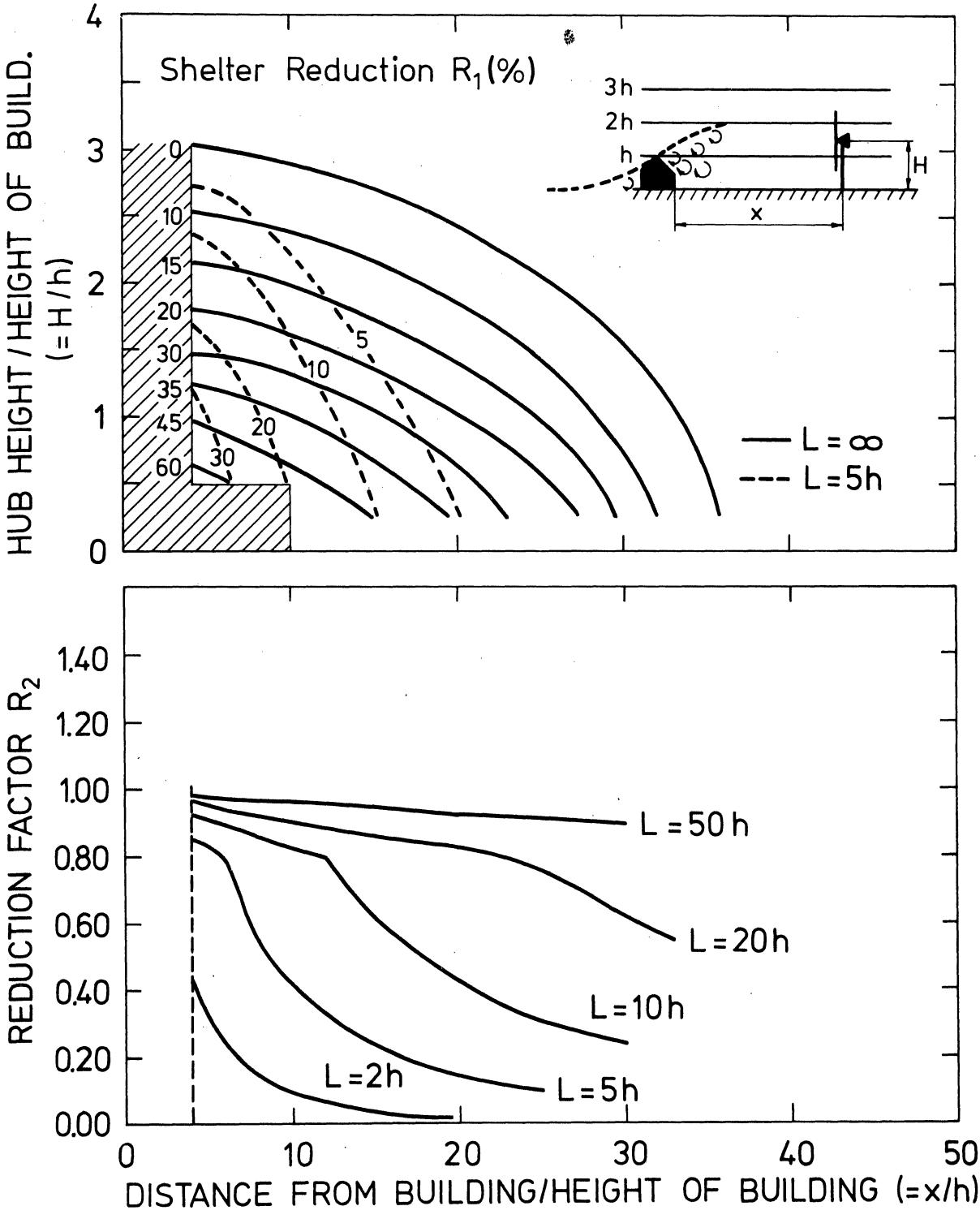

Fig. 5.8. Graphs giving the reduction of the A parameter behind a sheltering obstacle. L is the transverse dimension of the obstacle. The application is explained in the text.

Example 5.7

To illustrate the computation of the Weibull parameters in a situation where it is necessary to take into account the effect of shelter, the case of the airport at Skrydstrup has been chosen. This makes it possible to compare the results with the measurements taken there.

The anemometer is placed at a height of 9 metres, and the terrain is such that roughness class 1 must be used in all sectors. In the sectors E, SE, S and SW, buildings and windbreaks cover the whole sector.

Sector	distance x	height of obstacle h	length L
E	200 m	10 m	infinite
SE	200 m	10 m	-
S	100 m	5 m	-
SW	200 m	10 m	-

By choosing the hub height H equal to 9 metres, the following reduction factors can be obtained from figure 5.8:

Sector	x/h	H/h	R_1
E	20	0.9	22%
SE	20	0.9	22%
S	20	1.8	10%
SW	20	0.9	22%

For all the sectors, $R_2 = 1$. The Weibull parameters can now be obtained by using the corrected A parameters:

Sector/ class	A	C	F	M	V^2	fM	fV^2
N 1	4.7	1.70	0.065	4.19	24.0	0.272	1.56
NE 1	4.8	1.71	0.090	4.28	25.0	0.385	2.25
E 1*	4.3	1.98	0.125	3.81	18.6	0.476	2.33
SE 1*	4.6	1.92	0.122	4.08	21.5	0.498	2.62
S 1*	6.0	1.82	0.153	5.33	37.7	0.815	5.77
SW 1*	5.4	1.92	0.177	4.73	29.7	0.837	5.26
W 1	7.0	1.90	0.188	6.21	50.1	1.167	9.42
NW 1	5.0	1.57	0.080	4.49	28.7	0.359	2.30
			1.000			4.81	31.5
*Shelter reduction						4.81	31.5

$$\frac{M^2}{V^2} = 0.734$$

C = 1.71 A = 5.4 ms^{-1}

In Chapter 6 the measured wind speed distribution is shown together with the Weibull distribution corresponding to the above parameters. Also shown is the distribution which is obtained if the shelter correction is not taken into account. It is clear from the figure that the corrected curve provides a much better fit to the observations, than does the uncorrected curve.

5.7. The energy as function of the wind direction

It is obvious that a wind turbine should be placed so that the wind can blow towards it as unobstructed as possible. Regulatory and practical conditions, however, often result in sitings close to buildings. It is therefore important that the wind turbine be placed with respect to the buildings so that the energy production is as large as possible.

Sheltering effects from buildings and other obstructions, when unavoidable, should therefore preferably be in sectors where the contribution to the total energy production in any case is small.

Table 5.1 gives the mean energy in kWh/m^2/year in the eight direction sectors at 10 metres height as measured at Ålborg Airport (roughness class 1).

Table 5.1. Mean energy in the eight 45^o wind direction sectors. Measured at Ålborg Airport at the height of 10 metres.

Wind direction sector	Mean energy kWh/m^2/year
N	53
NE	90
E	185
SE	261
S	177
SW	411
W	641
NW	177

The table clearly shows that in Denmark a wind turbine should be placed with an unobstructed fetch in the SW and W sectors. If possible, it should be placed to the south of buildings or other sheltering elements.

5.8. Correction of the Weibull parameters for topographical effects

It is well known that the wind at the top of a hill often will be stronger than over the surrounding terrain. A turbine can therefore sometimes be placed with advantage on the top of a hill.

Letting V_2 and V_1 be the wind speeds at the same height over the surface over the top of the hill and over the terrain upstream of the hill, respectively, the relative speed-up ΔS is given by:

$$\Delta S = \frac{V_2 - V_1}{V_1} \tag{5.12}$$

An approximate expression for ΔS is given by (Jackson and Hunt, 1975):

$$\Delta S \cong 2\frac{h}{L} \quad , \quad L >> h \tag{5.13}$$

where h is the height of the hill over the surrounding terrain and L is a characteristic length of the hill, typically the half-width as shown on fig. 5.9. The dimension of the hill perpendicular to the wind direction has to be much greater than L so that the problem can be considered to be two-dimensional.

Above a certain height d, ΔS gradually decreases toward zero. This height d can be found approximately from

$$\frac{d}{z_o} \cong 0.5 \left(\frac{L}{z_o}\right)^{0.8} , \tag{5.14}$$

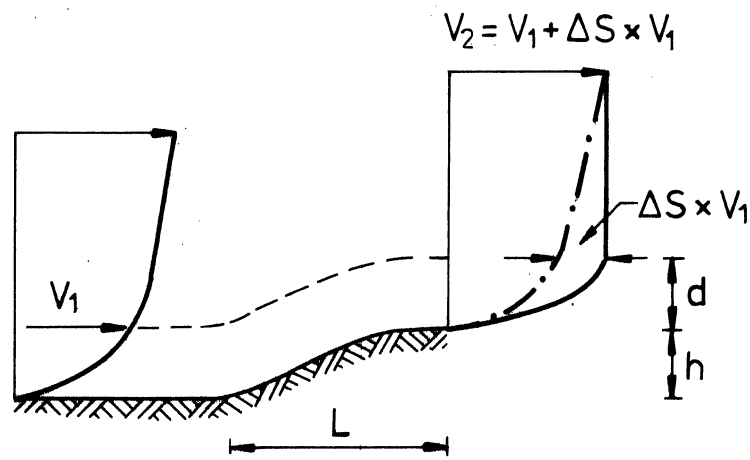

Fig. 5.9. The upstream-half of a two-dimensional hill together with typical wind profiles.

or fig. 5.5 can be used with d equal to 0.7 × h_2 where h_2 is read from the figure corresponding to a distance ℓ equal to L.

The effect of placing a wind turbine at the top of a hill can be taken into account in the determination of the Weibull parameters by increasing the A parameter from Appendix A for the sectors where the wind blows toward the hill:

$$A_{corrected} = A(1 + \Delta S) \qquad (5.15)$$

If the hub height H is not equal to the height d, ΔS is found for the height H as follows:

$$\Delta S_H = \Delta S_d \frac{\ln\left(\frac{H}{z_o}\right)}{\ln\left(\frac{d}{z_o}\right)} \quad \text{for } H < d$$

$$\Delta S_H = \Delta S_d \frac{\ln\left(\frac{H}{L}\right)}{\ln\left(\frac{d}{L}\right)} \quad \text{for } H > d \qquad (5.16)$$

where z_o is the roughness length corresponding to the surrounding terrain.

It should be noted that the considerations above only apply to hills of appreciable length perpendicular to the wind. With respect to a small single hill with an approximately circular base, the speedup ΔS will be around 20% less than that calculated for a corresponding long hill.

It should further be noted that the formulas only apply for smoothly shaped hills and not for cliffs where the strong deformation of the flow can result in localized shelter effects. Such effects can be found far downstream from the edge of the cliff, but they are usually limited to the lowest five to ten meters over the surface for the types of cliffs found in Denmark. Above a certain height over the cliff, a speed-up effect can be found as for flow over hills.

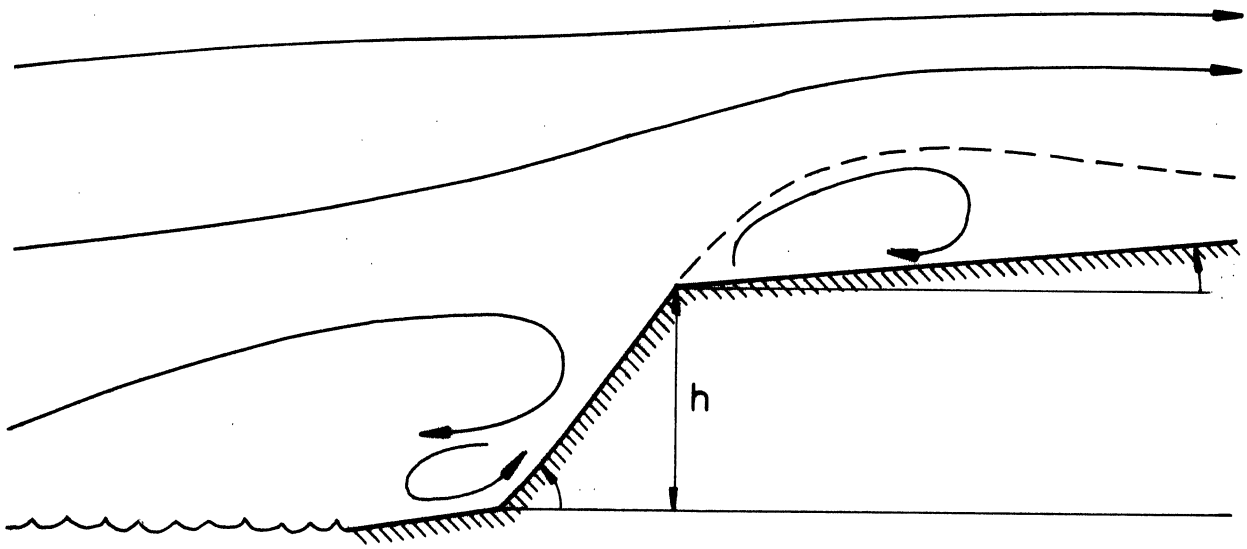

Fig. 5.10. Flow over a cliff.

5.9. Determination of mean power production

The mean power of a wind turbine can be computed by:

$$P = \int_0^\infty Pr(V)\,P(V)\,dV \qquad (5.17)$$

where Pr(V) is the probability density function of the wind speed and P(V) is the power delivered by the turbine at wind speed V. In terms of Weibull parameters the mean power can be expressed as:

$$P = \int_0^\infty \left(\frac{C}{A}\right)\left(\frac{V}{A}\right)^{C-1} \exp\left(-\left(\frac{V}{A}\right)^{C}\right) P(V)\,dV \qquad (5.18)$$

This integral cannot in general be computed analytically and numerical methods must be used.

Actual power curves are rather smooth and can be well approximated by a piecewise linear function with a few nodes. Using this approximation the power can be written as:

$$P(V) = \frac{P_{i+1}-P_i}{V_{i+1}-V_i}\,(V-V_i) + P_i \quad ; \quad V_i \leq V < V_{i+1} \tag{5.19}$$

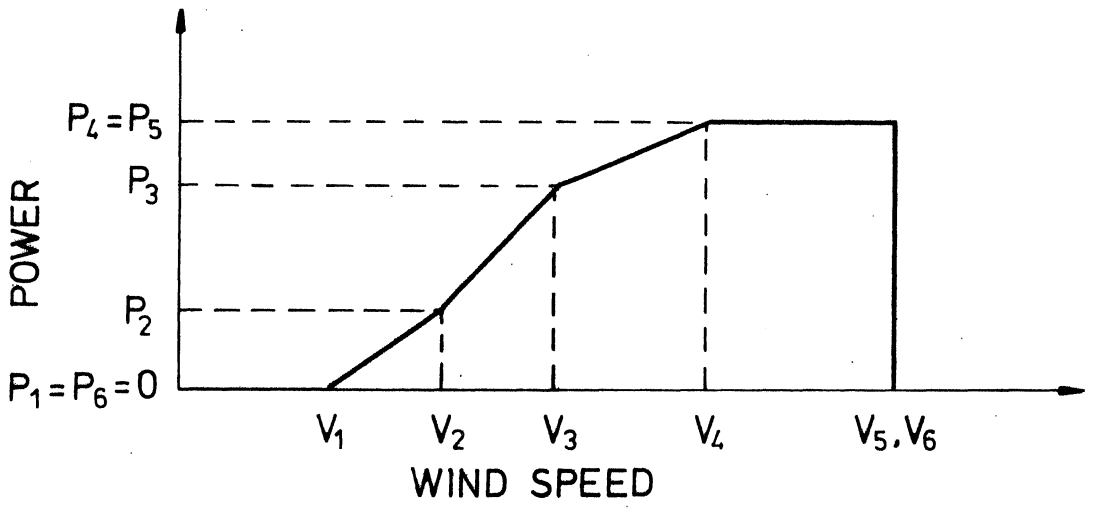

Fig. 5.11. Piecewise linear power curve

The integral in Eq. (5.18) can be simplified to

$$P = \int_0^\infty \exp(-x)\,P(V)\,dx \qquad \text{with} \qquad x = \left(\frac{V}{A}\right)^C. \tag{5.20}$$

By carrying out a partial integration this integral can be transformed to yield:

$$P = \left[-P(V)\exp(-x)\right]_0^\infty + \int_0^\infty \frac{dP}{dV} \cdot \frac{dV}{dx} \exp(-x)\,dx \qquad (5.21)$$

The first term is identically zero and with the piecewise linear power curve $\frac{dP}{dV}$, is piecewise constant. Introducing $\alpha_i = \frac{V_i}{A}$, the integral can be written as the sum:

$$P = \sum_i \frac{P_{i+1}-P_i}{V_{i+1}-V_i} \cdot \frac{1}{C} \cdot \int_{\alpha_i^C}^{\alpha_{i+1}^C} x^{\frac{1}{C}-1} \exp(-x)\,dx \qquad (5.22)$$

or

$$P = \sum_i \frac{P_{i+1}-P_i}{\alpha_{i+1}-\alpha_i} \cdot \left[\frac{1}{C}\,\gamma\left(\frac{1}{C},\ \alpha_{i+1}^C\right) - \frac{1}{C}\,\gamma\left(\frac{1}{C},\ \alpha_i^C\right)\right] \qquad (5.23)$$

where γ is the incomplete gamma function. Introducing $G_C(\alpha) = \frac{1}{C}\,\gamma(\frac{1}{C},\ \alpha^C)$, the expression for P can be more compactly written as:

$$P = \sum_i \frac{P_{i+1}-P_i}{\alpha_{i+1}-\alpha_i} \left[G_C(\alpha_{i+1}) - G_C(\alpha_i)\right] \qquad (5.24)$$

The function $G_C(\alpha)$ is tabulated in table A6. In some situations there is a discontinuity in the power curve (shown on figure 5.11 at $V_5 = V_6$). In the case of a jump in power from P_i to P_{i+1} at $V_i = V_{i+1}$ the contribution to the sum from this interval becomes

$$(P_{i+1} - P_i) \cdot \exp(-\alpha_i^C) \qquad (5.25)$$

By using Eqs. (5.24) and (5.25) the mean power can in principle be calculated for any power curve simply by dividing into a sufficient number of linear pieces. In practice the method will only be of use if the power curve can be approximated by a small number of linear pieces.

For many wind turbines the power curve is reasonably well approximated by the simple shape shown in 5.12.

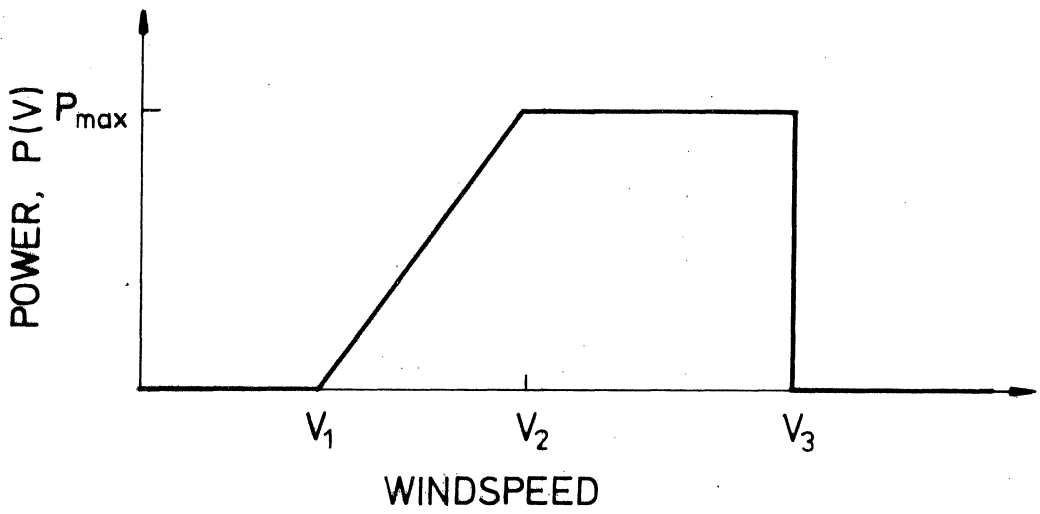

Fig. 5.12. Simple linear power curve

When the wind speed is less than V_1, the turbine will not be able to produce power (V_1 can be referred to as the starting speed). Between V_1 and V_2 the power output increases linearly with wind speed to the value P_{max} (rated power) at wind speed V_2; thereafter the output is constant until a (possible) maximum wind speed V_3 above which the turbine must be stopped for reasons of safety. The expression for the mean power becomes in this case

$$P = \frac{P_{max}}{\alpha_2 - \alpha_1} \left\{ G_C(\alpha_2) - G_C(\alpha_1) - \exp(-\alpha_3^C) \right\} . \qquad (5.26)$$

where

$$\alpha_1 = \frac{V_1}{A} \; ; \; \alpha_2 = \frac{V_2}{A} \; , \; \alpha_3 = \frac{V_3}{A} \qquad (5.27)$$

The function $G_C(\alpha)$ is tabulated in table A6. In practice the last term can often be neglected since the very high wind speeds at which the turbine must be stopped occur very infrequently.

Example 5.8

The power curve of the Gedser wind turbine has been measured and found to correspond quite accurately to the simple linear shape shown in fig. 5.12 with the parameters:

$V_1 = 5.7 \text{ ms}^{-1}$

$V_2 = 15 \text{ ms}^{-1}$

$P_{max} = 200 \text{ kW}.$

The hub height is 25 metres. The last term in Eq. (5.26), has been neglected (i.e. $V_3 = \infty$). The Gedser turbine is placed at a coast with the sea to the west, and the land sector has a roughness of class 2. The Weibull parameters are calculated as outlined in section 5.4:

Sector/ class	A	C	f	M	V^2	fM	fV^2
N 2	5.1	1.84	0.066	4.53	27.1	0.299	1.79
NE 2	5.3	1.92	0.092	4.70	28.6	0.432	2.63
E 2	6.0	2.23	0.127	5.32	34.6	0.676	4.39
SE 2	6.2	2.02	0.122	5.49	38.3	0.670	4.67
S 2	7.0	1.95	0.157	6.20	49.5	0.973	7.77
SW 0	9.7	2.06	0.172	8.59	93.0	1.478	16.00
W 0	10.0	2.03	0.198	8.86	99.4	1.754	19.68
NW 0	7.4	1.71	0.089	6.60	59.4	0.587	5.29
			1.02			6.87	62.2
						6.74	61.0
					$\frac{M^2}{V^2}$ =	0.744	

$C = 1.76$ (table A4)

$A = 6.74 \cdot F_A(1.76) = 7.6$ (table A5)

By using these parameters in Eqs. (5.27) and (5.26) the mean power output is computed by:

$\alpha_1 = \frac{5.7}{7.6} = 0.75$ then $G_C(\alpha_1) = 0.612$ (table A6)

$\alpha_2 = \frac{15}{7.6} = 1.97$ then $G_C(\alpha_2) = 0.879$ (table A6)

$\alpha_2 - \alpha_1 = 1.22$

from which it follows that

$$P = 200 \text{ kW} \cdot \frac{1}{1.22} \cdot (0.879 - 0.612) = 44 \text{ kW}.$$

This value can be compared with the value computed from wind speed measurements taken over the year 1978 at the Gedser site which is 40 kW. Note, that the starting speed V_1 should be used with care. The best results are obtained by calculating V_1 as $V_1 = \frac{2}{3} V_m$ (see section 5.10).

5.9.1. Power duration curve

From the Weibull parameters and the power curve the probability that the power will exceed a certain value can be calculated. The corresponding curve is called the power duration curve.

The probability that the power will exceed P between zero and P_{max} is given by

$$Pr(\text{Power} > P) = \exp(-(\frac{V_p}{A})^C) \qquad (5.28)$$

with

$$P = \frac{P_{max}}{V_2-V_1} (V_P-V_1) \quad \text{or} \quad V_P=V_1 + \frac{P}{P_{max}} (V_2-V_1)$$

then

$$Pr(\text{Power} > P) = \exp(-(\alpha_1 + \frac{P}{P_{max}} (\alpha_2-\alpha_1))^C) \; . \qquad (5.29)$$

Example 5.9

Using the parameters from the previous example the power duration curve for the Gedser wind turbine has been determined. The result is shown in fig. 5.13 together with the measured power duration curve for the year 1978. The curve shows that the turbine can be expected to produce 55% of the time. Furthermore, it can be expected to produce more than 100 kW 18% of the time, and to produce full power approximately 3% of the time.

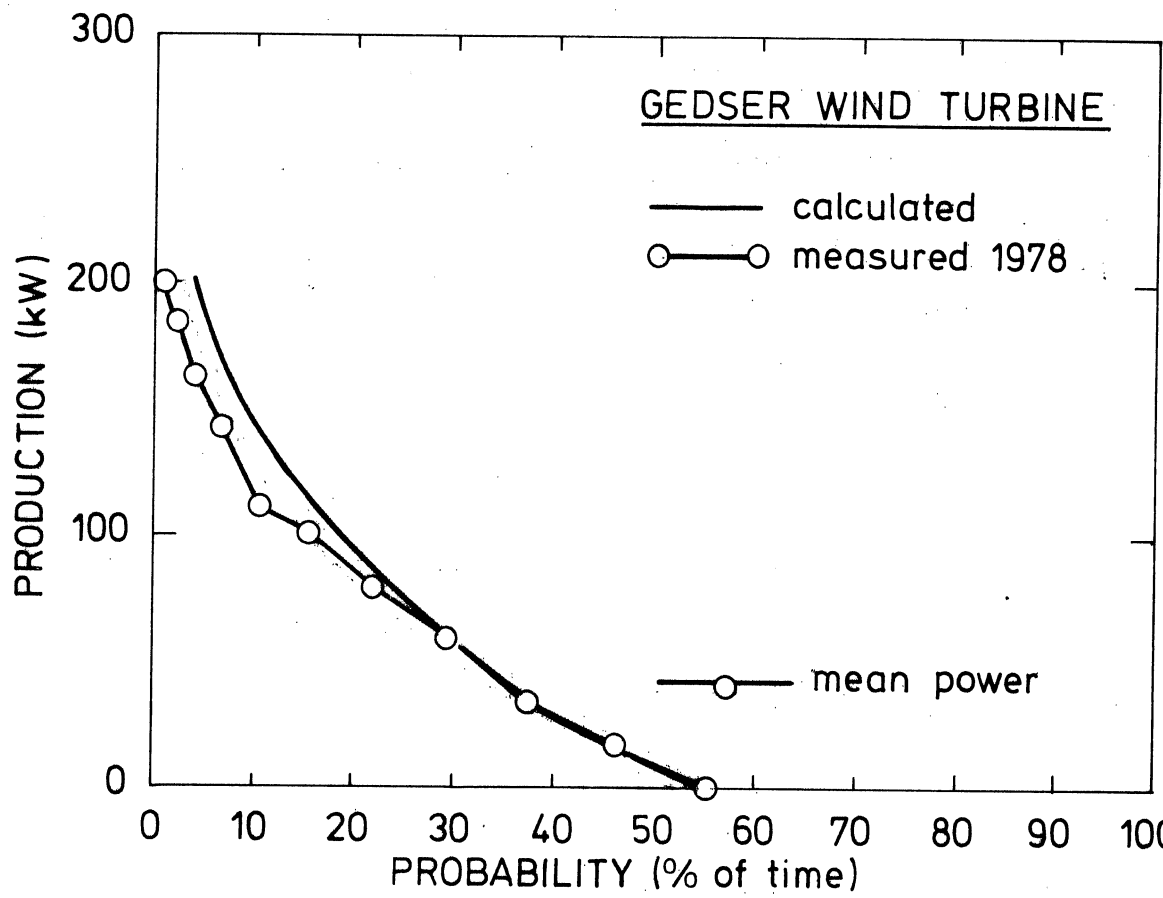

Fig. 5.13. Power duration curves for the Gedser wind turbine.

Example 5.10

A small wind turbine is to be placed in a homogeneous terrain of roughness class 1. The hub height is 18 meters and the power curve is measured to correspond to the simple linear shape with the parameters

starting speed $V_1 = 5\ ms^{-1}$

stalling speed $V_2 = 12\ ms^{-1}$

rated power $P_{max} = 50\ kW$

Since the terrain is assumed homogeneous the Weibull parameters can be read directly from the chart as:

$A = 6.9\ ms^{-1}$

$C = 1.85$

Using these as in example 5.8 the results are

$\alpha_1 = 0.72$ $\quad G_C(\alpha_1) = 0.594$

$\alpha_2 = 1.74$ $\quad G_C(\alpha_2) = 0.866$

$\alpha_2 - \alpha_1 = 1.02$

from which the mean power can be calculated as:

$$P = 50\ kW \cdot \frac{1}{1.02} \cdot (0.866 - 0.594) = 13.3\ kW$$

The corresponding calculation for the case where the same turbine is placed in a terrain of roughness class 2 yields

$P = 8.9\ kW$

The power duration curve can be calculated for both these situations as before; the results are shown in fig. 5.14.

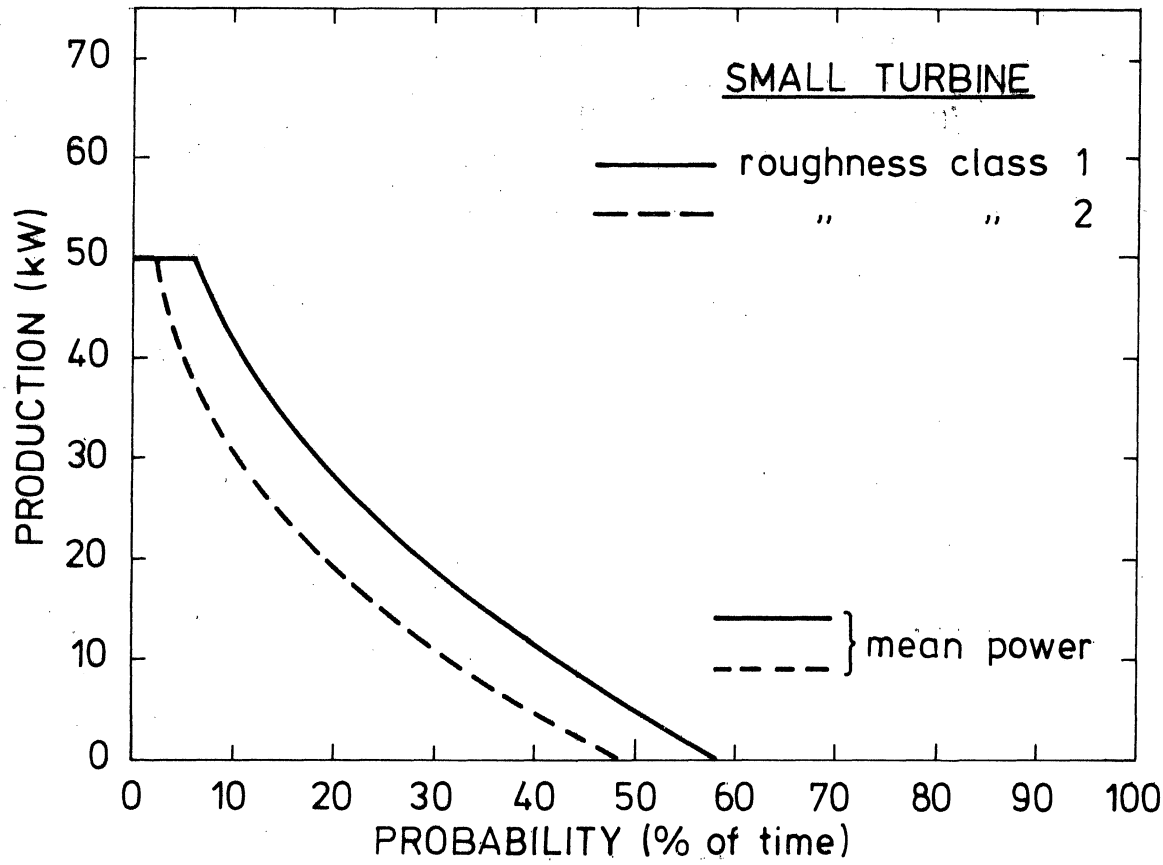

Fig. 5.14. Computed power duration curve for a small wind turbine placed in two different types of terrain.

5.9.2. Power density function

When designing wind turbines it is of interest to evaluate how different ranges of wind speeds will contribute to the power production. A very simple estimate can be made by evaluating the mean energy content in the wind for different wind speeds. The mean power density is given as

$$E(V) = \tfrac{1}{2}\rho\, V^3 \cdot Pr(V) \qquad (5.30)$$

where Pr(V) is the Weibull distribution corresponding to the situation considered. A graph of this function gives a picture of which wind speeds are important for the mean power production.

Example 5.11

At 10 meters height over a terrain of roughness class 1 the Weibull parameters are given as A = 6.2 ms^{-1} and C = 1.79. Introducing the parameters in Eq. (5.30) results in the graph labelled Windatlas in fig. 5.15. Also shown in fig. 5.15 is the measured power density E(V) from Ålborg Airport where there is a nearly ideal homogeneous terrain of roughness class 1 (flat grass field). The agreement between the measured and the estimated distributions is seen to be excellent, the difference in the total power density being less than 3%.

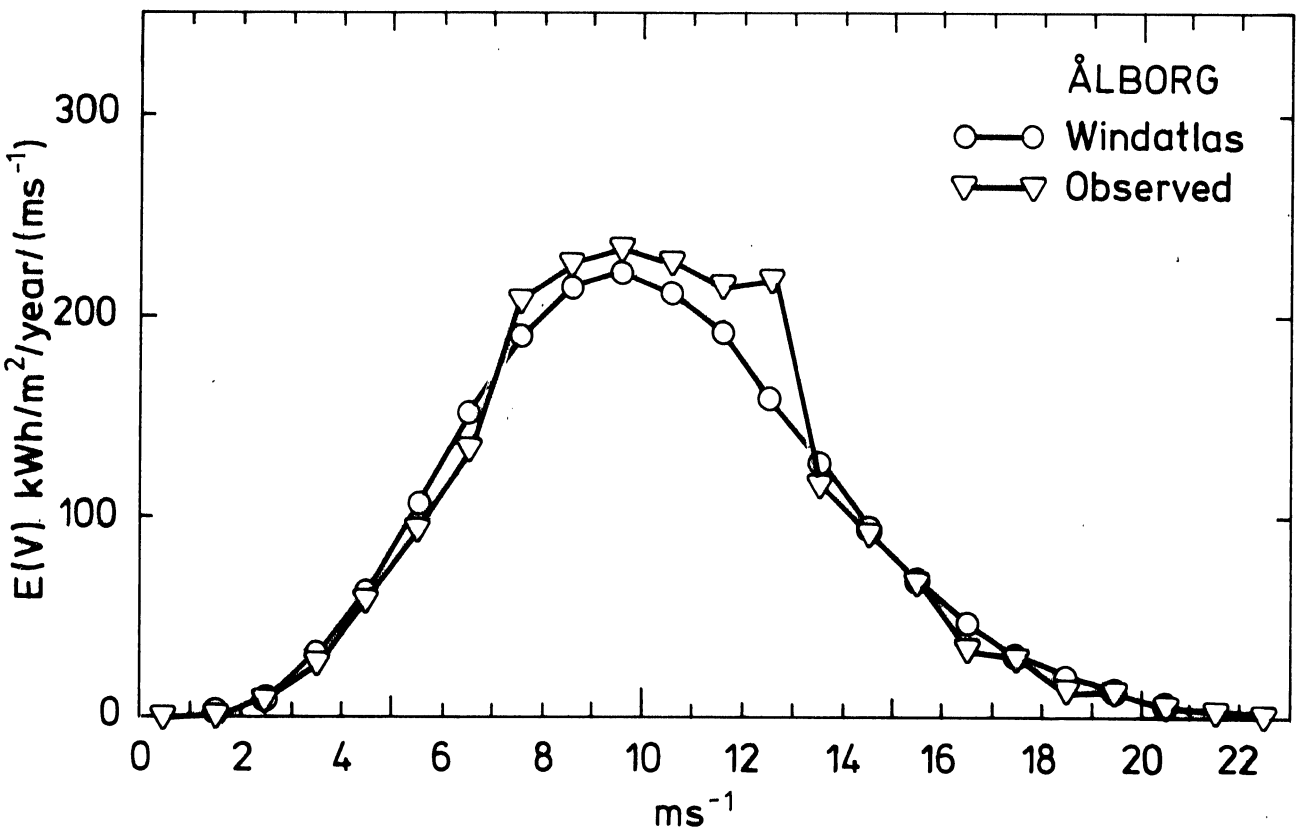

Fig. 5.15. Computed and measured power density functions for Ålborg Airport at 10 metres height.

5.10. Mean power and the choice of wind turbine parameters

For many applications it is useful to have a simple method for the estimation of the mean power output from a wind turbine. In section 5.9 it was shown how the mean production can be determined in a very simple manner directly from knowledge of the Weibull parameters when the power curve of the wind turbine is given by the simple piecewise linear shape shown in fig. 5.12. In this section this type of power curve is again employed in order to find a relation that expresses the mean power output as a function of the Weibull parameters and specific properties of the wind turbine.

The efficiency of a wind turbine is defined as the ratio of the actual power output at a given wind speed $P(V)$ to the total available power which passes through the swept area $E(V) \cdot A_R$. With the simple linear power curve the efficiency for $V_1 \leq V \leq V_2$ becomes:

$$\varepsilon(V) = \frac{P(V)}{E(V) \cdot A_R} = \frac{k(V-V_1)}{\frac{1}{2}\rho\, V^3 \cdot A_R} , \qquad (5.31)$$

where A_R is the swept area and k is the slope of the power curve ($k = P_{max}/(V_2-V_1)$). The efficiency has a maximum at wind speed V_m which can be determined by differentiating Eq. (5.31):

$$\frac{d\varepsilon}{dV} = \frac{k}{\frac{1}{2}\rho\, A_R\, V^4} (-2V + 3V_1)$$

The maximum efficiency occurs where this expression is zero; thus

$$V_m = \frac{3}{2} V_1 . \qquad (5.32)$$

Assuming that the maximum value of the efficiency $\varepsilon_m = \varepsilon(V_m)$ is known, the slope of the power curve can be found from Eq. (5.31) and Eq. (5.32) to be

$$k = \frac{3}{2} \rho \varepsilon_m \cdot A_R \cdot V_m^2 . \qquad (5.33)$$

The power curve can now be written as

$$P(V) = \frac{3}{2} \rho \varepsilon_m A_R \cdot V_m^2 \cdot (V - \frac{2}{3} V_m) \quad \text{for } V_1 \leq V \leq V_2$$

Substituting this expression into the expression for the mean power Eq. (5.26) yields the result:

$$P = \left[\tfrac{1}{2}\rho\varepsilon_m A_R \cdot A^3\right] \cdot \left[3\left(\frac{V_m}{A}\right)^2 \cdot \left\{G_C\left(\frac{V_2}{A}\right) - G_C\left(\frac{2}{3}\frac{V_m}{A}\right)\right\}\right] . \qquad (5.34)$$

This expression contains parameters which in a simple manner describe the wind turbine:

A_R = swept area
ε_m = maximum efficiency
V_m = wind speed at which the efficiency is maximum
V_2 = wind speed at which the power curve becomes constant.

It is important to note that the starting wind speed V_1 has been eliminated as a parameter. V_m should consequently <u>not</u> be calculated by means of Eq. (5.32), but rather by the actual wind speed at which the efficiency is maximum.

The right hand side of Eq. (5.34) consists of a product of two quantities $P = S \cdot K$ where

$$S = \tfrac{1}{2}\rho\varepsilon_m A^3 \cdot A_R \qquad (5.35)$$

is a scale factor, and

$$K = 3\alpha_m^2 \left\{G_C(\alpha_m + \delta) - G_C(\tfrac{2}{3}\alpha_m)\right\} \qquad (5.36)$$

where

$$\alpha_m = \frac{V_m}{A} \quad , \quad \alpha_m + \delta = \alpha_2 = \frac{V_2}{A} \qquad (5.37)$$

is the formfactor corresponding to the linear power curve. Equation (5.37) defines the quantity δ which is used in fig.

5.16. This figure shows the formfactor K as function of α_m and δ for four different choices of the parameter C. The graphs can be used directly to estimate mean power with the appropriate K value estimated from the graphs and P determined as $P = S \cdot K$ with S obtained from Eq. (5.35) (see example 5.12).

5.10.1. Optimization of design to maximum production

Obviously, the most advantageous shape of the power curve is the one for which the turbine has maximum efficiency at all wind speeds. In this case the power curve will not be linear but proportional to V^3 and the formfactor K becomes in this case a function of C only:

$$K = \Gamma(1 + \frac{3}{C}) \qquad (5.38)$$

C	1.5	1.6	1.7	1.8	1.9	2.0	2.1	2.2	2.3	2.4
K	2.00	1.79	1.63	1.50	1.41	1.33	1.27	1.21	1.17	1.13

Table 5.2. Formfactor for cubic power curve $P \propto V^3$.

Comparing with the formfactors corresponding to the linear power curve from fig. 5.16, it is seen that if α_m, δ and ε_m can be chosen independently it is possible to obtain a formfactor which is between 70% and 80% of the maximum, depending on C. This means that it is possible to obtain a mean efficiency for a wind turbine with linear power curve of approximately 75% of the maximum possible value. This is of interest since the linear power curve is a good representation of actual power curves for stall regulated horizontal axis propeller wind turbines with fixed blade pitch angle.

It is possible to show that for values of δ larger than 1 the best choice for α_m becomes

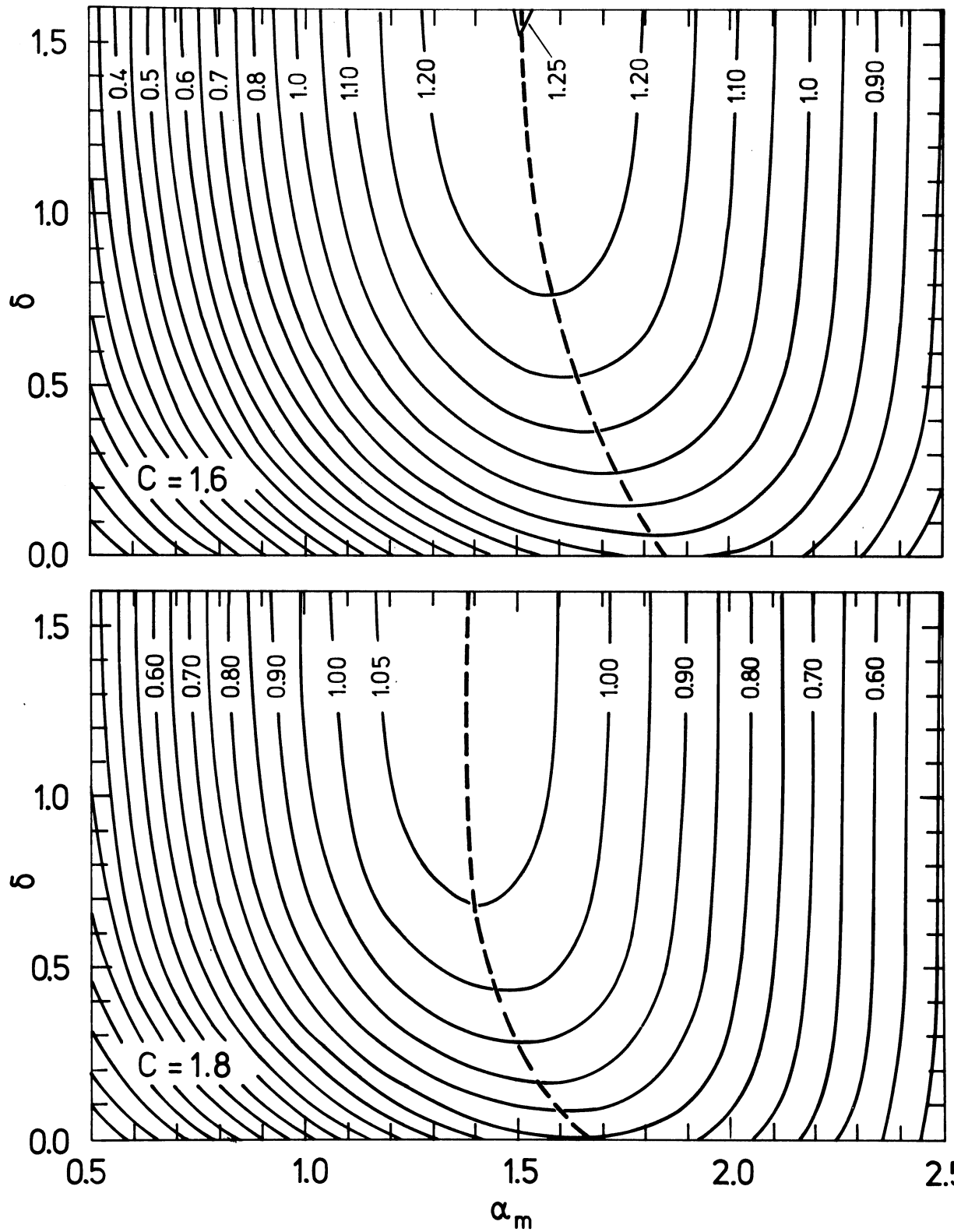

Fig. 5.16. The formfactor K as function of α_m and δ for four different values of the C parameter. The full lines are lines of a constant value of K indicated on each curve. The dashed lines shows the optimum value of α_m as function of δ.

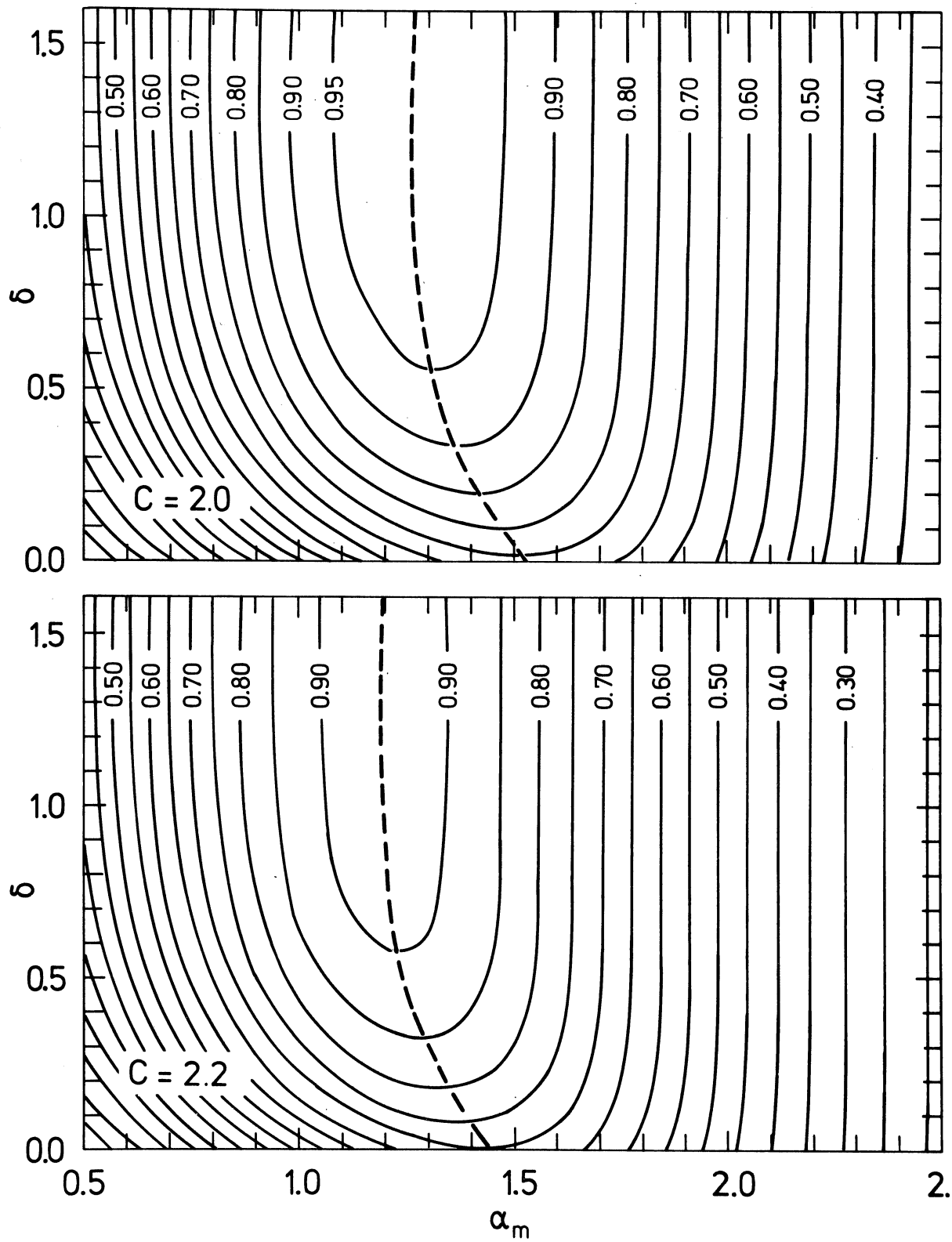

Fig. 5.16. Continued

$$\alpha_m = \left(\left(\frac{C+2}{C}\right)^{\frac{1}{C}} - 0.15\right) . \qquad (5.39)$$

This expression is not exact, but sufficiently accurate for realistic values for C. The first term in the parenthesis gives the wind speed scaled with A at which there is a maximum of the power density function for the wind (cf. section 5.9.2). The expression thus shows, that the maximum efficiency should be chosen at a wind speed somewhat lower than that corresponding to the maximum in the power density function of the wind. For smaller values of δ, the optimum value for V_m moves closer to the maximum in the power density curve for the wind, as can be seen in fig. 5.16. Each figure corresponds to one value of C and shows the formfactor K as function of α_m and δ. The dashed lines gives the optimum value of α_m as function of δ and the full lines are curves of a constant value of K as indicated on each curve.

Example 5.12

To illustrate the use of the above method for the estimation of mean production, data have been taken for four different large wind turbines and the mean power has been estimated using these data. The data are taken from Lundsager, Frandsen and Christensen (1980). The four wind turbines are: The Swedish wind turbine at "Kalkugnen", the American wind turbine "Mod-0", and the Danish wind turbines at Gedser and at Nibe (Nibe-A). The report contains a detailed calculation of the mean power output based on the measured power curves for the various wind turbines and for different choices of the Weibull parameters. This makes it possible to estimate the accuracy of the simple method described above.

Using C=2 and selecting for each wind turbine a value of A such that the measured value of V_m corresponds to the optimum choice according to Eq. (5.39) i.e. $\alpha_m = \frac{V_m}{A} = 1.26$ for C=2), leads to the results summarized in the table 5.3 below. The deviation of the results obtained by the simple procedure using K from

Table 5.3. Calculation of mean power as $P = S \cdot K$, where $S = \frac{1}{2}\rho\varepsilon_m A^3 \cdot A_R$ and K is estimated from figure 5.16.

Turbine	A ms^{-1}	C	V_m* ms^{-1}	V_2* ms^{-1}	A_R* m^2	ε_m*	α_m	δ	S kW	K	P kW	P' kW	P_m*	Δ
Kalkugnen	7.5	2.	9.5	11	254	0.32	1.26	0.21	21	0.83	17	28	19	11
Gedser	6.8	2.	8.5	15.5	452	0.32	1.26	1.02	28	0.95	27	37	28	4
Nibe-A	8.7	2.	11	15	1257	0.29	1.26	0.46	148	0.92	136	197	149	9
Mod-OA	6.0	2.	7.5	9.5	1134	0.33	1.26	0.32	50	0.88	44	66	49	10

P = computed mean power based on the assumption of a linear power curve.
P' = mean power if the efficiency of the turbines were equal to ε_m at all wind speeds.
P_m = mean power computed on basis of actual measured power curve.
Δ = percent deviation between P and P_m ($\Delta = (P_m - P)/P_m \times 100\%$).
Parameters marked with an asterisk are taken from Lundsager, Frandsen and Christensen (1980). Note that the wind speed distributions utilized differ from the actual wind speed distributions at the four sites. For this reason the values of the mean power in this table differ from the true values.

fig. 5.16 and the more accurate method only amounts to a few per cent. It should be noted, however, that the deviation becomes larger when the actual power curve deviates from the linear shape, and also when V_m is different from the optimum (according to Eq. (5.39)). For example, the deviation (Δ in table 5.3) becomes 15% if A = 8 ms^{-1} is used for the "Nibe-A" wind turbine, and the deviation Δ for the wind turbine "Kalkugnen" becomes 22% if A is 6 ms^{-1}.

5.10.2. Preliminary design considerations

The method described in the preceding section can be of use in preliminary investigations of the possibilities for the use of wind power to meet a certain need.

Traditionally, the procedure followed in such investigations is to calculate the mean production from one or more existing (or possibly only designed) wind turbines, and then select the turbine which seems the most appropriate for the purpose.

It can, however, be advantageous to take the starting point as the desired mean production, and from that deduce necessary specifications for the wind turbine. A possible procedure is to first decide on the desired mean power P and the site for the turbine, and to guess a reasonable hub height H. It is then possible to find appropriate values for the Weibull parameters as described in the bulk of this chapter. From Eq. (5.39) a first estimate of the best choice for V_m can now be obtained using $V_m = \alpha_m \cdot A$. The formfactor K can now be evaluated from Eq. (5.36) where a reasonable value for V_2 must be employed. Alternatively K can be read directly from fig. 5.16, which also makes it possible to evaluate the sensitivity of K to the choice for V_2. (Typical values for V_2 range between 12 to 15 ms^{-1}). From fig. 5.16 it is seen that if V_2 can be chosen larger than approximately twice V_m which is equivalent to the condition $\delta > 1$, the exact value for V_2 is of little importance.

The maximum efficiency ε_m is a parameter which is largely determined by the type of wind turbine. At this point in the

design considerations the wind turbine type should be chosen, together with a reasonable value for ε_m. (For horizontal axis propeller types, ε_m ranges between 0.25 and 0.40).

With the mean power P known, the necessary swept area A_R can be calculated using Eqs. (5.35) and (5.36). If the required rotor diameter is unrealistic when compared to the chosen hub height a new calculation is necessary.

When the above procedure has been satisfactorily carried out, a first rough estimate of the parameters describing an appropriate wind turbine will have been established. If the assumption that the power curve is approximately linear can be maintained and V_2 is sufficiently large compared to V_m, then the turbine has been optimized with respect to the chosen site and hub height.

The adjustment of the wind turbine parameters to the terrain at the site is expressed in the difference between the optimum value for V_m (Eq. 5.39) and the actual value. A small difference does not, however, have appreciable effect (cf. fig. 5.16).

The procedure is summarized below:

1) Decision about desired mean power P.
2) Choice of site and hub height (H).
3) Calculation of Weibull parameters A and C.
4) Determination of the wind speed V_m at which the efficiency must be at maximum. (Eq. 5.39).
5) Acquisition of wind turbine data giving realistic values for ε_m and V_2.
6) Calculation of K from Eq. (5.36) or from fig. 5.16.
7) Calculation of necessary swept area from Eq. (5.35).
8) Evaluation of whether the diameter is unrealistic when compared to the hub height. Typically, the rotor diameter must be in the interval from H/2 to H.
9) Recalculation from point 2) until 8) is satisfied.
10) A more accurate mean power calculation is made as described in section (5.9) using the final design.

This procedure is illustrated by the following example:

Example 5.13

It is desired to have a mean power from a wind turbine of 30,000 kWh per year. This corresponds to the mean power

1) $P = 30{,}000 \text{ kWh}/8760 \text{ h} = 3420 \text{ W}$.

The terrain where the turbine has to be placed is homogeneous and of roughness class 1.

2) The hub height is set to 10 metres.
3) From Appendix A the appropriate values of A and C are obtained:

   $A = 6.2 \text{ ms}^{-1}$ and $C = 1.79$

4) V_m is calculated using Eq. (5.39):

$$\alpha_m = \left(\left(\frac{3.79}{1.79}\right)^{\frac{1}{1.79}} - 0.15\right) = 1.37 \Rightarrow V_m = 1.37 \cdot A = 8.5 \text{ ms}^{-1}$$

5) The turbine is chosen to be a horizontal axis turbine with $\varepsilon_m = 0.3$ and $V_2 = 14 \text{ ms}^{-1}$.

6) From table A6, $G_C\left(\frac{V_2}{A}\right)$ and $G_C\left(\frac{2}{3}\frac{V_m}{A}\right)$ are found as $G_C\left(\frac{V_2}{A}\right) = 0.89$ and $G_C\left(\frac{2}{3}\frac{V_m}{A}\right) = 0.69$.

From these K is calculated to be

$$K = 3\left(\frac{V_m}{A}\right)^2\left\{G_C\left(\frac{V_m}{A}\right) - G_C\left(\frac{2}{3}\frac{V_m}{A}\right)\right\} = 1.13.$$

7) The necessary swept area is now be found from Eq. (5.35) as $A_R = P_m/(\frac{1}{2}\rho A^3 \cdot \varepsilon_m \cdot K) = 69 \text{ m}^2$ and $R = 4.7$ m.

A possible solution could thus be a construction with hub height 10 m, $V_m \simeq 8.5 \text{ ms}^{-1}$, $\varepsilon_m = 0.3$, $V_2 = 14 \text{ ms}^{-1}$ and radius $R = 4.7$ m.

6. VERIFICATION

This chapter presents a comparison between the distributions of wind speed predicted by the Windatlas and those which have actually been measured at nine airport stations evenly distributed over Denmark, at two tall meteorological masts and at one lightship. The airport stations were selected because of the sufficiently long, high quality measurement series available from these stations. The series consist primarily of 10 minute averages measured every third hour at a height of 10 meters over a relatively well-defined terrain. The measurements from the meteorological masts at Risø and Sprogø were especially valuable for comparison with the calculated height variation of the Weibull parameters, while data from the lightship Horns Rev (former Vyl) also made it possible to compare the predictions of the Windatlas with measurements over open water.

The primary purpose of the comparisons was to test the following three aspects of the Windatlas:

1) Whether the roughness classes employed were appropriately chosen.
2) Whether geographical variations over Denmark could be ignored.
3) Whether the similarity models were accurate and appropriate.

It is not possible to test these points independently by means of the chosen data series. However, since the similarity functions and the velocity and temperature profiles employed for use in the geostrophic resistance law were determined independently, and since the series did not enter into the Windatlas analyses, a comparison between Windatlas predictions and the measurements can be considered to be a reasonable test of all three points.

The roughness classification scheme is best tested by using the data from those areas displaying the most homogeneous roughness;

namely, Ålborg airport (roughness class 1), Tirstrup (roughness class 3 in the Southerly sectors), and Karup (roughness class 1). The airports are evenly distributed across the country; therefore, a systematic variation of the wind speed distribution across the country should be evident in deviations between the measured and predicted distributions. As has already been discussed in Chapter 4, no such deviations in either wind speed or wind direction distributions were present (other than those ascribable to the method of analysis).

While such geographical effects may still be present, they are so small that they are obscured by the uncertainties arising from the roughness classification and the natural variations of roughness within a particular area. It should be noted that only the surface winds are strongly influenced by the (local) surface conditions within a few hundred meters of the measuring point. At greater heights, however, the wind speeds are dependent on the surface roughness properties over a larger area, and therefore the small complicated details of the landscape can often be neglected.

A proper verification of the profile expressions and the resulting vertical variation of the Weibull parameters with height requires a comparison with data from heights greater than those normally available from the synoptic network. As a result, there are fewer possibilities for this kind of comparison, and there is little opportunity to look for geographical variations. As was mentioned in Chapter 2, the data from the meteorological mast at Risø was used to determine the atmospheric stability. However, since only the data from the lowest level (7-11 m) was used, the wind speed data from the 76 m level can be used for a reasonably independent verification. The meteorological mast on the island of Sprogø in the Great Belt (body of water between Zealand and Funen) is both sufficiently high for the height verification and has an ideal location with open water in all directions except the Westward sector. The location of the Sprogø mast also provides a further test of the Windatlas predictions in open water areas.

For each of the stations considered below, the period over which the observations were made is noted and a brief description of terrain surrounding the measuring site is given. In the accompanying figure, the observed frequencies of occurence of the wind speeds are presented as histograms in speed intervals of 1 m/s. The computed Weibull distributions are shown as continuous curves which ideally should pass through the midpoints of the histogram values. The figure also notes the roughness class used in the calculations. In those cases where roughness changes were present in one or more sectors, both the distance to the roughness change and the roughness before the change are given.

This chapter also includes comparisons with two other sets of measurements: The measurements taken by Martin Jensen in 1960 at three sites in Denmark,and measurements from the Cabauw mast in the Netherlands.

Ålborg Airport

The measurement series covers the period January 1, 1965 to December 12, 1977, and the measurements were taken at a height of 10 m.

The terrain surrounding the measurement site consists of grassy fields with scattered bushes and trees. The terrain is homogeneous in all directions and is accordingly assigned roughness class 1. Among all the airports for which data are available, this site is the best for verifying the Windatlas predictions for uniform roughness.

The comparison is done both for all wind directions and for the eight wind direction sectors separately. Further, an illustration is given of the difference between wind speed probabilities measured at night and day respectively.

The Weibull parameters are computed for roughness class 1 (z_0 = 1 cm) and for the half classes above and below it (z_0 = 2 cm, z_0 = 0.5 cm). The results are:

z_o = 2 cm : A = 5.8 ms^{-1}, C = 1.79

z_o = 1 cm : A = 6.2 ms^{-1}, C = 1.79

z_o = 0.5 cm: A = 6.5 ms^{-1}, C = 1.79

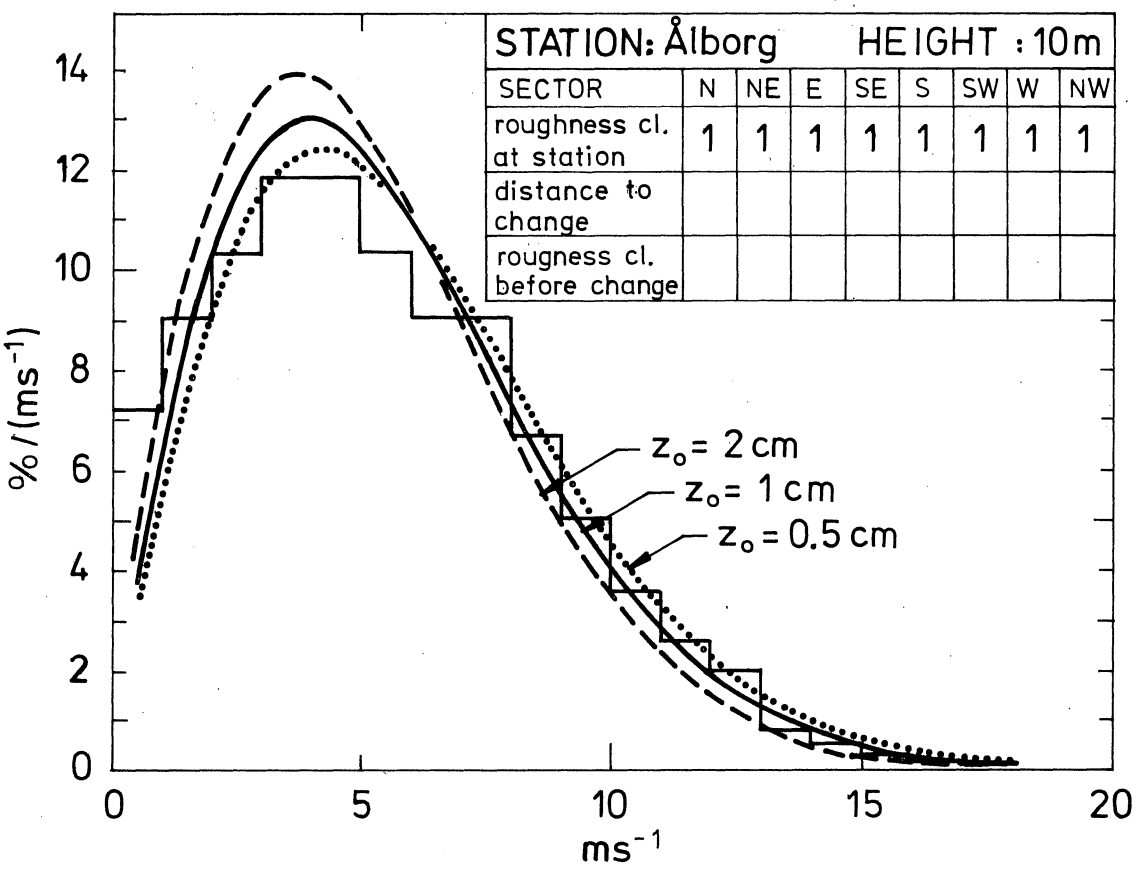
STATION: Ålborg HEIGHT : 10m
SECTOR N NE E SE S SW W NW
roughness cl. at station 1 1 1 1 1 1 1 1
distance to change
roughness cl. before change
z_o = 2 cm
z_o = 1 cm
z_o = 0.5 cm
%/(ms^{-1})
ms^{-1}
0 2 4 6 8 10 12 14
0 5 10 15 20

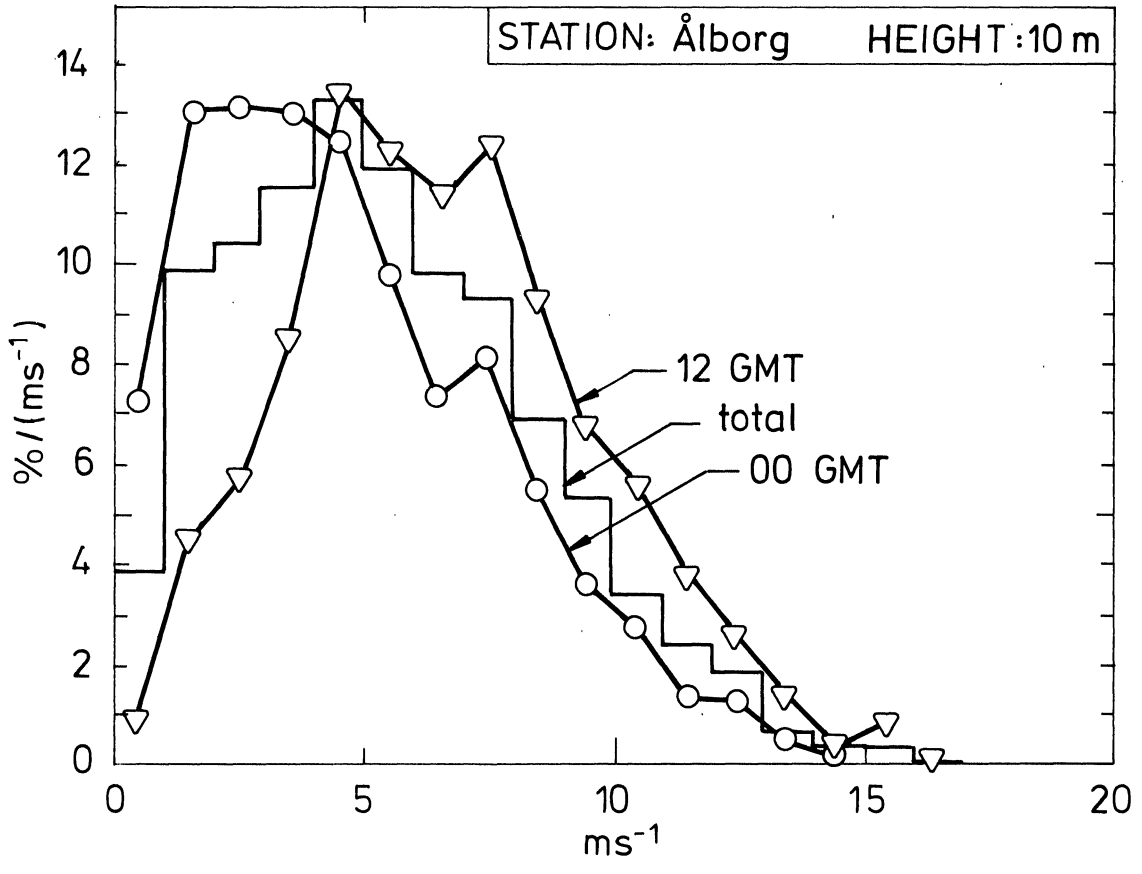
STATION: Ålborg HEIGHT : 10 m
12 GMT
total
00 GMT
%/(ms^{-1})
ms^{-1}
0 2 4 6 8 10 12 14
0 5 10 15 20

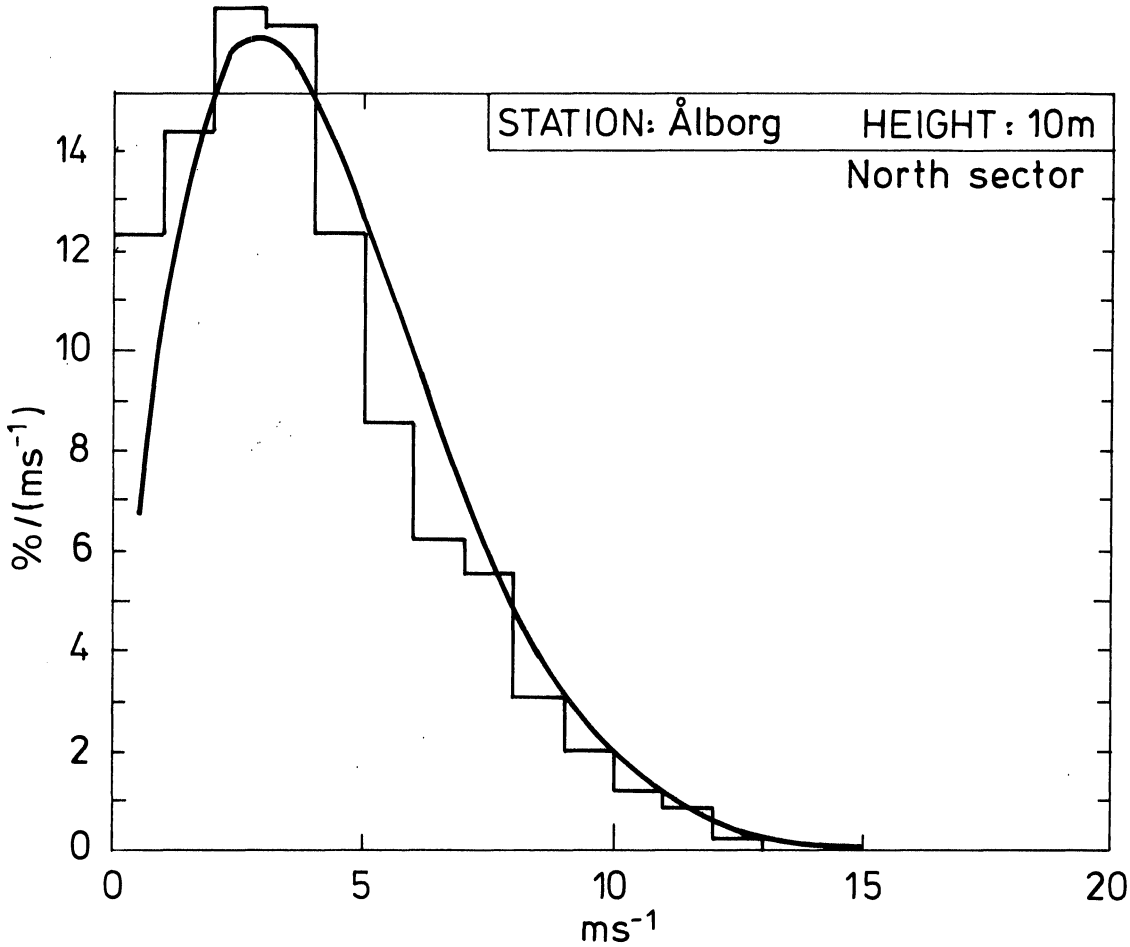
STATION: Ålborg
HEIGHT: 10m
North sector
%/(ms-1)
ms-1
0
2
4
6
8
10
12
14
0
5
10
15
20

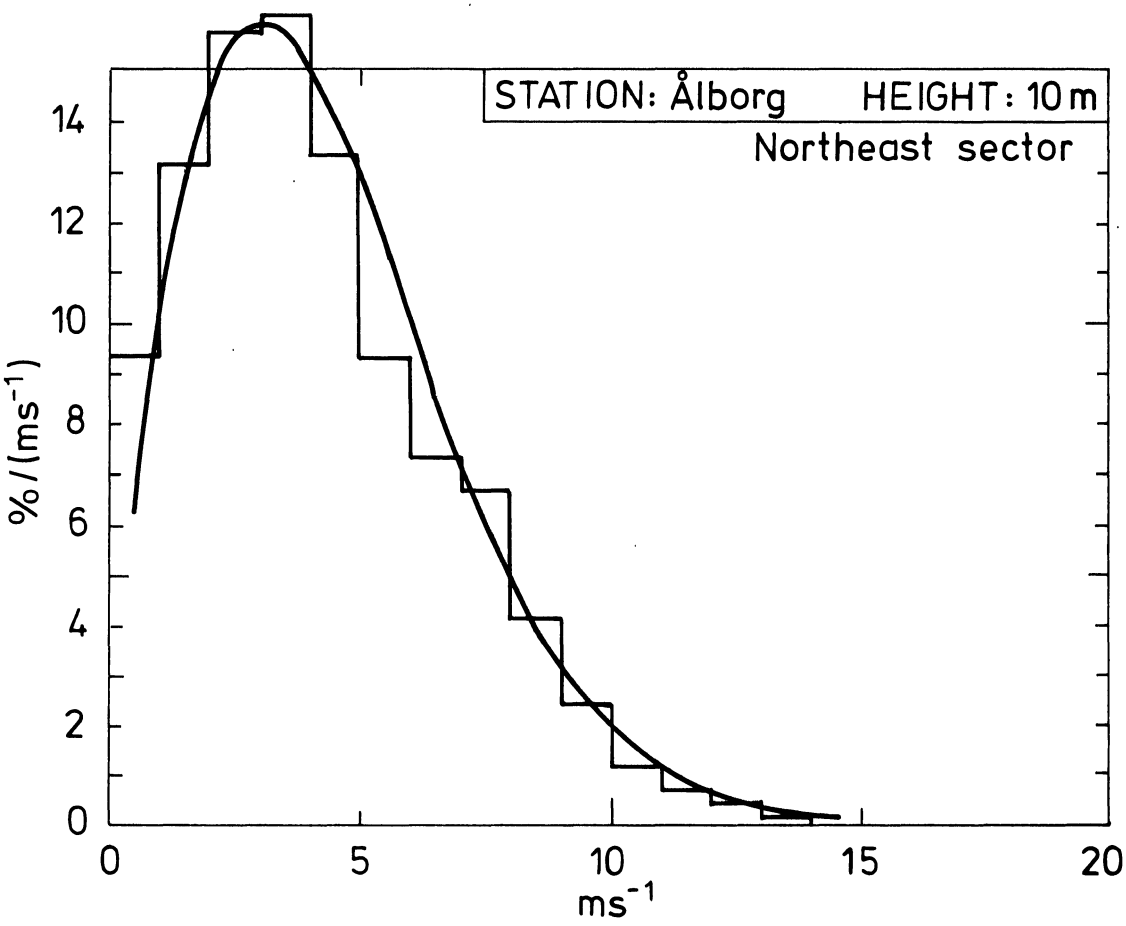
STATION: Ålborg
HEIGHT: 10m
Northeast sector
%/(ms-1)
ms-1
0
2
4
6
8
10
12
14
0
5
10
15
20

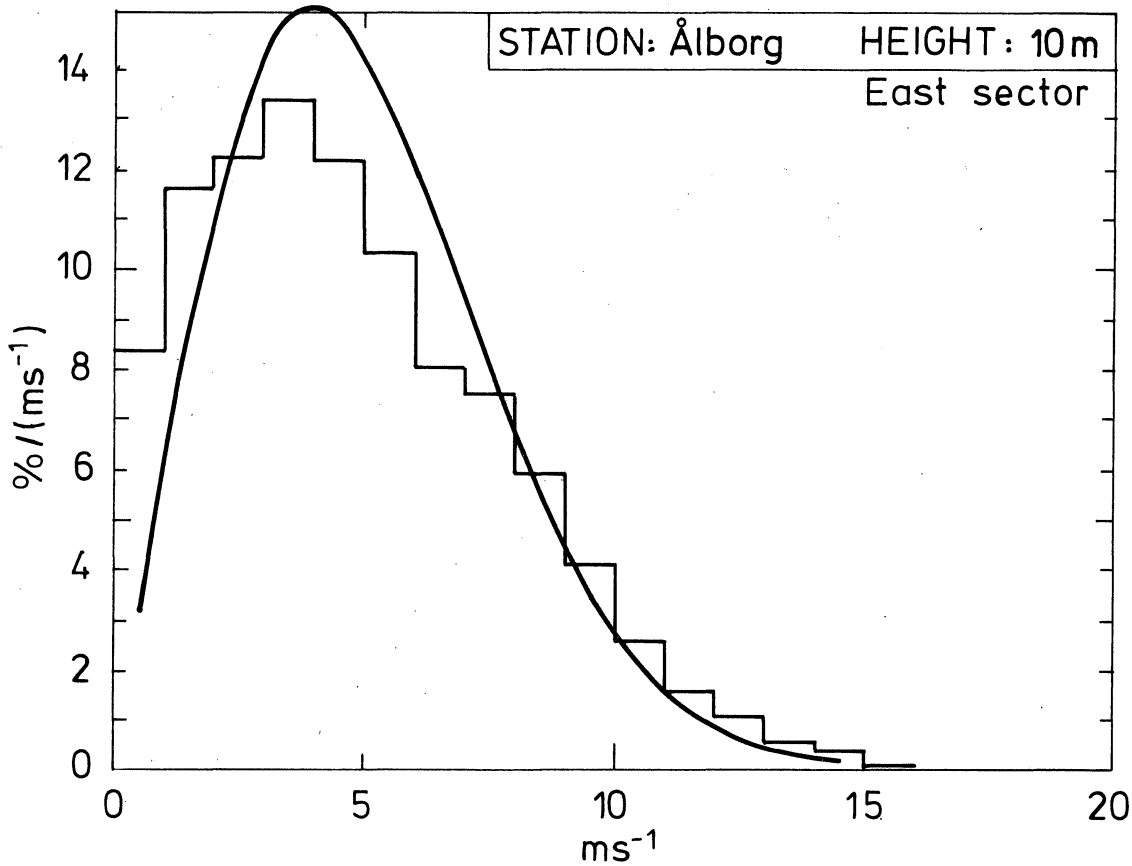
STATION: Ålborg HEIGHT: 10m
East sector
%/(ms-1)
ms-1
0
2
4
6
8
10
12
14
0
5
10
15
20

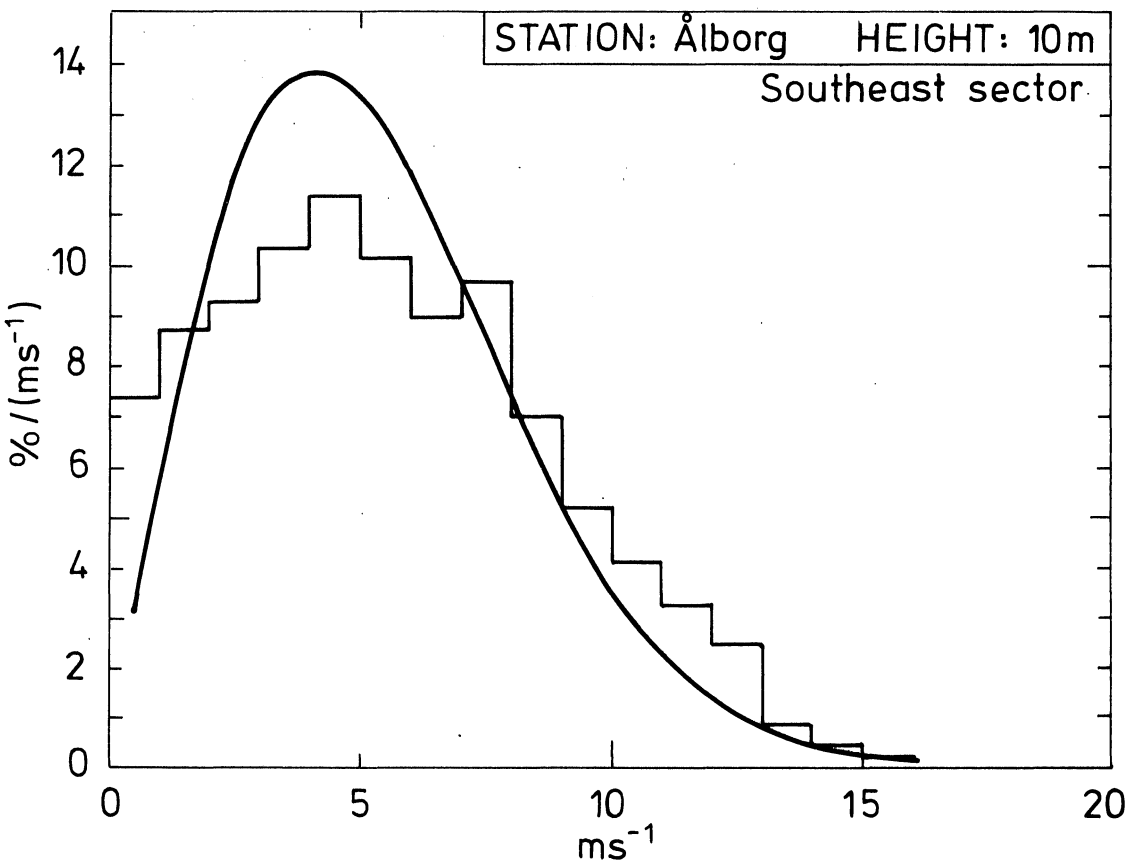
STATION: Ålborg HEIGHT: 10m
Southeast sector
%/(ms-1)
ms-1
0
2
4
6
8
10
12
14
0
5
10
15
20

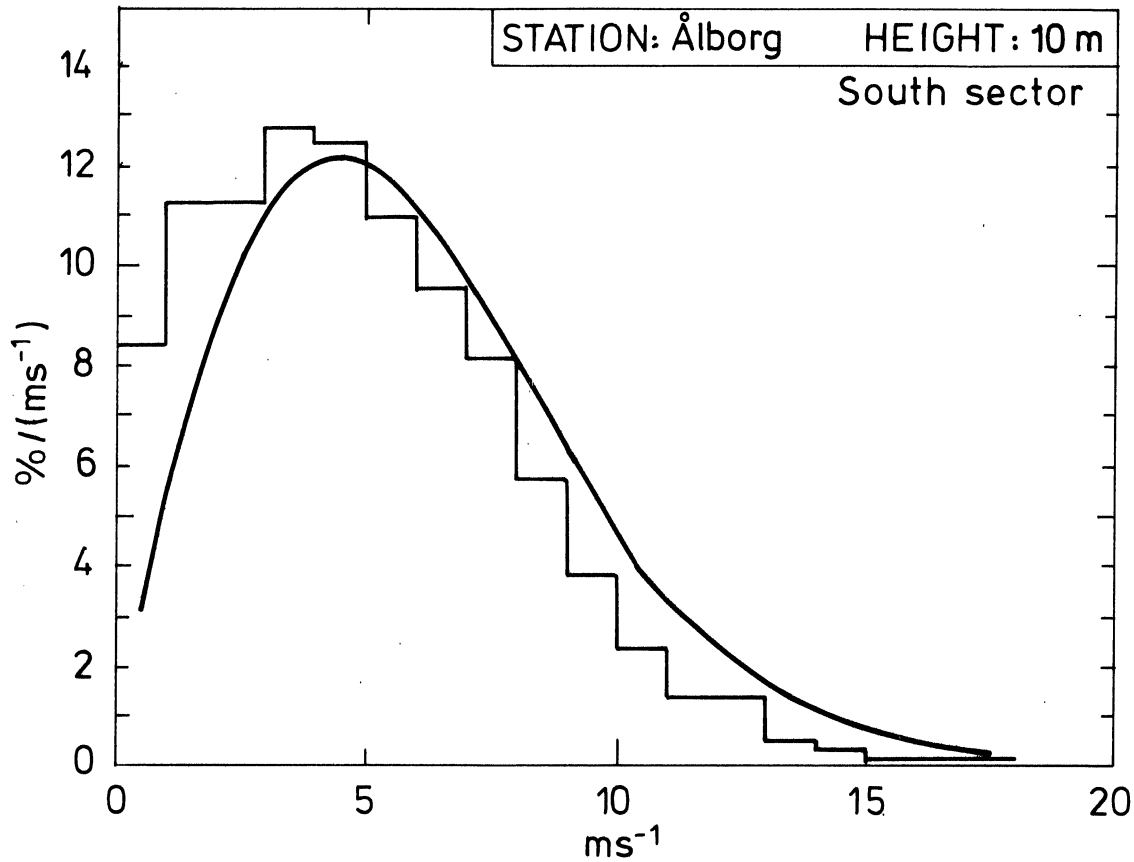
STATION: Ålborg
HEIGHT: 10 m
South sector
%/(ms⁻¹)
ms⁻¹
0
2
4
6
8
10
12
14
0
5
10
15
20

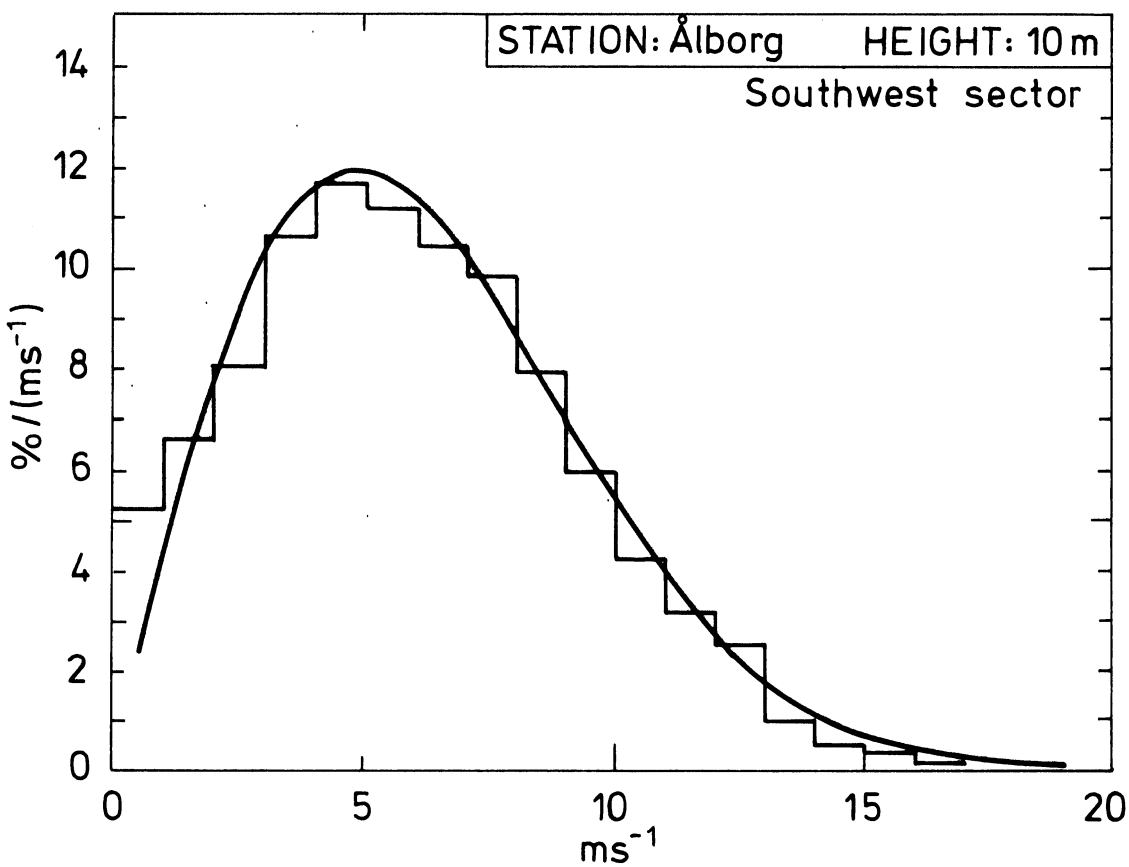
STATION: Ålborg
HEIGHT: 10 m
Southwest sector
%/(ms⁻¹)
ms⁻¹
0
2
4
6
8
10
12
14
0
5
10
15
20

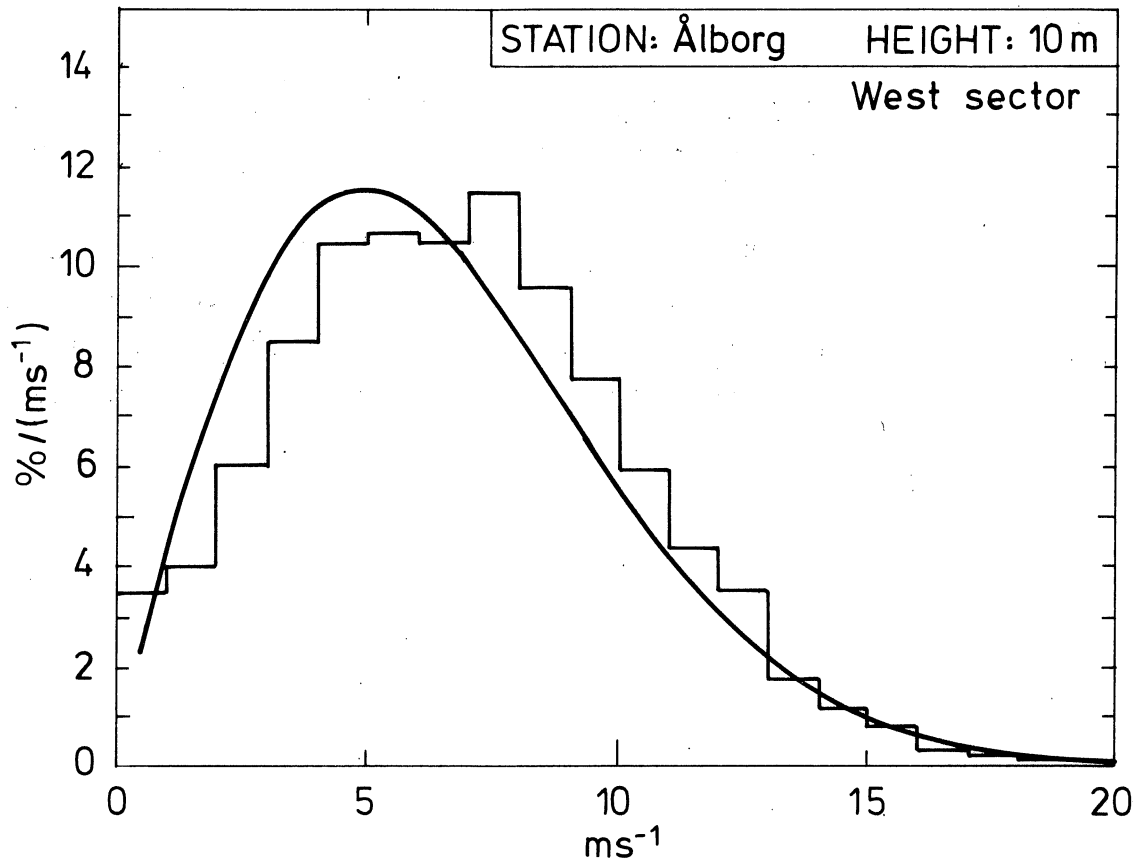
STATION: Ålborg HEIGHT: 10 m
West sector
%/(ms⁻¹)
ms⁻¹
0
2
4
6
8
10
12
14
0
5
10
15
20

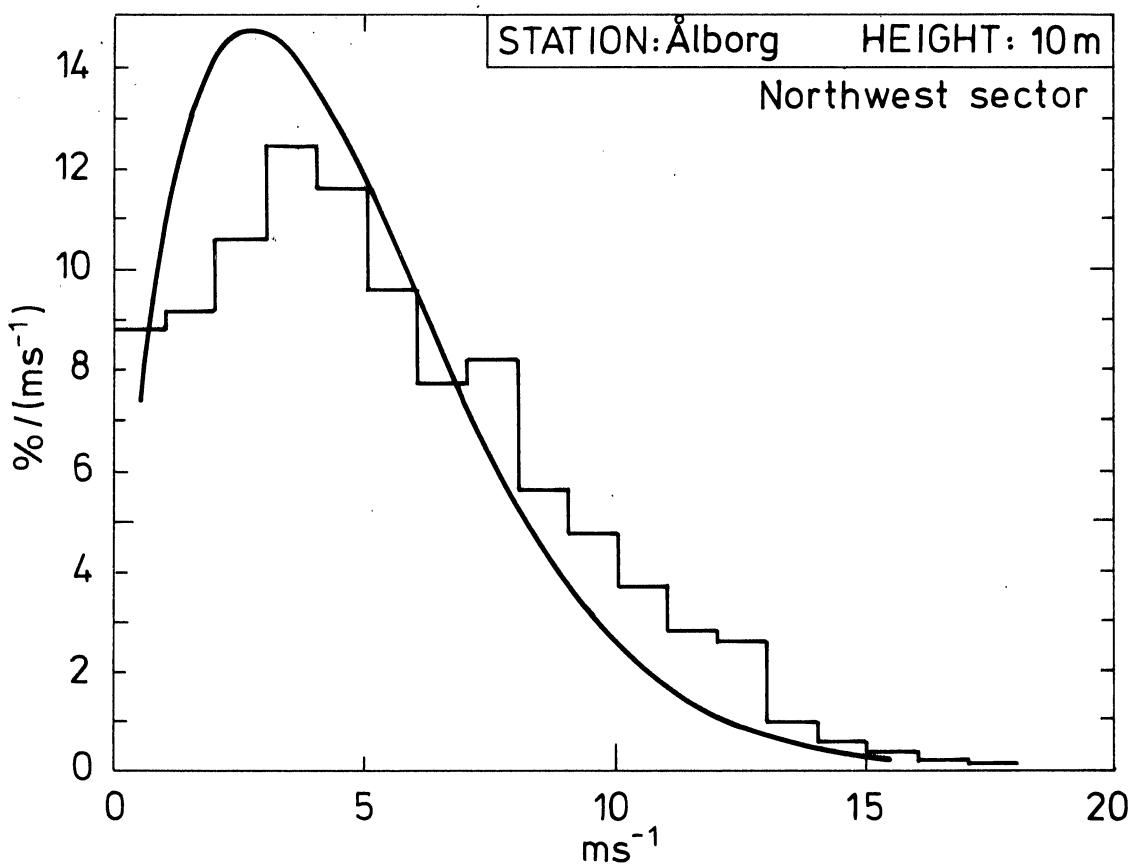
STATION: Ålborg HEIGHT: 10 m
Northwest sector
%/(ms⁻¹)
ms⁻¹
0
2
4
6
8
10
12
14
0
5
10
15
20

Karup Airport

The measurement series covers the period Oct. 10, 1971 to Dec. 31, 1977, and the measurements were taken at a height of 10 m.

Roughness class 1 is used for all sectors. However, in the NW, W, and NE sectors, stands of trees give rise to a roughness change at a distance of 300 m. The parts of these sectors before the roughness change are accordingly assigned roughness class 3.

The Weibull parameters are estimated as:

$$A = 5.9 \text{ ms}^{-1} \quad , \quad C = 1.69$$

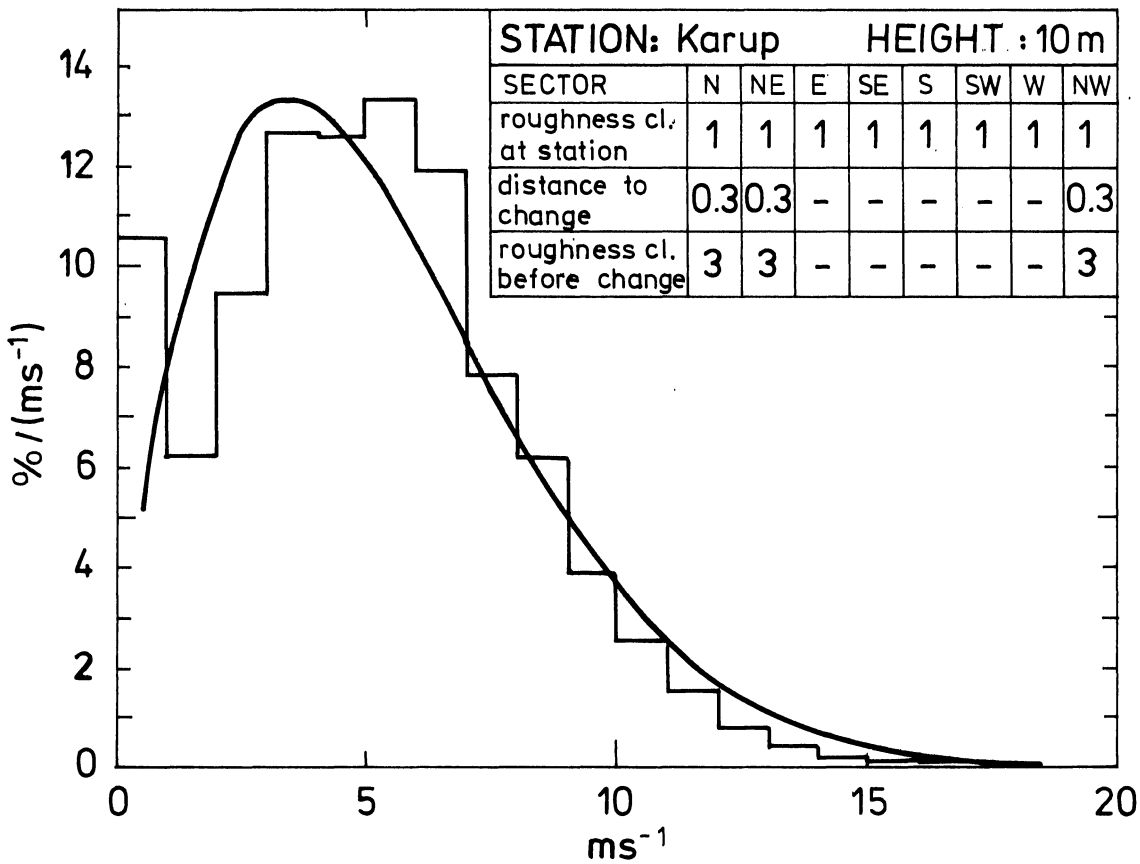

Skrydstrup Airport

The measurement interval was from September 1, 1969 to December 31, 1977, and the measurements were made at a height of 9 m.

The terrain surrounding the measuring site consists primarily of flat grassy fields. However, at a distance of only 200 m in several sectors there is a partial blockage of the wind by buildings and rows of trees. These effects can not be accounted for by a roughness change. The correction of the Weibull parameters for this data has been presented in Chapter 5 (example 5.7) as an illustration of the procedure for analyzing shelter effects.

The estimated Weibull parameters are:

Without shelter reduction: $A = 6.1\ ms^{-1}$; $C = 1.78$
With shelter reduction : $A = 5.4\ ms^{-1}$; $C = 1.71$

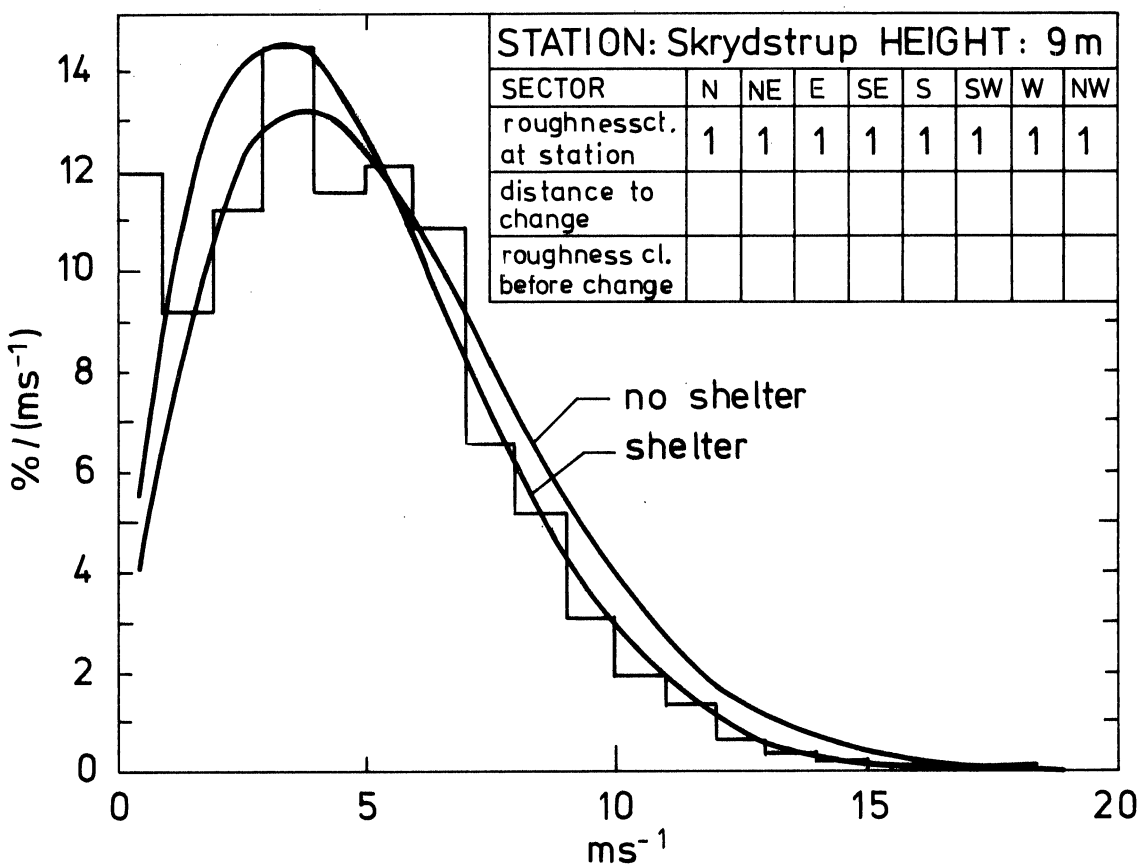

Tirstrup Airport

The measurement series covers the period from July 9, 1970 to December 31, 1977, and the measurements were made at a height of 10 m.

In the NW, N, NE, E and SE sectors the terrain is open and of roughness class 1. In the S and SW sectors are stands of fir trees at a distance of 50 m from the measuring site; accordingly, these sectors are assigned roughness class 3. The West sector is also partly influenced by the continuation of one of these stands to about 270°. To compensate for this influence, a roughness class of 2 is chosen as a compromise between 1 and 3.

The Weibull parameters are estimated as:

$A = 5.2\ ms^{-1}$; $C = 1.80$

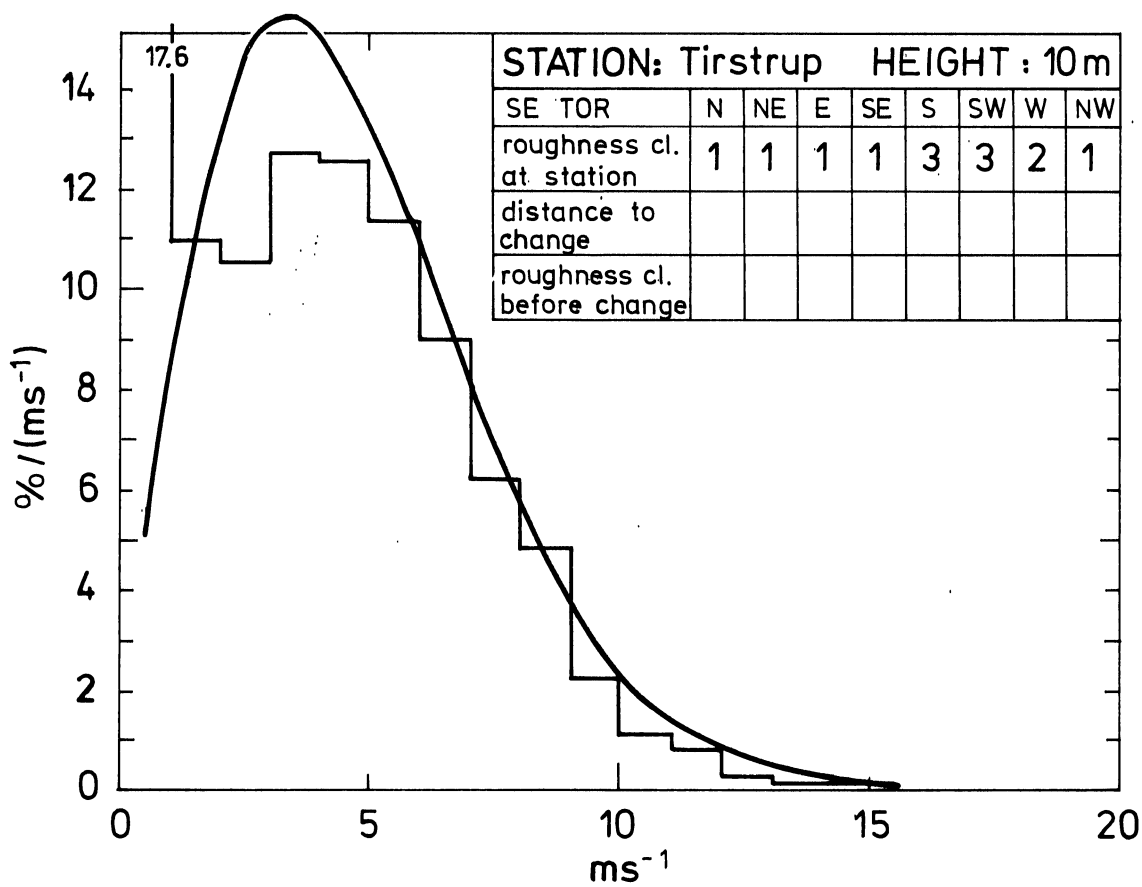

Avnø Airport

The measurement series extends from 1970 to 1977, although no measurements are available through this period from 00 and 03 GMT. All observations were made at a height of 10 m.

In all sectors except the N, NE, and E, the terrain consists of flat grassy fields and is assigned roughness class 1. Because of obstructions in the vicinity of the measuring site, no measurements from the aforementioned sectors are used. The wind is observed to be in the other sectors (SE, S, SW and NW) 71% of the time which can be compared to the Windatlas predictions of 72%.

The Weibull parameters are estimated as:

$$A = 6.6 \text{ ms}^{-1} \quad ; \quad C = 1.83$$

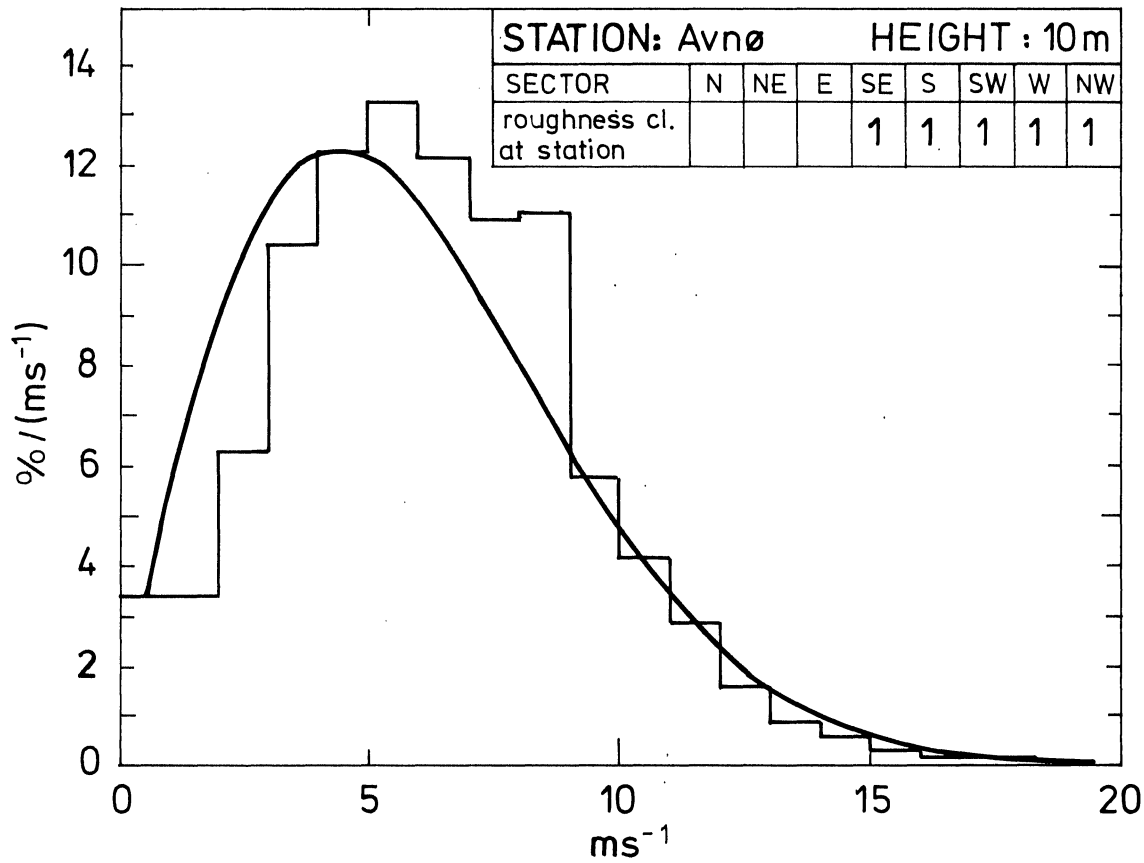

Værløse Airport

The measurement series covers the period January 10, 1972 to December 31, 1977, and all measurements were made at a height of 10 m.

The roughness length is chosen as 1 cm (class 1) in all sectors. It is necessary, however, to account for roughness changes in the SE, S and SW sectors because the measurements were made relatively near the airport perimeter. Outside of this boundary in these sectors the terrain alternates between woods, collected buildings, and scattered buildings and windbreaks. The former corresponds to roughness class 3 while the latter corresponds to class 2. Because of the difficulty in making this particular assignment, the Weibull parameters are calculated for both roughness classes. In addition, since the West sector is the best with regard to uniform roughness, this sector is computed separately.

The Weibull parameters are:

1) West sector alone (roughness class 1)
   A = 7.1 m/s, C = 1.91, f_v = 18.8%.
2) All sectors (with change from class 1 to class 2 in SE, S and SW directions at 700, 700 and 500 respectively)
   A = 5.9 m/s, C = 1.80.
3) Same as above but with change to class 3:
   A = 5.5 m/s, C = 1.78.

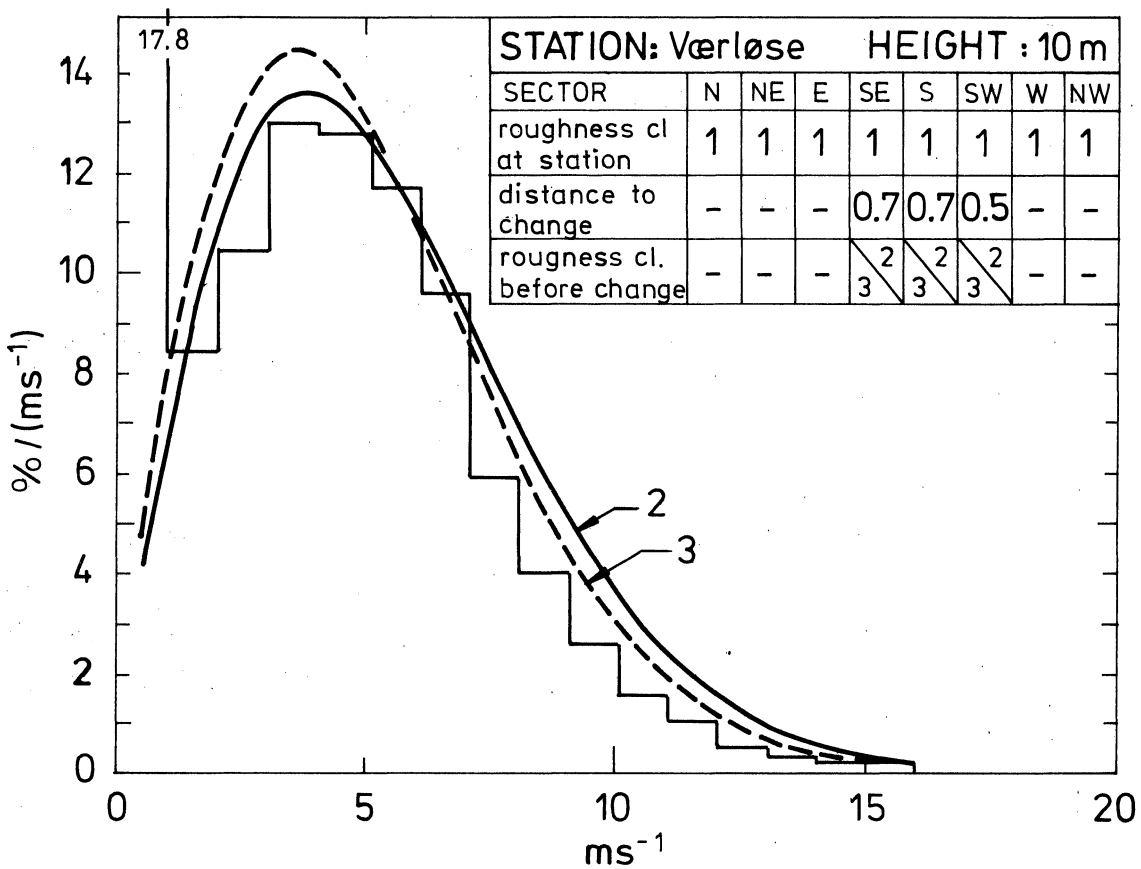
17.8
STATION: Værløse HEIGHT : 10 m
SECTOR N NE E SE S SW W NW
roughness cl at station 1 1 1 1 1 1 1 1
distance to change - - - 0.7 0.7 0.5 - -
rougness cl. before change - - - 2/3 2/3 2/3 - -
2
3
%/(ms⁻¹)
ms⁻¹
0 2 4 6 8 10 12 14
0 5 10 15 20

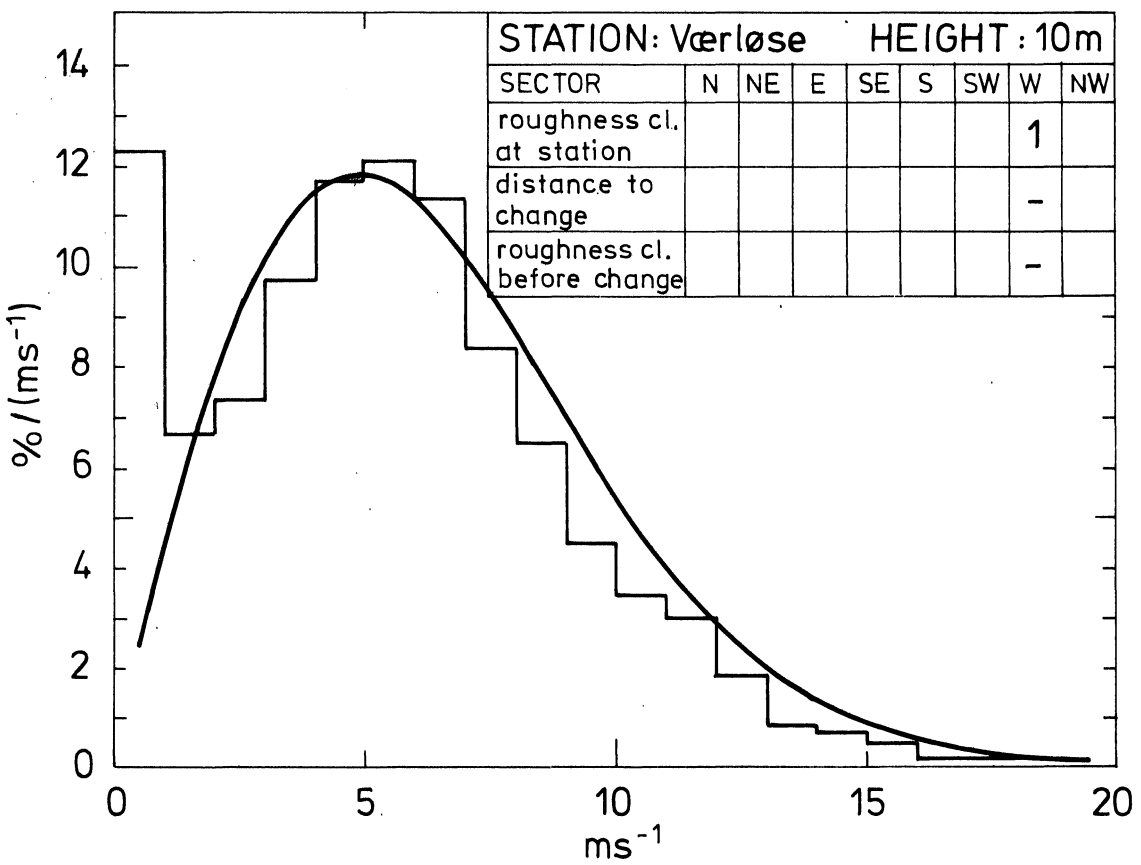
STATION: Værløse HEIGHT : 10m
SECTOR N NE E SE S SW W NW
roughness cl. at station 1
distance to change -
roughness cl. before change -
%/(ms⁻¹)
ms⁻¹
0 2 4 6 8 10 12 14
0 5 10 15 20

Rønne Airport

The measurements cover the period January 1, 1965 to December 12, 1977, and are made at a height of 10 m. No observations were made at 00 or 03 GMT daily.

The area in which the measurements were made corresponds to roughness class 1. The terrain is complicated, however, because at a distance of 300 m toward the southwest is the coastline (to the Baltic sea) with a cliff 20 m high. In the other directions, there are also roughness changes at the airport's boundary which must be taken into consideration. Because of the influence of the cliff on the flow, it is uncertain whether the roughness change calculation is reasonable. Therefore the wind speed distribution is calculated both with and without the roughness change.

The Weibull parameters for the two cases are:

No roughness change A = 6.2, C = 1.79
With roughness change A = 6.7, C = 1.68

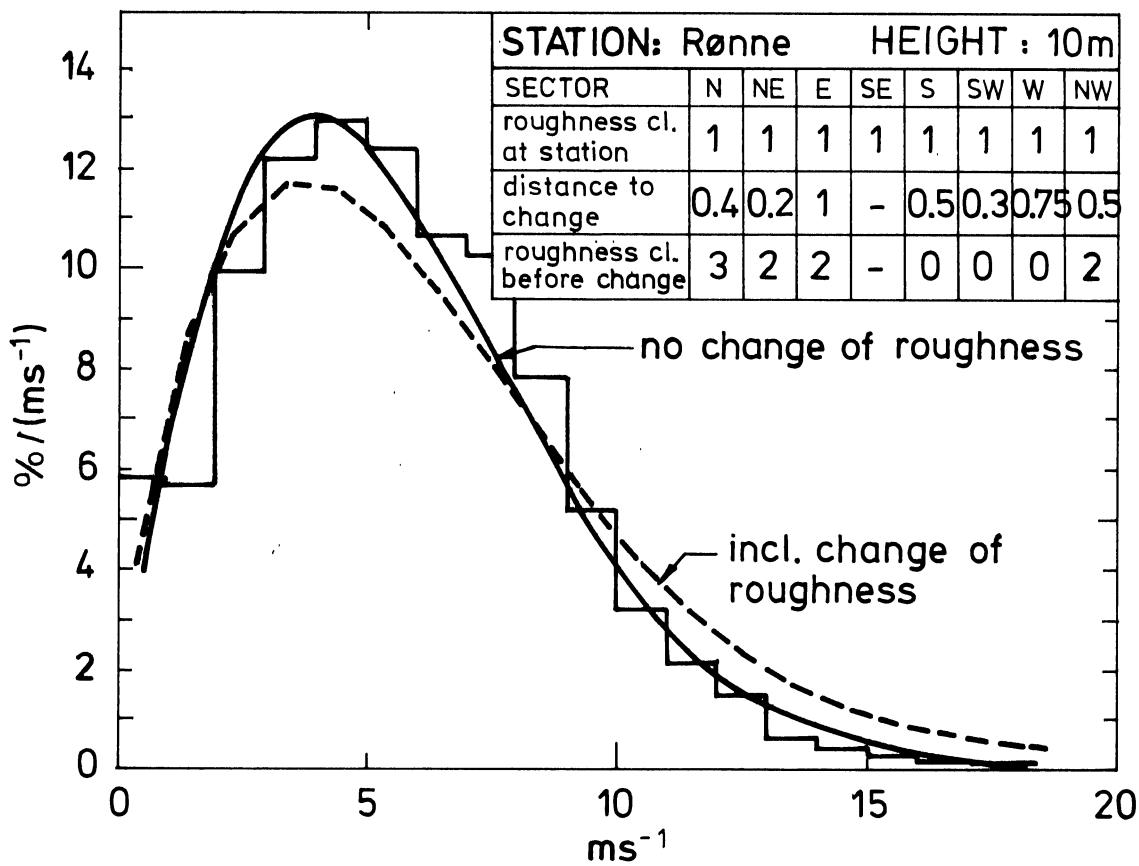

Beldringe Airport

The measurement series spans the period from January 1, 1965 to December 31, 1977, and was obtained at a height of 8 m.

The measurement site is placed in the open on a flat grassy field, and it is therefore characterized by roughness class 1 in all sectors. Outside of the airport's immediate area the terrain can be characterized by roughness class 2. The Weibull distributions are calculated both without roughness changes and with roughness changes at the distances given in the figure below.

The Weibull parameters for the two estimates are:

No roughness change : A = 5.6 m/s, C = 1.73
With roughness change : A = 5.9 m/s, C = 1.77.

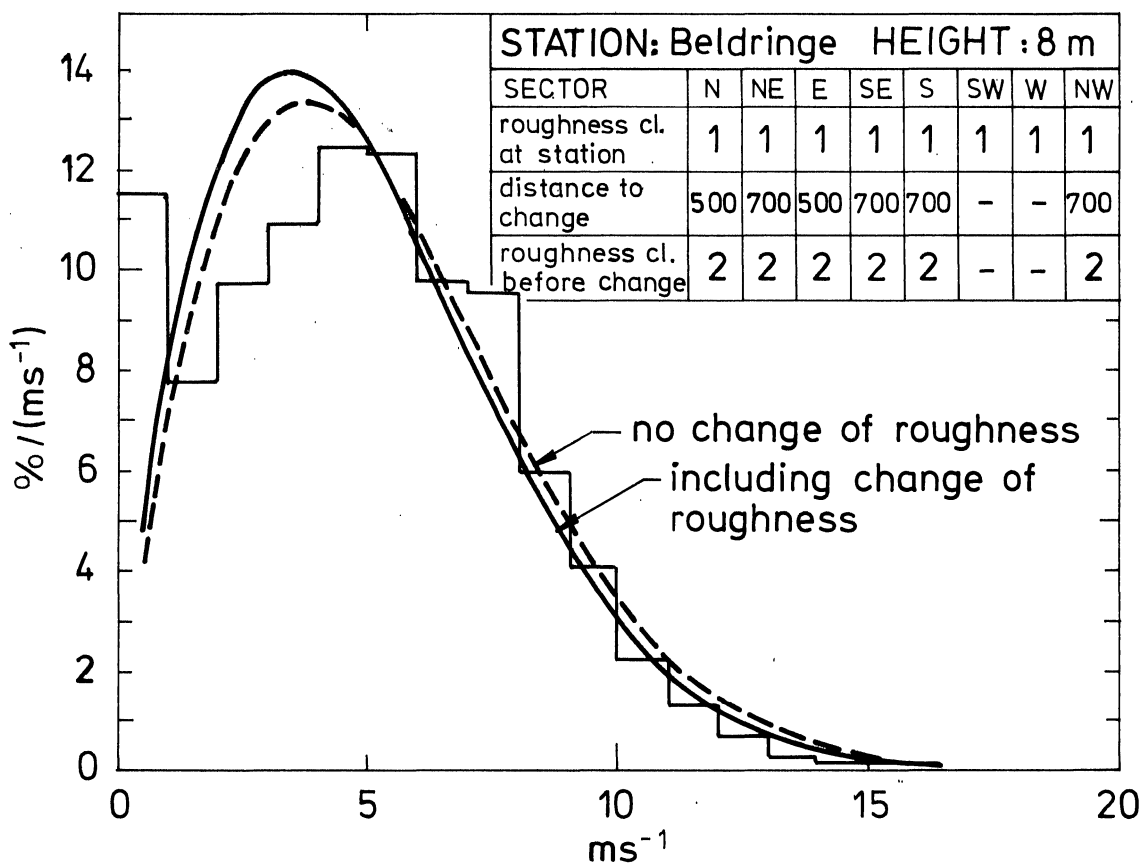

Sprogø Mast

Measurements are available from the period September 13, 1977 to January 12, 1979, and the mast has a height of 70 m.

The mast is placed on the east tip of Sprogø and is surrounded by open water in all directions except to the West where the shelter effects of the island can be expected to significantly influence the flow. Because of this, calculations are carried out for all sectors except the West sector. The computed Weibull parameters are

A = 9.2 m/s, C = 1.92,

and the frequency with which the wind is expected outside the West sector is given by

f = 80.2%.

The observed frequency of occurrence of the wind outside the West sector is 82%.

The error arising from using the wind speed distribution as calculated from the Windatlas can be quantified by computing the mean production using a reasonable power curve together with the calculated and the observed distributions respectively. For example,when the theoretical power curve for the Nibe-A turbine (Appendix B, fig. B1) is employed the two production estimates for the Sprogø data becomes:

Windatlas distribution: P = 223 kW
Observed distribution: P = 219 kW

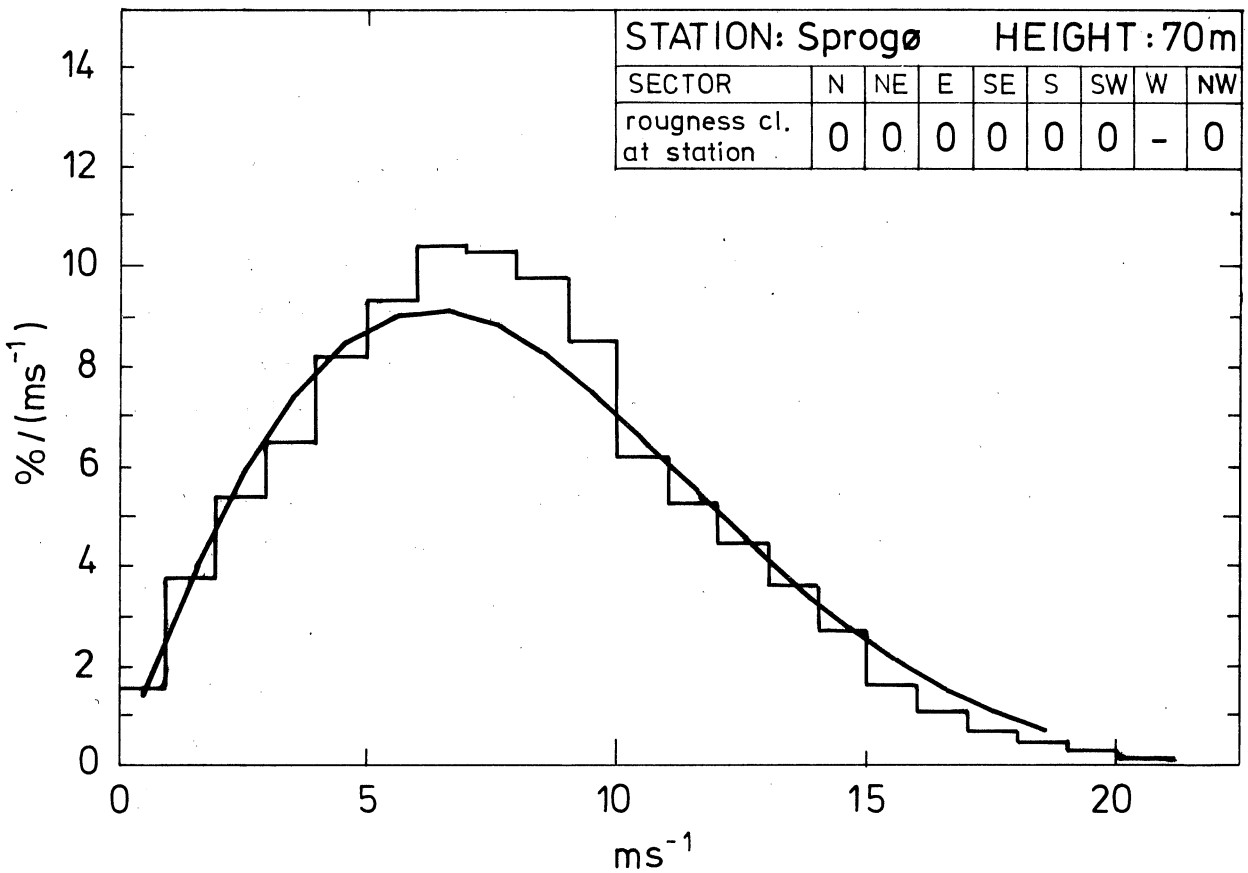
STATION: Sprogø HEIGHT: 70m
SECTOR N NE E SE S SW W NW
rougness cl. at station 0 0 0 0 0 0 - 0
%/(ms-1)
ms-1
0
2
4
6
8
10
12
14
0
5
10
15
20

Risø Mast

The Risø mast is placed in rather complicated terrain on the East coast of the Roskilde Fjord. Application of the classification scheme of Chapter 5 leads to the roughness class assignments shown in the figure. Note that roughness class 2 is used in the sectors where the wind speed at the chosen height is expected to be primarily determined by the land conditions, even though the air passes over water for a limited distance (several hundred meters) in front of the mast. In the West sector, roughness class 1 is selected since the wind speed at 76 m is influenced both by the fjord (class 0) and the conditions beyond the opposite shore (class 2).

The figure illustrates both the observed distributions for single years and for 20 years, and thereby illustrates the magnitude of the annual variations of the wind distribution.

The estimated Weibull parameters are:

A = 8.3 m/s, C = 1.96.

As in the case of the Sprogø data, the mean power of a Nibe-A turbine based on the Risø data has been computed, the result is:

Windatlas distribution: P = 187 kW
Observed distribution: P = 187 kW.

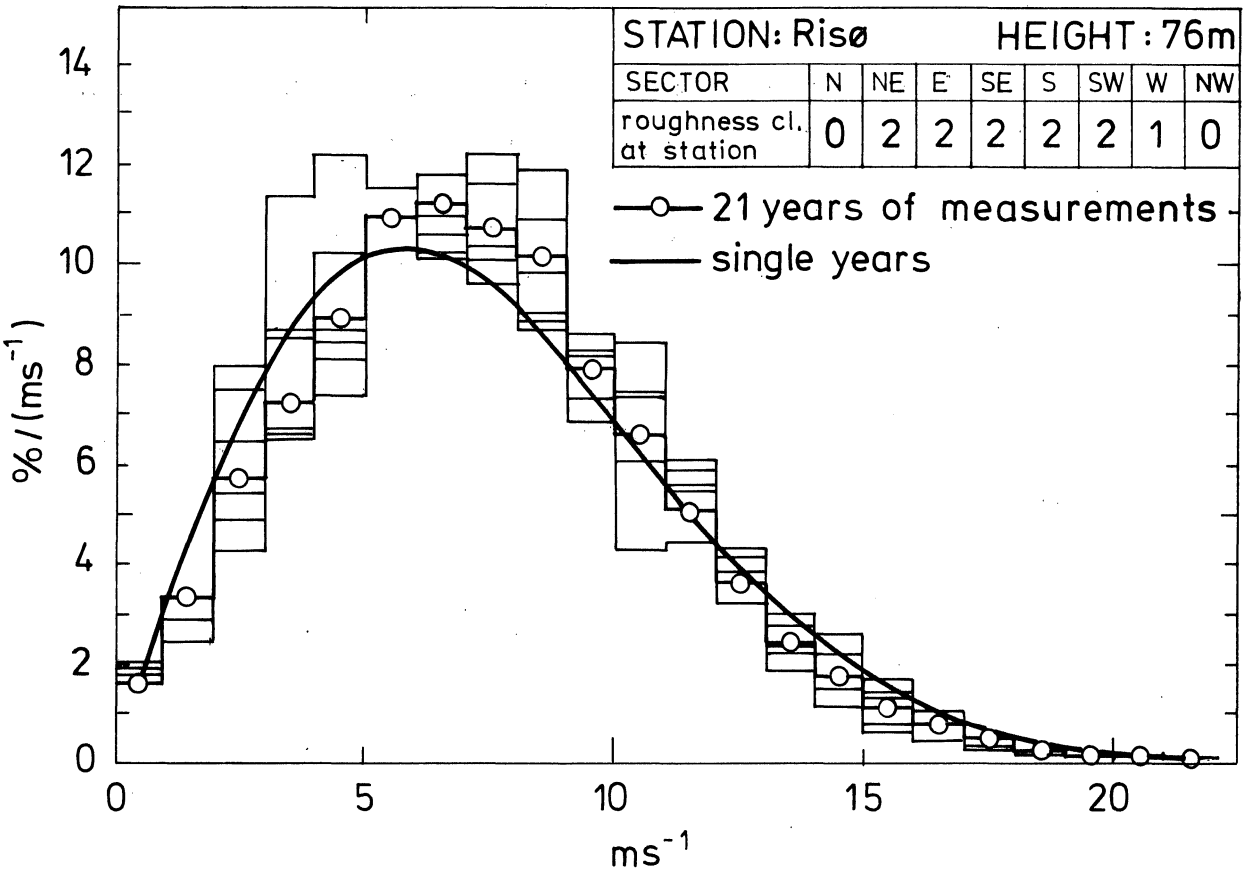
STATION: Risø
HEIGHT: 76m
SECTOR N NE E SE S SW W NW
roughness cl. at station 0 2 2 2 2 2 1 0
21 years of measurements
single years
%/(ms-1)
ms-1
0
2
4
6
8
10
12
14
0
5
10
15
20

Lightship Horns Rev

The measurements cover the years 1965-1978, and the anemometer height was 20 m. The terrain is open sea in all directions.

The lightship was named the Vyl at position 55°24' N, 07°34' E until March 6 1975, and renamed the Horns Rev when relocated to 55°34' N, 07°20' E thereafter.

The estimated Weibull parameters are:

$A = 8.5\ ms^{-1}$, $C = 1.92$

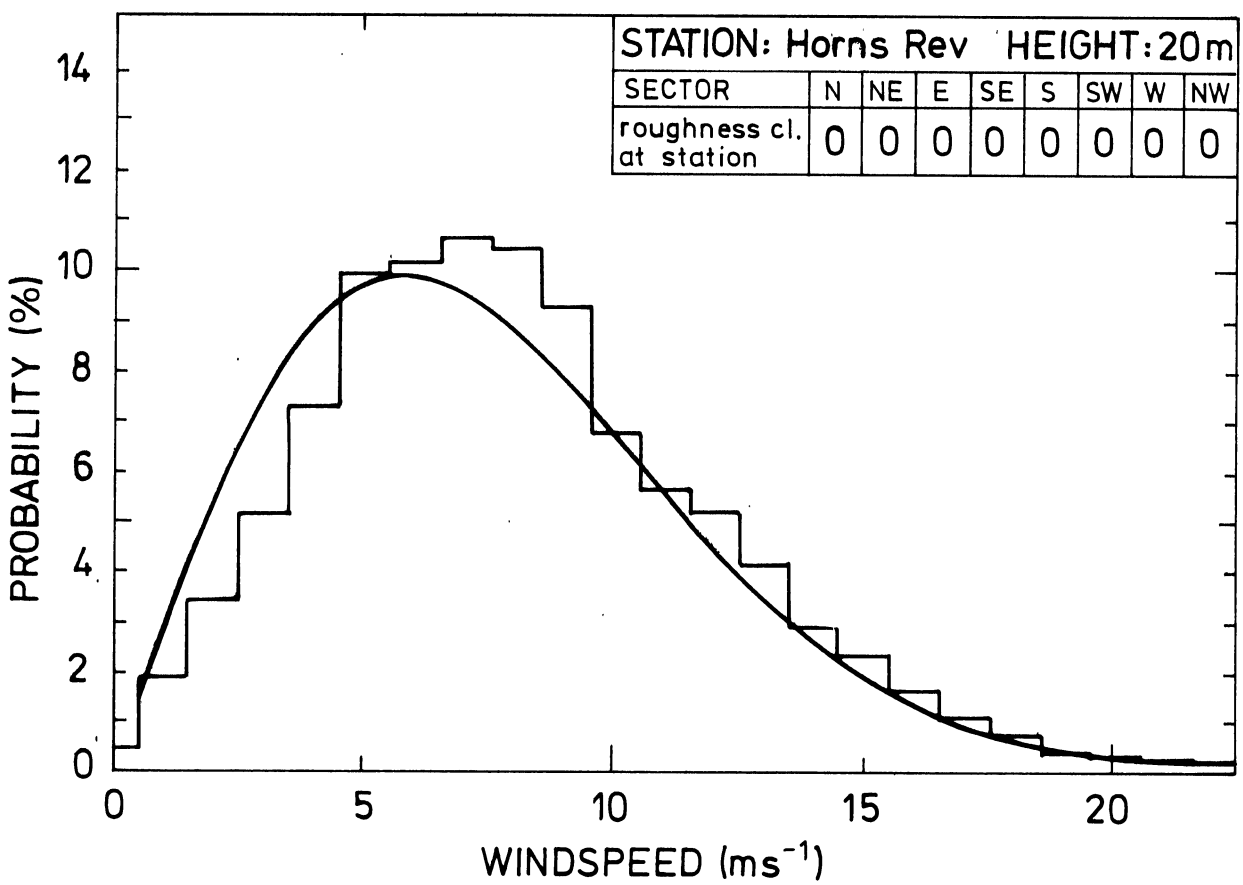

Tune, Gedser and Torsminde

These measurement series were obtained by Martin Jensen in the year 1960. Measuring height is 25 m.

Three masts, each equipped with a specially designed anemometer, were placed at sites thought to be especially suitable for wind power production, and they were operated from 1957 to 1961 (but not continuously). The anemometers were especially constructed to be able to respond rapidly to wind speed fluctuations, but only slowly to directional changes. The accumulated probability distributions for the wind speed at 25 m height were measured directly by a system of spring-loaded plates which were calibrated to switch on an electrical contact when the wind speed exceeded a predetermined value. The system was used at Tune, Gedser and Torsminde. Torsminde was chosen as representing the most extreme winds in Jutland. Gedser was selected as being representative of a nearly ideal coastal site, while Tune was representative of a good inland site.

The mode of operation of the measuring apparatus and a description of the terrain surrounding the masts is given by Martin Jensen (1962). By using his descriptions of the terrain, it is possible to assign the roughness classes and to calculate the Weibull parameters for the three locations. The results are:

Torsminde: A = 7.9 , C = 1.86
Gedser: A = 7.7 , C = 1.88
Tune: A = 7.2 , C = 1.88

The measurements were carried out over the entire period (1957-1961); however, because of interruptions, unbroken series exist only for the year 1960. Therefore, the comparison with the Windatlas predictions is made for only this year.

The figures for Tune, Gedser and Torsminde show the accumulated probability distribution for the wind speed and the corresponding Windatlas predictions. For the Gedser site, the result of an

additional data series obtained in 1978 is also shown. These measurements consist of ten minute averages and were the basis for the production probability curve estimates shown in example 5.9.

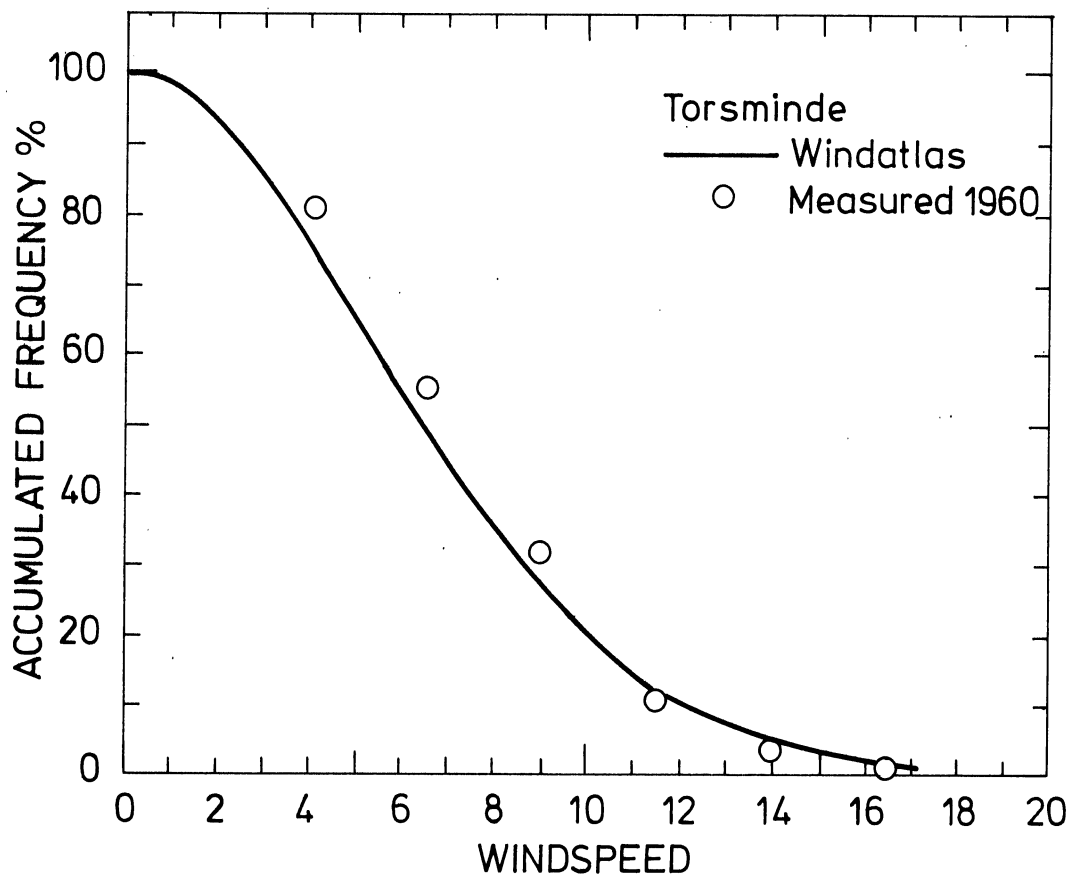

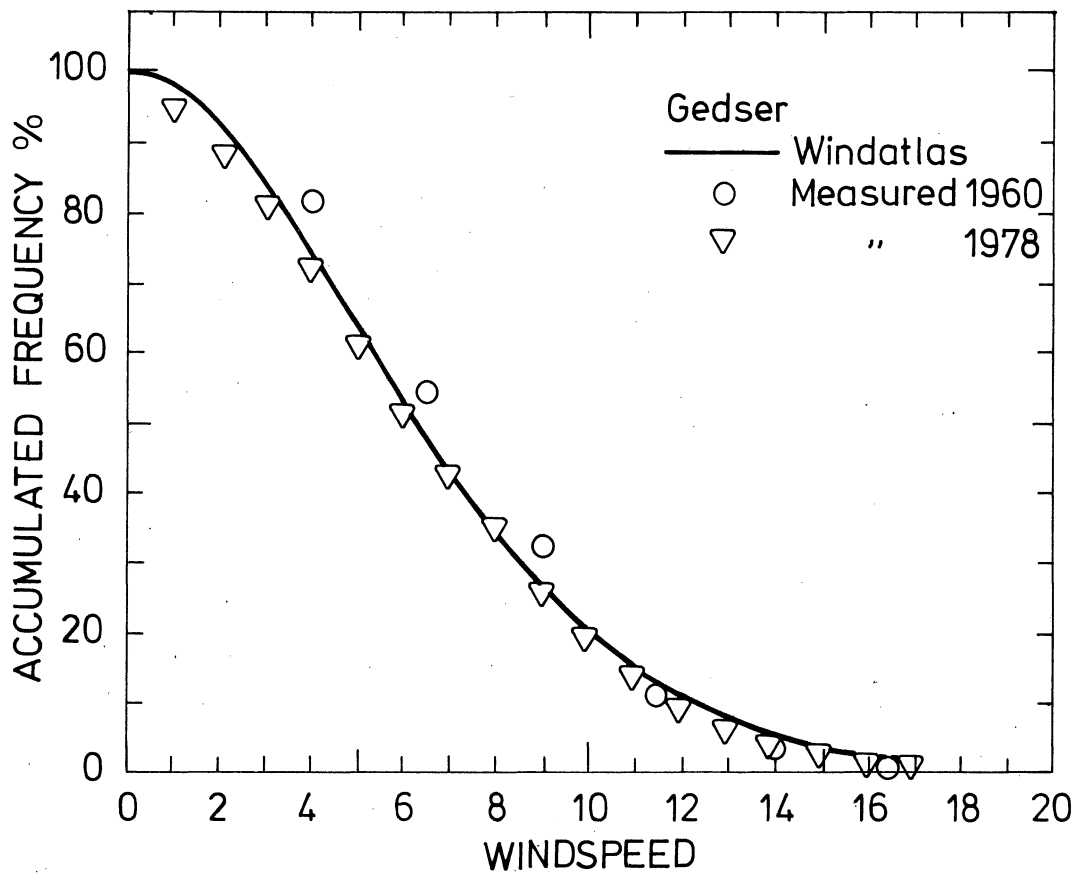
Gedser
Windatlas
Measured 1960
" 1978
ACCUMULATED FREQUENCY %
WINDSPEED
0
20
40
60
80
100
0 2 4 6 8 10 12 14 16 18 20

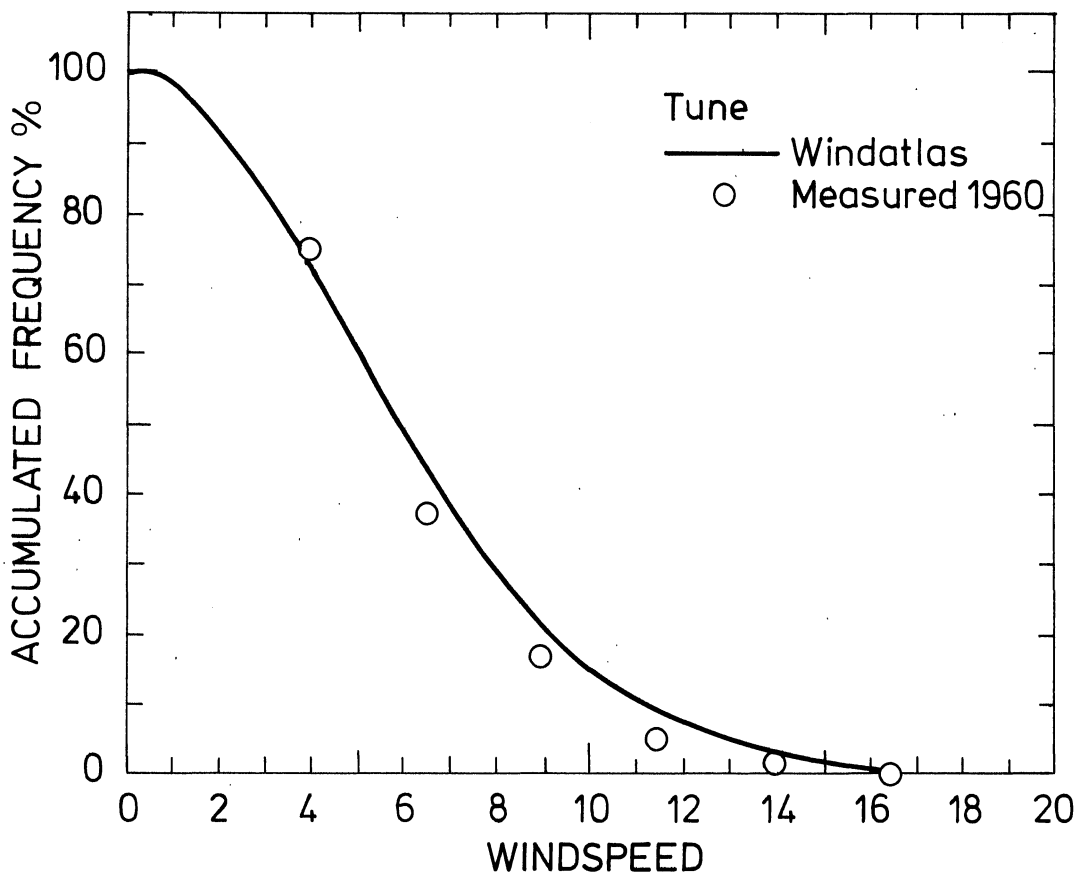
Tune
Windatlas
Measured 1960
ACCUMULATED FREQUENCY %
WINDSPEED
0
20
40
60
80
100
0 2 4 6 8 10 12 14 16 18 20

From the figures it is clear that the deviations between Martin Jensen's measurements and the calculated distributions have the same form for the three cases. Because of the excellent agreement between the 1978 measurements at Gedser and the calculated distribution, it seems reasonable to attribute these deviations to the difference in averaging time. This argument can be substantiated qualitatively, at least, by the fact that the deviations are in the direction that would be expected if the averaging times were too short for the 1960 measurements.

Cabauw mast in the Netherlands

The 215 m high meteorological mast at Cabauw in the Netherlands is placed in an ideally homogeneous terrain which according to the classification in the Windatlas is of class 2. Although the Netherlands is outside the analyzed region and climatological differences should be expected, because of the unusual homogeneity of the surrounding terrain and the height above terrain of the measurements it is of interest to compare the Windatlas prediction with the measured wind distribution at the 200 m height.

The measured wind speed distribution is for the year 1973 and has been supplied by Dr. J. Wieringa of The Netherlands Meteorological Institute.

The estimated Weibull parameters are:

$A = 9.2\ ms^{-1}$, $C = 1.97$

The full line is the accumulated probability distribution based on the above parameters, and the circles are the observed values.

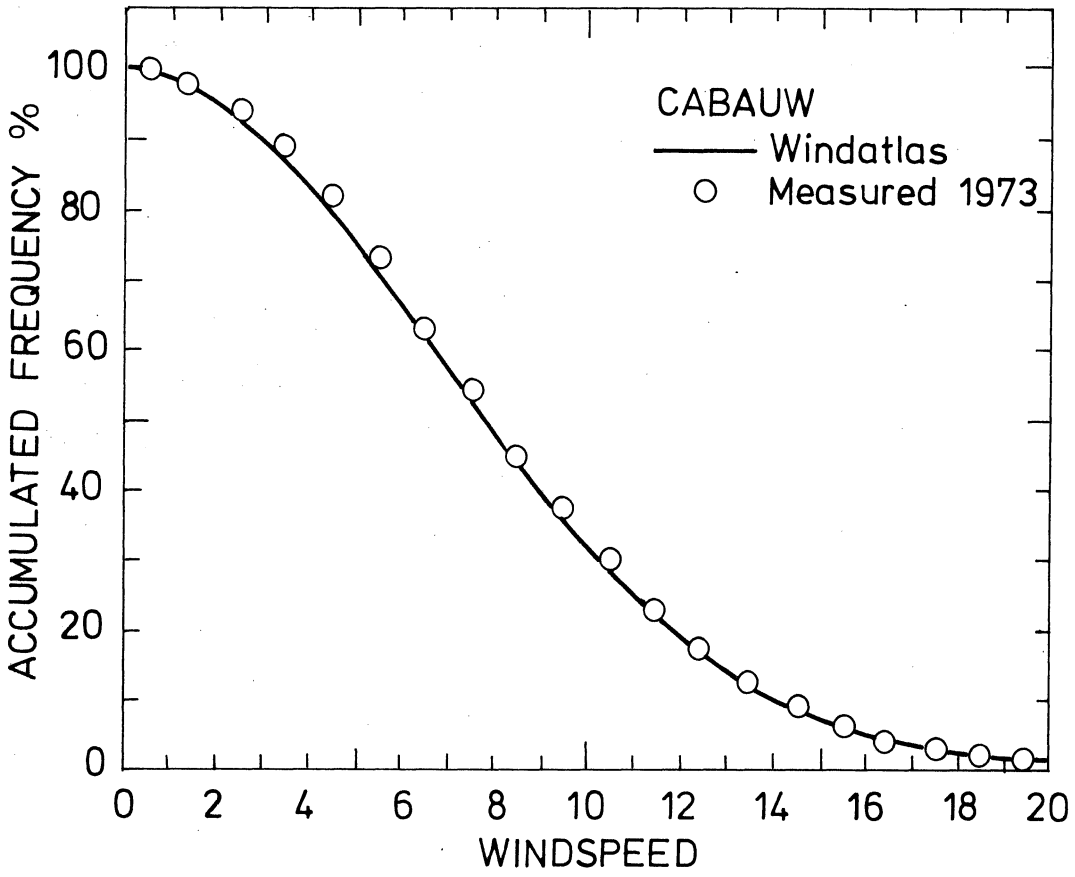

6.1. Summary of verifications

A judgement as to whether the Windatlas methods have, in fact, proven to be capable of determining wind speed distributions with sufficient accuracy for wind energy estimates, is in the final analysis partially subjective. Nonetheless, there does seem to have been an especially good agreement between measurements and predictions in the foregoing comparisons. In situations where relatively large deviations have appeared between measured and predicted distributions, it has often been possible to give a reasonable explanation without carrying out a detailed analysis. For example, the missing nighttime observations at Avnø are probably responsible for the deviations between analysis and measurement there. Evidence supporting such an argument is presented for Ålborg in the figure showing the wind speed distributions at 00 and 12 GMT respectively. The figure

shows a rather large variation in the wind speed distribution over the course of a day. (This, of course, could have been expected from the frequent differences in stability between night and day). Similar effects are present in the data for the Risø mast presented in figure 3.5.

The best agreement is seen when the terrain in the least complicated, as one might have expected. Especially interesting in this regard is the Lightship Horns Rev Comparison because the terrain is open water in all directions. The agreement between the predicted and measured distributions shows that the chosen water roughness (Appendix C) and the assumptions in the physical model are both reasonable and consistent.

The eight figures in the Ålborg airport verification show the sectorwise distributions for the Ålborg airport together with the distributions calculated from the Windatlas. The good agreement testifies to the ability of the Windatlas methods to predict even sectorwise differences in the wind speed distributions.

The West coast of Jutland is different from the rest of the country in a meteorological sense since, especially in the winter months, it is not uncommon to encounter situations where the prevailing westerlies cause a strong flow of cold and stable air from the west or northwest over the relatively warmer sea. The resulting instability might be expected to give rise to stronger wind speeds at the coast than farther inland. This possible effect was one of the reasons for the comparison with data of Martin Jensen taken at Torsminde, Gedser, and Tune. The data from Torsminde at the West coast of Jutland and the data from Gedser at a West coast in Eastern Denmark make possible a relative evaluation since the data were taken concurrently. The comparison of the data with the Windatlas predictions shows that the difference between the two stations is (in a statistical sense at least) primarily due to the difference in terrain roughness at the two sites, and not to the aforementioned meteorological conditions. This conclusion should be regarded as tentative since measurements were available for only one year.

As has been discussed above, it is difficult to make a direct comparison between the Windatlas predictions and Martin Jensen's measurements because of the short averaging times which were built into his measuring technique. However, measurements performed at Gedser at nearly the same site at Jensen's mast, but averaged over 10 minutes, show excellent agreement with the Windatlas predictions, thereby indicating that the deviations between predictions and measurements are probably primarily due to these averaging time differences. (The extra variance which is included by a shorter averaging time would be expected to cause positive deviations in the accumulated distribution, the largest effect occurring at moderate wind speeds).

From the perspective of the verification analyses of this chapter, it seems reasonable to conclude that the procedures and physical models of the Windatlas are useful and sufficiently accurate for estimating the wind speed distribution at a given locality and height in Denmark, especially for wind power production estimation purposes.

7. DISCUSSION

The Windatlas is a climatological investigation which has the aim of establishing a rational method for the siting of wind turbines in Denmark. It is important to keep this goal in mind, especially when the Windatlas is used for other purposes such as air pollution studies and wind loads on building structures. With regard to air pollution, it is often situations with low wind speeds which are of interest. Unfortunately, in such situations the method that forms the basis for the Windatlas is less reasonable. Nonetheless, meteorological objections not withstanding, various verifications in Chapter 6 show that the Windatlas gives wind speed distributions which are in good agreement with the observed distributions, even for low wind speeds. This is especially true for stations where measurements

have been taken at relatively large heights such as Sprogø, Risø and Gedser.

The high frequency of wind speeds less than 1 m/sec observed at some of the airports can to a large extent be attributed to observational practice and the instrument threshold. Part of the anomaly may also be caused by local microclimatological effects.

The occurence of extremely high wind speeds are of interest for many types of wind loading problems. While the Windatlas provides a probability of occurrence, it has not been investigated to what extent it is justifiable to use the calculated distributions in this extreme limit.

The physical method which was chosen for the Windatlas and the necessary assumptions are discussed in Chapter 2, the pressure analysis is discussed in Chapter 4 and the statistical basis in Chapter 3. The most important assumptions, namely a uniform geostrophic wind and a uniform atmospheric stability over the country - in a statistical sense - are justified independently. The uniformity of the geostrophic wind distribution is argued in Chapter 4, and the validity of the stability assumption is discussed in Chapter 2. Further, the verifications in Chapter 6 serve as a documentation of the validity of both assumptions.

Chapter 5 and Appendix A consitute a "Users Guide" and can be used independently of the rest of the Windatlas. Following the guidelines, a user without special qualifications can calculate wind speed distributions and energy productions from wind turbines with known power curves.

The correlation analysis in Appendix B is concerned with the possible advantage of having a geographical distribution inside Denmark of electricity producing wind turbines. The conclusion is that separations of the order of a thousand kilometers would be required in order to be of significance.

The persistence analysis in Appendix B is relevant for evaluations of the supply reliability and the gain obtained by com-

bining wind turbines with storage facilities. A detailed analysis of combined systems of generators, storages and time-dependent loads is, however, only possible by means of computer simulations of the systems using long recorded series of the wind speed.

The method used in the Windatlas has not previously been applied to wind climatological investigations. It was not obvious at the start of the project whether the method would lead to a usable result, or whether the many complications (as discussed in Chapter 2) would render this impossible and necessitate a resort to traditional analysis of existing wind data. That the method has proven useful has been demonstrated in the previous chapters, and it can be recommended for use in other parts of the world where the topographical and climatological conditions are similar to those of Denmark.

The discussion in Chapter 2 suggests that it may be possible to improve the physical model so that it can be used to accurately predict the wind speed from forecasted or actually analyzed fields of surface pressure and other routine meteorological data. The results of the Windatlas show that such a model has a good chance of leading to an improvement of local forecasts of wind speed. Such forecasts might be important, for example, for the control of a power grid which has a number of large wind turbines connected, as well as for a number of other important technical applications.

LIST OF SYMBOLS

Superscript "→" denotes vector, underlining "$\underline{=}$" denotes matrix, apostrophe "′" denotes deviation from mean, bracket "< >" denotes mean value, "×" denotes vectorial product.

A $a^{-1/C}$	scale parameter in the Weibull distribution
$\underline{\underline{A}}$	station matrix (in pressure analysis)
A_R	rotor area
A_{rs}	element of $\underline{\underline{A}}$ with row number r and column number s
$A(\mu_o)$	empirical function in geostrophic drag law
A_ϕ	anisometry function in map projection
A_H	horizontal area per roughness element
$B(\mu_o)$	empirical function in geostrophic drag law
b	constant
C	shape parameter in the Weibull distribution
D	displacement length
dsx, dsy	curvelinear increments
E	available power density (energy flux)
E(V)	available power density at wind speed V
exp(x)	exponential function
f	Coriolis parameter, frequency of occurrence
f(V)	probability density function
F(V)	accumulated probability function

$F_A(C)$ $F_C(M^2/V^2)$ $F_M(C)$ $F_V(C)$	functions entering into the calculation of the Weibull parameters; tabulated in appendix A
$F_E(C)$	function entering in mean power calculation; tabulated in appendix A
g	acceleration of gravity
G	geostrophic wind speed
$G_C(\xi)$	function entering into the calculation of mean power output; tabulated in appendix A
GMT	Greenwich mean time, Danish local time is GMT + 1 hour
h	height
H	hub height, when used as subscript it denotes horizontal
h_1	height of "computational" layer
h_2	height of internal boundary layer
i	index
j	index
k	index, von Kármàn constant, slope of power curve
$\vec{k}$	unit vector in vertical direction
K	formfactor in mean power
ℓ,l	distance, distance to roughness change
L	distance, half width of hill, Monin-Obukhov length
L(a,c)	maximum likelihood function
ln(x)	natural logaritm function
M	mean value
n	frequency, order of polynomial
N	number of observational points

p	pressure
P	mean power (long term average)
$P(V)$	mean power at wind speed V
Pr	probability
$Pr(V)$	probability density function
P_{max}	rated power
r	index
R	shelter reduction, radius of curvature, radius, gas constant for air
R_1	shelter reduction
R_2	shelter reduction factor
Ri_B	bulk Richardson number
Ro	surface Rossby number
s	index
S	standard deviation, power scale factor, cross section
$S(n)$	spectral density function
t	time
T	averaging time, absolute temperature
T_o	surface absolute temperature
$\tan^{-1}(x)$	arctangent function
u_*	friction velocity
u_g	Eastward component of geostrophic wind
V	wind speed
$\vec{V}$	wind velocity vector
V_T	thermal wind speed
V_{gr}	gradient wind speed
v_g	Northward component of the geostrophic wind
V^2	mean square value
V_1	starting speed

V_2	wind speed above which $P = P_{max}$
V_m	wind speed at which efficiency is maximum
W_1	weighting factor
W_2	weighting factor
x_1	distance
x_2	distance
x	distance to the East
y	distance to the North
z	height above ground
z_o	roughness length
α	wind speed divided by A
α_m	V_m divided by A
β_{jk}	coefficient in polynomial fitted to surface pressure
$\sqrt{\beta_1}$	skewness
γ	dry adiabatic lapse rate
$\gamma(x,y)$	incomplete gamma function
$\Gamma(x)$	gamma function
δ	difference of α_2 and α_m
Δ	difference operator, relative error, weighting factor
ΔS	relative speed up
$\vec{\nabla}$	gradient operator
$\varepsilon(V)$	efficiency at wind speed V
ε_m	maximum efficiency, $\varepsilon_m = \varepsilon(V_m)$
η	constant
θ	potential temperature
θ_*	scaling temperature of surface heat flux
λ	longitude
μ_o	stability parameter

ν	kinematic viscosity
ψ_1	empirical stability function in wind profile
ψ_2	empirical stability function in temperature profile
χ	concentration
ϕ	latitude, angle
σ	standard deviation, index of curvature
Ω	angular speed in the earth's rotation.

REFERENCES

ARYA, S.P.S. and WYNGAARD, J.C. (1975). Effect of Baroclincity on Wind Profiles and the Geostrophic Drag Law for the Convective Planetary Boundary Layer, Atmos. Sci. 32, 767-778.

BAKER, R.W. et al. (1979). Wind power potential in the Pacific Northwest. J. Appl. Meteor. 17, 1814-1826.

BARNDORFF-NIELSEN, O. (1977). Exponentially decreasing distributions for the logarithm of particle size. Proc. R. Soc. Lond. Ser. A. 353. 401-419.

BUSINGER, J.A. (1973). Turbulent transfer in the atmospheric surface layer. In: Workshop on micrometeorology. Ed. by D.A. Haugen. Held by the American Meteorological Society, Boston, Mass., 14-18 August 1972. 67-100.

BUSINGER, J.A. (1975). Aerodynamics of vegetated surfaces. In: Heat and mass transfer in the biosphere, Pt. I. Transfer processes in the plant environment. (Wiley, New York) 594 p.

CHARNOCK, H. (1955). Wind stress on a water surface. Quart. J. Roy. Meteor. Soc. 81, 639.

DANSK INGENIØRFORENING (1978). Code for Actions on building structures. 2. Wind load. Dansk Standard DS 410.2. Translated edition.

ESKINAZI, S. (1975). Fluid Mechanics and Thermodynamics of our environment. (Academic Press, New York, San Francisco and London) 422 p.

GARRATT, J.R. (1977). Review of drag coefficients over oceans and continents. Mon. Wea. Rev. 105, 915-929.

GUMBEL, E.J. (1958). Statistics of Extremes. (Columbia University Press, New York) 375 p.

HASSE, L. (1976). A Resistance-Law Hypothesis for the Non-Stationary Advective Planetary Boundary Layer. Boundary-Layer Meteor. 10, 393-407.

HALTINER, G.J. and MARTIN, F.L. (1957). Dynamical and Physical Meteorology. (McGraw-Hill, New York) 470 p.

HENNESSEY, J.P. (1977). Some aspects of wind power statistics. J. Appl. Meteor. 16, 119-128.

HESS, G.D. (1973). On Rossby-Number Similarity Theory for a Baroclinic Planetary Boundary Layer. J. Atmos. Sci. 30, 1722-1723.

JENSEN, M. (1959). Aerodynamik i den naturlige vind. (Teknisk Forlag, København) 248 p.

JENSEN, N.O. (1973). Occurrences of stability classes, wind speeds, and wind directions as observed at Risø. Risø-M-1666, 37 p.

JUSTUS, C.G. and MIKHAIL, A. (1976). Height variation of wind speed and wind distribution statistics. Geophys. Res. Lett. 3, 261-264.

JUSTUS, C.G. et al. (1976). Nationwide assessment of potential output from wind-powered generators. J. Appl. Meteor. 15, 673-678.

JUSTUS, C.G. (1978). Wind energy statistics for large arrays of wind turbines (New England and central U.S. regions). Solar Energy 20, 379-386.

KOSTADINOV, L. and DZHOLOV, G. (1977). The universal functions in the resistance and heat-exchange laws for the Ekman boundary layer. Izv. Acad. Sci. USSR Atmos. Oceanic Phys. Engl. Transl. 13, 673-675.

KVICK, T. och KARLSTRÖM, C. (1977). Sammanställning av vindstatistik för projektet Vindenergiprospektering. Del I. (Sveriges Meteorologiska och Hydrologiska Institut. Klimatbyrån, Norrköbing) 155 s.

LOUIS, J.-F. (1977). Parameterisation of the surface fluxes. European Centre for Medium Range Weather Forecasts. Research Dept., Bracknell) Internal Report 4, 15 p.

GEDSER TEST GROUP (1979). The measurements on the Gedser windmill 1977-1979. Edited by Per Lundsager, C.J. Christensen and Sten Frandsen. (The Wind Power Program of the Ministry of Commerce and the Electric Utilities in Denmark). 195 p.

LUNDSAGER, P., FRANDSEN, S. and CHRISTENSEN, C.J. (1980). Analysis of data from the Gedser wind turbine 1977-1979, Risø-M-2242.

PAULSON, C.A. (1970). The Mathematical representation of Wind-Speed and Temperature Profiles in the Unstable Atmospheric Surface Layer. J. Appl. Meteor. 9, 857-861.

PETERSEN, E.L. (1975). On the kinetic energy spectrum of atmospheric motions in the Planetary boundary layer. Risø Rep. 285, 103 p.

PETERSON, E.W. and HENNESSEY, J.P. (1978). On the use of power laws for estimates of wind power potential. J. Appl. Meteor. 17, 390-394.

PRINSENMOLEN-COMMITTEE (1958). Research inspired by the Dutch windmills. (H. Veenman en Zonen, Wageningen) 184 p.

ROMANOV, V.F. (1977). Similarity theory for the baroclinic planetary boundary layer of the atmosphere. Izv. Akad. Nauk SSSR Fiz. Atmos. & Okeana 13, 1081-1086.

SMEDMAN-HÖGSTRÖM, A.-S. and HÖGSTRÖM, U. (1978). A practical method for determining wind frequency distributions for the lowest 200 m from routine meteorological data. J. App. Meteor. 17, 942-954.

STEWART, D.A. and ESSENWANGER, O.M. (1978). Frequency distribution of wind speed near the surface. J. Appl. Meteorol. 17, 1633-1642.

TENNEKES, H. and LUMLEY, J.L. (1972). A first Course in Turbulence. (MIT Press, Cambridge (Mass.) and London) 299 p.

VINDKRAFTUDVALGET (1962). Betænkning. Wind Power Committee's report. (Danske elværkers Forening, København) 74 p.

APPENDIX A

Weibull parameter charts and tables

The Weibull parameters are presented as function of roughness class, wind direction and height on the following 36 charts. At the top of each chart it is noted which wind direction sector and roughness class the chart refers to. Further the frequency with which the wind appears in the sector is given. The Weibull parameters A and C for the chosen height (vertical scale) can be read with reference to the bottom and top horizontal scales respectively. The symbols denote the calculated values at the heights 10, 25, 50, 100, and 200 meters.

For each roughness class a separate chart is supplied which gives the Weibull parameters irrespective of the wind direction, i.e. for use in a terrain where there is no change of roughness with direction. These four charts which are marked "TOTAL". Also shown are the Weibull parameters for the geostrophic wind at a height of 1000 m (arbitrarily chosen). The extensions of the curves to the geostrophic values are shown as dotted times.

Applications using the tables following the charts are given in Chapter 5.

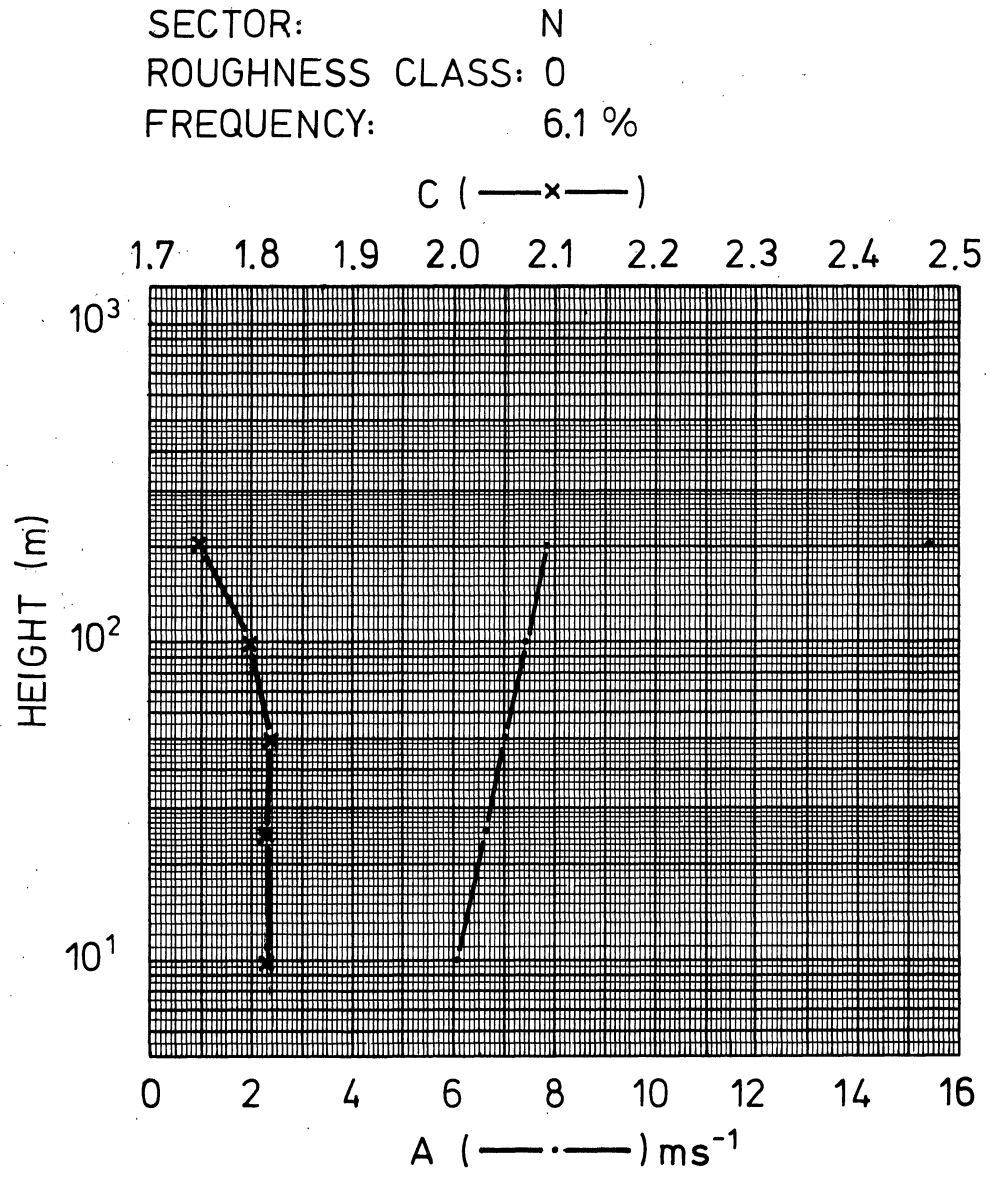
SECTOR: N
ROUGHNESS CLASS: 0
FREQUENCY: 6.1 %
C (—×—)
1.7 1.8 1.9 2.0 2.1 2.2 2.3 2.4 2.5
HEIGHT (m)
10³
10²
10¹
0 2 4 6 8 10 12 14 16
A (—·—) ms⁻¹

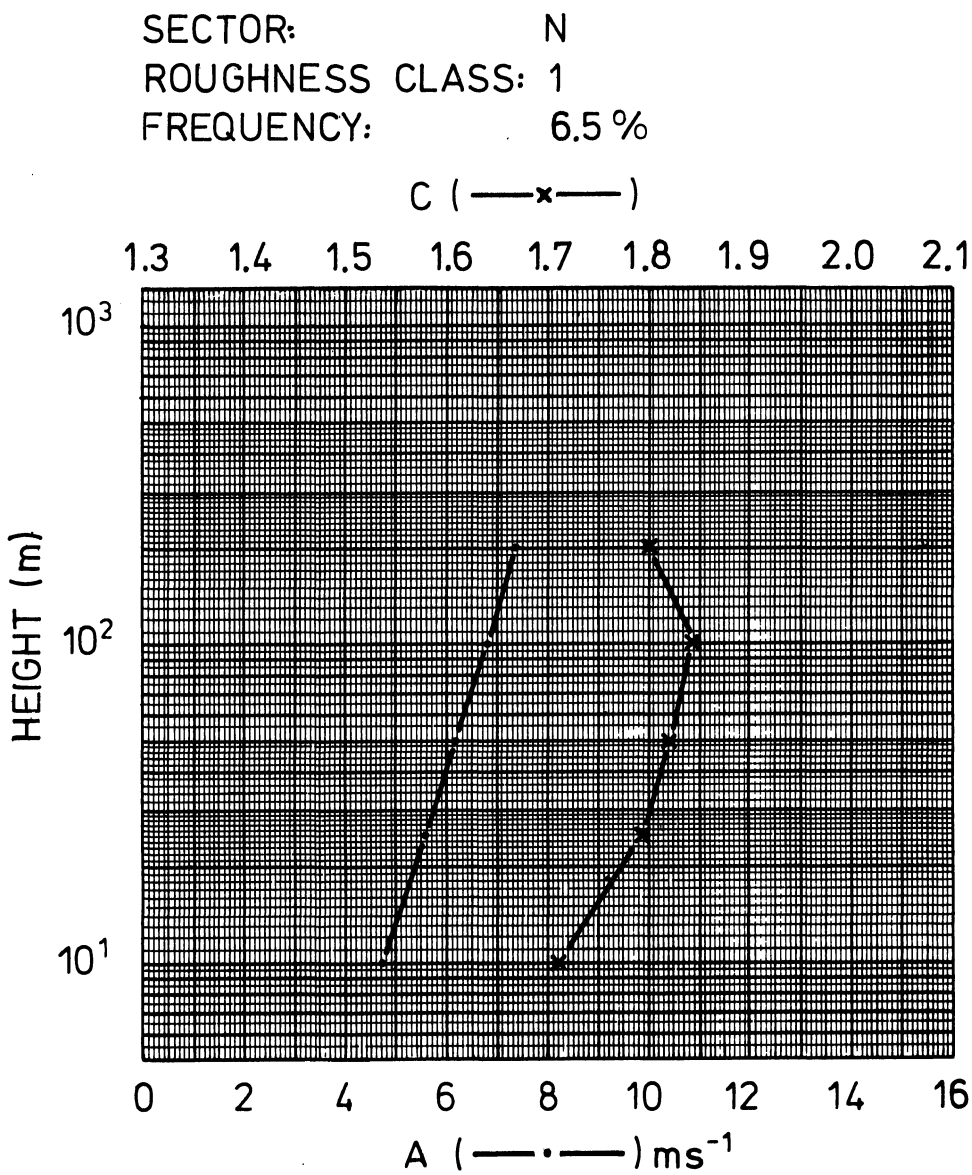
SECTOR: N
ROUGHNESS CLASS: 1
FREQUENCY: 6.5 %
C (—×—)
1.3 1.4 1.5 1.6 1.7 1.8 1.9 2.0 2.1
HEIGHT (m)
10³
10²
10¹
0 2 4 6 8 10 12 14 16
A (—·—) ms⁻¹

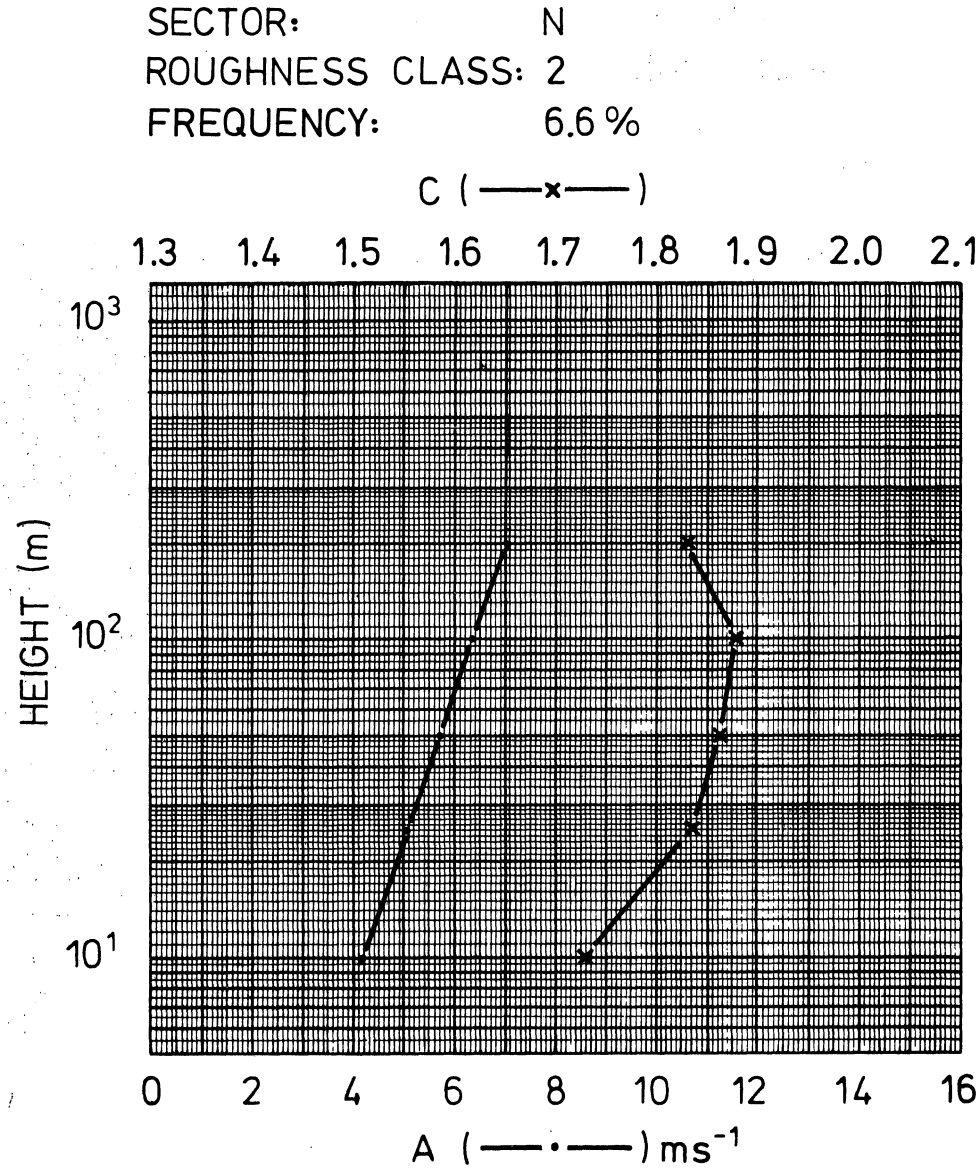
SECTOR: N
ROUGHNESS CLASS: 2
FREQUENCY: 6.6 %
C (—×—)
1.3 1.4 1.5 1.6 1.7 1.8 1.9 2.0 2.1
10^3
10^2
10^1
HEIGHT (m)
0 2 4 6 8 10 12 14 16
A (—·—) ms^{-1}

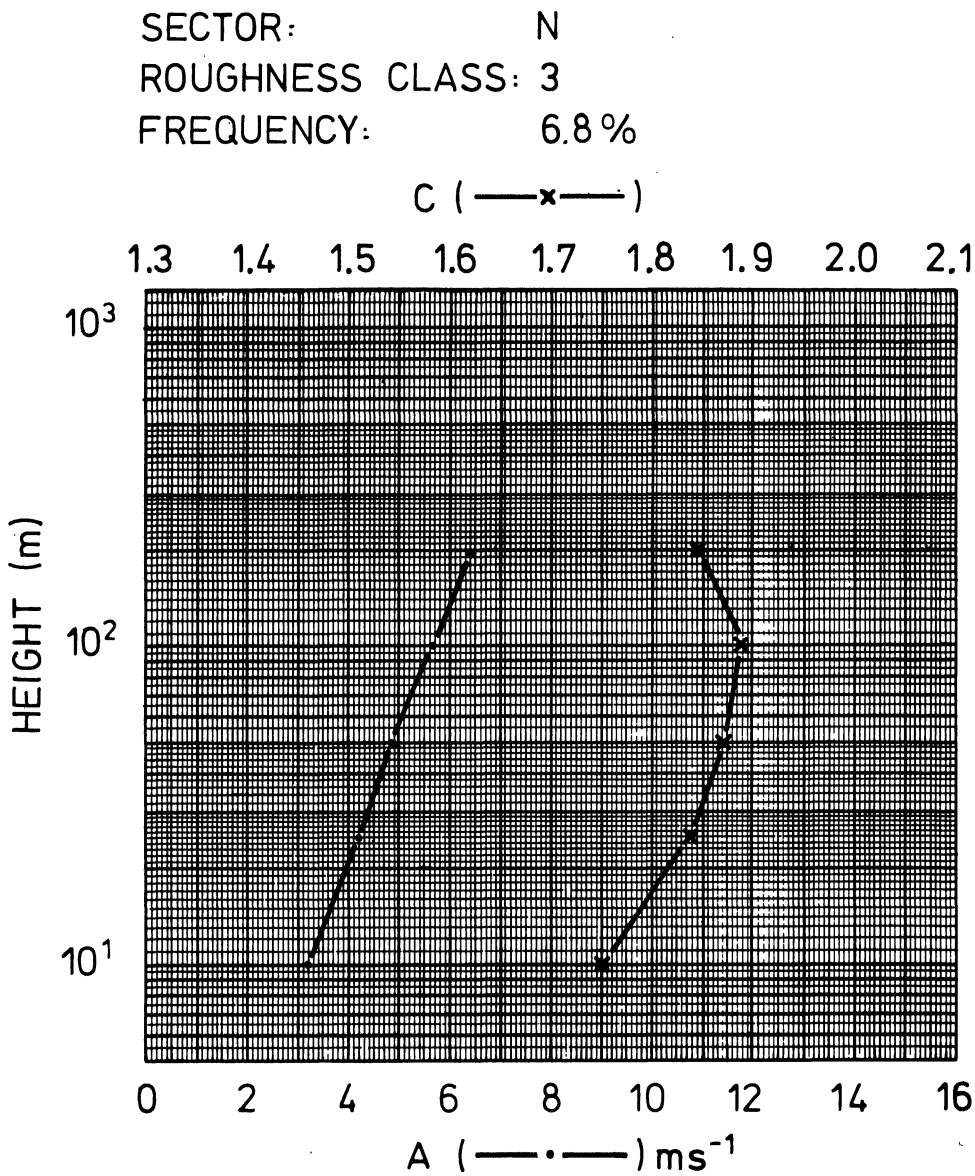
SECTOR: N
ROUGHNESS CLASS: 3
FREQUENCY: 6.8 %
C (—×—)
1.3 1.4 1.5 1.6 1.7 1.8 1.9 2.0 2.1
HEIGHT (m)
10³
10²
10¹
0 2 4 6 8 10 12 14 16
A (—•—) ms⁻¹

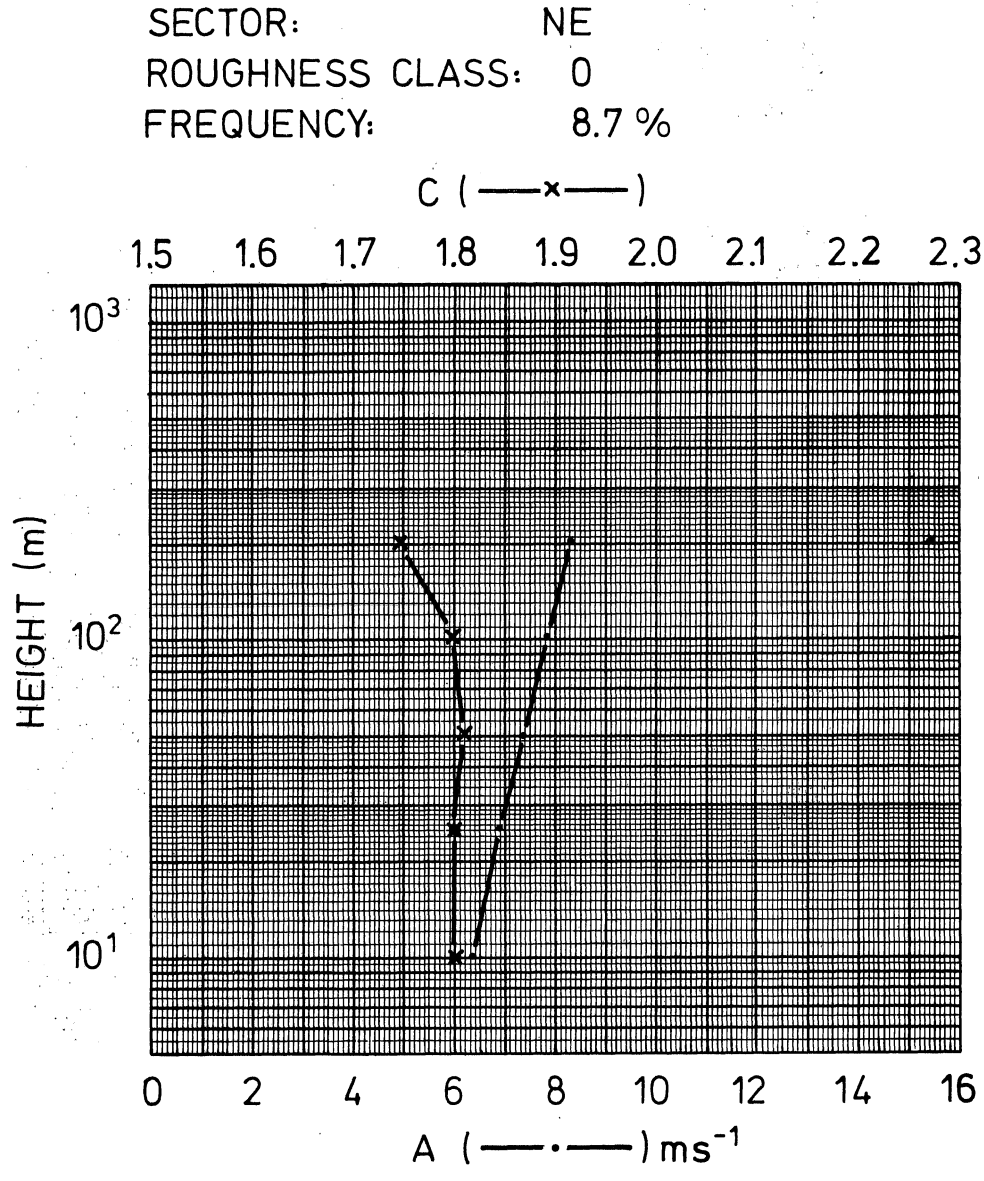
SECTOR: NE
ROUGHNESS CLASS: 0
FREQUENCY: 8.7 %
C (—×—)
1.5 1.6 1.7 1.8 1.9 2.0 2.1 2.2 2.3
HEIGHT (m)
10³
10²
10¹
0 2 4 6 8 10 12 14 16
A (—·—) ms⁻¹

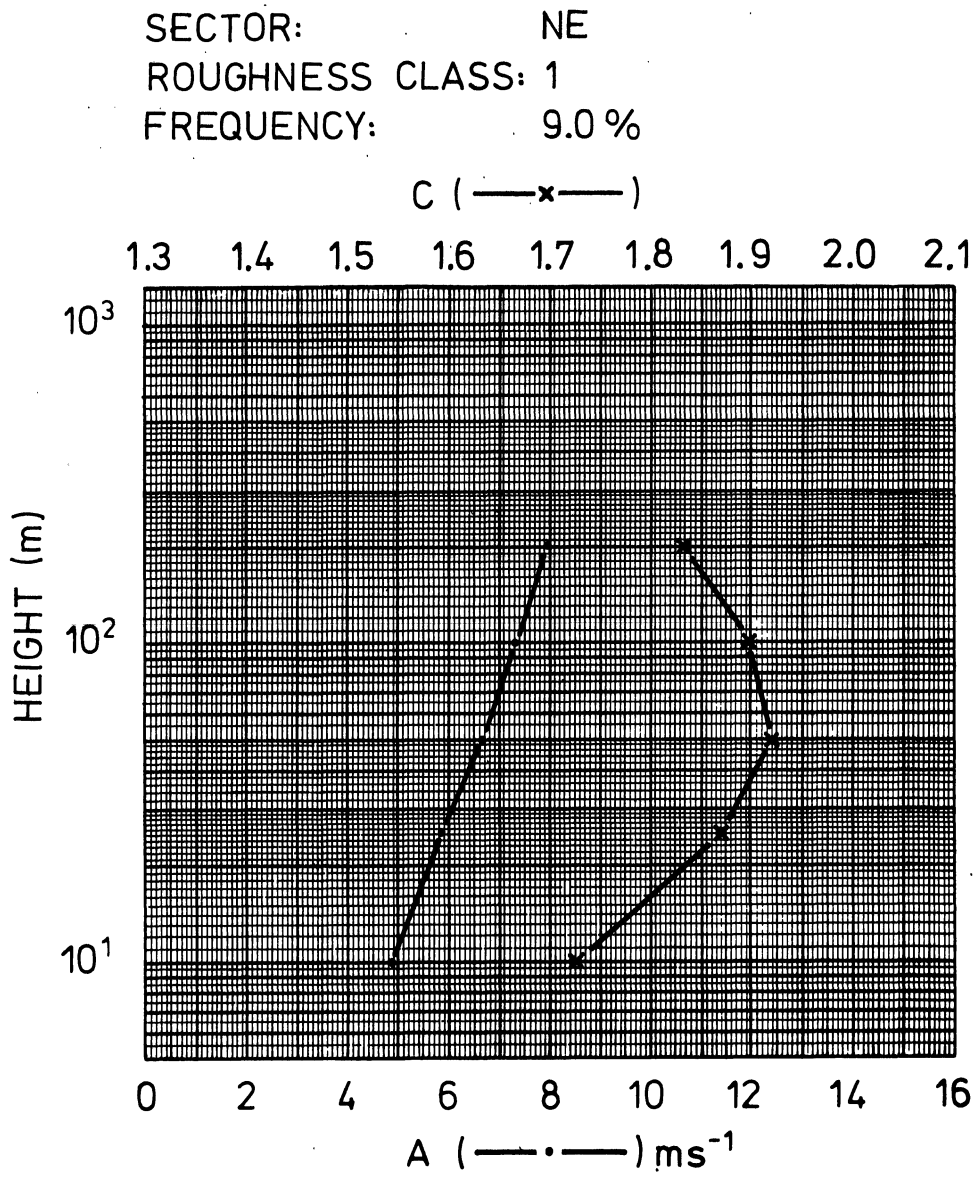
SECTOR: NE
ROUGHNESS CLASS: 1
FREQUENCY: 9.0 %
C (—×—)
1.3 1.4 1.5 1.6 1.7 1.8 1.9 2.0 2.1
HEIGHT (m)
10³
10²
10¹
0 2 4 6 8 10 12 14 16
A (—·—) ms⁻¹

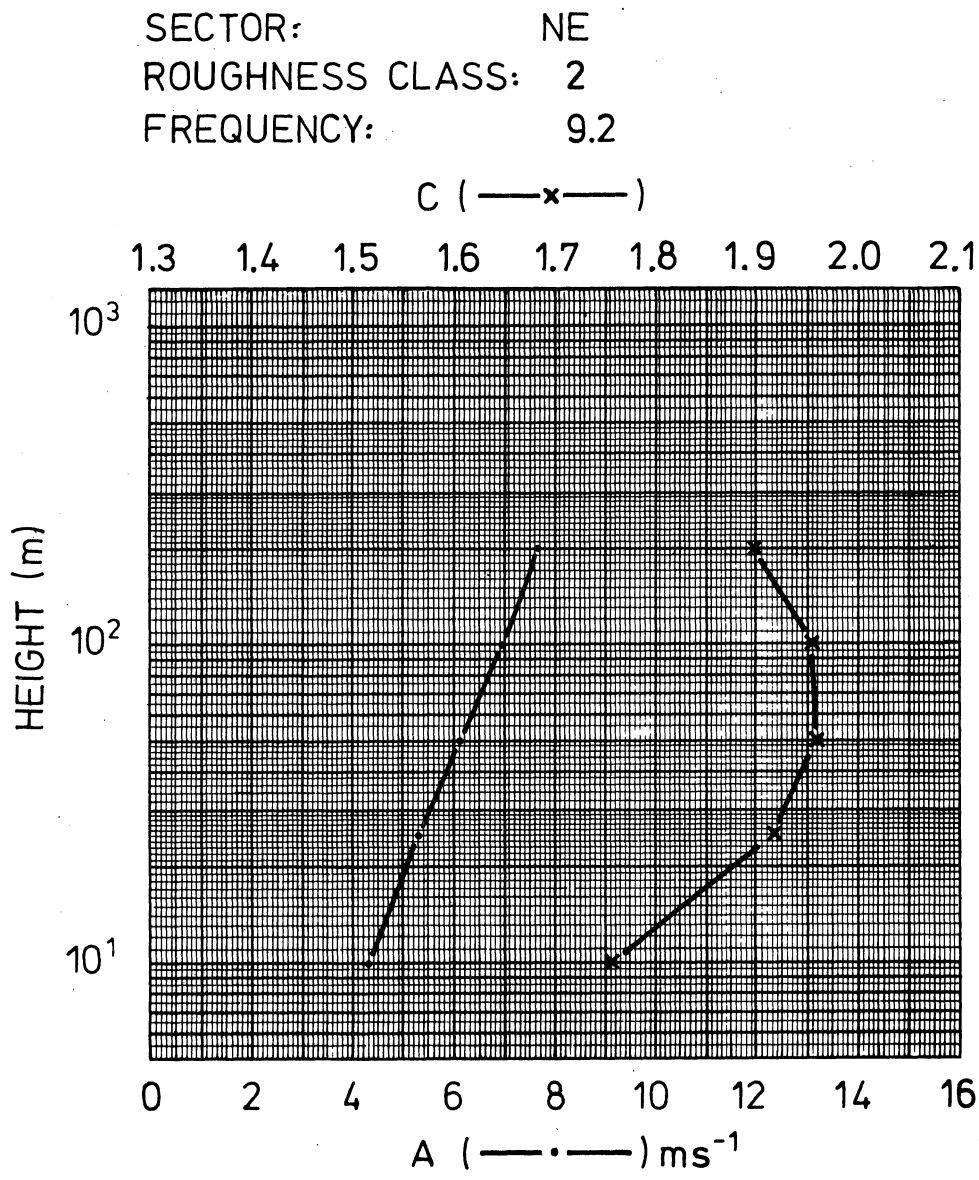
SECTOR: NE
ROUGHNESS CLASS: 2
FREQUENCY: 9.2
C (—×—)
1.3 1.4 1.5 1.6 1.7 1.8 1.9 2.0 2.1
HEIGHT (m)
10³
10²
10¹
0 2 4 6 8 10 12 14 16
A (—·—) ms⁻¹

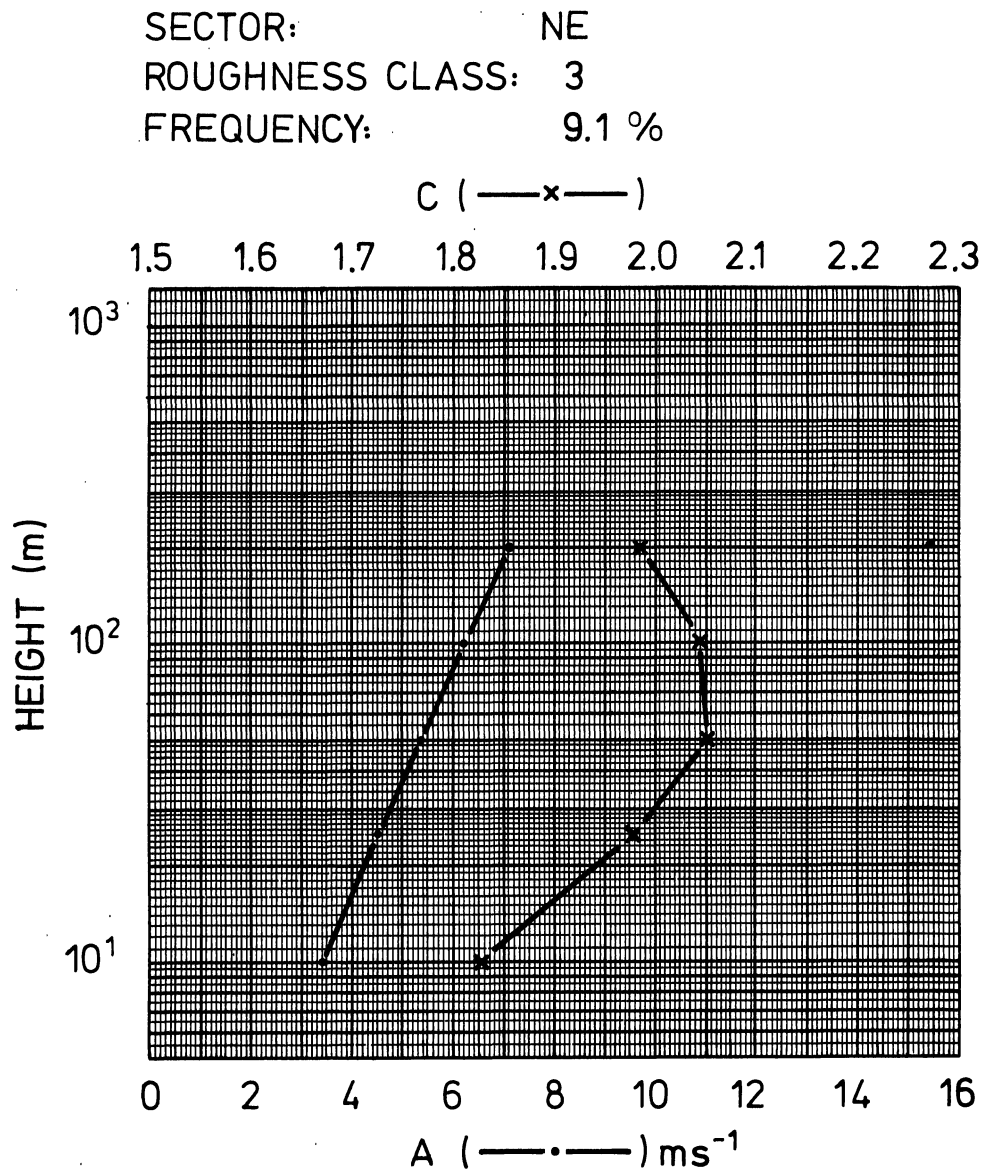
SECTOR: NE
ROUGHNESS CLASS: 3
FREQUENCY: 9.1 %
C (—×—)
1.5 1.6 1.7 1.8 1.9 2.0 2.1 2.2 2.3
HEIGHT (m)
10³
10²
10¹
0 2 4 6 8 10 12 14 16
A (—·—) ms⁻¹

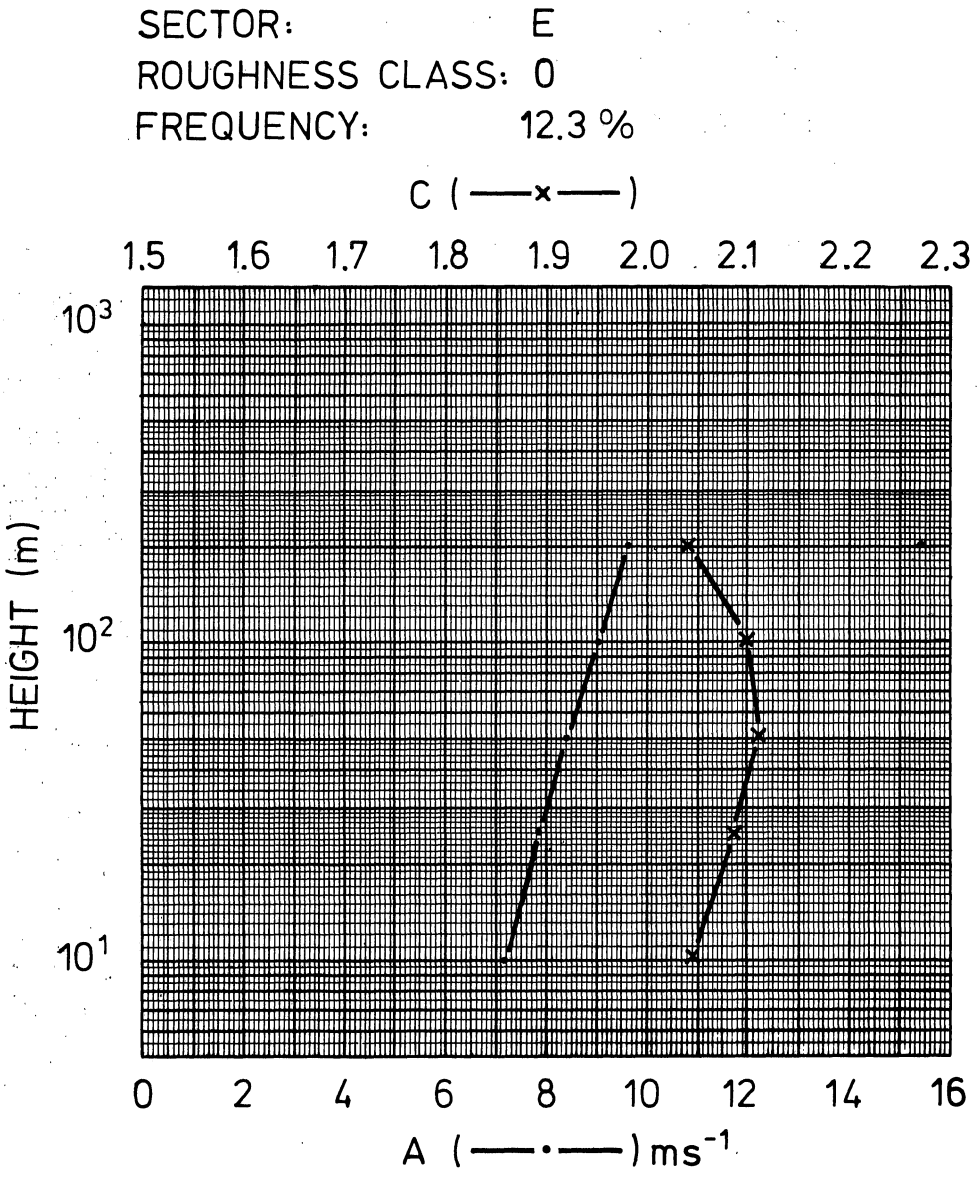
SECTOR: E
ROUGHNESS CLASS: 0
FREQUENCY: 12.3 %
C (—×—)
1.5 1.6 1.7 1.8 1.9 2.0 2.1 2.2 2.3
HEIGHT (m)
10³
10²
10¹
0 2 4 6 8 10 12 14 16
A (—·—) ms⁻¹

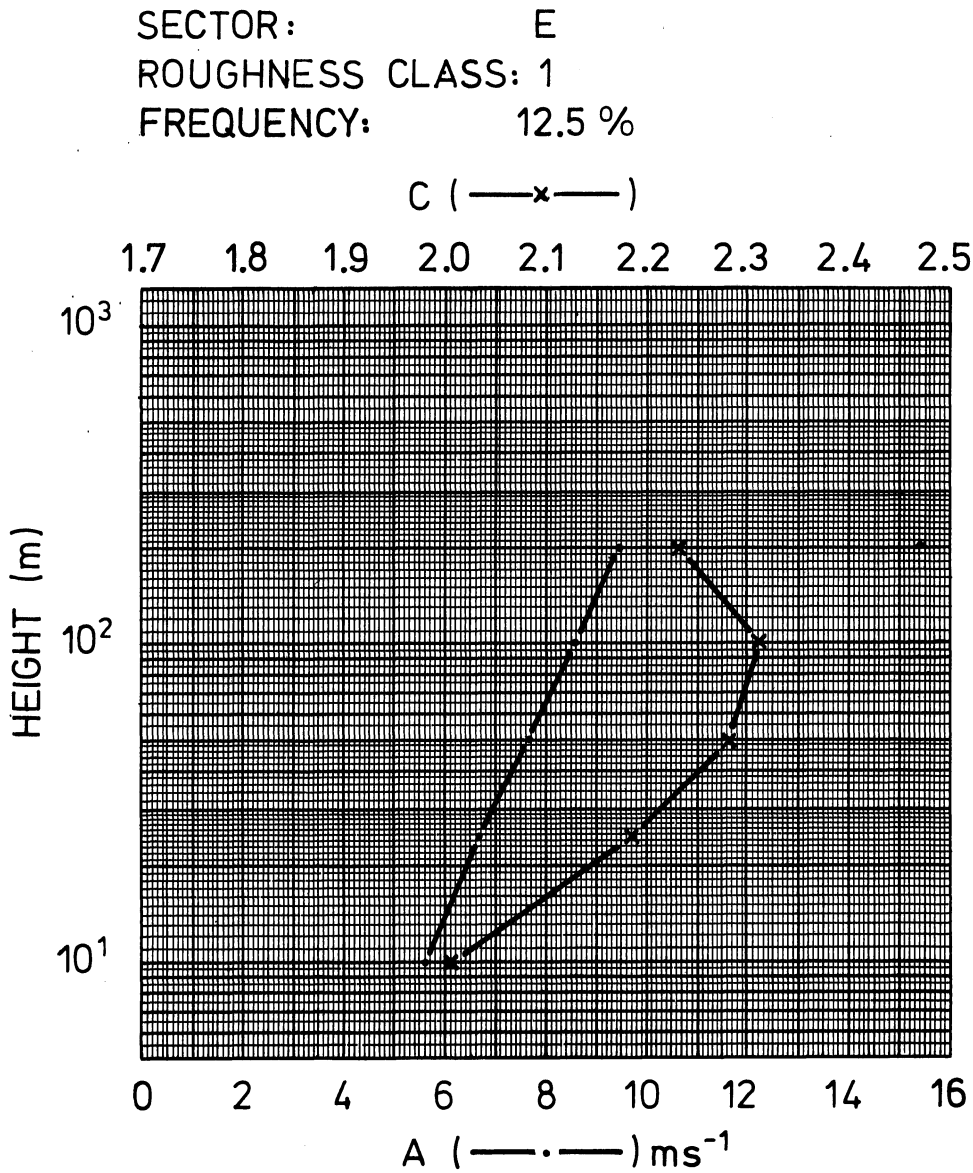
SECTOR: E
ROUGHNESS CLASS: 1
FREQUENCY: 12.5 %
C (—×—)
1.7 1.8 1.9 2.0 2.1 2.2 2.3 2.4 2.5
HEIGHT (m)
10³
10²
10¹
0 2 4 6 8 10 12 14 16
A (—·—) ms⁻¹

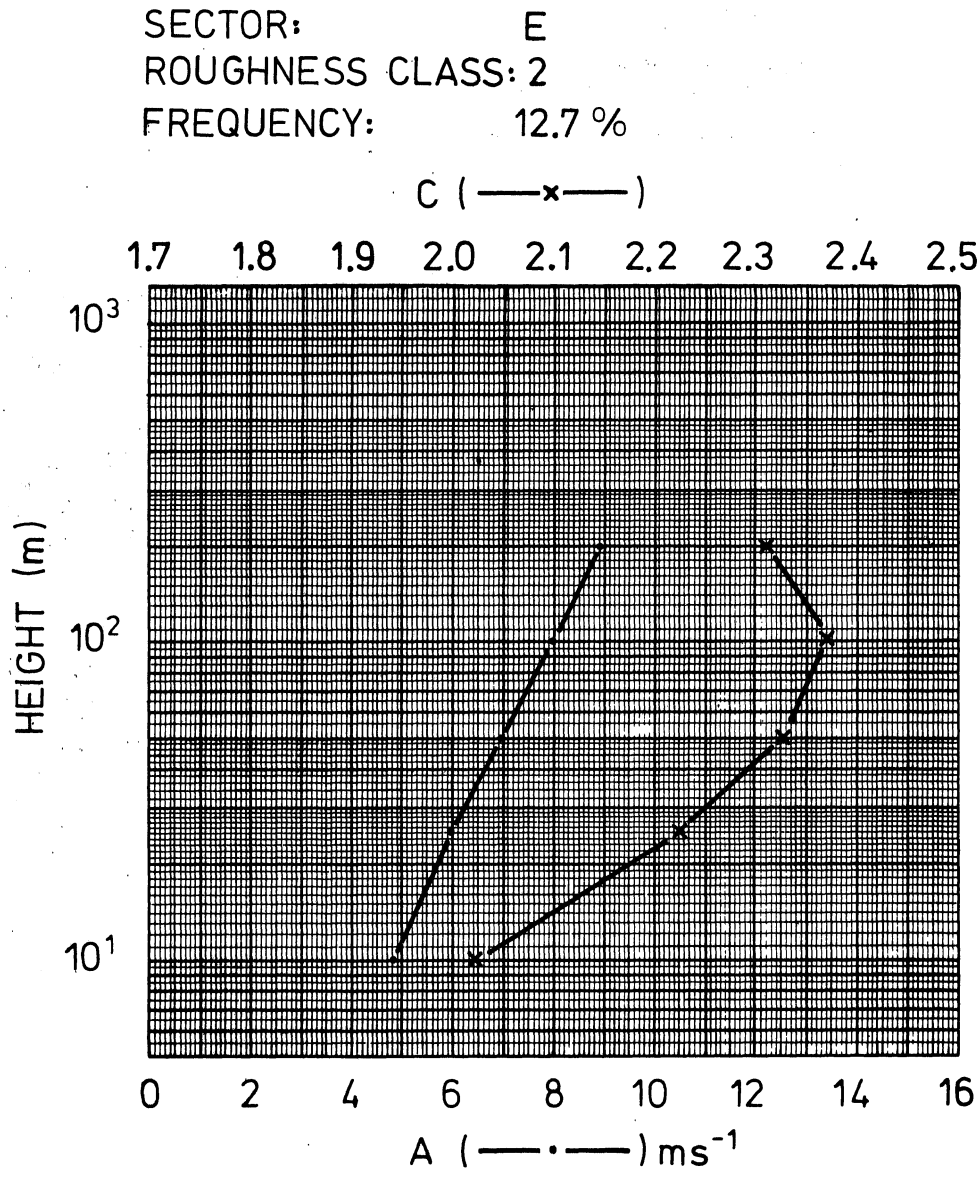
SECTOR: E
ROUGHNESS CLASS: 2
FREQUENCY: 12.7 %
C (—×—)
1.7 1.8 1.9 2.0 2.1 2.2 2.3 2.4 2.5
HEIGHT (m)
10³
10²
10¹
0 2 4 6 8 10 12 14 16
A (—·—) ms⁻¹

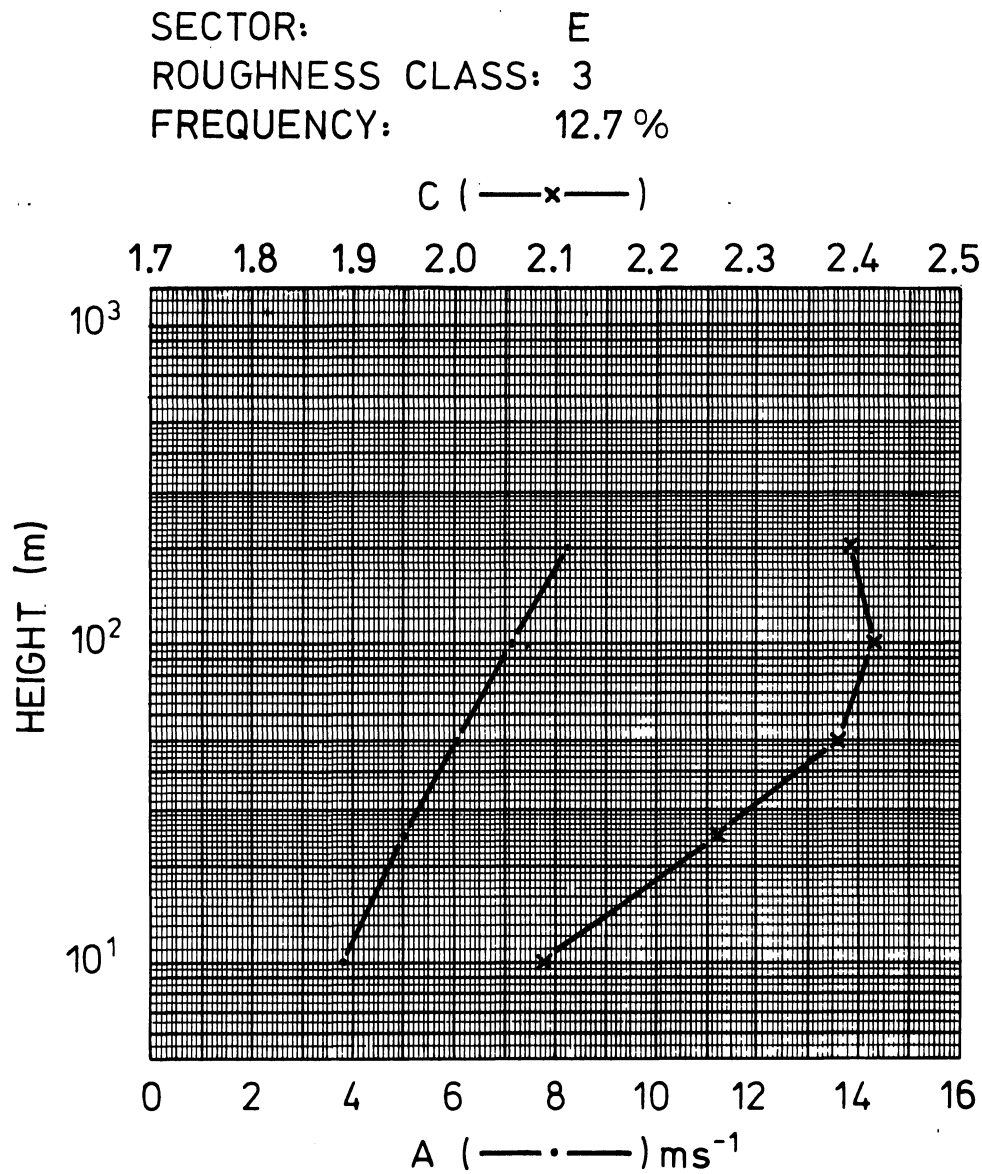
SECTOR: E
ROUGHNESS CLASS: 3
FREQUENCY: 12.7 %
C (—×—)
1.7 1.8 1.9 2.0 2.1 2.2 2.3 2.4 2.5
HEIGHT (m)
10³
10²
10¹
0 2 4 6 8 10 12 14 16
A (—·—) ms⁻¹

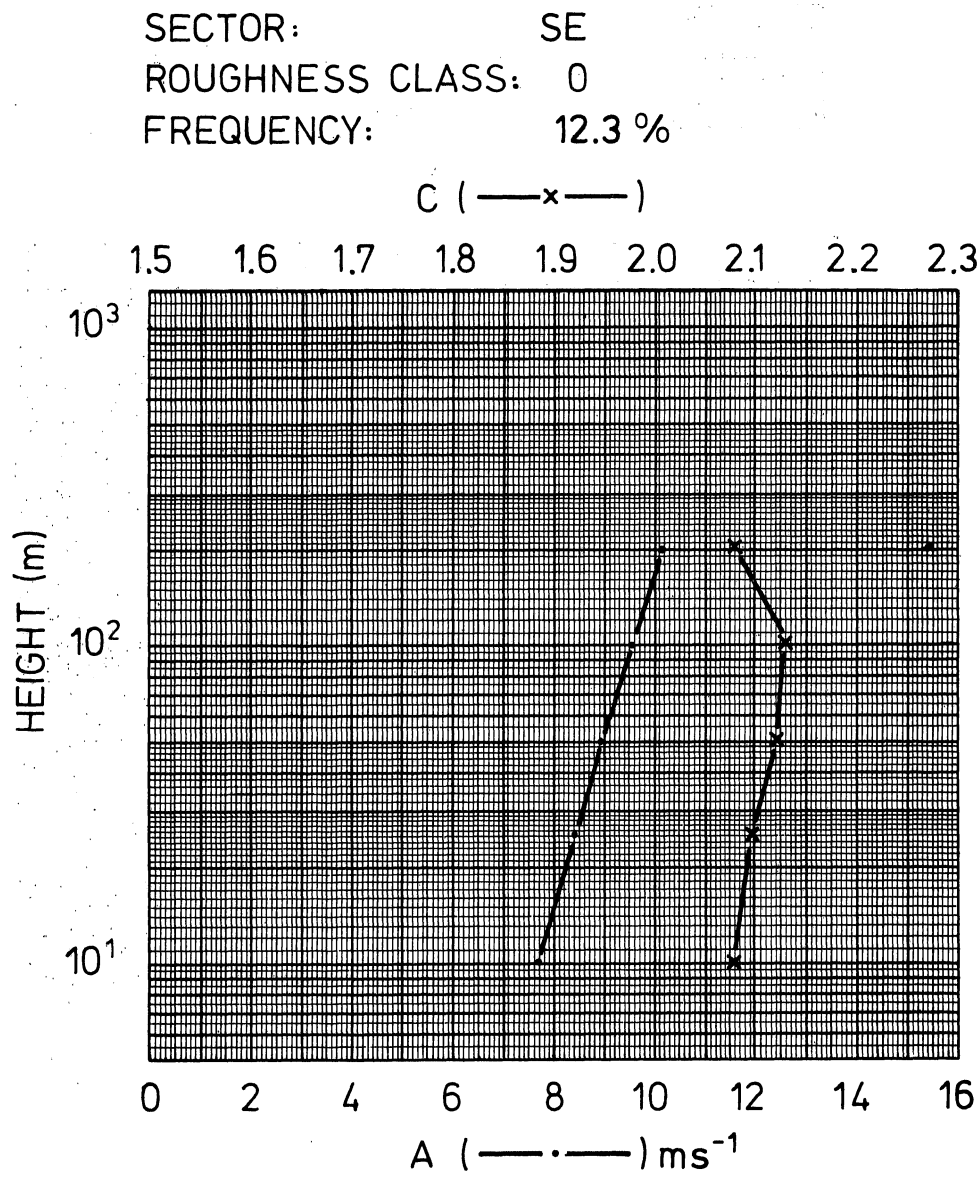
SECTOR: SE
ROUGHNESS CLASS: 0
FREQUENCY: 12.3 %
C (——x——)
1.5 1.6 1.7 1.8 1.9 2.0 2.1 2.2 2.3
HEIGHT (m)
10³
10²
10¹
0 2 4 6 8 10 12 14 16
A (——·——) ms⁻¹

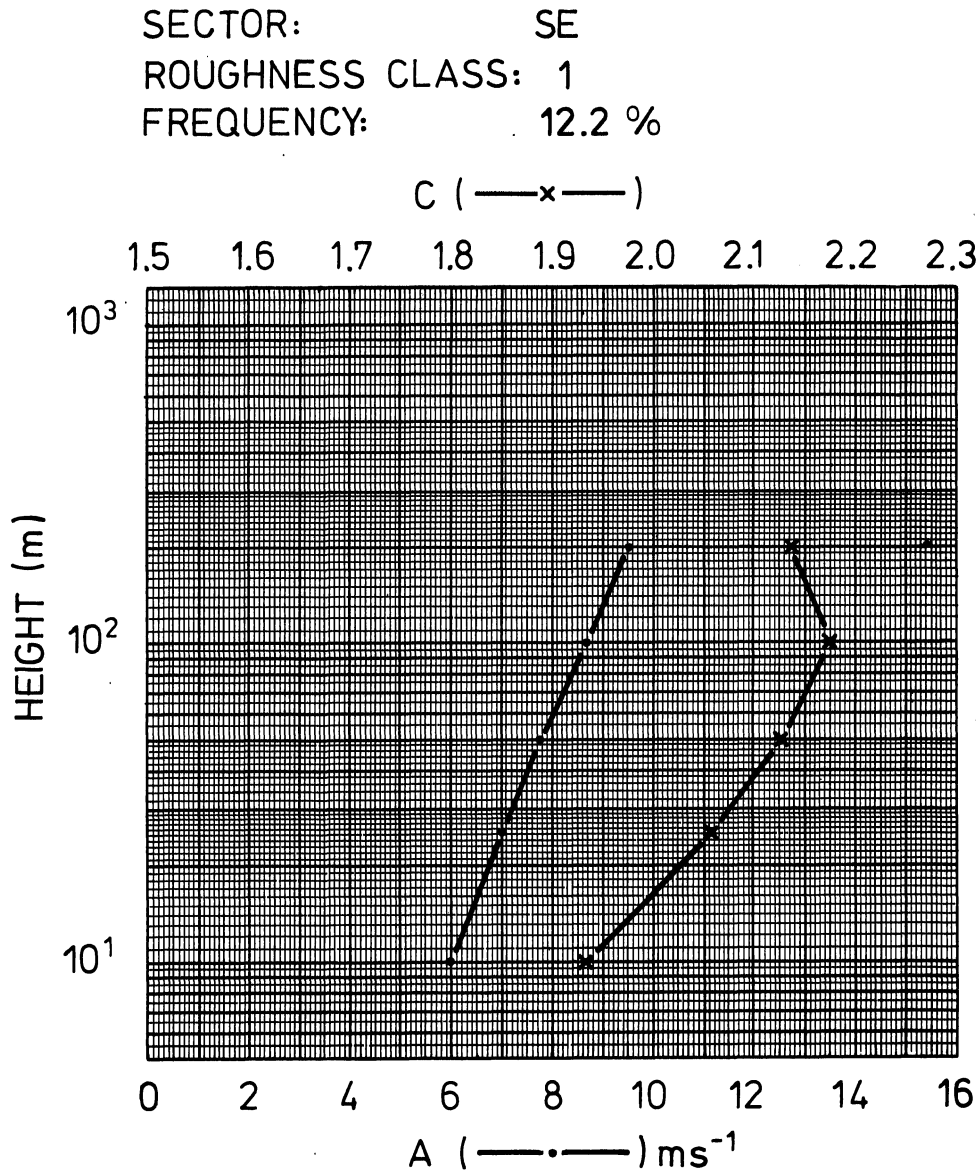
SECTOR: SE
ROUGHNESS CLASS: 1
FREQUENCY: 12.2 %
C (—×—)
1.5 1.6 1.7 1.8 1.9 2.0 2.1 2.2 2.3
HEIGHT (m)
10³
10²
10¹
0 2 4 6 8 10 12 14 16
A (—·—) ms⁻¹

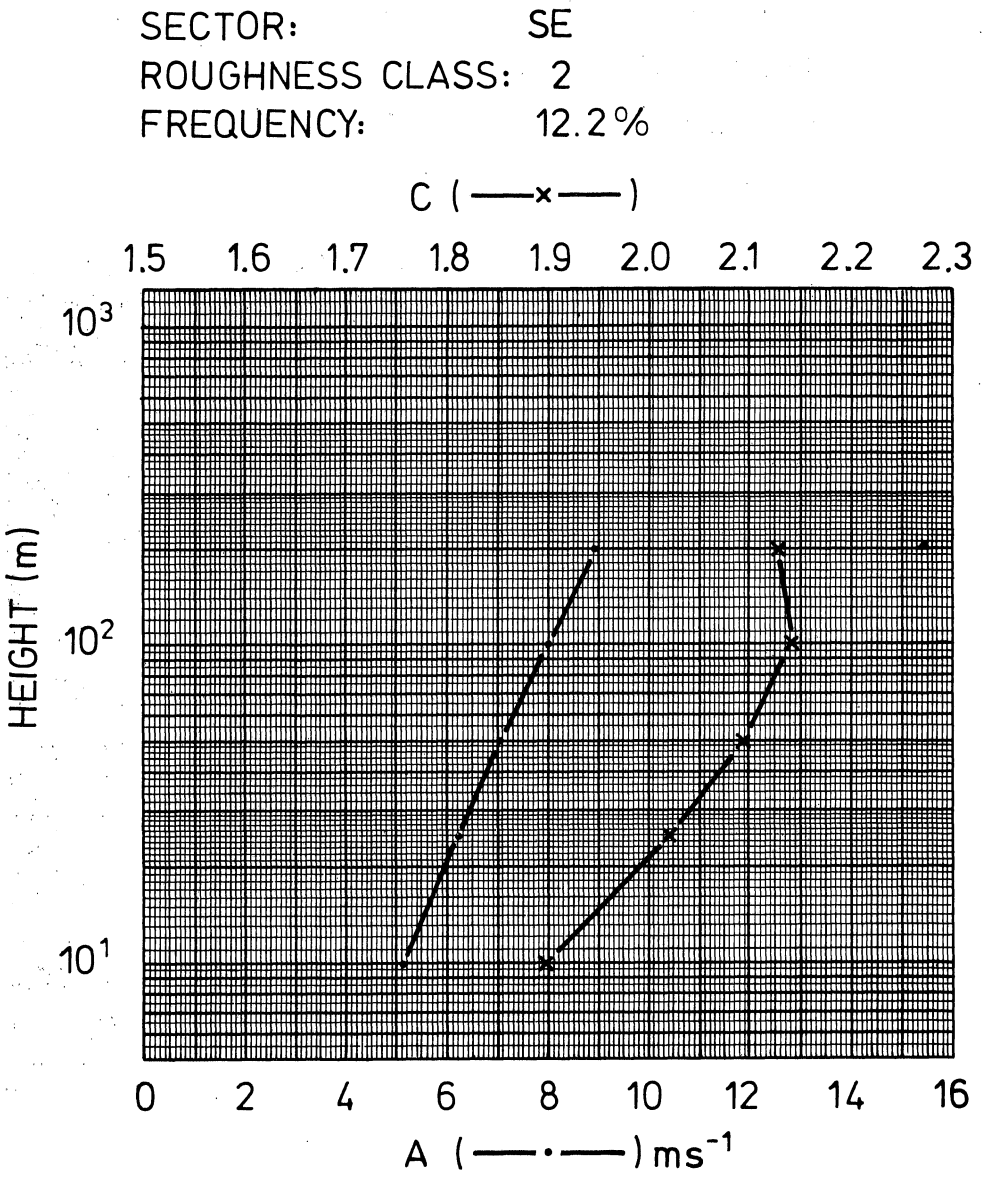
SECTOR: SE
ROUGHNESS CLASS: 2
FREQUENCY: 12.2%
C (——×——)
1.5 1.6 1.7 1.8 1.9 2.0 2.1 2.2 2.3
HEIGHT (m)
10³
10²
10¹
0 2 4 6 8 10 12 14 16
A (——·——) ms⁻¹

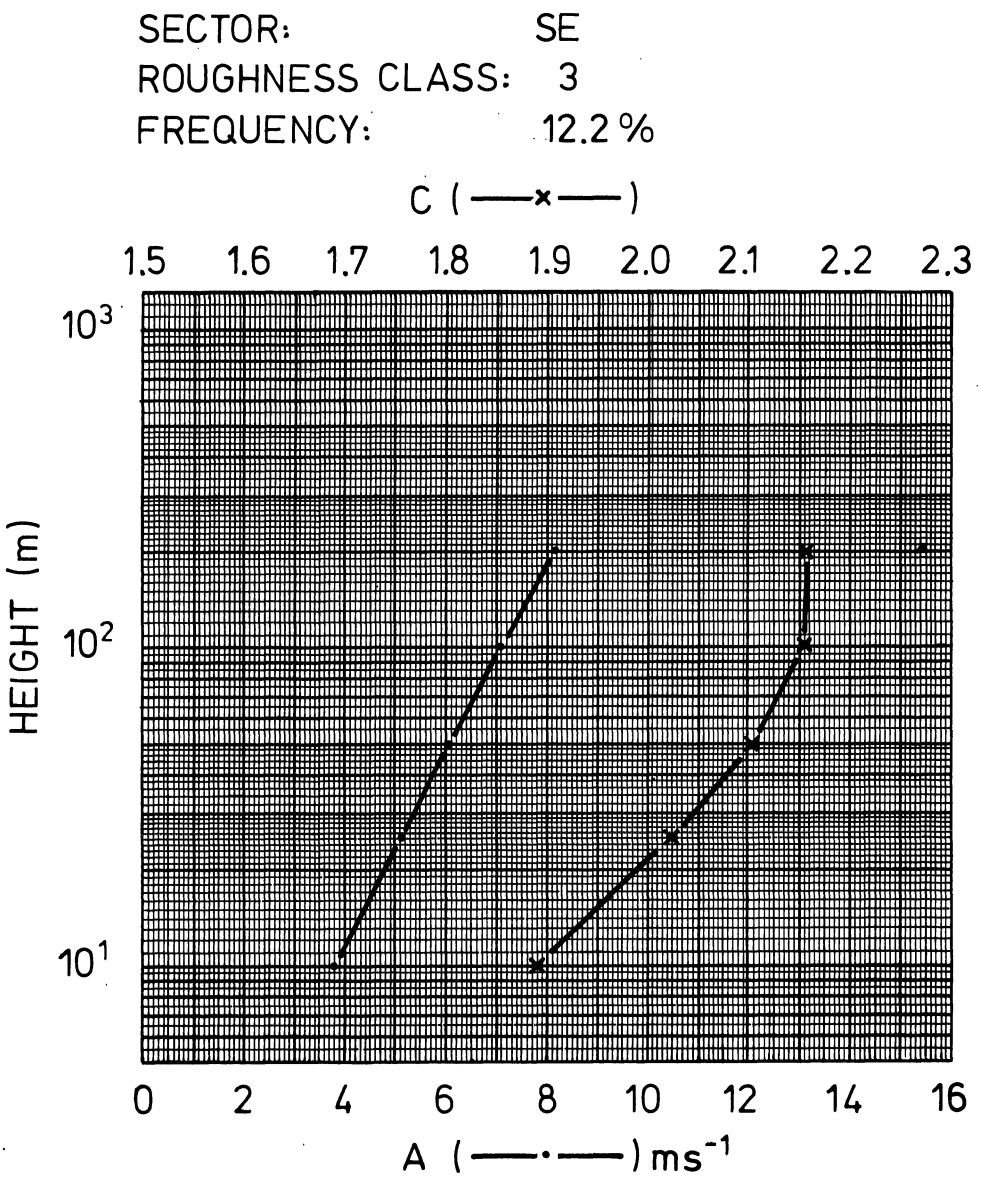
SECTOR: SE
ROUGHNESS CLASS: 3
FREQUENCY: 12.2 %
C (—×—)
1.5 1.6 1.7 1.8 1.9 2.0 2.1 2.2 2.3
HEIGHT (m)
10³
10²
10¹
0 2 4 6 8 10 12 14 16
A (—·—) ms⁻¹

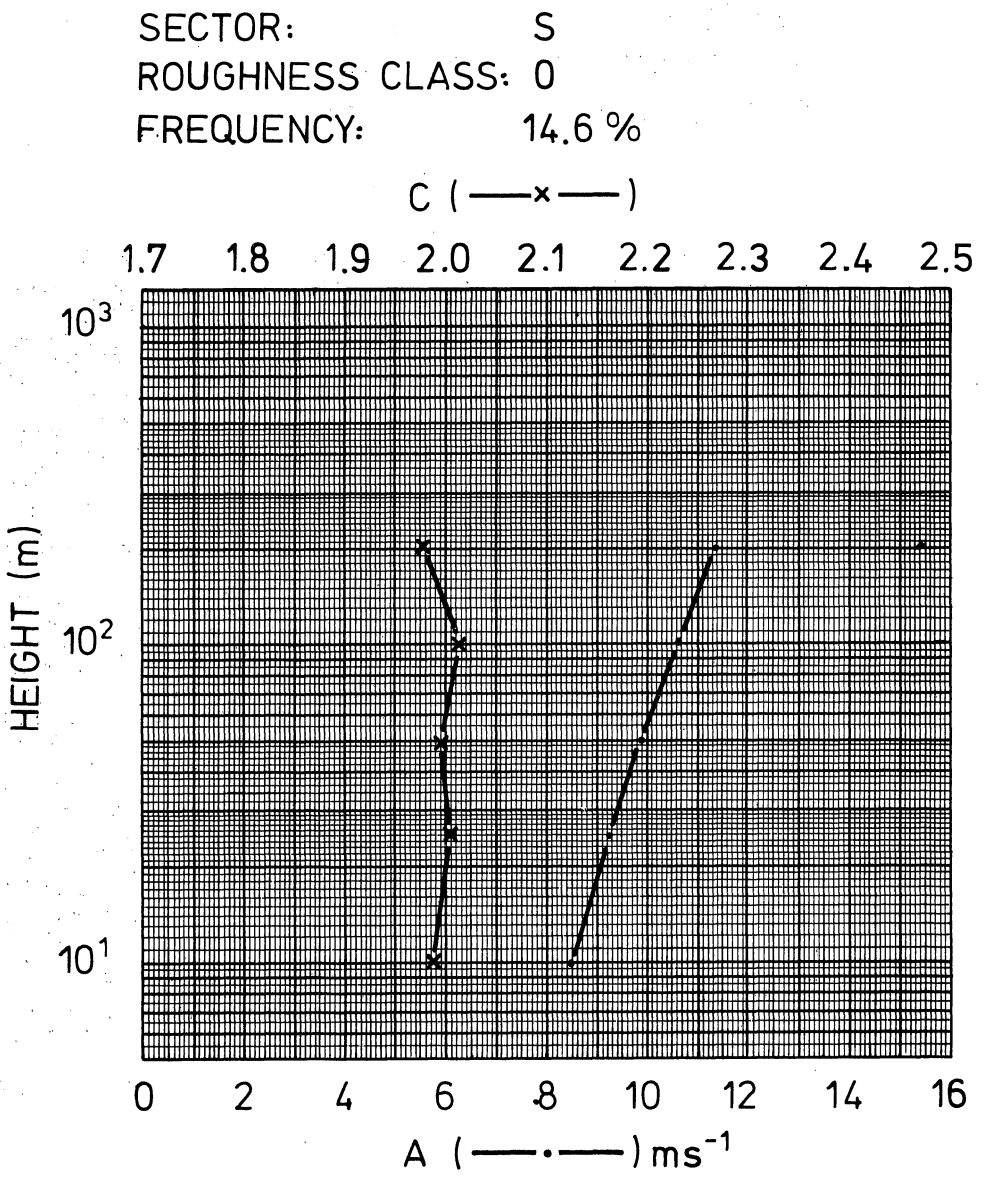
SECTOR: S
ROUGHNESS CLASS: 0
FREQUENCY: 14.6 %
C (—×—)
1.7 1.8 1.9 2.0 2.1 2.2 2.3 2.4 2.5
HEIGHT (m)
10³
10²
10¹
0 2 4 6 8 10 12 14 16
A (—·—) ms⁻¹

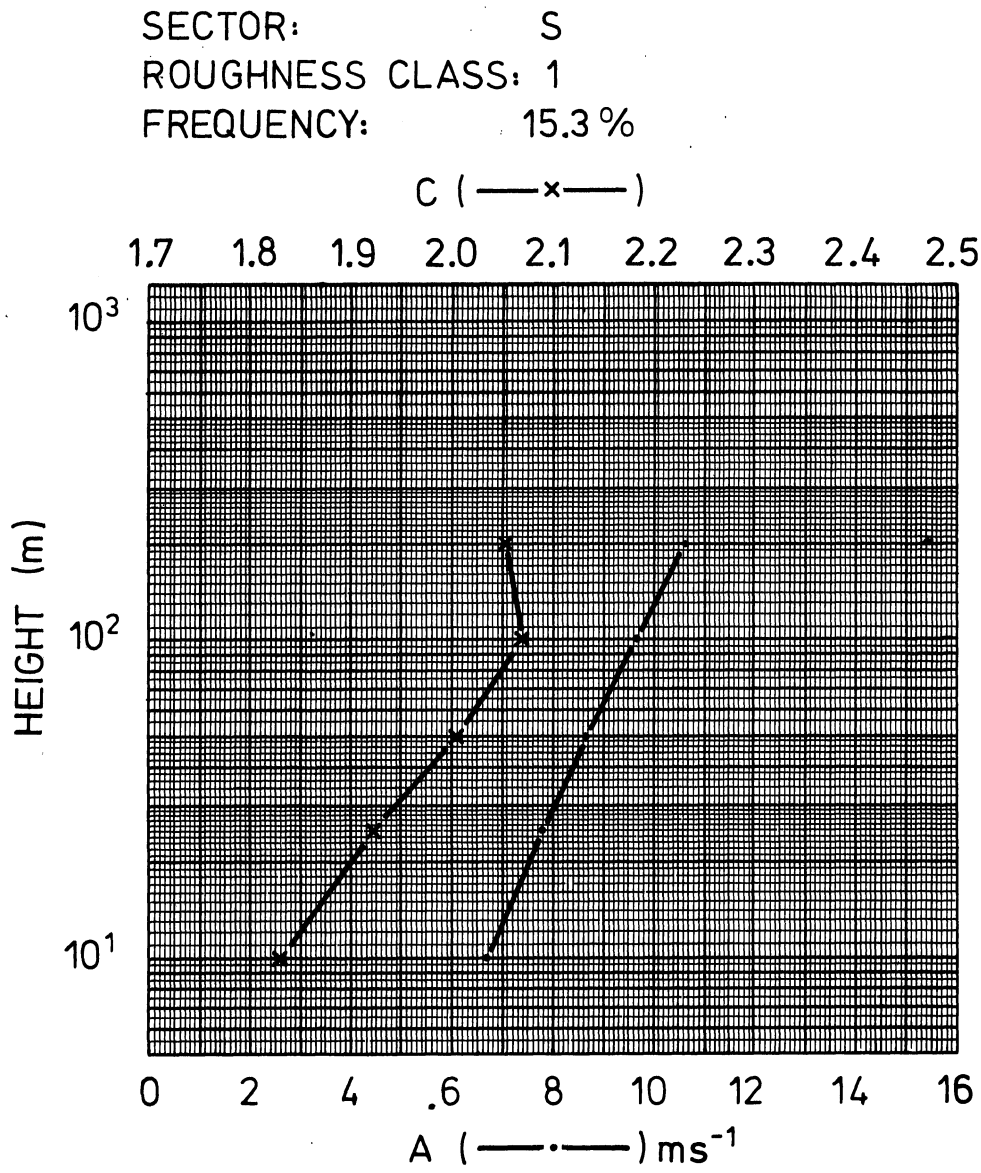
SECTOR: S
ROUGHNESS CLASS: 1
FREQUENCY: 15.3 %
C (—×—)
1.7 1.8 1.9 2.0 2.1 2.2 2.3 2.4 2.5
10^3
10^2
10^1
HEIGHT (m)
0 2 4 6 8 10 12 14 16
A (—·—) ms^{-1}

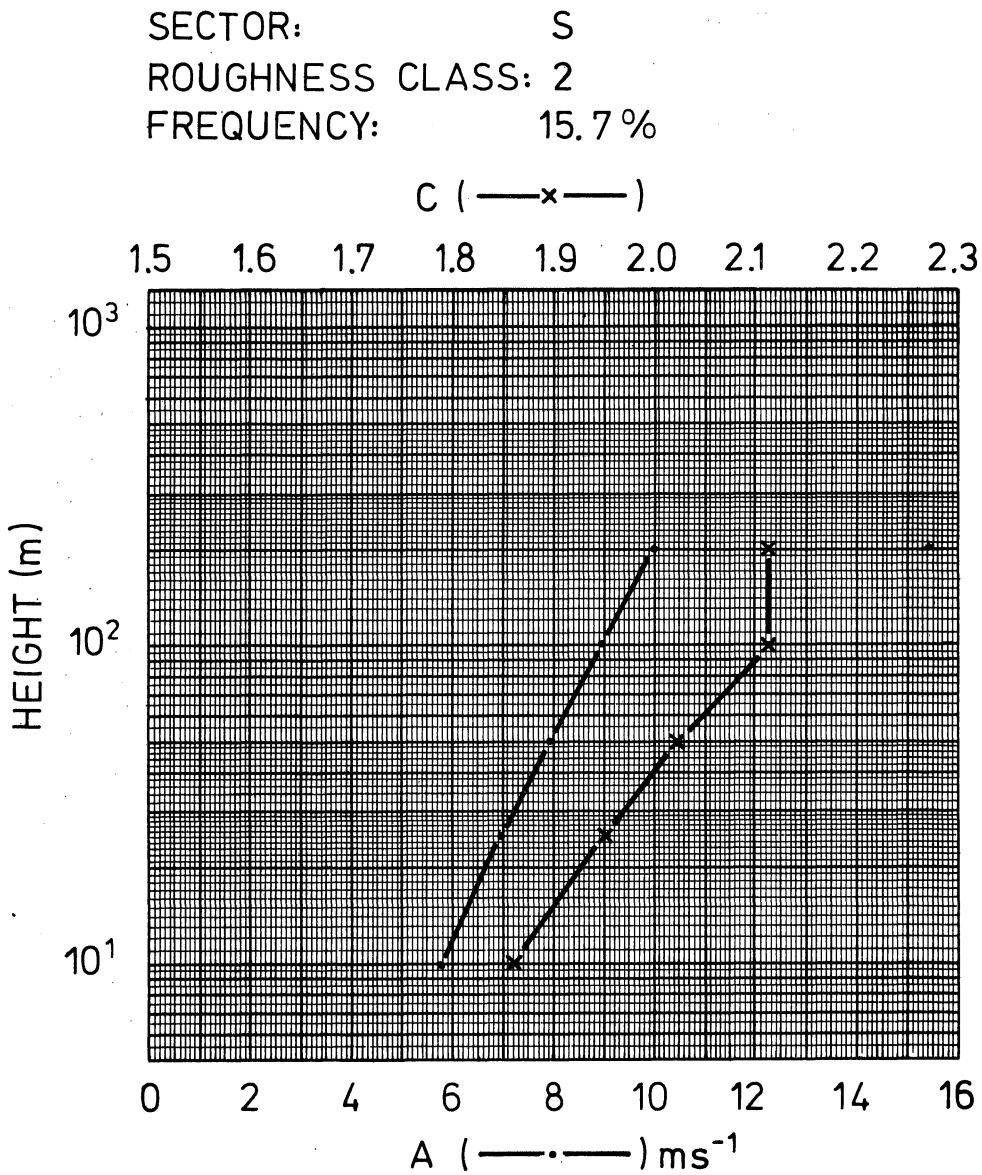
SECTOR: S
ROUGHNESS CLASS: 2
FREQUENCY: 15.7 %
C (——×——)
1.5 1.6 1.7 1.8 1.9 2.0 2.1 2.2 2.3
10^3
10^2
10^1
HEIGHT (m)
0 2 4 6 8 10 12 14 16
A (——·——) ms^{-1}

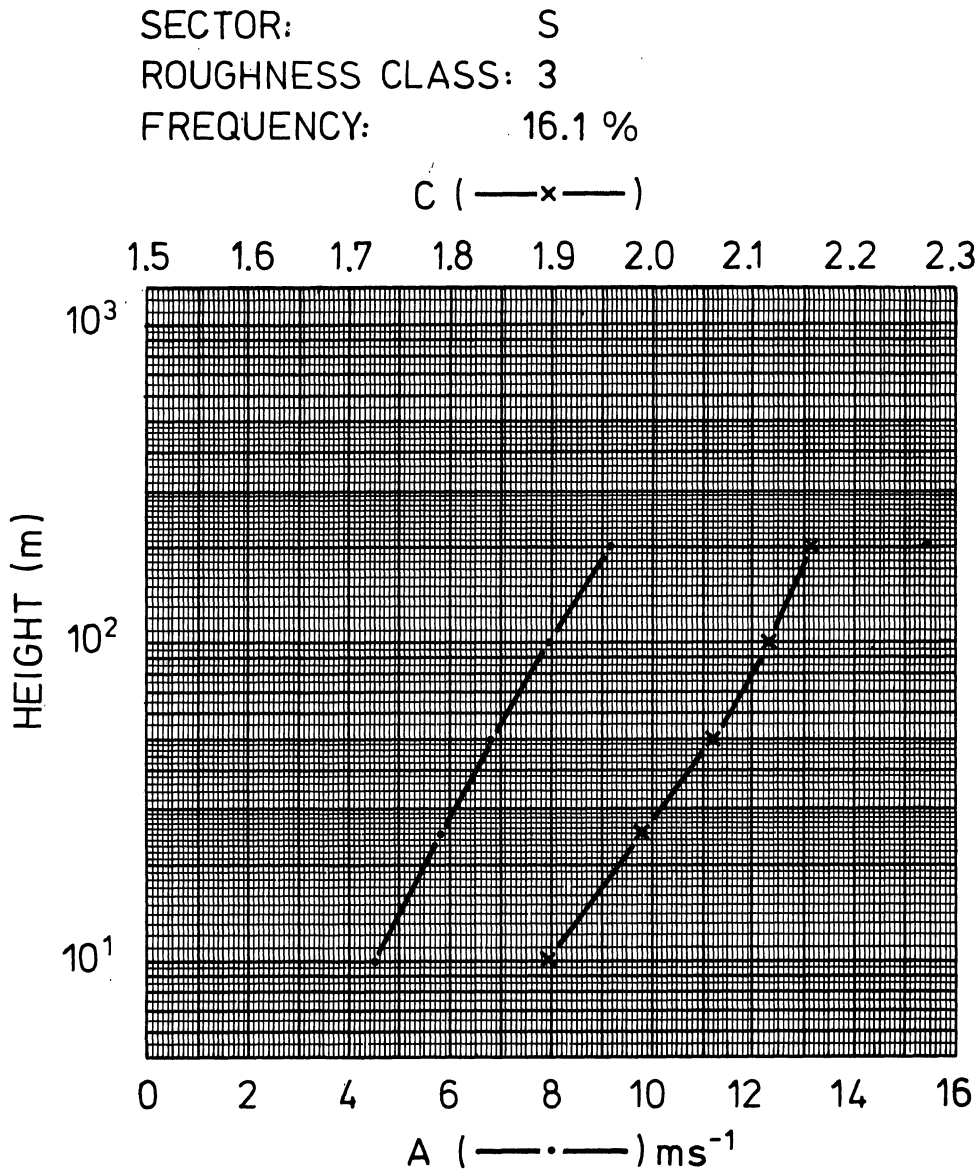
SECTOR: S
ROUGHNESS CLASS: 3
FREQUENCY: 16.1 %
C (——×——)
1.5 1.6 1.7 1.8 1.9 2.0 2.1 2.2 2.3
HEIGHT (m)
10³
10²
10¹
0 2 4 6 8 10 12 14 16
A (——·——) ms⁻¹

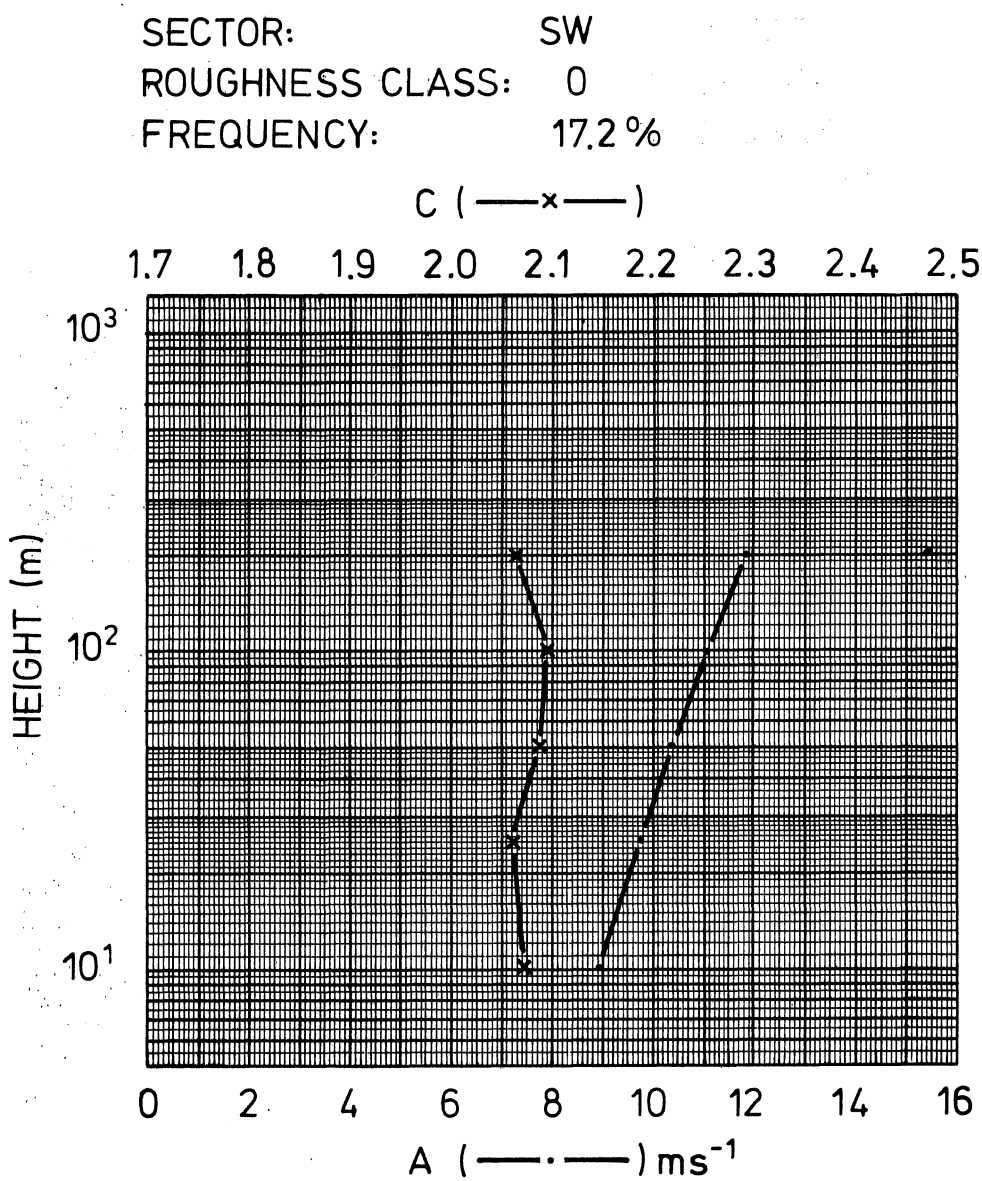
SECTOR: SW
ROUGHNESS CLASS: 0
FREQUENCY: 17.2 %
C (——×——)
1.7 1.8 1.9 2.0 2.1 2.2 2.3 2.4 2.5
HEIGHT (m)
10³
10²
10¹
0 2 4 6 8 10 12 14 16
A (——·——) ms⁻¹

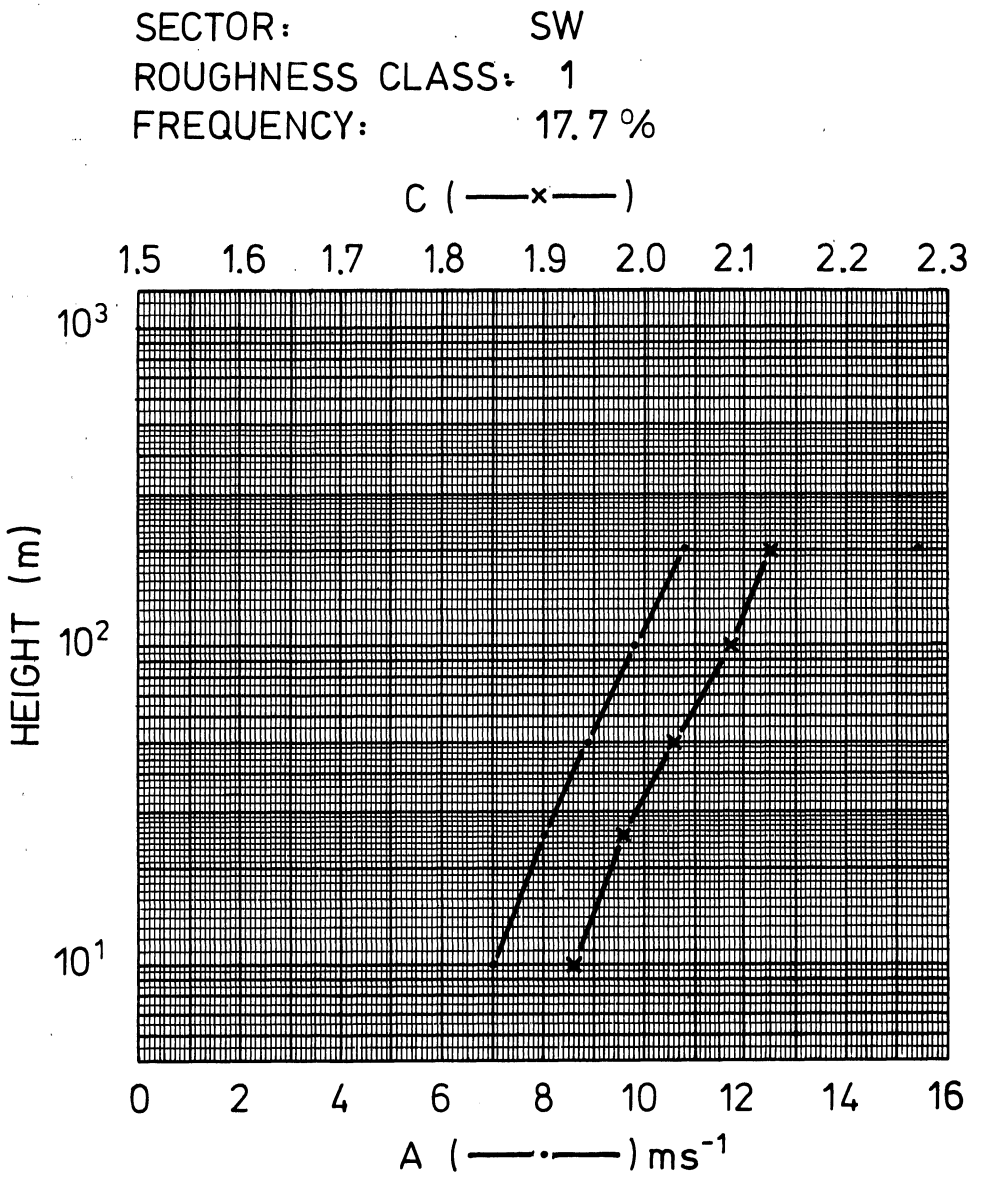
SECTOR: SW
ROUGHNESS CLASS: 1
FREQUENCY: 17.7 %
C (——×——)
1.5 1.6 1.7 1.8 1.9 2.0 2.1 2.2 2.3
HEIGHT (m)
10³
10²
10¹
0 2 4 6 8 10 12 14 16
A (——·——) ms⁻¹

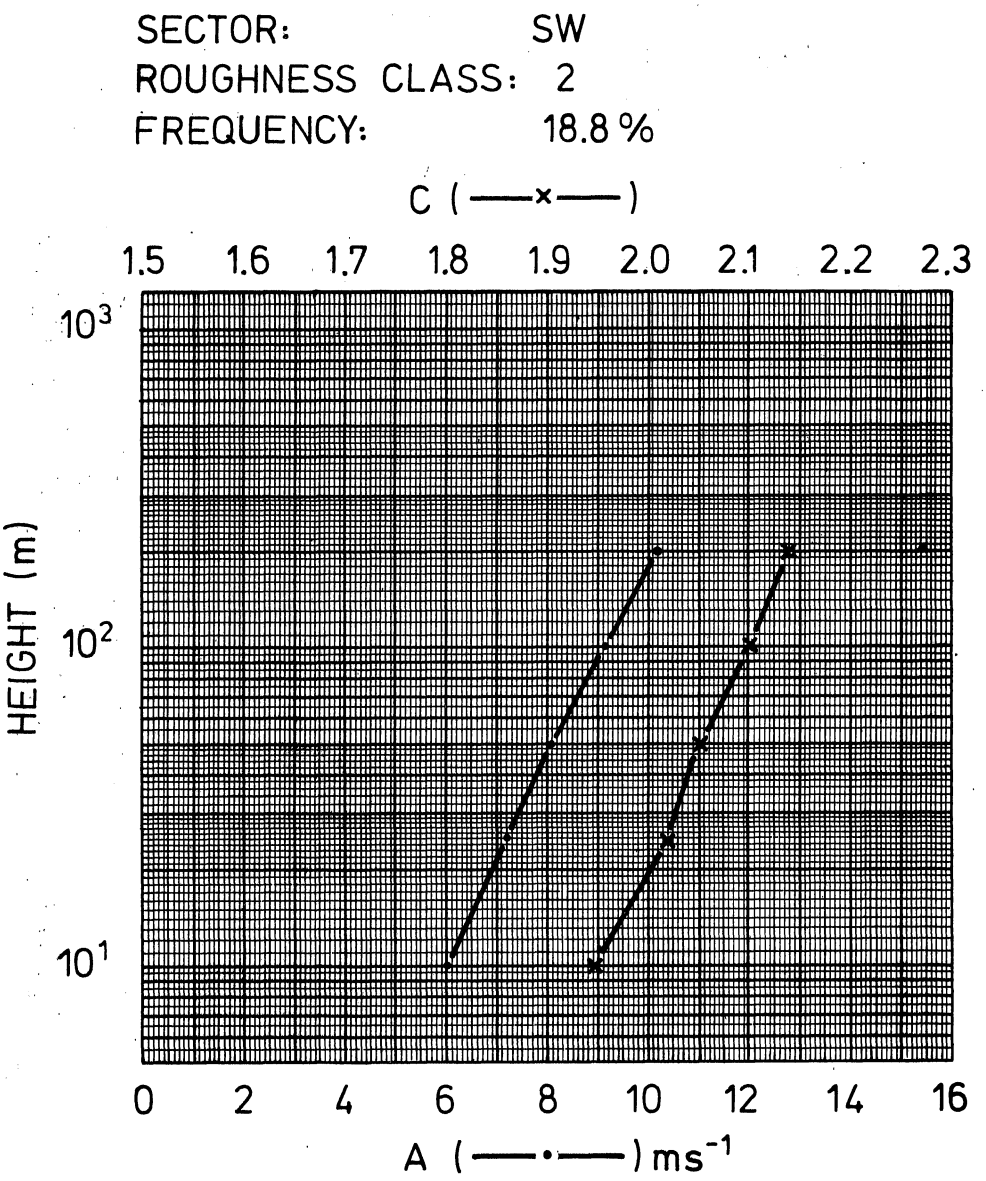
SECTOR: SW
ROUGHNESS CLASS: 2
FREQUENCY: 18.8 %
C (—×—)
1.5 1.6 1.7 1.8 1.9 2.0 2.1 2.2 2.3
HEIGHT (m)
10³
10²
10¹
0 2 4 6 8 10 12 14 16
A (—•—) ms⁻¹

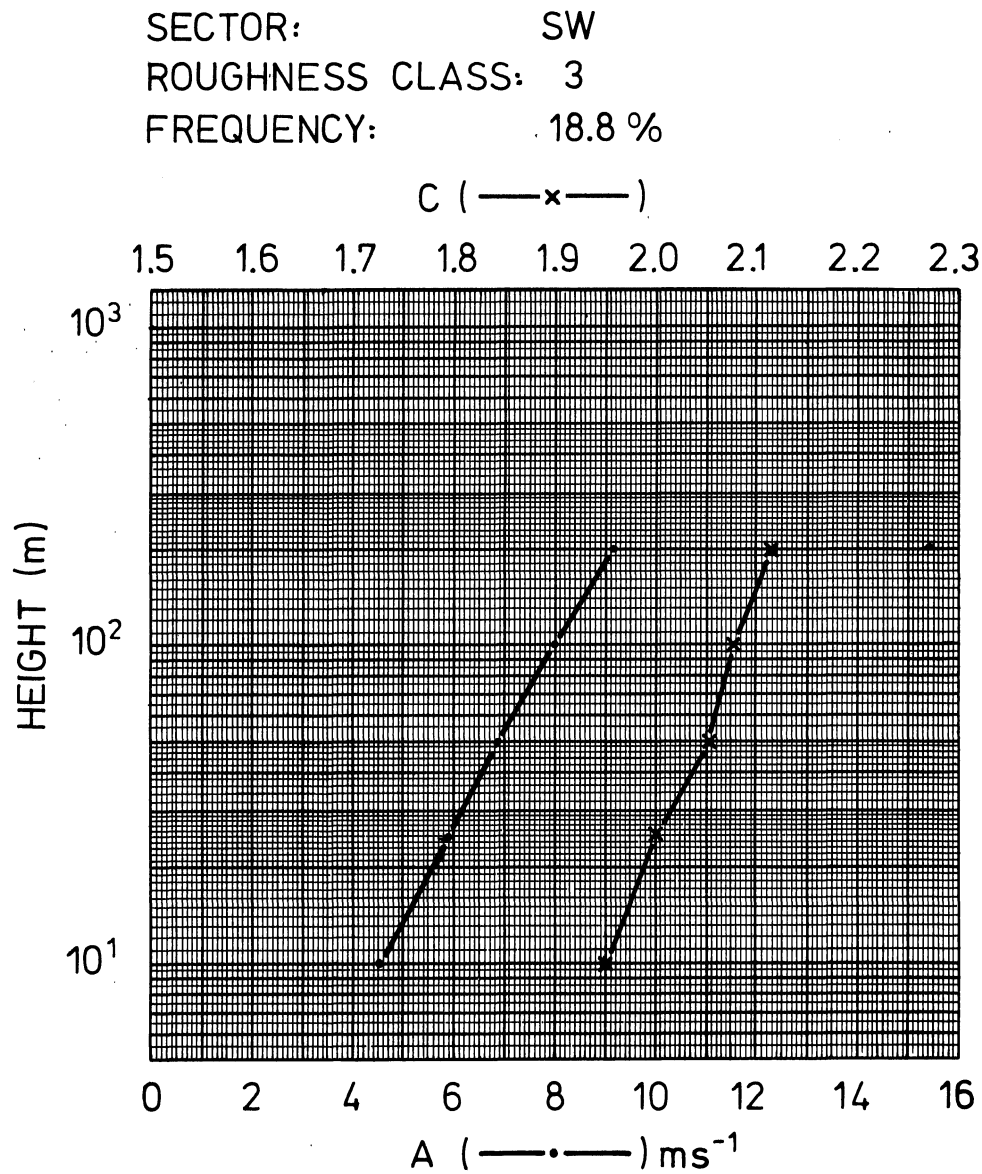
SECTOR: SW
ROUGHNESS CLASS: 3
FREQUENCY: 18.8 %
C (—×—)
1.5 1.6 1.7 1.8 1.9 2.0 2.1 2.2 2.3
HEIGHT (m)
10³
10²
10¹
0 2 4 6 8 10 12 14 16
A (—•—) ms⁻¹

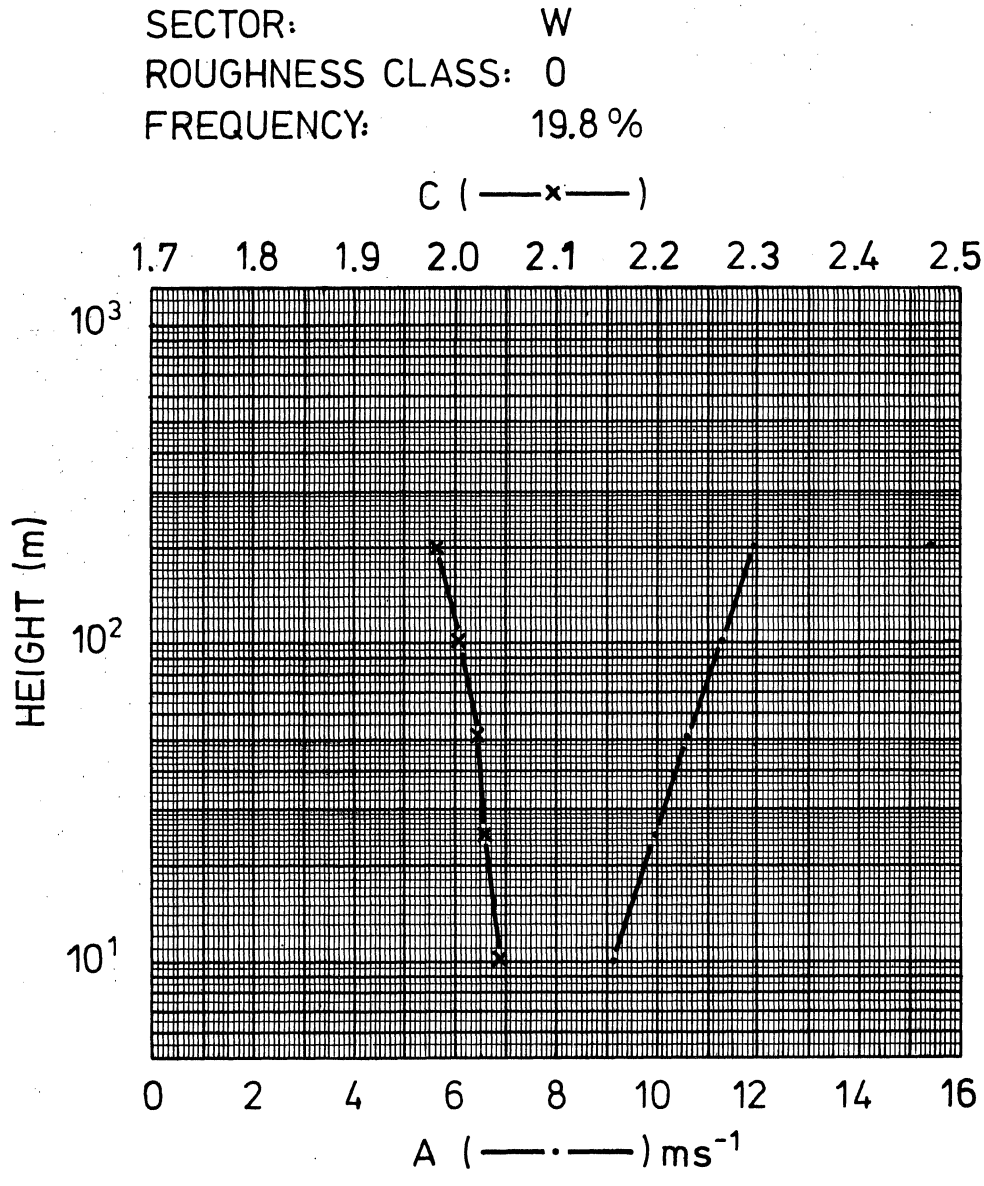
SECTOR: W
ROUGHNESS CLASS: 0
FREQUENCY: 19.8 %
C (——×——)
1.7 1.8 1.9 2.0 2.1 2.2 2.3 2.4 2.5
HEIGHT (m)
10³
10²
10¹
0 2 4 6 8 10 12 14 16
A (——·——) ms⁻¹

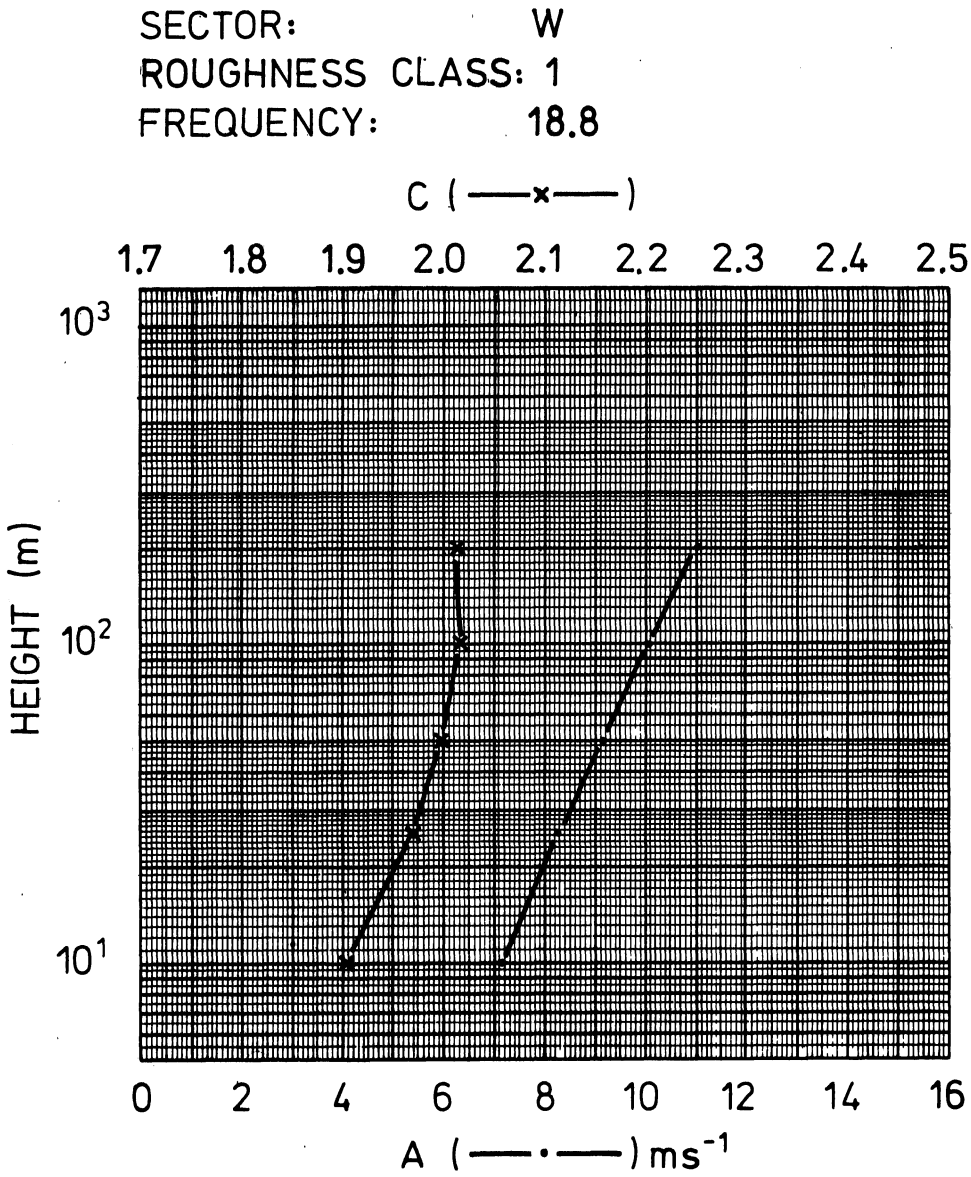
SECTOR: W
ROUGHNESS CLASS: 1
FREQUENCY: 18.8
C (—×—)
1.7 1.8 1.9 2.0 2.1 2.2 2.3 2.4 2.5
HEIGHT (m)
10³
10²
10¹
0 2 4 6 8 10 12 14 16
A (—·—) ms⁻¹

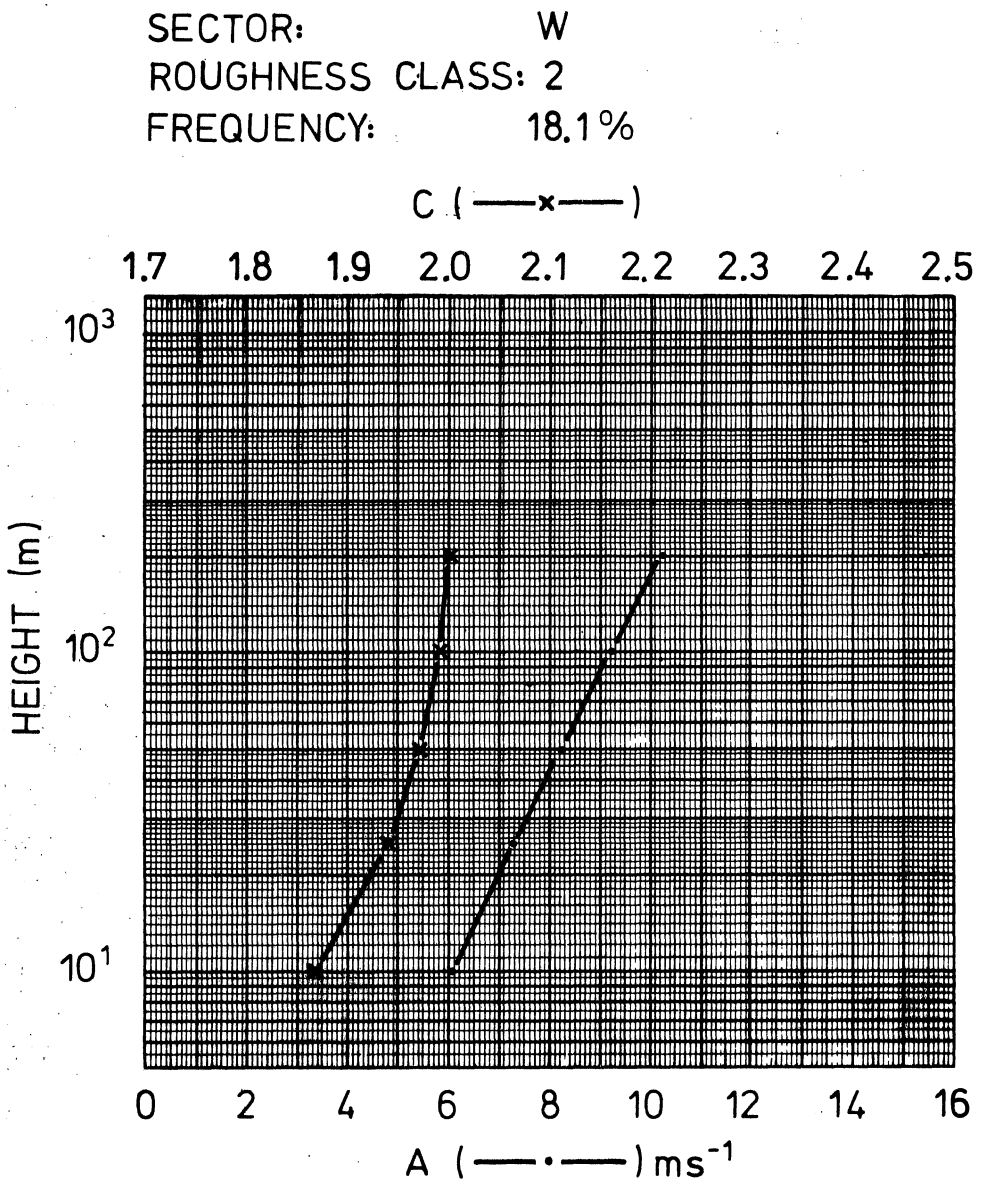
SECTOR: W
ROUGHNESS CLASS: 2
FREQUENCY: 18.1%
C (—×—)
1.7 1.8 1.9 2.0 2.1 2.2 2.3 2.4 2.5
HEIGHT (m)
10³
10²
10¹
0 2 4 6 8 10 12 14 16
A (—·—) ms⁻¹

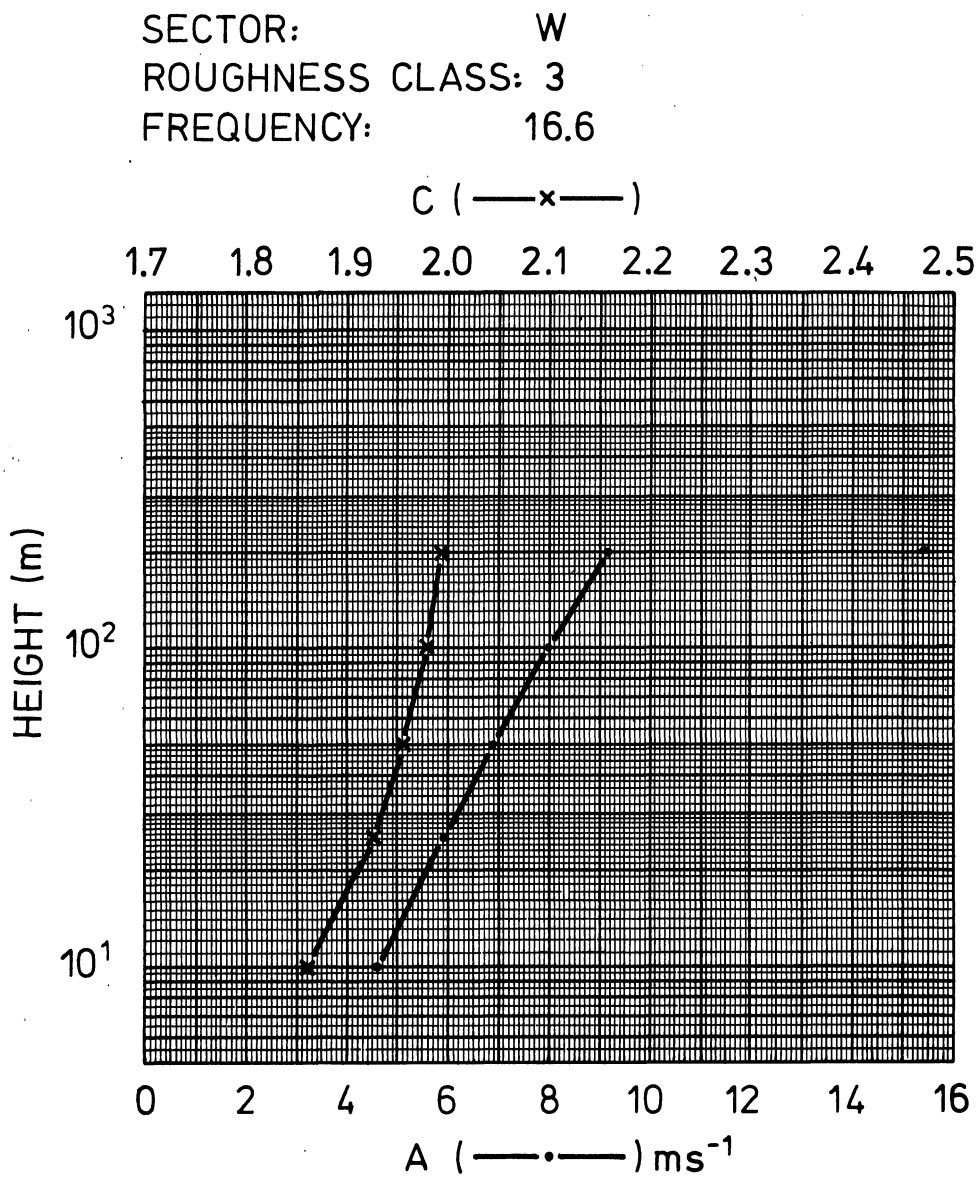
SECTOR: W
ROUGHNESS CLASS: 3
FREQUENCY: 16.6
C (—×—)
1.7 1.8 1.9 2.0 2.1 2.2 2.3 2.4 2.5
HEIGHT (m)
10³
10²
10¹
0 2 4 6 8 10 12 14 16
A (—•—) ms⁻¹

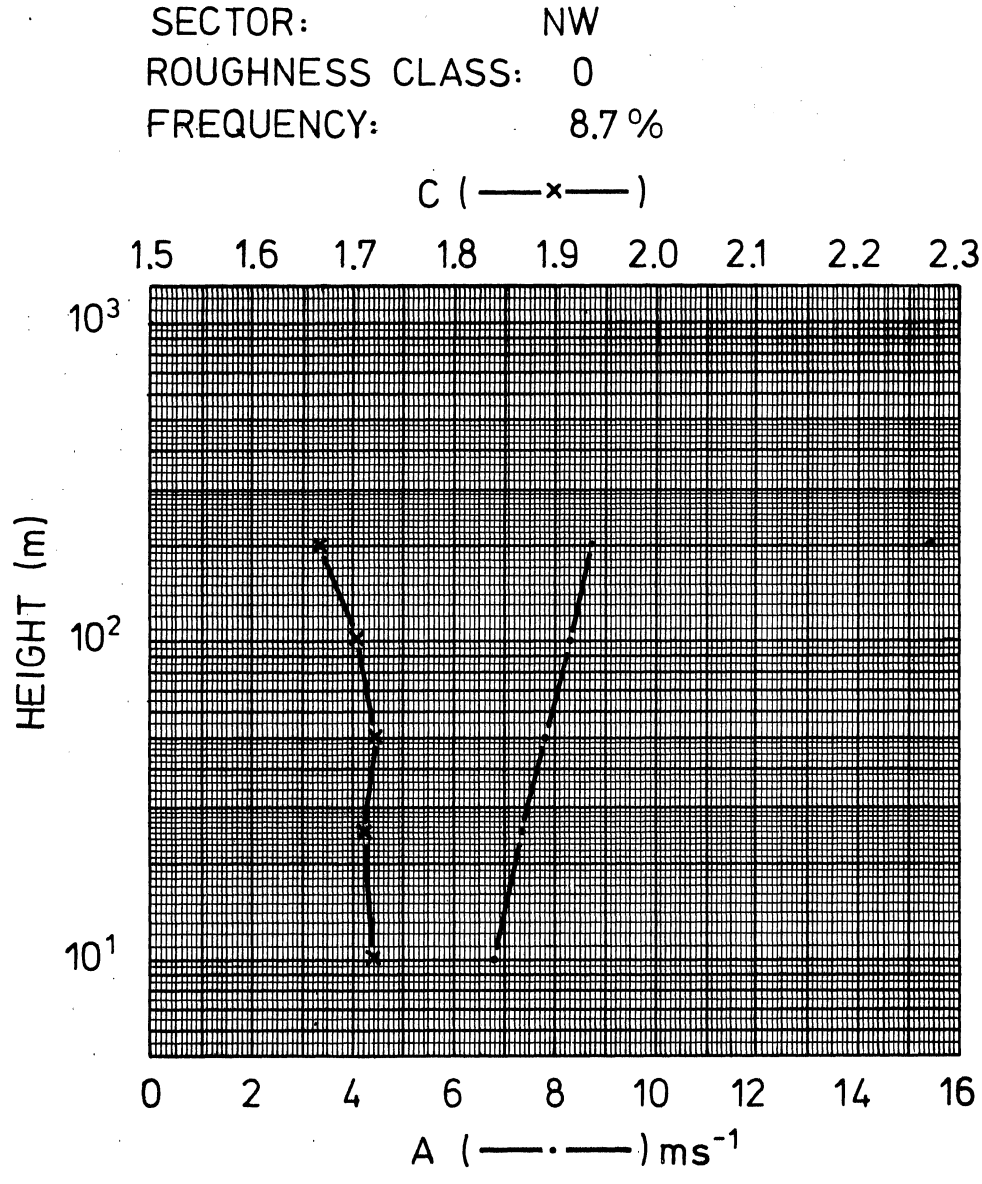
SECTOR: NW
ROUGHNESS CLASS: 0
FREQUENCY: 8.7 %
C (—×—)
1.5 1.6 1.7 1.8 1.9 2.0 2.1 2.2 2.3
HEIGHT (m)
10³
10²
10¹
0 2 4 6 8 10 12 14 16
A (—·—) ms⁻¹

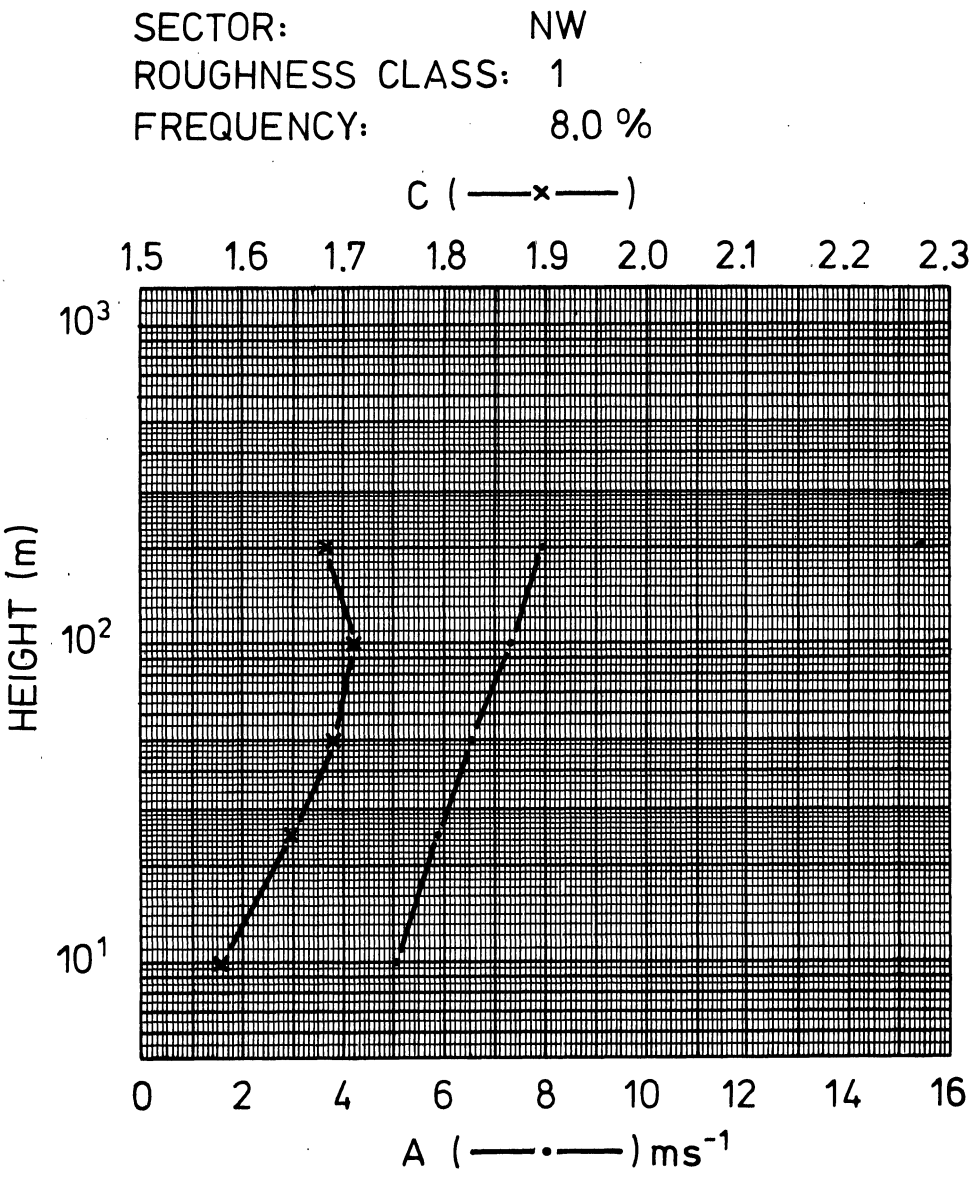
SECTOR: NW
ROUGHNESS CLASS: 1
FREQUENCY: 8.0 %
C (—×—)
1.5 1.6 1.7 1.8 1.9 2.0 2.1 2.2 2.3
HEIGHT (m)
10³
10²
10¹
0 2 4 6 8 10 12 14 16
A (—•—) ms⁻¹

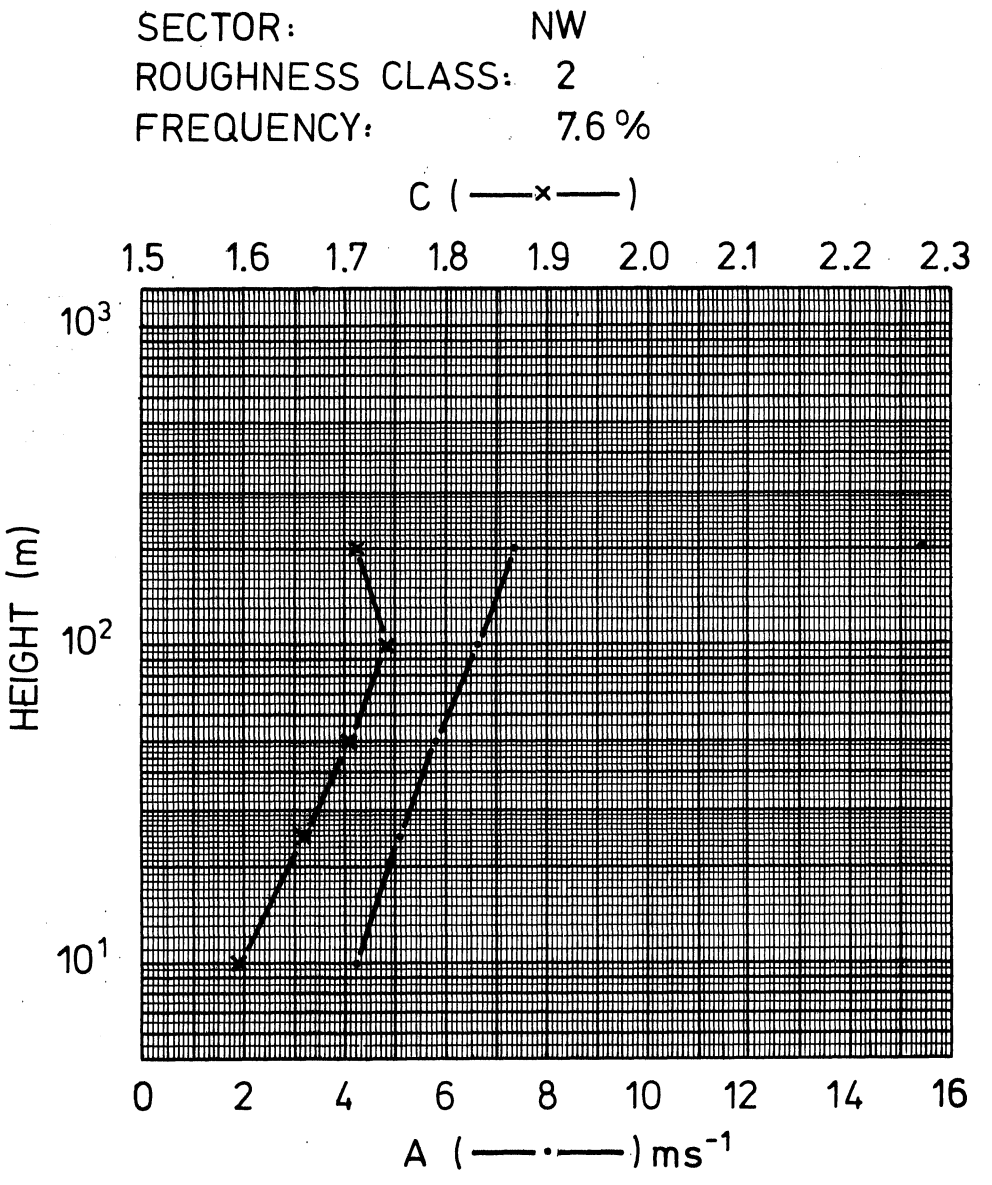
SECTOR: NW
ROUGHNESS CLASS: 2
FREQUENCY: 7.6 %
C (——×——)
1.5 1.6 1.7 1.8 1.9 2.0 2.1 2.2 2.3
HEIGHT (m)
10³
10²
10¹
0 2 4 6 8 10 12 14 16
A (——·——) ms⁻¹

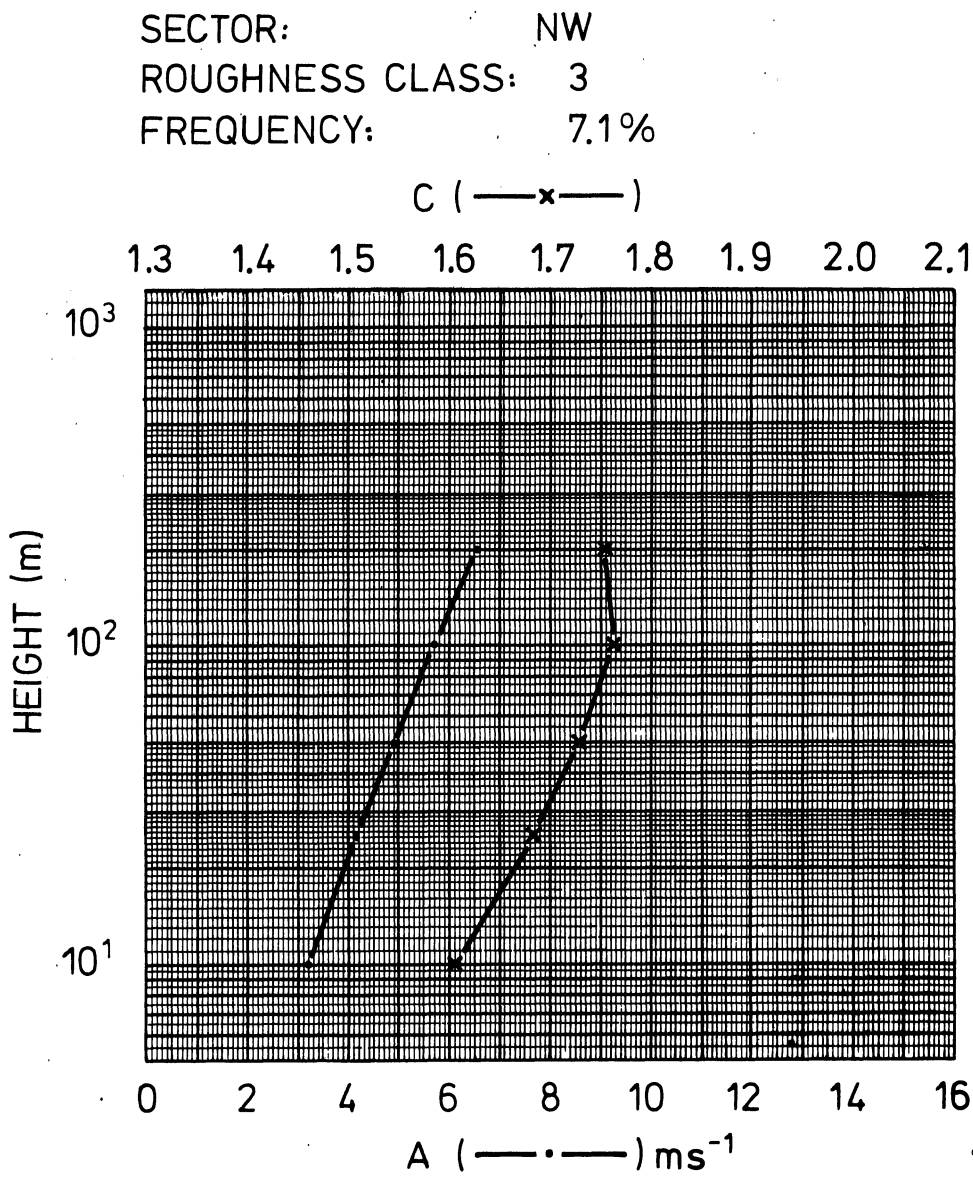
SECTOR: NW
ROUGHNESS CLASS: 3
FREQUENCY: 7.1%
C (—×—)
1.3 1.4 1.5 1.6 1.7 1.8 1.9 2.0 2.1
HEIGHT (m)
10³
10²
10¹
0 2 4 6 8 10 12 14 16
A (—·—) ms⁻¹

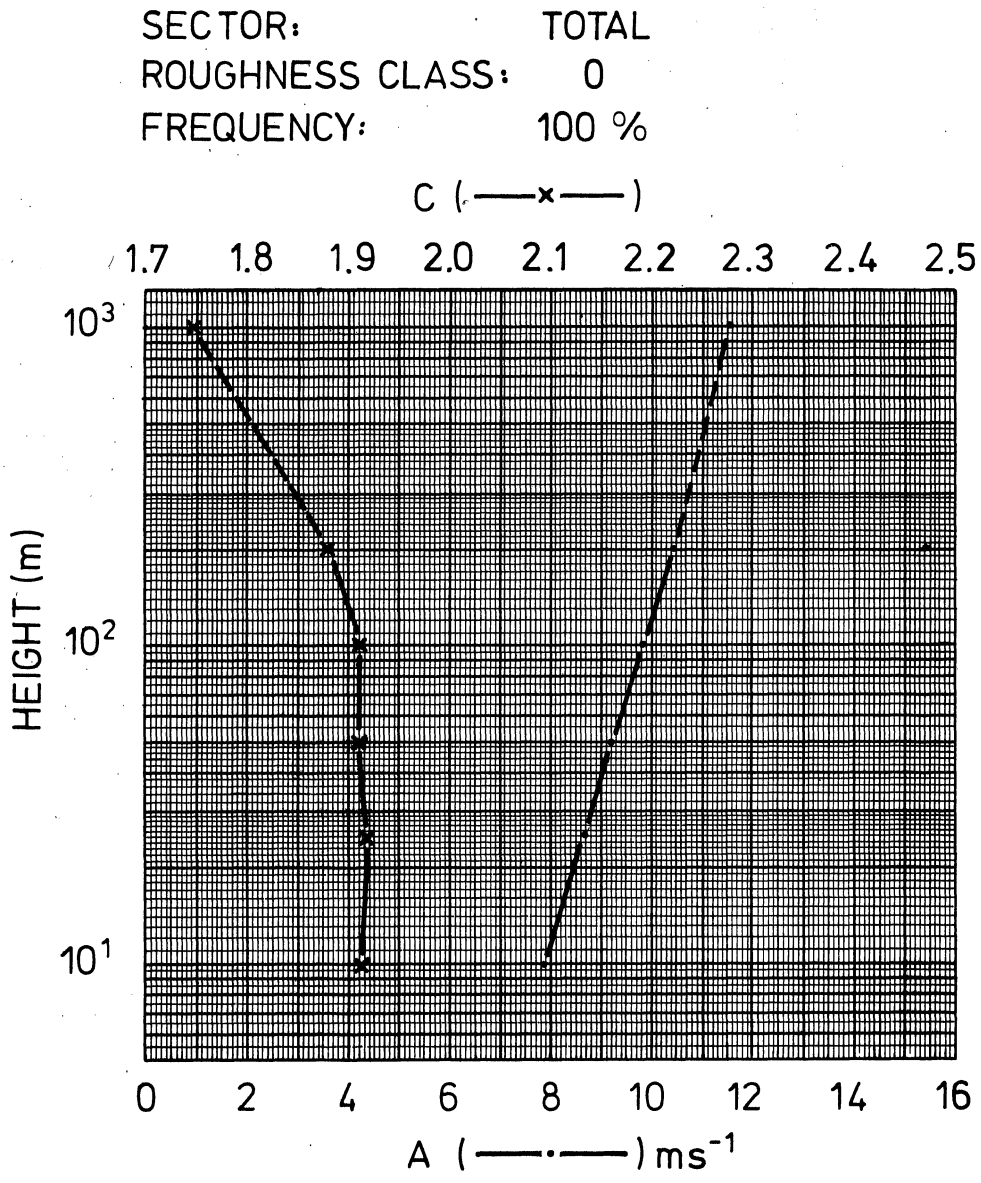
SECTOR: TOTAL
ROUGHNESS CLASS: 0
FREQUENCY: 100 %
C (—×—)
1.7 1.8 1.9 2.0 2.1 2.2 2.3 2.4 2.5
HEIGHT (m)
10³
10²
10¹
0 2 4 6 8 10 12 14 16
A (—·—) ms⁻¹

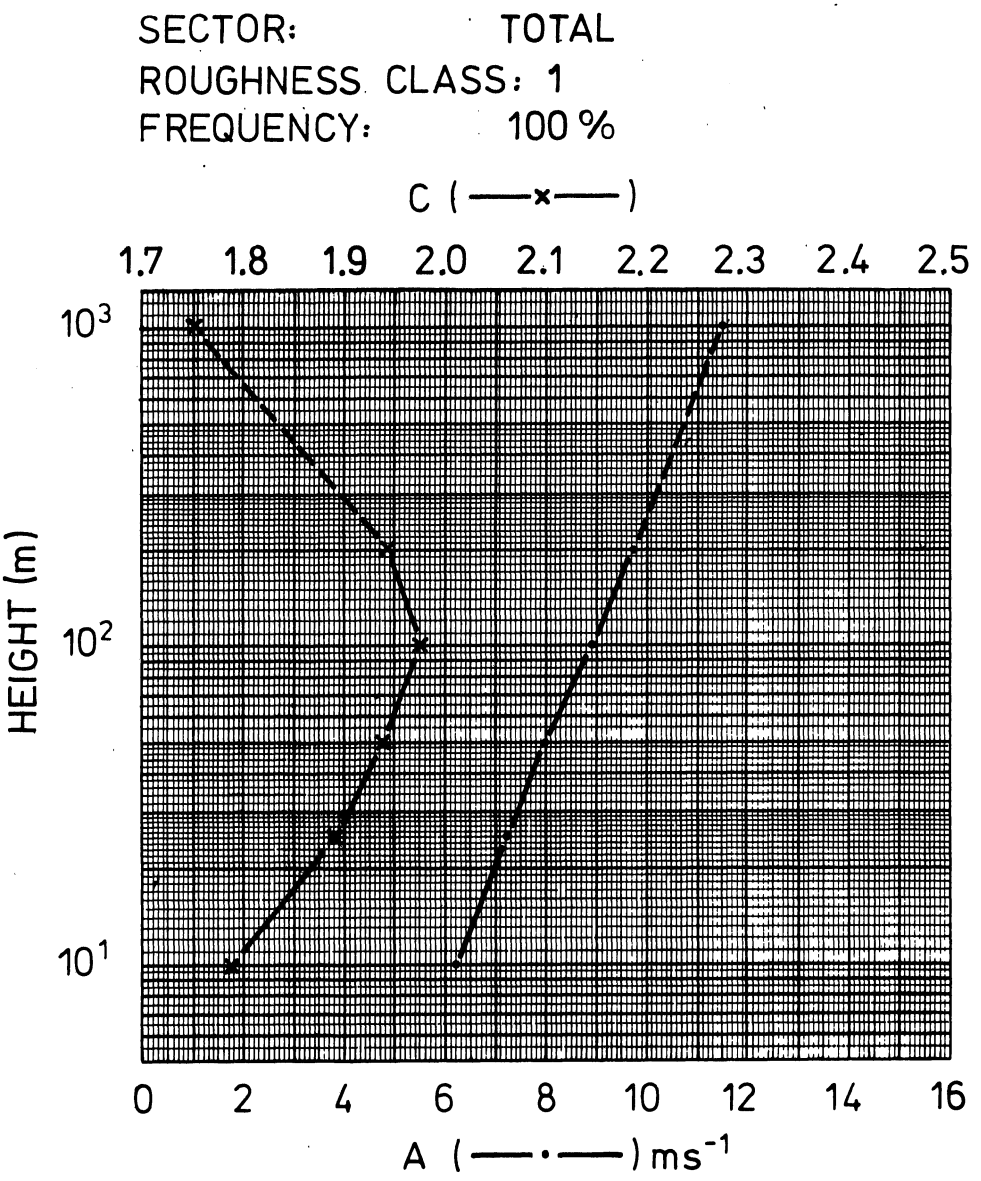
SECTOR: TOTAL
ROUGHNESS CLASS: 1
FREQUENCY: 100 %
C (—×—)
1.7 1.8 1.9 2.0 2.1 2.2 2.3 2.4 2.5
HEIGHT (m)
10³
10²
10¹
0 2 4 6 8 10 12 14 16
A (—·—) ms⁻¹

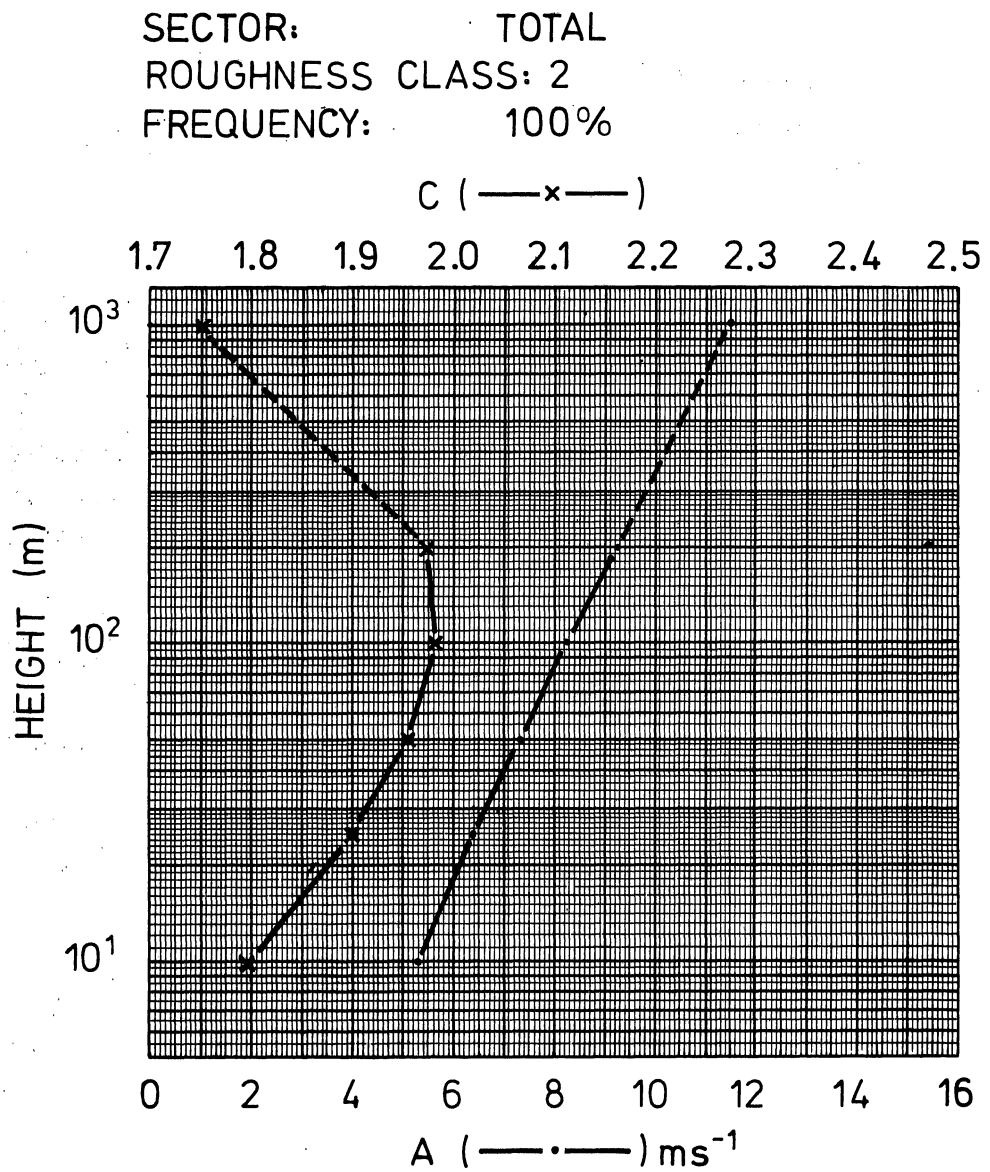
SECTOR: TOTAL
ROUGHNESS CLASS: 2
FREQUENCY: 100%
C (—×—)
1.7 1.8 1.9 2.0 2.1 2.2 2.3 2.4 2.5
HEIGHT (m)
10^3
10^2
10^1
0 2 4 6 8 10 12 14 16
A (—·—) ms^{-1}

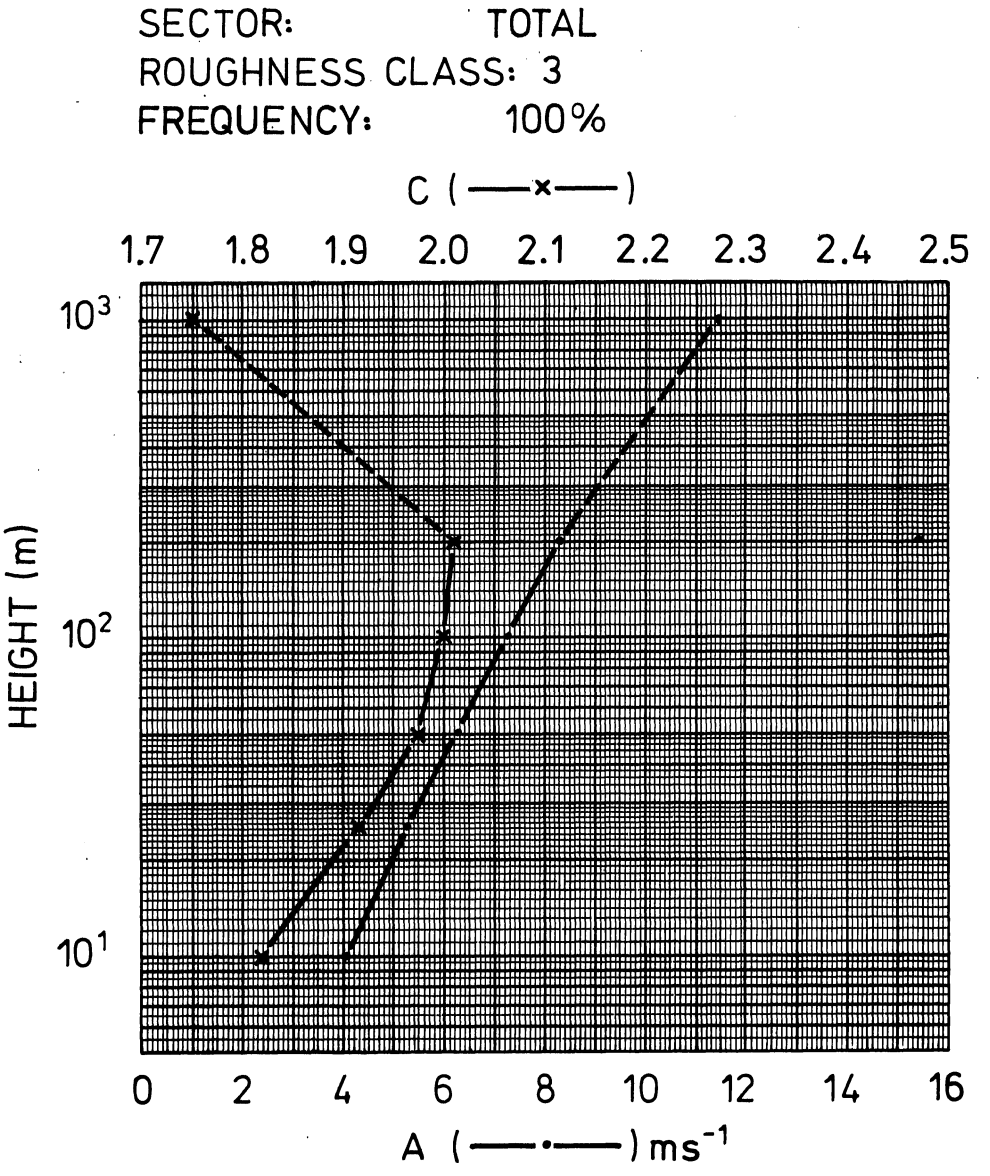
SECTOR: TOTAL
ROUGHNESS CLASS: 3
FREQUENCY: 100%
C (—×—)
1.7 1.8 1.9 2.0 2.1 2.2 2.3 2.4 2.5
HEIGHT (m)
10³
10²
10¹
0 2 4 6 8 10 12 14 16
A (—·—) ms⁻¹

Table A1. Table for the calculation of the total power density in the wind from the Weibull parameters A and C. The value of $F_E(C)$ is found from the table entry corresponding to the value of C by entering the row given by the first two ciphers in C and the coloumn given by the third cipher in C. The power density with dimension kWh m^{-2} $year^{-1}$ is then: $E = A^3 F_E(C)$.

	0	1	2	3	4	5	6	7	8	9
1.0	32.347	31.166	30.057	29.016	28.036	27.113	26.242	25.420	24.644	23.910
1.1	23.214	22.555	21.931	21.337	20.774	20.238	19.728	19.242	18.779	18.338
1.2	17.916	17.514	17.129	16.761	16.409	16.072	15.749	15.439	15.142	14.856
1.3	14.582	14.319	14.066	13.822	13.588	13.362	13.145	12.935	12.733	12.538
1.4	12.350	12.169	11.993	11.824	11.660	11.501	11.348	11.200	11.056	10.917
1.5	10.782	10.652	10.525	10.402	10.283	10.167	10.055	9.946	9.840	9.738
1.6	9.638	9.541	9.446	9.354	9.265	9.178	9.093	9.011	8.931	8.852
1.7	8.776	8.702	8.630	8.559	8.490	8.423	8.358	8.294	8.232	8.171
1.8	8.111	8.053	7.997	7.941	7.887	7.834	7.783	7.732	7.683	7.634
1.9	7.587	7.541	7.496	7.451	7.408	7.366	7.324	7.284	7.244	7.205
2.0	7.167	7.129	7.093	7.057	7.021	6.987	6.953	6.920	6.887	6.855
2.1	6.824	6.793	6.763	6.734	6.705	6.676	6.648	6.621	6.594	6.568
2.2	6.542	6.516	6.491	6.467	6.443	6.419	6.396	6.373	6.350	6.328
2.3	6.306	6.285	6.264	6.243	6.223	6.203	6.183	6.164	6.145	6.126
2.4	6.108	6.090	6.072	6.055	6.038	6.021	6.004	5.988	5.971	5.956
2.5	5.940	5.925	5.909	5.894	5.880	5.865	5.851	5.837	5.823	5.810
2.6	5.796	5.783	5.770	5.757	5.744	5.732	5.720	5.708	5.696	5.684
2.7	5.672	5.661	5.650	5.639	5.628	5.617	5.606	5.596	5.586	5.575
2.8	5.565	5.555	5.546	5.536	5.527	5.517	5.508	5.499	5.490	5.481
2.9	5.472	5.464	5.455	5.447	5.439	5.430	5.422	5.414	5.406	5.399
3.0	5.391	5.384	5.376	5.369	5.361	5.354	5.347	5.340	5.333	5.327

Table A2. Table for the calculation of the mean value from Weibull parameters A and C. The value of $F_M(C)$ is found from the table entry corresponding to the value of C by entering the row given by first two ciphers in C and the column given by the third cipher in C. The mean value is then: $M = AF_M(C)$ (ms^{-1}). Note that the value of $F_M(C)$ varies only slightly, and that the value usually can be chosen as 0.888.

	0	1	2	3	4	5	6	7	8	9
1.0	1.000	0.996	0.992	0.988	0.984	0.981	0.977	0.974	0.971	0.968
1.1	0.965	0.962	0.959	0.957	0.954	0.952	0.949	0.947	0.945	0.943
1.2	0.941	0.939	0.937	0.935	0.933	0.931	0.930	0.928	0.927	0.925
1.3	0.924	0.922	0.921	0.919	0.918	0.917	0.916	0.915	0.914	0.912
1.4	0.911	0.910	0.909	0.909	0.908	0.907	0.906	0.905	0.904	0.903
1.5	0.903	0.902	0.901	0.901	0.900	0.899	0.899	0.898	0.898	0.897
1.6	0.897	0.896	0.896	0.895	0.895	0.894	0.894	0.893	0.893	0.893
1.7	0.892	0.892	0.892	0.891	0.891	0.891	0.890	0.890	0.890	0.890
1.8	0.889	0.889	0.889	0.889	0.888	0.888	0.888	0.888	0.888	0.886
1.9	0.887	0.887	0.886	0.886	0.886	0.886	0.886	0.886	0.886	0.886
2.0	0.886	0.886	0.886	0.886	0.886	0.886	0.886	0.886	0.886	0.886
2.1	0.886	0.886	0.886	0.886	0.886	0.886	0.886	0.886	0.886	0.886
2.2	0.886	0.886	0.886	0.886	0.886	0.886	0.886	0.886	0.886	0.886
2.3	0.886	0.886	0.886	0.886	0.886	0.886	0.886	0.886	0.886	0.886
2.4	0.886	0.887	0.887	0.887	0.887	0.887	0.887	0.887	0.887	0.887
2.5	0.887	0.887	0.887	0.888	0.888	0.888	0.888	0.888	0.888	0.888
2.6	0.888	0.888	0.888	0.889	0.889	0.889	0.889	0.889	0.889	0.889
2.7	0.889	0.889	0.890	0.890	0.890	0.890	0.890	0.890	0.890	0.890
2.8	0.890	0.891	0.891	0.891	0.891	0.891	0.891	0.891	0.891	0.892
2.9	0.892	0.892	0.892	0.892	0.892	0.892	0.892	0.893	0.893	0.893
3.0	0.893	0.893	0.893	0.893	0.894	0.894	0.894	0.894	0.894	0.894

Table A3. Table for the calculation of the mean square speed from Weibull parameters A and C. The value of $F_V(C)$ is found in the table and V^2 is then: $V^2 = A^2 F_V(C)$ $(m^2 s^{-2})$.

	0	1	2	3	4	5	6	7	8	9
1.0	2.000	1.964	1.930	1.897	1.865	1.835	1.806	1.779	1.752	1.727
1.1	1.702	1.679	1.657	1.635	1.614	1.594	1.575	1.556	1.538	1.521
1.2	1.505	1.489	1.473	1.458	1.444	1.430	1.416	1.403	1.390	1.378
1.3	1.366	1.355	1.344	1.333	1.322	1.312	1.302	1.293	1.284	1.275
1.4	1.266	1.257	1.249	1.241	1.233	1.226	1.218	1.211	1.204	1.197
1.5	1.191	1.184	1.178	1.172	1.166	1.160	1.154	1.149	1.143	1.138
1.6	1.133	1.128	1.123	1.118	1.114	1.109	1.105	1.100	1.096	1.092
1.7	1.088	1.084	1.080	1.076	1.073	1.069	1.066	1.062	1.059	1.055
1.8	1.052	1.049	1.046	1.043	1.040	1.037	1.034	1.031	1.029	1.026
1.9	1.023	1.021	1.018	1.016	1.013	1.011	1.009	1.007	1.004	1.002
2.0	1.000	0.998	0.996	0.994	0.992	0.990	0.988	0.986	0.984	0.983
2.1	0.981	0.979	0.977	0.976	0.974	0.972	0.971	0.969	0.968	0.966
2.2	0.965	0.963	0.962	0.961	0.959	0.958	0.957	0.955	0.954	0.953
2.3	0.952	0.951	0.949	0.948	0.947	0.946	0.945	0.944	0.943	0.942
2.4	0.941	0.940	0.939	0.938	0.937	0.936	0.935	0.934	0.933	0.932
2.5	0.931	0.931	0.930	0.929	0.928	0.927	0.927	0.926	0.925	0.924
2.6	0.924	0.923	0.922	0.921	0.921	0.920	0.919	0.919	0.918	0.918
2.7	0.917	0.916	0.916	0.915	0.915	0.914	0.914	0.913	0.912	0.912
2.8	0.911	0.911	0.910	0.910	0.909	0.909	0.909	0.908	0.908	0.907
2.9	0.907	0.906	0.906	0.905	0.905	0.905	0.904	0.904	0.903	0.903
3.0	0.903	0.902	0.902	0.902	0.901	0.901	0.901	0.900	0.900	0.900

Table A4. Table of F_C for the calculation of the Weibull parameter C from the mean and the mean square in a Weibull distribution (cfr. section 5.4).

	0	1	2	3	4	5	6	7	8	9
.60	1.231	1.234	1.237	1.240	1.242	1.245	1.248	1.251	1.253	1.256
.61	1.259	1.262	1.265	1.267	1.270	1.273	1.276	1.279	1.282	1.284
.62	1.287	1.290	1.293	1.296	1.299	1.302	1.305	1.308	1.311	1.314
.63	1.317	1.320	1.323	1.326	1.329	1.332	1.335	1.338	1.341	1.344
.64	1.348	1.351	1.354	1.357	1.360	1.363	1.367	1.370	1.373	1.376
.65	1.379	1.383	1.386	1.389	1.393	1.396	1.399	1.403	1.406	1.409
.66	1.413	1.416	1.419	1.423	1.426	1.430	1.433	1.437	1.440	1.444
.67	1.447	1.451	1.454	1.458	1.461	1.465	1.469	1.472	1.476	1.480
.68	1.483	1.487	1.491	1.495	1.498	1.502	1.506	1.510	1.513	1.517
.69	1.521	1.525	1.529	1.533	1.537	1.541	1.545	1.549	1.553	1.557
.70	1.561	1.565	1.569	1.573	1.577	1.581	1.585	1.590	1.594	1.598
.71	1.602	1.606	1.611	1.615	1.619	1.624	1.628	1.633	1.637	1.641
.72	1.646	1.650	1.655	1.659	1.664	1.668	1.673	1.678	1.682	1.687
.73	1.692	1.696	1.701	1.706	1.711	1.716	1.721	1.725	1.730	1.735
.74	1.740	1.745	1.750	1.755	1.760	1.765	1.771	1.776	1.781	1.786
.75	1.791	1.797	1.802	1.807	1.813	1.818	1.824	1.829	1.835	1.840
.76	1.846	1.851	1.857	1.863	1.868	1.874	1.880	1.886	1.892	1.898
.77	1.904	1.910	1.916	1.922	1.928	1.934	1.940	1.946	1.952	1.959
.78	1.965	1.971	1.978	1.984	1.991	1.997	2.004	2.011	2.017	2.024
.79	2.031	2.038	2.045	2.051	2.058	2.065	2.073	2.080	2.087	2.094
.80	2.101	2.109	2.116	2.124	2.131	2.139	2.146	2.154	2.162	2.170
.81	2.177	2.185	2.193	2.201	2.209	2.218	2.226	2.234	2.242	2.251
.82	2.259	2.268	2.277	2.285	2.294	2.303	2.312	2.321	2.330	2.339
.83	2.348	2.358	2.367	2.377	2.386	2.396	2.406	2.415	2.425	2.435
.84	2.445	2.456	2.466	2.476	2.487	2.498	2.508	2.519	2.530	2.541
.85	2.552	2.563	2.575	2.586	2.598	2.609	2.621	2.633	2.645	2.657
.86	2.670	2.682	2.695	2.707	2.720	2.733	2.746	2.760	2.773	2.787
.87	2.801	2.814	2.829	2.843	2.857	2.872	2.886	2.901	2.916	2.932
.88	2.947	2.963	2.979	2.995	3.011	3.028	3.044	3.061	3.078	3.096
.89	3.113	3.131	3.149	3.168	3.186	3.205	3.224	3.244	3.263	3.283
.90	3.304	3.324	3.345	3.366	3.388	3.410	3.432	3.454	3.477	3.501

Table A5. Table of F_A for the calculation of the Weibull parameter A from the mean and the mean square in a Weibull distribution (cfr. section 5.4). Note that the value of F_A varies only slightly, and that the value usually can be chosen as 1.126.

	0	1	2	3	4	5	6	7	8	9
1.0	1.000	1.004	1.008	1.012	1.016	1.020	1.023	1.027	1.030	1.033
1.1	1.036	1.039	1.042	1.045	1.048	1.051	1.053	1.056	1.058	1.061
1.2	1.063	1.065	1.068	1.070	1.072	1.074	1.076	1.077	1.079	1.081
1.3	1.083	1.084	1.086	1.088	1.089	1.091	1.092	1.093	1.095	1.096
1.4	1.097	1.098	1.100	1.101	1.102	1.103	1.104	1.105	1.106	1.107
1.5	1.108	1.109	1.109	1.110	1.111	1.112	1.113	1.113	1.114	1.115
1.6	1.115	1.116	1.117	1.117	1.118	1.118	1.119	1.119	1.120	1.120
1.7	1.121	1.121	1.122	1.122	1.122	1.123	1.123	1.124	1.124	1.124
1.8	1.124	1.125	1.125	1.125	1.126	1.126	1.126	1.126	1.127	1.127
1.9	1.127	1.127	1.127	1.127	1.128	1.128	1.128	1.128	1.128	1.128
2.0	1.128	1.128	1.129	1.129	1.129	1.129	1.129	1.129	1.129	1.129
2.1	1.129	1.129	1.129	1.129	1.129	1.129	1.129	1.129	1.129	1.129
2.2	1.129	1.129	1.129	1.129	1.129	1.129	1.129	1.129	1.129	1.129
2.3	1.129	1.129	1.129	1.129	1.129	1.128	1.128	1.128	1.128	1.128
2.4	1.128	1.128	1.128	1.128	1.128	1.128	1.127	1.127	1.127	1.127
2.5	1.127	1.127	1.127	1.127	1.127	1.126	1.126	1.126	1.126	1.126
2.6	1.126	1.126	1.126	1.125	1.125	1.125	1.125	1.125	1.125	1.125
2.7	1.125	1.124	1.124	1.124	1.124	1.124	1.124	1.123	1.123	1.123
2.8	1.123	1.123	1.123	1.123	1.122	1.122	1.122	1.122	1.122	1.122
2.9	1.121	1.121	1.121	1.121	1.121	1.121	1.121	1.120	1.120	1.120
3.0	1.120	1.120	1.120	1.119	1.119	1.119	1.119	1.119	1.119	1.118

Table A6. Table for the calculation of the mean power. The table gives the value of $G_C(\xi)$ (cfr. section 5.9).

	C										
	1.5	1.6	1.7	1.8	1.9	2.0	2.1	2.2	2.3	2.4	2.5
ξ 0.00	0.000	0.000	0.000	0.000	0.000	0.000	0.000	0.000	0.000	0.000	0.000
0.05	0.050	0.050	0.050	0.050	0.050	0.050	0.050	0.050	0.050	0.050	0.050
0.10	0.099	0.099	0.099	0.099	0.100	0.100	0.100	0.100	0.100	0.100	0.100
0.15	0.147	0.147	0.148	0.148	0.149	0.149	0.149	0.149	0.149	0.150	0.150
0.20	0.193	0.194	0.195	0.196	0.197	0.197	0.198	0.198	0.199	0.199	0.199
0.25	0.238	0.240	0.241	0.243	0.244	0.245	0.246	0.246	0.247	0.247	0.248
0.30	0.281	0.284	0.286	0.288	0.290	0.291	0.292	0.294	0.294	0.295	0.296
0.35	0.323	0.326	0.329	0.332	0.334	0.336	0.338	0.339	0.341	0.342	0.343
0.40	0.363	0.367	0.371	0.374	0.377	0.380	0.382	0.384	0.386	0.387	0.389
0.45	0.400	0.406	0.410	0.414	0.418	0.421	0.424	0.427	0.429	0.431	0.433
0.50	0.436	0.443	0.448	0.453	0.457	0.461	0.465	0.468	0.471	0.474	0.476
0.55	0.471	0.478	0.484	0.489	0.495	0.499	0.503	0.507	0.511	0.514	0.517
0.60	0.503	0.511	0.518	0.524	0.530	0.535	0.540	0.544	0.549	0.552	0.556
0.65	0.533	0.542	0.550	0.557	0.563	0.569	0.574	0.580	0.584	0.589	0.593
0.70	0.562	0.571	0.579	0.587	0.594	0.601	0.607	0.612	0.618	0.622	0.627
0.75	0.589	0.599	0.607	0.616	0.623	0.630	0.637	0.643	0.649	0.654	0.659
0.80	0.614	0.624	0.634	0.642	0.650	0.658	0.665	0.671	0.677	0.683	0.688
0.85	0.638	0.648	0.658	0.667	0.675	0.683	0.690	0.697	0.704	0.710	0.715
0.90	0.660	0.671	0.680	0.690	0.698	0.706	0.714	0.721	0.727	0.734	0.740
0.95	0.681	0.691	0.701	0.711	0.719	0.727	0.735	0.742	0.749	0.756	0.762
1.00	0.700	0.710	0.720	0.730	0.739	0.747	0.755	0.762	0.769	0.775	0.781
1.05	0.717	0.728	0.738	0.747	0.756	0.764	0.772	0.779	0.786	0.792	0.798
1.10	0.734	0.744	0.754	0.763	0.772	0.780	0.788	0.795	0.801	0.808	0.814
1.15	0.749	0.759	0.769	0.778	0.786	0.794	0.801	0.808	0.815	0.821	0.827
1.20	0.763	0.773	0.782	0.791	0.799	0.807	0.814	0.820	0.827	0.832	0.838

Table A6. continued

ξ \ C	1.5	1.6	1.7	1.8	1.9	2.0	2.1	2.2	2.3	2.4	2.5
1.25	0.776	0.786	0.795	0.803	0.811	0.818	0.825	0.831	0.837	0.842	0.847
1.30	0.788	0.797	0.806	0.814	0.821	0.828	0.834	0.840	0.845	0.851	0.855
1.35	0.799	0.807	0.816	0.823	0.830	0.836	0.842	0.848	0.853	0.858	0.862
1.40	0.809	0.817	0.825	0.832	0.838	0.844	0.849	0.854	0.859	0.863	0.867
1.45	0.818	0.826	0.833	0.839	0.845	0.850	0.855	0.860	0.864	0.868	0.872
1.50	0.826	0.833	0.840	0.846	0.851	0.856	0.861	0.865	0.869	0.872	0.875
1.55	0.834	0.840	0.846	0.852	0.857	0.861	0.865	0.869	0.872	0.875	0.878
1.60	0.841	0.847	0.852	0.857	0.861	0.865	0.869	0.872	0.875	0.878	0.880
1.65	0.847	0.852	0.857	0.861	0.865	0.869	0.872	0.875	0.877	0.880	0.882
1.70	0.853	0.857	0.862	0.865	0.869	0.872	0.875	0.877	0.879	0.882	0.884
1.75	0.858	0.862	0.866	0.869	0.872	0.874	0.877	0.879	0.881	0.883	0.885
1.80	0.863	0.866	0.869	0.872	0.874	0.877	0.879	0.880	0.882	0.884	0.885
1.85	0.867	0.870	0.872	0.874	0.877	0.878	0.880	0.882	0.883	0.884	0.886
1.90	0.871	0.873	0.875	0.877	0.878	0.880	0.881	0.882	0.884	0.885	0.886
1.95	0.874	0.876	0.877	0.879	0.880	0.881	0.882	0.883	0.884	0.885	0.887
2.00	0.877	0.878	0.879	0.880	0.881	0.882	0.883	0.884	0.885	0.886	0.887
2.05	0.880	0.881	0.881	0.882	0.882	0.883	0.884	0.884	0.885	0.886	0.887
2.10	0.882	0.883	0.883	0.883	0.883	0.884	0.884	0.885	0.885	0.886	0.887
2.15	0.885	0.884	0.884	0.884	0.884	0.884	0.884	0.885	0.885	0.886	0.887
2.20	0.887	0.886	0.885	0.885	0.885	0.885	0.885	0.885	0.886	0.886	0.887
2.25	0.889	0.887	0.886	0.886	0.885	0.885	0.885	0.885	0.886	0.886	0.887
2.30	0.890	0.889	0.887	0.886	0.886	0.885	0.885	0.885	0.886	0.886	0.887
2.35	0.892	0.890	0.888	0.887	0.886	0.885	0.885	0.885	0.886	0.886	0.887
2.40	0.893	0.891	0.889	0.887	0.886	0.886	0.885	0.885	0.886	0.886	0.887
2.45	0.894	0.891	0.889	0.888	0.886	0.886	0.885	0.885	0.886	0.886	0.887

Table A6. continued

ξ \ C	1.5	1.6	1.7	1.8	1.9	2.0	2.1	2.2	2.3	2.4	2.5
2.50	0.895	0.892	0.890	0.888	0.887	0.886	0.886	0.886	0.886	0.886	0.887
2.55	0.896	0.893	0.890	0.888	0.887	0.886	0.886	0.886	0.886	0.886	0.887
2.60	0.897	0.893	0.890	0.888	0.887	0.886	0.886	0.886	0.886	0.886	0.887
2.65	0.898	0.894	0.891	0.888	0.887	0.886	0.886	0.886	0.886	0.886	0.887
2.70	0.898	0.894	0.891	0.889	0.887	0.886	0.886	0.886	0.886	0.886	0.887
2.75	0.899	0.894	0.891	0.889	0.887	0.886	0.886	0.886	0.886	0.886	0.887
2.80	0.899	0.895	0.891	0.889	0.887	0.886	0.886	0.886	0.886	0.886	0.887
2.85	0.900	0.895	0.891	0.889	0.887	0.886	0.886	0.886	0.886	0.886	0.887
2.90	0.900	0.895	0.892	0.889	0.887	0.886	0.886	0.886	0.886	0.886	0.887
2.95	0.900	0.895	0.892	0.889	0.887	0.886	0.886	0.886	0.886	0.886	0.887
3.00	0.901	0.896	0.892	0.889	0.887	0.886	0.886	0.886	0.886	0.886	0.887
3.05	0.901	0.896	0.892	0.889	0.887	0.886	0.886	0.886	0.886	0.886	0.887
3.10	0.901	0.896	0.892	0.889	0.887	0.886	0.886	0.886	0.886	0.886	0.887
3.15	0.901	0.896	0.892	0.889	0.887	0.886	0.886	0.886	0.886	0.886	0.887
3.20	0.902	0.896	0.892	0.889	0.887	0.886	0.886	0.886	0.886	0.886	0.887
∞	0.903	0.897	0.892	0.889	0.887	0.886	0.886	0.886	0.886	0.886	0.887

APPENDIX B

Production probability, power duration and persistence

B1. Power duration

The production probability curve was defined in Chapter 3 as the accumulated probability density distribution of the power produced by a wind turbine. The curve gives therefore the expected percent of the time that the produced power exceeds a certain level. The curve is also called the power duration curve although it does not contain any information about the length of the periods having a given production. Two examples were given in Chapter 5 of the calculation of the power duration curve for a single wind turbine with a given power curve and placed in a given terrain.

This section investigates how the mean power duration curve for a number of wind turbines is affected by their geographical distribution within Denmark.

The calculations were performed using measurements from the six airport stations Ålborg, Karup, Tirstrup, Skrydstrup, Beldringe and Værløse; these give a good geographical coverage. The type of turbine chosen for the calculations corresponds to the Nibe turbine A (hub height 45 m). Further, the type of terrain chosen is that of the terrain in which the Nibe turbine is situated. This means that for each airport station the wind speed was extrapolated to a height of 45 m over a terrain of roughness class 1 in all sectors except SW, W and NW where the roughness class 0 was used. The extrapolation was carried out with the help of the roughness classification (Chapter 5) and the height variation of the Weibull parameter A (Appendix A). In other words, the calculations were made for six Nibe turbines, each placed in a terrain corresponding to that of Nibe and with the largest possible separations inside Denmark.

By means of the theoretical curve for the mechanical shaft power of the Nibe turbine A (shown in fig. B1) and the calculated wind speed at 45 m, a time series of the power production was calculated for each of the airport stations. The six time series were then used for calculating the production probability curve for each airport station and the corresponding curve for the mean production obtained if the six turbines were connected.

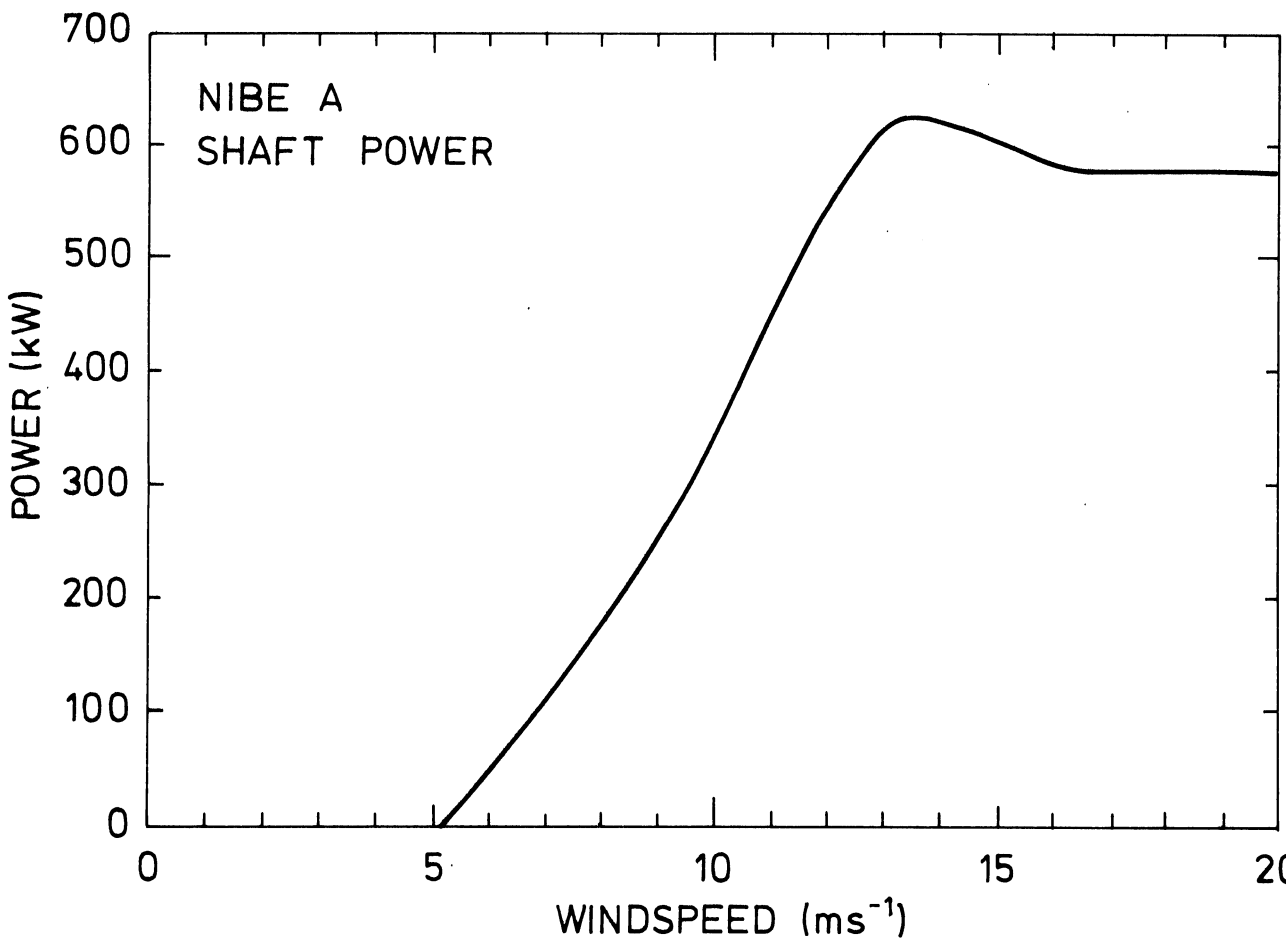

Fig. B1. Theoretical curve for the mechanical shaft power of the Nibe turbine A.

Figure B2 shows the mean of the production probability curve for one turbine compared with the production per turbine in the interconnected grid of six geographically separated wind turbines. It appears, as expected, that the system of separated wind turbines has both a reduced probability of no production and of maximum production. Hence the system of turbines provides a more stable production than does a single turbine. However, it also appears that a really effective improvement demands a much larger separation of the wind turbines, a result that is

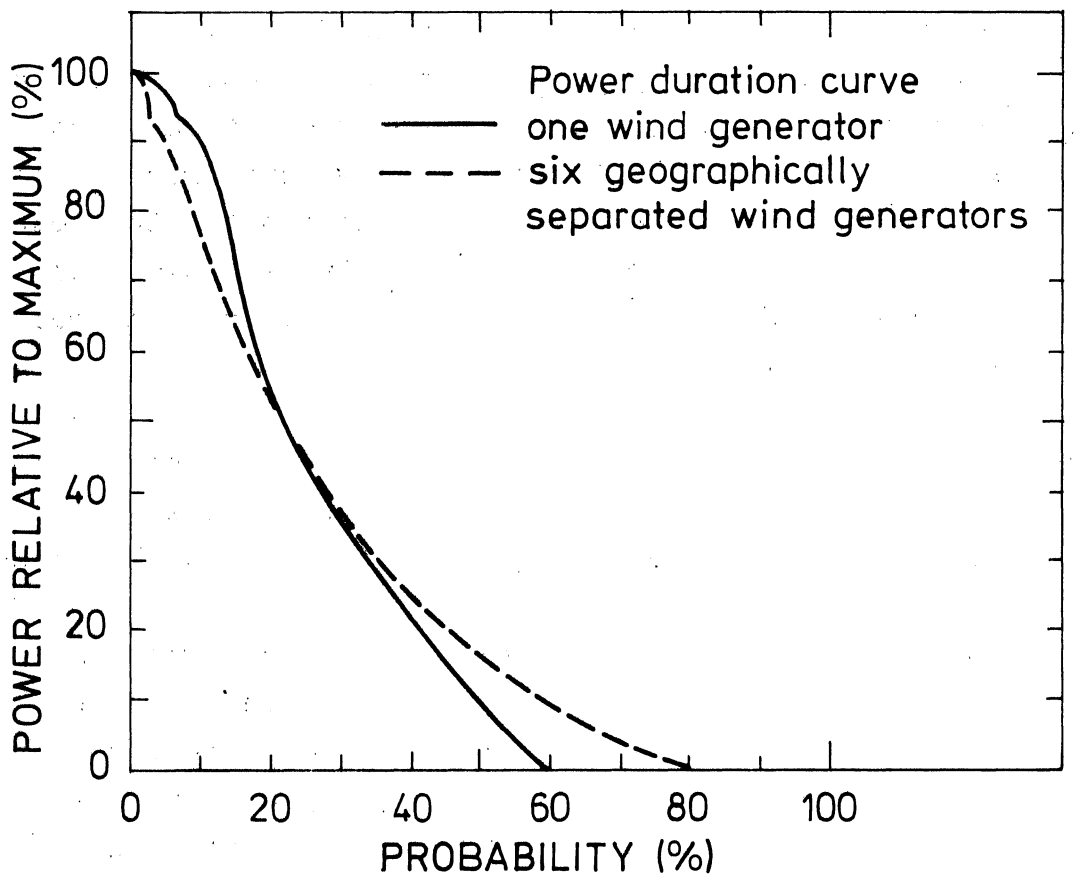

Fig. B2. Production probability curves for one wind turbine and for six geographically distributed turbines.

the direct consequence of the fact that weather systems usually have dimensions of thousands of kilometers. Thus an effective improvement would first be obtained with a geographical separation of the wind turbines that is several times the extent of the weather systems, i.e. thousands of kilometers.

B2. Persistence

It is often important to know whether the production from a wind turbine is produced in long, but relatively infrequent periods, or whether the production takes place in shorter and more frequent periods. To investigate the persistence of power production, a specific power curve and a long time series of the wind speed at the hub height are required. As in the previous section, use will be made of the power curve for the Nibe wind turbine (fig. B1) and the time series of the wind speed measured at Risø at the height of 76 meters. Due to the higher mean roughness at Risø than at the Nibe site, the mean production calculated from the Risø series is very close to the expected mean production of the Nibe wind turbine as calculated by the Windatlas.

Twenty-one years of hourly measurements of the wind speed and the Nibe power curve were used to produce a time series of hourly power production, and by means of this series the probability density functions for mean production over periods ranging from one hour in one year were calculated. The result is shown in fig. B3. The horizontal axis gives the averaging time *T on a logarithmic scale and the vertical axis gives the accumulated probability for the relative power averaged over T (100% corresponds to maximum production. For the chosen

---

*Note that T is the averaging time defining a mean power and should not be confused with the averaging time of the mean wind discussed in Chapter 3.

type of wind turbine the mechanical shaft power is 622 kW. The curves on the figure are lines of constant relative power. The curves are a generalization of the power duration curve. The power duration curve is obtained from the intersection between the lines of constant relative power and the vertical axis. As an example, it is found from the figure that the 40% line intersects at 70%, which means that the wind turbine produces more than 0.40·622 kW = 249 kW in (100-70)% = 30% of the time. The rest of the power duration curve can be obtained following the same procedure.

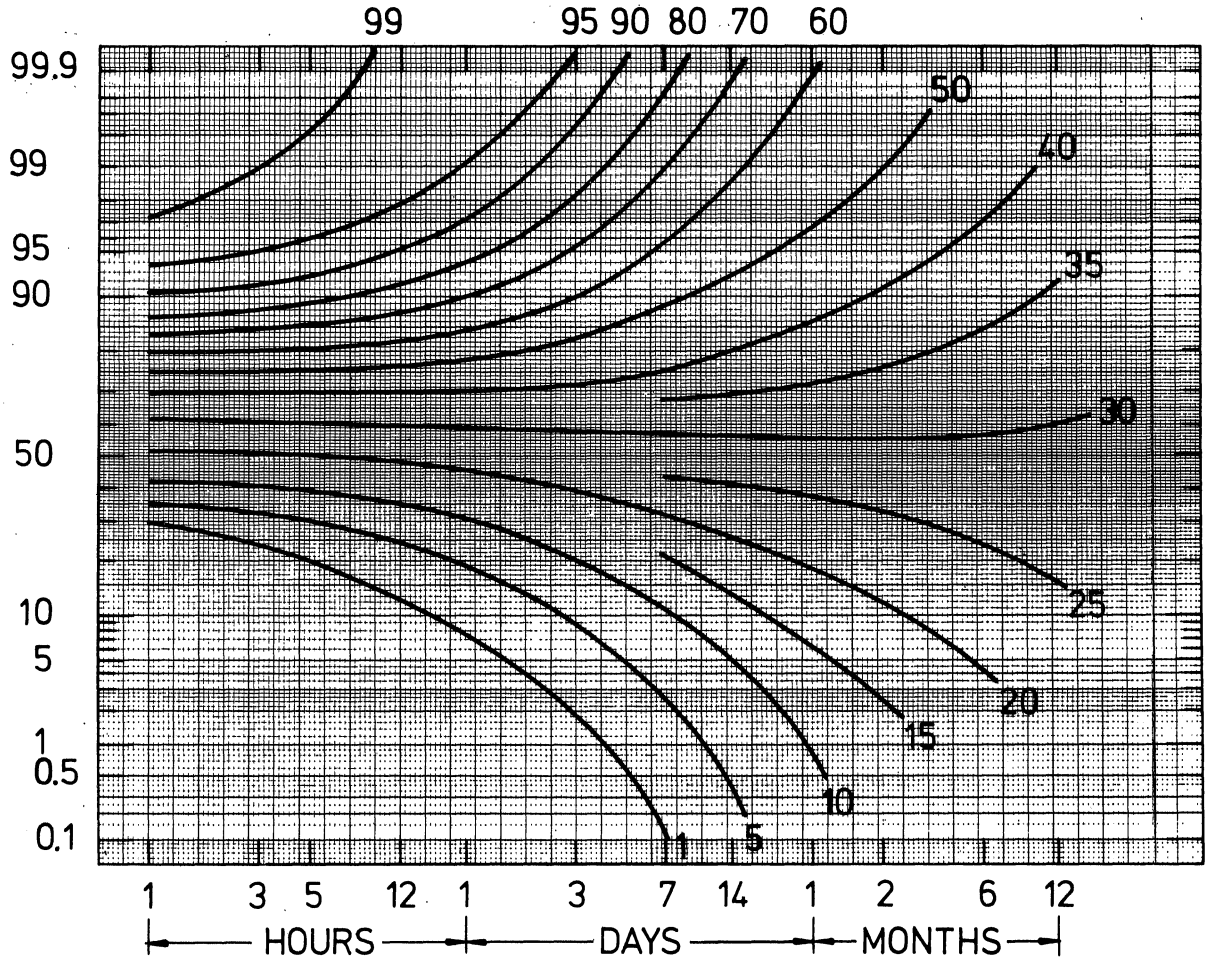

Fig. B3. The accumulated probability for the mean power as function of the averaging line T shown as isolines for the power relative to maximum power. The numbers on the isolines denote percent of maximum power.

For each choice of averaging time T a generalized power duration curve can be constructed. For example, for a choice of T equal to 14 days it can be seen from fig. B3 that the probability of having a mean production over a period of 14 days of less than 10% of the maximum production is 5%; further, the probability for a production less than 30% of maximum is 55%. Hence it is found that the mean production over a period of 14 days can be expected in the interval from 62 kW to 187 kW with a probability of 50%.

The standard deviation of the mean production for various choices of T can also be obtained from fig. B3. Figure B4 shows this standard deviation relative to the mean value for values of T larger than one day. It appears that the standard deviation is 90% of the mean value for the daily production and 12% for the yearly production.

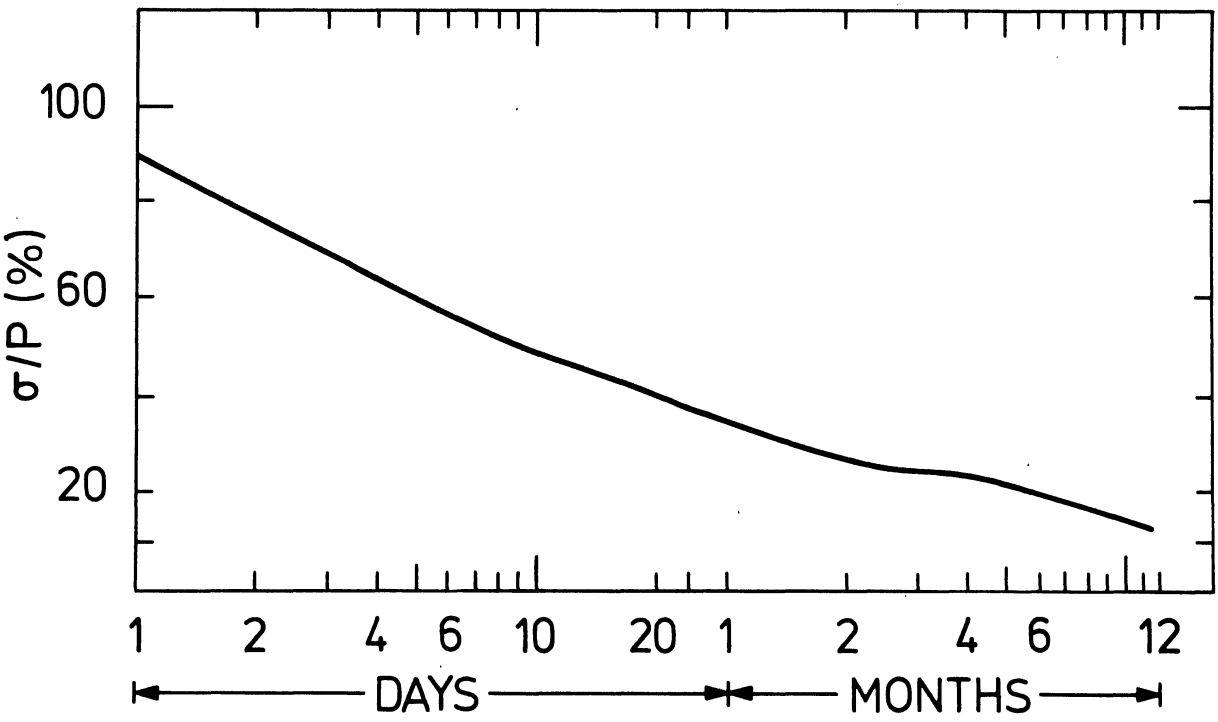

Fig. B4. The standard deviation (σ) of the power averaged over the period T relative to the mean power (P).

The existence and probability of long periods with almost no production, say 1% of maximum production, is of special concern with regard to the power production reliability of wind turbines. The probability of having a production of less than 1% of the maximum can be read from fig. B3 using the line of constant relative power marked "1". For example, the probability of having less than 1% production over a period of 24 hours is 8%.

It is further of interest to evaluate how much a geographical separation of interconnected wind turbines diminishes the probability of having long periods with low production. This question was investigated following the same procedure as in section B1 using six Nibe A wind turbines and six small wind turbines (example 5.10) respectively. The result is given in Table B1.

			Days				
		Turbine(s)	1	2	4	10	30
Power relative to maximum	1%	1 Nibe A turbine	8.1	3.5	0.8	0.04	-
		6 Nibe A turbines	2.6	0.6	0.1		
		1 Small turbine	9.3	3.9	0.8		
		6 Small turbines	1.2	0.1	-		
	5%	1 Nibe A turbine	20.0	13.1	6.8	1.7	-
		6 Nibe A turbines	11.7	5.9	1.8		
		1 Small turbine	19.4	12.4	7.0		
		6 Small turbines	7.5	3.5	1.2		
	10%	1 Nibe A turbine	30.9	24.2	16.6	8.2	0.8
		6 Nibe A turbines	23.5	14.4	7.6		
		1 Small turbine	29.2	22.3	15.2		
		6 Small turbines	17.2	9.1	2.9		
			Probability %				

Table B1. The probability of having a period of 1, 2, 4, 10 or 30 days with a production less than 1%, 5%, and 10% of maximum production. Blank spaces have not been calculated whereas a hyphen indicates that the quantity did not appear in the data used.

B3. Annual variation of mean power production

The wind speed distribution, and therefore the power output from a wind turbine, has a pronounced annual variation. Part of the variance of the production averaged over one month (which can be read from fig. B4) is caused by a mean annual variation and part is caused by random variations. The division into these components can be seen from fig. B5, which was constructed from the 21 years of wind data from the Risø mast and the power curve from the Nibe-A wind turbine. The figure shows the mean annual variation of the monthly means expressed as deviation in percent from the long term mean value, together with the standard deviation in the distribution of the individual monthly means (shown as bars of length twice the standard deviation). The 95% confidence interval for the mean values is 47% of the interval shown by the bars, and the 95% confidence intervals for the standard deviations are from 0.76 to 1.46 times the standard deviations.

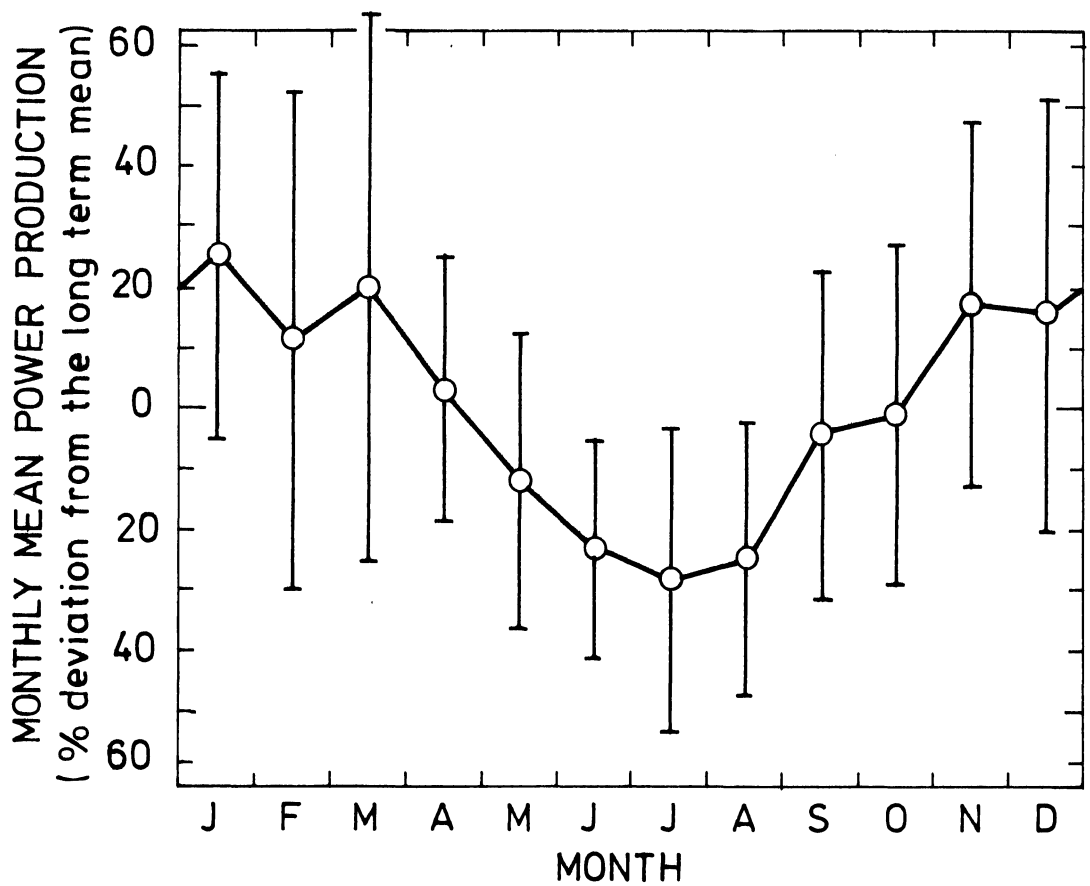

Fig. B5. Annual variation of monthly mean production and standard deviation in the distribution of the monthly means, shown as bars of length twice the standard deviation.

APPENDIX C

C1. The roughness length

Close to the surface of the terrain at heights comparable to the height of the elements obstructing the flow (e.g. buildings, trees, bushes), the mean wind will depend considerably on the shape and spacing of the elements and will be different above the elements and above the space between them. Hence the flow close to the surface is of a complexity which makes any attempt to apply simple general laws impossible. At heights much larger than the height of the roughness elements the local properties of the surface of the terrain will not have any effect on the mean wind. The only essential feature is a constant flux of momentum in the vertical direction toward the surface. Because the heights of interest are far larger than the friction length (~ thickness of layer where viscous effects are important ~ ν/u_* ~ tenth of a millimeter; ν is the kinematic viscosity of air) and because of the Galilean invariance of the equations of mechanics, it follows that the addition of a constant to all velocities cannot change the momentum flux through the fluid. Hence for a flow at vanishing pressure gradient nothing can be said about the absolute value of the wind speed at a given height. This leaves the gradient of the mean wind as the only quantity for a general study.

Considering a flow without buoyancy effects, the value of the gradient of the mean wind at heights far larger than the friction length must be independent of the viscosity and can thus depend only on the momentum flux, the density, and the height. Therefore, on dimensional grounds the following relationship

---

*)see Monin and Yaglom (1975) for a comprehensive treatment of flow close to rigid walls.

must be valid:

$$\frac{d\langle v(z)\rangle}{dz} = \frac{1}{k}\frac{u_*}{z} \qquad (C1)$$

This can be integrated to yield

$$\langle v(z)\rangle = \frac{u_*}{k} \ln(z/z_o) \qquad (C2)$$

where the von Karman constant k has been introduced ($k \cong 0.4$).

The constant z_o in Eq. (C2) is determined by the lower boundary conditions, and depends therefore on the variation of the mean wind close to the surface. This can differ considerably depending on whether the surface is rough or smooth, i.e. whether the roughness elements are larger or smaller than the friction length ν/u_*. As the friction length is of order tenth of a millimeter, a solid natural surface will always be classified as rough. However, the surface of water areas can often during low wind speeds be classified as smooth; this case will be considered later. For a rough surface z_o will be independent of viscosity and is determined only by the roughness elements.

The height z_o is formally the height where the mean wind speed becomes zero if the logarithmic variation were applicable down to this height. This creates no problem with the physics since in fact, the logarithmic variation ceases to apply at much larger values of z.

The roughness length z_o is dependent on the properties of the surface as described above, and from experiments where the variation of the mean wind with height has been measured, the profiles have been extrapolated to zero velocity and the z_o's obtained have been compared with various types of roughness elements (indicated on fig. C1). Since the height z_o is a characteristic length for a rough surface it is usually called the roughness length.

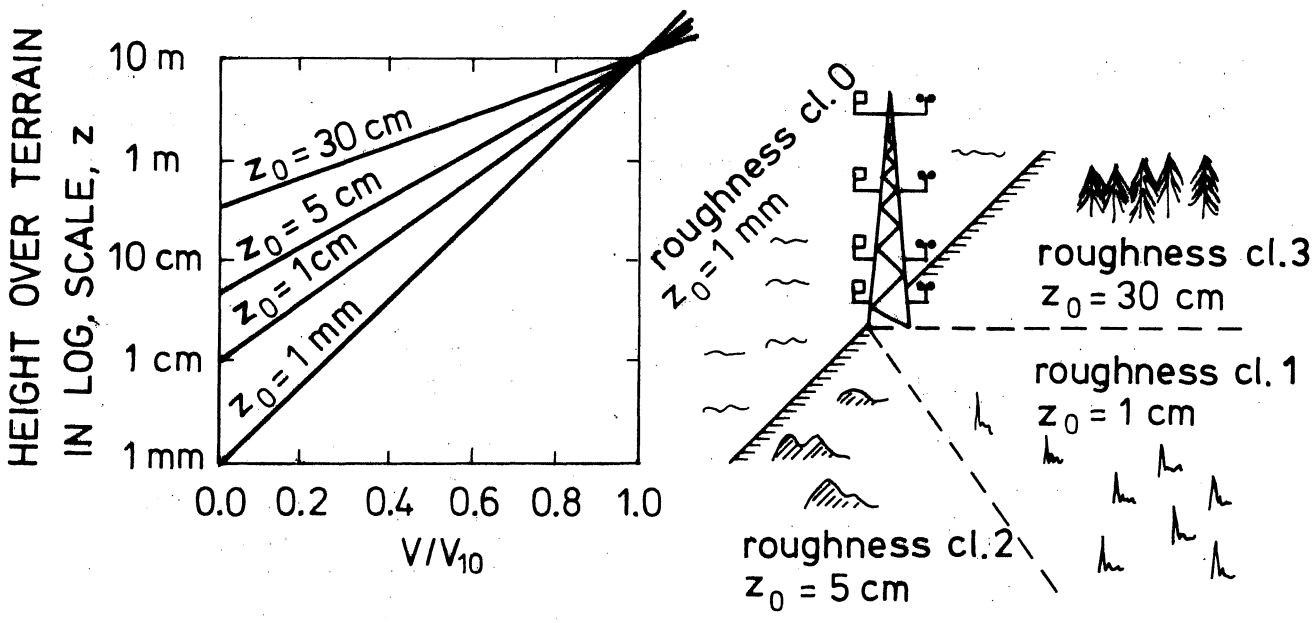

Fig. C1. Experimental determination of the roughness length z_o.

The correct choice of origin of the height z can be a problem if the height of the roughness elements is comparable to the height of interest. In this case the height of the elements will also influence the mean flow. Introducing the height into Eq. (C1) leads to an equation of the form:

$$\langle v(z) \rangle = \frac{u_*}{k} \ln \frac{z-D}{z_o} \qquad (C3)$$

The mean wind speed profile is still seen to be logarithmic and to depend only on the roughness length z_o when the height z is now measured from the level z = D. The height D is called the displacement length.

For vegetation of not too great a height, D may generally be taken equal to zero.

For high vegetation D must often be taken between the height and half the height of the vegetation. Figure C2 illustrates the wind profile over a forrest.

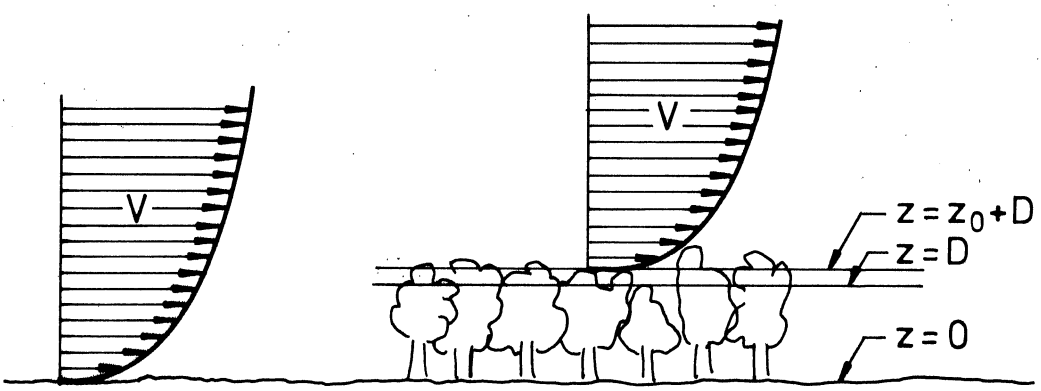

Fig. C2. The wind profile over a forrest, showing the displacement length D.

The roughness length of vegetated surfaces may also depend on the wind speed itself. For example, the bending of stalks by the wind can change the form of the surface. A similar phenomenon occur for water waves where both the height and the form of the waves are dependent on the wind speed. From dimensional arguments the following equation can be obtained for the roughness over water when viscous effects and the surface tension of the water are neglected (Charnock, 1955):

$$z_o = b \frac{u_*^2}{g} , \qquad (C4)$$

where b is a constant and g the gravitational acceleration.

In the Windatlas the roughness of water areas, roughness class 0, is obtained using Eq. (C4) with b = 0.014 (Garratt, 1977), and an approximation to the geostrophic drag law for neutral conditions (Eq. 2.1):

$$\frac{u_*}{G} = \frac{0.5}{\ln(Ro)}$$
$$Ro = \frac{G}{fz_o} \qquad \text{(C5)}$$

The values of $z_o(G)$ are obtained by an iterative process. The range of z_o can be illustrated by an example:

$$z_o \ (G = 4 \text{ m/sec}) = 2 \cdot 10^{-5} \text{m}$$
$$z_o \ (G = 23 \text{ m/sec}) = 1.6 \cdot 10^{-3} \text{m}$$

It follows that for low geostrophic wind speed, the roughness of the surface is smaller than the friction length: $\nu/u_* \sim 10^{-4}$m, hence the surface cannot be considered to be rough, but rather dynamically smooth. The assumption of negligble viscous effects in Eq. (C4) is not fulfilled for low wind speeds either; however, as low wind speeds are of little concern for wind energy purposes and further because the roughness of a dynamically smooth surface is approximately $1/9 \ \nu/u_* \sim 10^{-5}$ m, it is reasonable to use the Eqs. (C4) and (C5) in the whole geostrophic wind speed range.

It should further be noted that in general the roughness length as applied in the Windatlas has to be considered a climatological parameter. The roughness of an area changes with foliation, vegetation, snowcover and so on. The reason for requiring the determination of a wind turbines power production to be performed on a climatological basis is primarily for the climatological variations of the weather, however, the seasonal variations of the local terrain characteristics can also have a profound influence.

C2. Roughness elements

Not all the elements in the terrain contribute to the roughness of the terrain. In order to act as a roughness element, it is necessary for the element to cause an increased turbulence in the flow over and around the element. This happens when vortex shedding and flow seperation is created by the element, (fig. C3) and thereby extracting energy from the flow and acting as an increased resistance to the flow. Long smooth hills, for example, are not roughness elements because they do not themselves cause vortex shedding and separation.

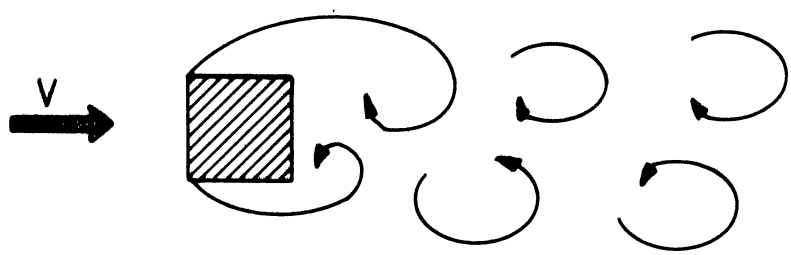

Fig. C3. Vortex shedding and separation from a roughness element

A roughness element can be characterized by a height h, a cross section to the wind S, and a porosity to the wind. Further, for a population of roughness elements distributed over an area, the horizontal area A_H per roughness element also enters the considerations.

Through a series of experiments, a simple empirical relation based on the above-mentioned characteristics Eq. C6, assuming that porosity does not play an important role (Businger, 1974):

$$z_o = 0.5\ h\ \frac{S}{A_H} \qquad (C6)$$

The relation gives reasonable estimates of z_o when A_H is much larger than S; it tends to overestimate z_o when A_H becomes of the order of S.

Example C1.

In a terrain of roughness class 1, z_o = 1 cm, a large number of houses are constructed. The increase in roughness is estimated from: h = 5 m, S = 100 m^2, A_H = 1000 m^2:

$$z_o = 0.5 \cdot 5 \cdot \frac{100}{1000} = 0.25 \text{ m} ,$$

i.e. the resulting z_o ~ 1 + 25 cm ~ 30 cm corresponding to roughness class 3.

Example C2

A very large number of wind turbines are erected in an area of roughness class 2, z_o = 5 cm. The hub height and rotordiameter is 50 m and the distance between the generators is ten times the diameter, i.e. 500 m. By assuming the rotor to be the roughness element, h becomes equal to 50 m and S is equal to the rotorarea, 2000 m^2 which gives:

$$z_o = 0.5 \cdot 50 \cdot \frac{2000}{250000} = 0.20 \text{ m}$$

i.e. the resulting z_o ~ 5 + 20 ~ 30 cm corresponding to roughness class 3.

It should be noted that this result is based on the assumption of a very large number of wind turbines, hence it cannot be used directly for wind turbine parks with a few wind turbines.

——— • ———

The results in the two examples have to be viewed as rough estimates. It is worthwhile noting that although it seems quite resonable to add roughness lengths, there is no theoretical basis for doing so.

Equation (C6) can also be applied to windbreaks by letting $S \sim hL$ and $A_H \sim \ell L$, where L is the length of the windbreak and ℓ the distance between the windbreaks:

$$z_o = 0.5 \frac{h^2}{\ell} \qquad (C7)$$

For a typical height of h equal to 10 m the influence on z_o of ℓ is illustrated below:

ℓ (m)	1000	500	200
z_o (m)	0.05	0.1	0.25

C3. A simplified roughness model

When the roughness determination is done in practice it is useful to have a feeling for what area in each direction is important for the windspeed within the swept area of the wind turbine. For a turbine fifty meters high, say, the windspeed at hub height will not be influenced by trees five meters high and bushes out to a distance upstream of a few hundred meters. Similarly it is obvious that roughness elements at large distances cannot have a significant influence. These qualitative considerations can be quantified somewhat by utilization of a simplified roughness model, which is based on an analogy from dispersion

meteorology. The effect of a single roughness element is thought of as a source of velocity deficit, which by the action of large eddies is dispersed upwards. The model does not account for the shelter effect and the flow disturbance immediately behind a isolated roughness element. The effect of shelter is treated in section 5.6.

It has been found from dispersion experiments that a passive contaminant (such as smoke) emitted from a point source at the surface under conditions of near neutral stratification are dispersed approximately according to the expression

$$C(x) \sim \frac{1}{\sigma_z \sigma_y} \exp\left(-\frac{h^2}{2\sigma_z^2}\right) \qquad (C8)$$

with

$$\sigma_y \sim x^{0.8}, \quad \sigma_z \cong \eta\, x^{0.8} \quad \text{and} \quad \eta = 60\ \text{m(km)}^{-0.8},$$

where C is the concentration at distance x downstream from the source and at height h above the surface; hence:

$$C(x) \sim \sigma_z^{-2} \exp\left(-\frac{1}{2} h^2 \sigma_z^{-2}\right) . \qquad (C9)$$

This function has a maximum for

$$\sigma_z = \eta\, x^{0.8} = h/\sqrt{2} ,$$

and the value of C has decreased to 10% of the maximum value at the distances determined by

$$\left(\frac{h}{\sigma_z}\right)^2 \exp\left(-\frac{1}{2}\left(\frac{h}{\sigma_z}\right)^2\right) = 0.074$$

with the solutions

$$\frac{h}{\sigma_z} \cong 3.1 \quad \text{and} \quad \frac{h}{\sigma_z} = 0.28 \ .$$

Using the expression above for σ_z as function of distance x the following results are obtained:

1) The maximum influence is from an area upstream at a distance

$$x \cong [0.012 \cdot h]^{1.25} \qquad [x \text{ in km, } h \text{ in m}]$$

2) The zone of influence larger than 10% of the maximum ranges between distances x_1 and x_2 determined from:

$$x_1 \cong [0.0054 \cdot h]^{1.25} \qquad [x \text{ in km, } h \text{ in m}]$$

$$x_2 \cong [0.060 \cdot h]^{1.25} \qquad [x \text{ in km, } h \text{ in m}]$$

The relations are plotted in fig. C4.

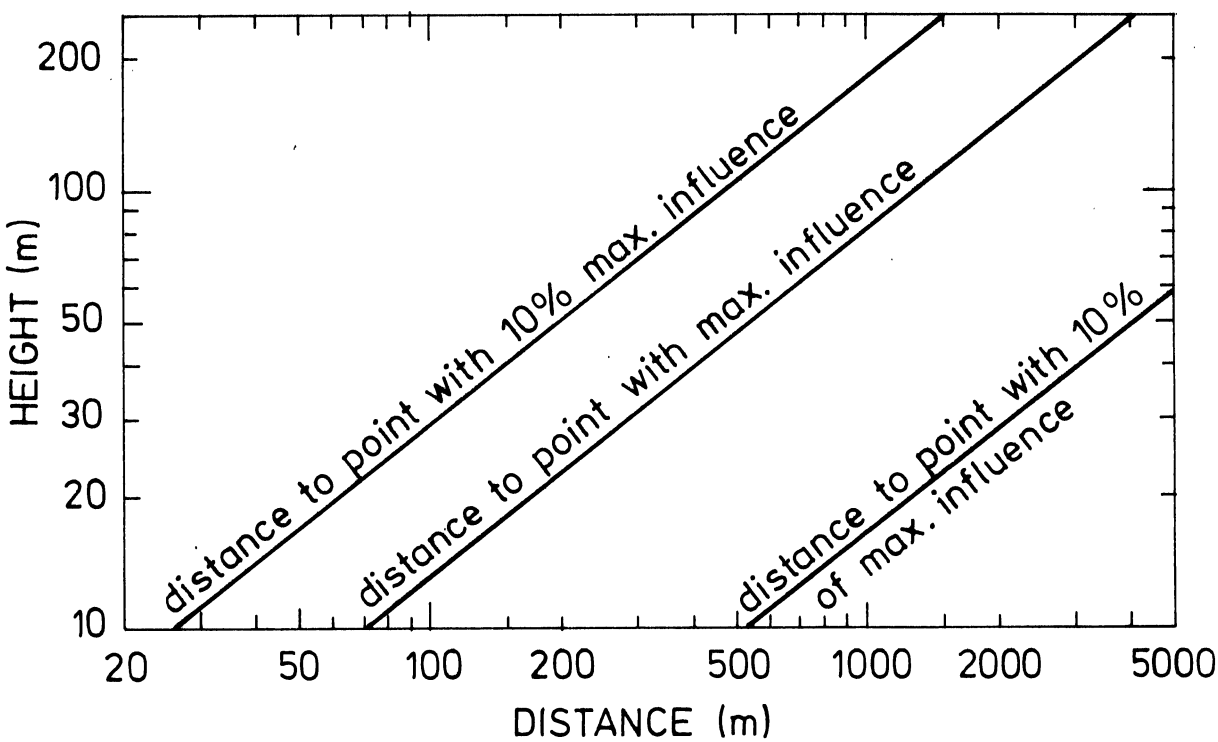

Fig. C4. Rule of thumb for the evaluation of the area in which the roughness has the greatest effect on the wind-speed.

This roughness model is, as noted above, very simplified, but it provides in any case a usefull "rule-of-thumb" for which areas are most important when determining the roughness of a terrain. The model furthermore shows that the roughness elements in different directions cannot be considered independently; that is, roughness elements which are not directly in the upwind direction can influene the windspeed. On fig. C5 is shown as an example the situation at a point situated above the borderline between two areas of well-defined roughness. When the wind direction is close to the direction of the coastline the speed deficit from the more rough terrain is dispersed across the coastline and as a consequence, the windspeed at the point considered is determined by both roughnesses.

When it is necessary to take into account roughness changes in the computation of the wind distribution at a given point, the model described above cannot be used, and the procedure desscribed in section 5.5 must be employed.

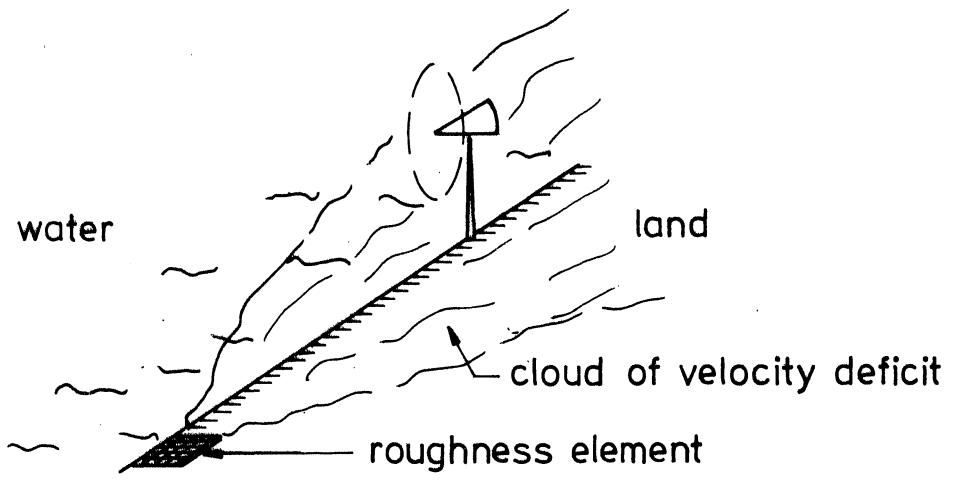

Fig. C5. The simple roughness model and the situation at a coastline.